Low-Valent Main Group Complexes and their Transition Metal-like Reactivity

by

Matthew M. D. Roy

A thesis submitted in partial fulfillment of the requirements for the degree of

Doctor of Philosophy

Department of Chemistry
University of Alberta

Abstract

The work presented in this thesis describes the isolation of novel low-valent Group 12 and p-block element-containing molecules. Some of these molecules are shown to exhibit reactivity which mimics that of the transition metals; specifically, with respect to strong bond activation and catalysis. In order to isolate these reactive main group compounds, several stabilization strategies were employed. Lewis base stabilization using bulky *N*-heterocyclic carbene (NHC) ligands proved to be highly valuable in the formation of reactive sites involving electropositive elements. Using NHCs, both cadmium and germanium-based molecules are shown to be active ketone reduction catalysts. Additionally, an extremely bulky NHC ligand was synthesized and demonstrated to stabilize low-coordinate inorganic cations of silver, thallium and germanium. Finally, a bulky anionic (vinylic) donor based on an *N*-heterocyclic carbene framework proved to be highly effective in the stabilization of low-coordinate, reduced main group environments. This includes the synthesis of two-coordinate silicon compounds which, at the present time, are still exceedingly rare owing to their high degree of reactivity. One such species is shown to cleave strong organic and inorganic σ-bonds, thus demonstrating transition metal-like reactivity with the 2nd most abundant element in the Earth's crust.

Preface

A portion of the work presented in this thesis has been done in collaboration with others within the Department of Chemistry, University of Alberta. Crystallographic studies of all compounds presented in this thesis were performed by Dr. Robert McDonald, Dr. Michael J. Ferguson and Dr. Yuqiao Zhou including mounting of the crystals, operation of the diffractometer, refinement of the structures and preparation of the crystallographic data tables. Elemental analyses were performed by the Analytical and Instrumentation Laboratory in the Department of Chemistry, University of Alberta. $^{199}Hg\{^{1}H\}$ NMR spectra, variable temperature NMR and DOSY experiments were conducted with the assistance of Mark Miskolzie at the Nuclear Magnetic Resonance Laboratory in the Department of Chemistry, University of Alberta.

Chapter 3: The reactivity of imine-substituted phosphines towards electrophiles was investigated in collaboration with Linkun Miao.

Chapter 4: The initial synthesis of the bulky *N*-heterocyclic carbene ITr (ITr = $[(HCNCPh_3)_2C:]$) was conducted by Dr. Paul A. Lummis.

Chapter 5: The synthesis and characterization of all new compounds reported was done in collaboration with Dr. Shiori Fujimori from the group of Prof. Norihiro Tokitoh.

Chapter 7: Characterization of the precursor compounds ^{Me}IPr=CH(I) and (^{Me}IPrCH)Li was done in collaboration with Samuel R. Baird.

According to the policy of our research group, each chapter of this thesis is essentially self-contained, and prepared in the form of a manuscript that is intended for publication in a peer-reviewed journal. A portion of this thesis has been previously

published in peer-reviewed journals and the publications are listed below with their associated chapters.

Chapter 1:

Roy, M. M. D.; Rivard, E. *Acc. Chem. Res.* **2017**, *50*, 2017.

Chapter 2:

(a) Roy, M. M. D.; Ferguson, M. J.; McDonald, R.; Rivard, E. *Chem. Eur. J.* **2016**, *22*, 18236; (b) Roy, M. M. D.; Ferguson, M. J.; Rivard, E. *Z. Anorg. Allg. Chem.* **2016**, *642*, 1232.

Chapter 3:

Roy, M. M. D.; Miao, L.; Ferguson, M. J.; McDonald, R.; Rivard, E. *Can. J. Chem.* **2018**, *96*, 543.

Chapter 4:

(a) Roy, M. M. D.; Lummis, P. A.; Ferguson, M. J.; McDonald, R.; Rivard, E. *Chem. Eur. J.* **2017**, *23*, 11249; (b) Roy, M. M. D.; Ferguson, M. J.; McDonald, R.; Rivard, E. *Chem. Commun.* **2018**, *54*, 483.

Chapter 5:

Roy, M. M. D.; Fujimori, S.; Ferguson, M. J.; McDonald, R.; Tokitoh, N.; Rivard, E. *Chem. Eur. J.* **2018**, *24*, 14392.

Chapter 6:

Roy, M. M. D.; Ferguson, M. J.; McDonald, R.; Zhou, Y.; Rivard, E. *Chem. Sci.* **2019**, *10*, 6476.

Dedicated to my Grandmother

Beverly Jean George

Acknowledgements

First, I must thank my supervisor and mentor Prof. Eric Rivard. His continuous support and guidance throughout the course of my PhD has helped me to grow as a researcher, writer and presenter. I am especially grateful that he gave me the freedom to pursue whichever topics interested me most and he constantly pushed me to be more creative. Additionally, Eric has been immensely helpful giving career advice and I know his support will continue as I pursue a career in chemistry.

I would also like my supervisory committee members Prof. Jon Veinot and Prof. Alex Brown for their support and advice throughout my PhD. Additionally, I would like to thank all my thesis defense examiners, Prof. Georgii Nikonov, Prof. Jon Veinot, Prof. Alex Brown, and Prof. Arthur Mar for providing valuable insight and feedback. Finally, I would like to thank the non-examining defense chair Prof. Josef Takats.

Next, I would like to express my most sincere gratitude for my wonderful and supportive girlfriend Dr. Shiori Fujimori, who I met at the University of Alberta during my studies (and who was a collaborator on Chapter 5 of this thesis). I would also like to thank my family; parents Brent and Mary-Jo, my brother Gabe, my sister Laura, my grandfather Ronald Roy and my grandmother Beverly George for their support and encouragement throughout my studies.

My time at the University of Alberta would not have been nearly as enjoyable without the fantastic members of the Rivard group. Dr. Mike Boone and Dr. Christian Hering-Junghans were both great sources of comic relief and advice during the formative years of my PhD. I would also like to thank Sarah Parke who started in the Rivard group

with me in 2014 and who, over the years, has helped me book flights, find apartments, remember meetings, do taxes and listened to my endless complaining. Finally, I am especially grateful to all past and present Rivard group members and visiting students who I have had the pleasure of working with: Dr. Paul Lummis, Kate Powers, Dr. Olena Shynkaruk, Dr. Melanie Lui, Nathan Paisley, Derek Zomerman, Dr. William Torres Delgado, Dr. Anindya Swarnakar, Dr. Felix Kaiser, Dr. Emanuel Hupf, Christina Braun, Bruno Luppi, Jocelyn Sinclair, Ian Watson, Alvaro Omana, Sam Baird, Matthias Ackermann, Gunwant Matharu and my trusty sidekick, Linkun Miao.

Additionally, I would like to thank crystallographers Dr. Robert McDonald and Dr. Michael Ferguson for allowing me to drink coffee in the X-ray lab instead of working while they picked through my dubious "crystals". Also, all members of the Department of Chemistry support staff who make doing research at the U of A easy.

Finally, I have made many great friends in the department since arriving in 2014 who made living here the last five years extremely enjoyable. Those who I would especially like to thank are my close friends Patrick "Party Pat" Moon, Kevin Hooton, Anis Fahandej-Sadi, Benjamin Rehl and the staff at Sherlock's pub who never cut us off or kicked us out.

Table of Contents

List of Tables

List of Figures

List of Schemes

List of Symbols and Abbreviations

Å	Angstrom
Ad	Adamantyl
Ar	Aryl
avg.	Average
*n*Bu	Normal butyl
*s*Bu	Secondary butyl
*t*Bu	Tertiary butyl
ca.	Approximately; *circa*
CAAC	Cyclic(alkyl)amino carbene
Cp	Cyclopentadienyl
Cp*	Pentamethylcyclopentadienyl
Cy	Cyclohexyl
°C	Degrees Celsius
δ	Chemical shift
δ^+/δ^-	Partial positive/negative charge
d	doublet
DFT	Density functional theory
diox	Dioxane
Dipp	2,6-*i*$Pr_2C_6H_3$
DMAP	4-Dimethylaminopyridine

DOSY	Diffusion ordered NMR spectroscopy
Dur	1,2,4,5-Tetramethylbenzene
η^n	Indicates hapticity (*n*)
FT	Fourier transform
g	Gram
HOMO	Highest occupied molecular orbital
Hz	Hertz
HSQC	Heteronuclear single quantum coherence
IMe	$(HCNCH_3)_2C$:
IPr	$(HCNDipp)_2C$:
^{Me}IPr	$(MeCNDipp)_2C$:
IR	Infrared
ITr	$(HCNCPh_3)_2C$:
K	Kelvin
kJ	Kilojoule
kcal	Kilocalorie
L	General neutral ligand
LA	Lewis acid
LB	Lewis base
LUMO	Lowest unoccupied molecular orbital
Me	Methyl
Mes	Mesityl
Mes*	2,4,6-*t*BuC_6H_2

mol	Mole
M.p.	Melting point
NBO	Natural bonding orbital
NacNac	General β-diketimine ligand
NHC	*N*-Heterocyclic carbene
NHI	*N*-Heterocyclic imine
NHO	*N*-Heterocyclic olefin
$^{n}J_{AB}$	n-Bond coupling constant between A and B
NMR	Nuclear magnetic resonance
OTf	Trifluoromethanesulfonate
Ph	Phenyl
ppm	Parts per million
q	Quartet
R	General anionic ligand
s	Singlet
sept	Septet
t	Triplet
Tbt	2,4,6-$\{CH(SiMe_3)_2\}_3C_6H_2$
THF	Tetrahydrofuran
TOF	Turnover frequency
TON	Turnover number
Trip	2,4,6-iPr$_3$C$_6$H$_2$

vide infra	See below
vide supra	See above
WBI	Wiberg bond index

Chapter 1: Introduction

1.1. The Resurgence of Main Group Element Chemistry

The discovery of ferrocene in the 1950s[1] sparked great interest in the field of organometallic chemistry, leading to seminal discoveries such as Vaska's complex, $[IrCl(CO)(PPh_3)_2]$ (which was later shown to reversibly bind H_2),[2] Wilkinson's catalyst, $[RhCl(PPh_3)_3]$ (shown to catalytically hydrogenate olefins)[3] and the first activation of aliphatic C–H bonds using Graham's $[Cp^*Ir(CO)_2]$ ($Cp^* = Me_5C_5$) complex.[4] While organometallic chemistry flourished, leading to the development of a plethora of *homogeneous* catalytic reactions, the chemistry of the main group elements (s- and p-block) was, at this time, thought to be well understood. Specifically, main group elements were generally considered to form relatively stable complexes which did not promote the cleavage of strong organic bonds, thus precluding their use in catalysis as offered by the transition metals. For example, an excerpt from Cotton and Wilkinson's *Advanced Inorganic Chemistry, Fourth Edition* (1980) concerning multiple bonding of the Group 14 elements reads: "Silicon, germanium, tin and lead do not form multiple bonds using $p\pi$ orbitals. Consequently, numerous types of carbon compounds, such as alkenes, alkynes, ketones, and nitriles have no analogues."[4] This notion was commonly referred to as the "double bond rule" which states that elements having a principal quantum number greater than 2 will not form double bonds with themselves or any other elements.[5] The rule was first broken in 1981 with West's groundbreaking isolation of the first disilene, $Mes_2Si{=}SiMes_2$ (Mes = 2,4,6-$Me_3C_6H_2$), representing the first example of a heavy

unsaturated carbon analogue (heavy alkene)[6] and Yoshifuji's diphosphene Mes*P=PMes* (Mes* = 2,4,6-*t*BuC_6H_2).[7] These early discoveries were made possible by the use of a *kinetic stabilization* strategy which spurred the burgeoning field of modern main group chemistry.

1.2. Kinetic Stabilization of Low-Valent Main Group Compounds

Kinetic stabilization refers to the use of sterically encumbering groups to kinetically mitigate oligomerization processes of otherwise unstable fragments. This can be illustrated by the formation of polydimethylsilane from dimethyldichlorosilane (Reaction A, Scheme 1.1). The reduction of Me_2SiCl_2 with sodium metal (Wurtz coupling) affords the dimethylsilane polymer, presumably via the low-valent Si^{II} intermediate Me_2Si:, which later undergoes oligomerization.[8] In support of this postulate, the intermediary silylene Me_2Si: has been observed by low-temperature matrix isolation.[9] This polymerization illustrates that, unlike carbon which forms stable alkenes, silicon prefers to form 4-coordinate products with Si–Si σ-bonds rather than engaging in π-bonding. By replacing the methyl groups of Me_2SiCl_2 with bulky aryl substituents, West and coworkers were able to halt oligomerization at the disilene dimer, $Mes_2Si{=}SiMes_2$ (Reaction B, Scheme 1.1), forming the first isolable compound featuring an Si–Si π-bond. Evidence for the initially formed silylene, $:SiMes_2$ was also confirmed by low-temperature chemical trapping experiments.[6]

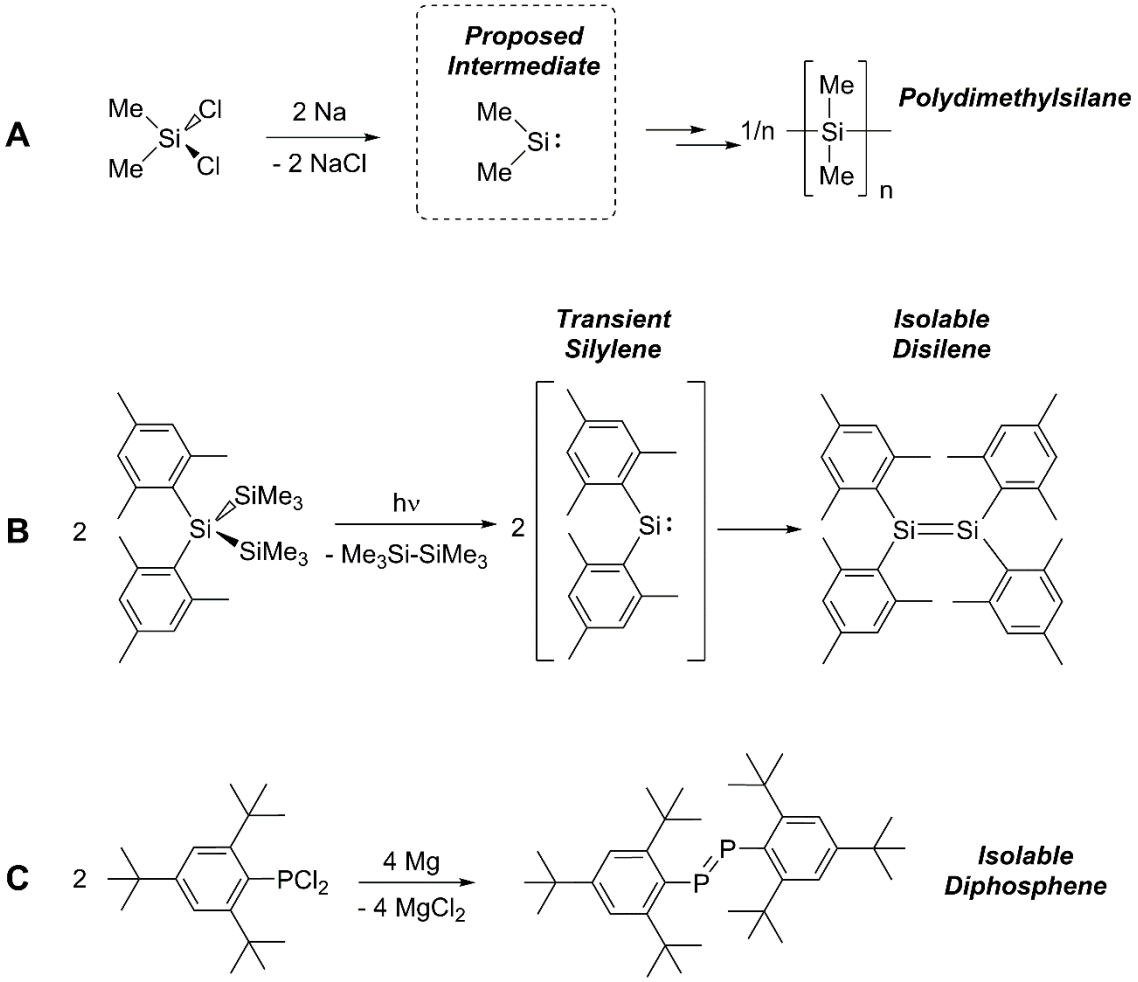

Scheme 1.1. A) The reduction of dimethyldichlorosilane leading to polydimethylsilane, B) the formation of an isolable disilene by photolytic reduction of a Si^{IV} precursor, and C) the formation of an isolable diphosphene by magnesium reduction of a P^{III} precursor.

In the same year, the diphosphene Mes*P=PMes* was isolated by the reductive coupling of a P^{III} precursor Mes^*PCl_2 (Reaction C, Scheme 1.1).[7] Again, the presence of sterically hindered aryl groups prevented oligomerization thus allowing for the formation of a stable P=P double bond with a short P–P bond length of 2.034(2) Å, far shorter than typical P–P single bonds [*cf.* average P–P single bond length in *cyclo*-$(PhP)_5$ = 2.217(6) Å].[10] Both the diphosphene and disilene represent dimers of their respective parent phosphinidene ($Mes^*\ddot{P}$:) and silylene (Mes_2Si:) forms. While stable silylenes had

not yet been isolated at this time, heavier tetrelenes R_2E: (R = bulky anionic organic group, E = Ge, Sn, Pb) had been synthesized using bulky alkyl substituents (*vide infra*).

1.2.1. Kinetic Stabilization of Heavy Alkenes and the Inert Pair Effect

Prior to West's discovery of the stable disilene $Mes_2Si{=}SiMes_2$, Lappert and coworkers described a distannene, a tin analogue of an alkene, using the bulky bis(trimethylsilyl)methyl ligand $CH(SiMe_3)_2$.[11] Unlike the disilene $Mes_2Si{=}SiMes_2$, Lappert's distannene $\{(Me_3Si)_2HC\}_2SnSn\{CH(SiMe_3)_2\}_2$ (**1**) was found to dissociate to the stannylene (**2**) form in solution (Figure 1.1). Additionally, while the disilene $Mes_2Si{=}SiMes_2$ has a nearly planar geometry as expected for an alkene (sum of interligand angles = 356°),[12] the tin atoms in Lappert's distannene exhibit significant pyramidalization, indicating a high degree of lone pair character on each tin center ($\sum\alpha$ = 340°). Another indication of lone pair character is that the ligands are 41° out-of-plane of the Sn–Sn bond (fold angle). These observations suggest that if multiple bonding is present in $\{(Me_3Si)_2HC\}_2SnSn\{CH(SiMe_3)_2\}_2$, it is quite weak. As a result, the bonding situation in **1** is best illustrated by two zwitterionic resonance structures with a Sn–Sn σ-bond (Figure 1.1). The preference for tin to maintain non-bonding lone pair character rather than form an Sn=Sn bond can be partially explained by the *inert pair effect*.[13]

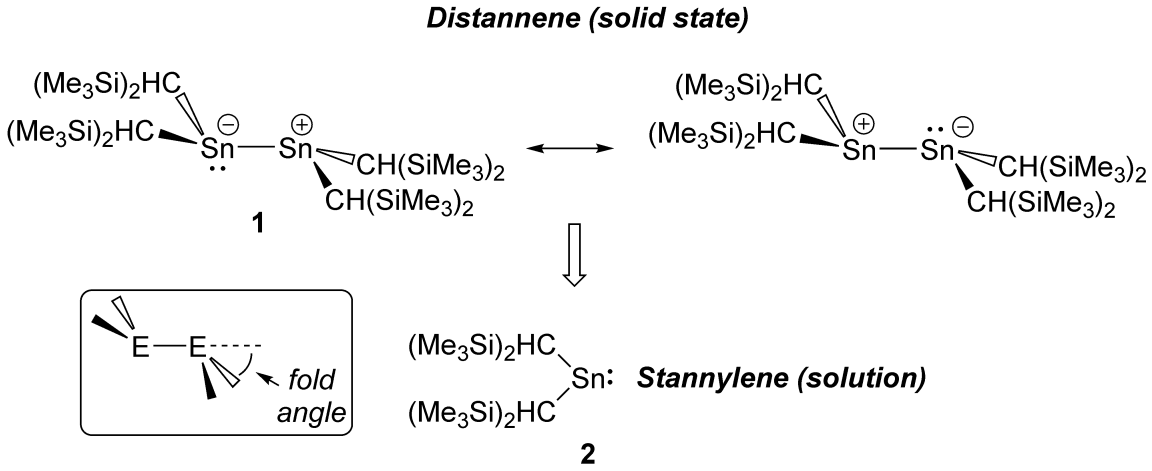

Figure 1.1. Illustration of the *trans*-pyramidal distannene (**1**) geometry in the solid state (top) and its stannylene (**2**) form in solution (bottom).

The *inert pair effect* describes the increasing stability of oxidation states two less the Group valency for the Group 13–16 elements upon descending the group. For example, boron is most commonly found in its +3 oxidation state, whereas thallium prefers Tl^{I}. Thallium(I) has a $6s^2$ "inert pair" which is resistant to oxidation. This preference for heavy p-block elements to occupy lower oxidation states is due to several factors: (1) the relatively diffuse *d*- and *f*-orbitals poorly shield n*s* electrons; (2) relativistic effects and (3) decreasing bond enthalpies upon descending a group.[13]

Table 1.1. Structural features of the heavy alkene series illustrating the inert pair effect.

	E–E [Å]	∑α [°]	fold angle [°]
Mes$_2$SiSiMes$_2$[12]	2.16	356	18
R$_2$GeGeR$_2$[11c]	2.35	348	32
R$_2$SnSnR$_2$[11b]	2.76	340	41
R$_2$PbPbR$_2$[14]	4.13	–	34.2

R = $\{CH(SiMe_3)_2\}^-$

Following the trend predicted by the inert pair effect, the structure of the germanium analogue of $\{(Me_3Si)_2HC\}_2SnSn\{CH(SiMe_3)_2\}_2$ (**1**) shows less

pyramidalization at each germanium atom relative to **1**, with a fold angle of 32° and a sum of the interligand angles at germanium of 348°. Unlike its lighter congeners, the lead derivative essentially exists as a monomer :Pb{CH(SiMe$_3$)$_2$}$_2$ in the solid state, with a very long Pb···Pb contact of 4.13 Å.[14] The important structural features for the Group 14 series of heavy alkenes are listed in Table 1.1.

1.2.2 Kinetic Stabilization of Heavy Alkynes and their *trans*-Bent Geometries

Following the stabilization of the heavy Group 14 alkenes using bulky alkyl and aryl substituents, a similar kinetic strategy was used to isolate the heavy Group 14 alkynes. Using a bulky silyl substituent, the disilyne RSiSiR (**3**, R = Si(*i*Pr){CH(SiMe$_3$)}$_2$) was isolated by Sekiguchi and coworkers in 2004 (Figure 1.2).[15] Similar to Mes$_2$Si=SiMes$_2$ (*vide supra*), disilyne **3** shows structural distortion relative to its alkyne hydrocarbon congeners. In the case of **3**, the distortion from linearity (or *trans*-bending) is evident by an R-Si-Si angle of 137.4°.[15] Prior to the isolation of **3**, bulky *meta*-terphenyl ligands were used by Power and coworkers for the isolation of the Ge–Pb analogues ArEEAr (**4**–**6**; Figure 1.2; Ar = bulky aryl group). Like with the alkene analogues, upon descending Group 14, multiple bond character decreases (and *trans*-bending becomes more pronounced). The Pb^{I} dimer **6** exhibits a C-Pb-Pb angle of 94.3° indicating that ligand-metal and metal-metal bonding is dominated by orbitals of high *p*-character, whereas an "inert" lone pair resides in a low-energy 6*s* orbital on lead. This may also be thought of as a decreased degree of orbital *s*/*p* orbital mixing (hybridization) upon descending the group.

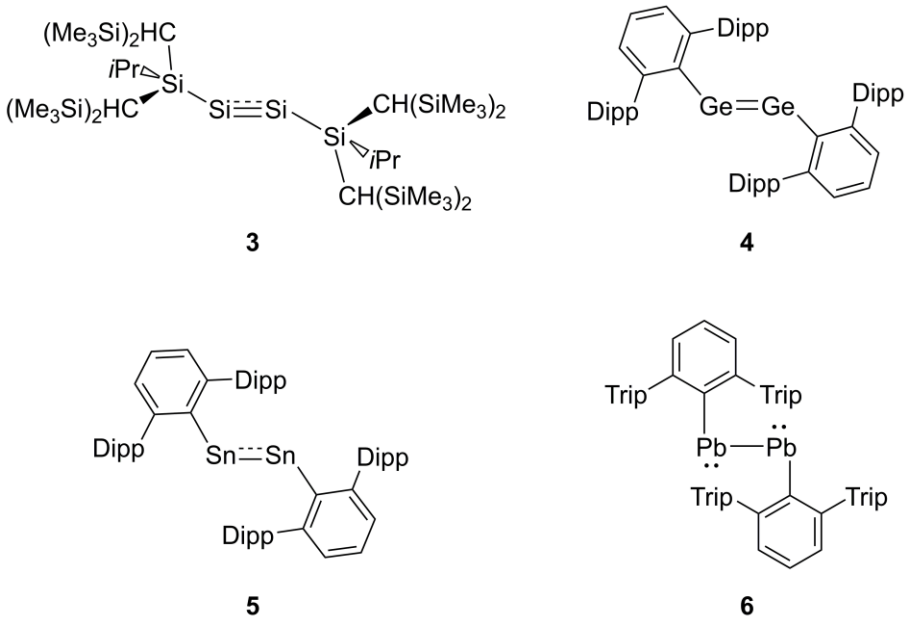

Figure 1.2. Heavy alkyne analogues REER **3**–**6** illustrating a decrease in multiple bond character upon descending Group 14 (Dipp = 2,6-*i*Pr$_2$C$_6$H$_3$; Trip = 2,4,6-*i*Pr$_3$C$_6$H$_2$).

From a molecular orbital perspective, the *trans*-bent geometries of compounds **3**–**6** may be understood as arising from second order Jahn-Teller mixing. The frontier molecular orbitals of a general linear ($D_{\infty h}$) alkyne REER (E = Group 14 element) consist of a σ-bonding orbital, two degenerate π-bonding orbitals and their corresponding antibonding combinations (Figure 1.3, left).[16] Since these orbitals are orthogonal to one another, mixing cannot occur. This picture changes upon distortion to a *trans*-bent (C_{2h}) geometry (Figure 1.3, right). Upon distortion, the degeneracy of the π and π* orbitals is broken, and a new occupied orbital of lone-pair character (n_-) is generated. Formerly symmetry forbidden σ/π* and π/σ* mixing (in the linear case) becomes allowed upon *trans*-bending, thus lowering the energy of σ- and π- type bonding orbitals through a second order Jahn Teller mixing.[16] As *trans*-bending increases, E–E π-bonding character decreases (and lone pair character increases) thus *trans*-bending becomes more favorable for heavy elements.

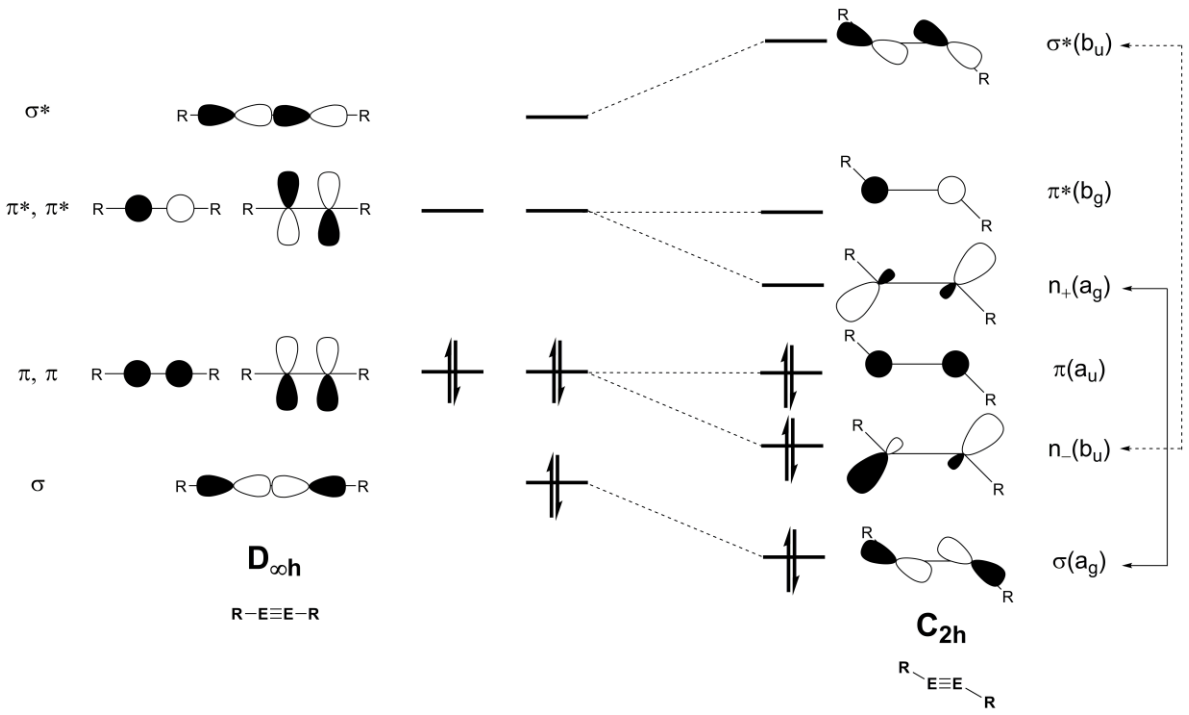

Figure 1.3. Molecular orbital depiction of a linear ($D_{\infty h}$) alkyne (left) and a *trans*-bent (C_{2h}) alkyne (right). Arrows indicate symmetry allowed orbital mixing; Mulliken symbols are in parentheses. Adapted from Figure 9 of reference 16.

1.2.3. Kinetic Stabilization of Univalent Group 13 and Group 15 Elements

The series of heavy Group 14 alkenes and alkynes provides a good comparison to their hydrocarbon analogues and gives insight into the multiple bond character trends for a given group. Similar trends in multiple bonding character can also be seen for the Group 13 and Group 15 elements in their +1 oxidation states. For example, heavy triel dimers REER (R = bulky aryl group, E = Group 13 element) are known for gallium, indium and thallium whereas their lighter congeners (boron, aluminum) are too reactive to be observed.

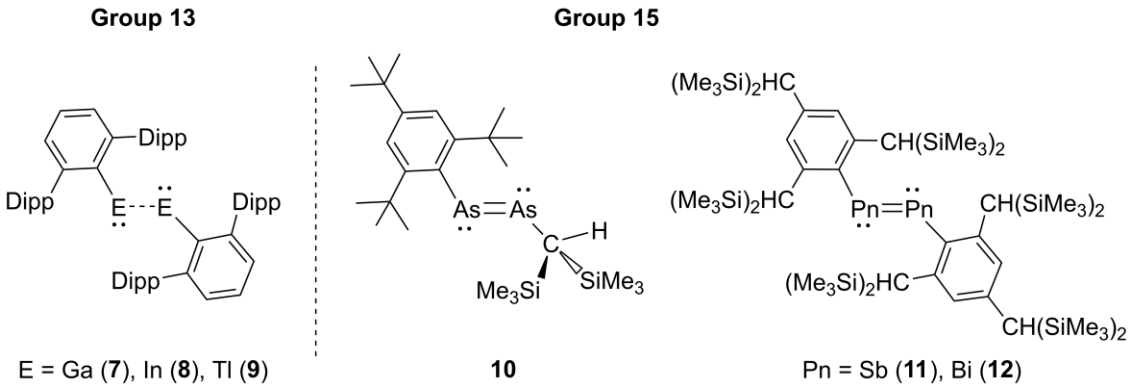

Figure 1.4. Group 13 (left) and Group 15 (right) dimers stabilized by bulky aryl and alky groups.

Using the same bulky *meta*-terphenyl ligands used to isolate compounds **4**–**6**, Power and coworkers were able to prepare the Group 13 E^{I} dimers of gallium (**7**),[17] indium (**8**)[18] and thallium (**9**) (Figure 1.4).[19] Notably, attempts to form analogous boron and aluminum derivatives gave intramolecular ligand activation products in the former case[20] and solvent activation (benzene or toluene) products in the latter.[21] A few years following the first report of a stable diphosphene (Scheme 1.1), Cowley and coworkers prepared the diarsene Mes*As=As{$CH(SiMe_3)_2$} **10**.[22] More than a decade later, this was followed by the report of a distibene (Tbt)Sb=Sb(Tbt)[23] and dibismuthene (Tbt)Bi=Bi(Tbt)[24] (Tbt = 2,4,6-{$CH(SiMe_3)_2$}$_3C_6H_2$) by Tokitoh and coworkers, using very bulky aryl groups appended with {$CH(SiMe_3)_2$}$^-$ substituents (Figure 1.4). As with the Group 14 elements, multiple bonding in REER systems (E = Group 13 or Group 15 element) becomes weaker upon descending the group.

1.3. Thermodynamic Stabilization of Low-Valent Main Group Compounds

The low oxidation state main group compounds discussed thus far have all been stabilized using bulky carbon (or silicon) based anionic ligands, with the steric protection preventing oligomerization of reactive main group multiple bonds. As described above, the alkylated

tetrelenes :E{CH(SiMe$_3$)$_2$}$_2$ (E = Ge–Pb) are monomeric in solution and form dimers with varying degrees of E–E bonding in the solid state.[11] Lappert and coworkers also reported the amide derivatives :E{N(SiMe$_3$)$_2$}$_2$ which are monomeric both in solution and the solid state.[11] In this case, the bulky amide groups provide *thermodynamic* stabilization in addition to kinetic stabilization. Thermodynamic stabilization refers to ligands whose electronic properties stabilize the element to which they are bound. As illustrated in Figure 1.5 (using germanium as an example), the electronegative nitrogen atom of the amide donor is σ-withdrawing which serves to stabilize the highest occupied molecular orbital (HOMO): a germanium lone pair. Additionally, the nitrogen atom of the amide group has a π-symmetry lone pair which can donate into the lowest unoccupied molecular orbital (LUMO) located at Ge (empty *p*-orbital) thereby increasing its energy. This concept has led to the design of a myriad of heteroatom-based anionic (and neutral) ligands which have been used to support previously unprecedented bonding environments.

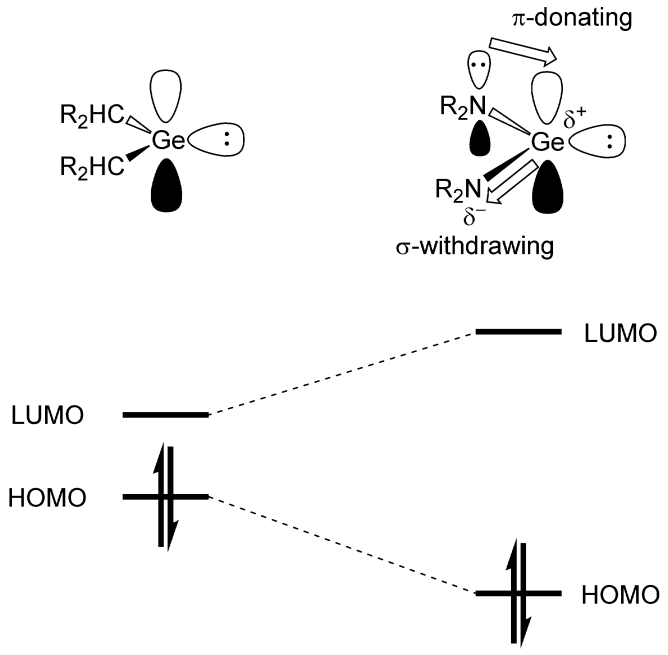

Figure 1.5. Illustration of the effect of the σ-withdrawing/π-donating effect of an amide group on the frontier molecular orbitals of a germylene (R = SiMe$_3$).

1.3.1. Anionic Heteroatom Donors in Main Group Chemistry

By taking advantage of the dual σ-withdrawing/π-donating nature of nitrogen, several bulky ligand classes have been developed using this element (Figure 1.6). One of the most widely used ligands by organometallic and main group chemists alike are the bidentate β-diketiminate ligands (also referred to as NacNac$^-$ ligands). The ease of synthesis and structural tunability in addition to their stabilizing ability makes NacNac$^-$ ligands highly desirable.[25] Other bulky nitrogen-based ligands such as bulky silyl amides,[26] and *N*-heterocyclic imines (NHIs)[27] have been employed in low-valent main group chemistry. As illustrated in Figure 1.6, *N*-heterocyclic imines donate up to 6 electrons (2σ, 4π).

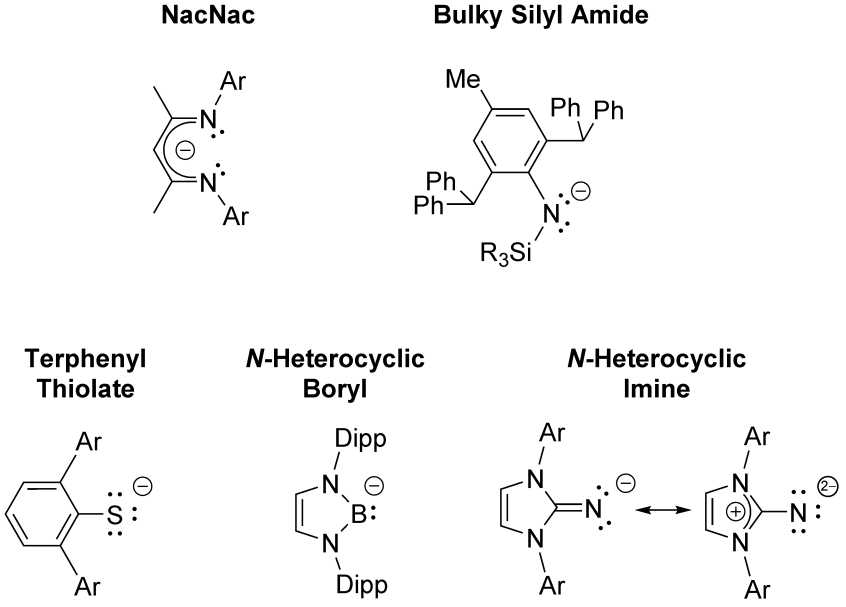

Figure 1.6. General structures of commonly employed monoanionic heteroatom ligands (Ar = bulky aryl group; R = Me/Ph).

Using bulky *meta*-terphenyl ligands as a building block, these aryl substituents can be further functionalized to their corresponding thiols which, upon deprotonation, afford bulky sulfur-based thiolate ligands (Figure 1.6) with multiple lone pairs available for added π-donation.[28] By using an *N*-heterocycle framework, Yamashita, Nozaki and coworkers

isolated the remarkable *N*-heterocyclic boryl anion $[(HCNDipp)_2B]^-$ (Figure 1.6).[29] This species has also been used as a ligand in main group chemistry[30] and offers different stabilizing effects than the ligands discussed thus far. The highly electropositive boron center renders the boryl anion a very strong σ-donor, while the presence of a vacant boron-based *p*-orbital makes the ligand an effective π-acceptor. Anionic heteroatom ligands are a ligand class which offer thermodynamic stabilization (often in addition to kinetic stabilization). The use of these heteroatom donors has allowed for the isolation of a diverse array of unprecedented main group compounds.

1.3.2. Examples of Low-Valent Main Group Compounds Stabilized by Anionic Heteroatom Ligands

Using thermodynamically stabilizing ligands, the first examples of two-coordinate acyclic silylenes were published simultaneously. As described above, using the bulky mesityl ligand, silylene (Mes_2Si:) is unstable and rapidly dimerizes to a disilene (Scheme 1.1). In 2012, the Power group used bulky thiolate ligands to form a stable two-coordinate acyclic silylene **13**,[31] while Aldridge and coworkers utilized both a boryl ligand and an amide ligand to stabilize silylene **14** (Scheme 1.7).[32] Though attempts by several groups to form an aluminum(I) dimer RAl=AlR using bulky aryl ligands have failed,[21] Roesky and coworkers employed a bulky β-dikeminate to isolate the Al^I monomer **15** in 2000.[33]

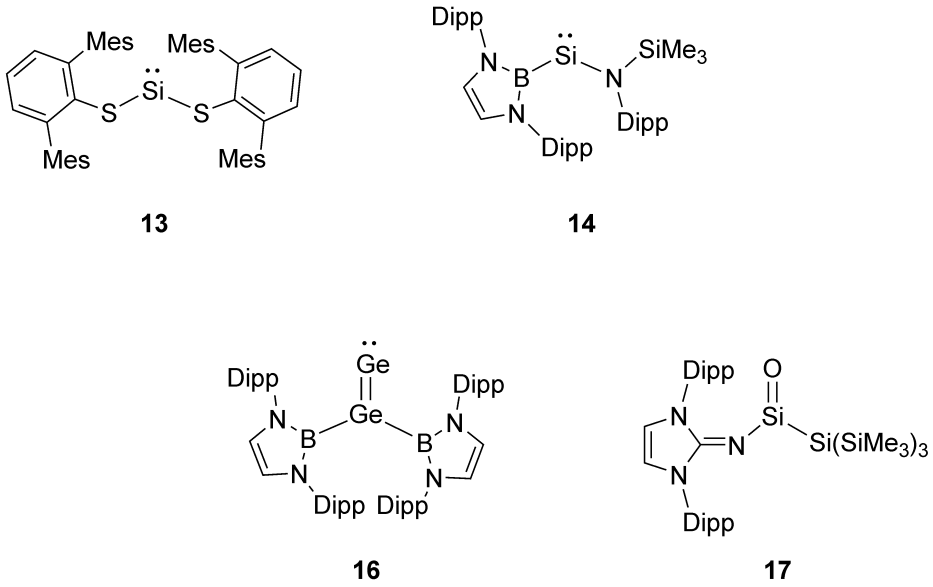

Figure 1.7. Selected examples of previously unprecedented main group bonding environments using heteroatom-based donor ligands.

Aldridge and coworkers have also taken advantage of the *N*-heterocyclic boryl anion for germanium chemistry. Specifically, the mixed oxidation state $R_2Ge^{II}=Ge^0$ vinylidene complex **16** was prepared (R = boryl ligand).[34] Interestingly, this compound represents an alternate isomeric form of the previously discussed *trans*-bent digermyne, ArGeGeAr (**4**). Recently, the groups of Inoue and Rieger utilized a bulky silyl substituent in combination with an *N*-heterocyclic imine to form an acyclic silanone-type compound **17**.[35] Remarkably, the highly polarized $^{\delta+}Si=O^{\delta-}$ π-bond was found to be stable with respect to oligomerization using this stabilization strategy.

These selected examples demonstrate the power of anionic heteroatom stabilization, often allowing for the isolation of compounds which would be unstable with kinetic stabilization alone. Along these lines, thermodynamically stabilizing *neutral* donor ligands have also been explored in the stabilization of low-oxidation state main group elements.

1.3.3. Neutral Donor Ligands in the Main Group

Carbenes are molecules containing a divalent carbon atom (with six valence electrons) and have become common ligands in main group and transition metal chemistry (Figure 1.8). The two unshared electrons of a carbene may either be paired and reside in an sp^2 orbital (singlet state) or unpaired (triplet state). The strong σ-donor character of the carbon-based lone pair makes carbenes highly desirable, but in order to be of widespread synthetic utility, stable carbenes had to be designed so that their singlet state is more stable than the very reactive triplet state. As shown in Figure 1.8, adjacent π-donor substituents stabilize the singlet state by partially occupying the empty carbene *p*-orbital. In 1988, Bertrand and coworkers utilized this strategy using an adjacent phosphorus donor to form the first isolable carbene $\{(Me_3Si)_2N\}_2PC(SiMe_3)$ (**18**), however this compound was found to be a weak donor.[36] A few years later, Arduengo and coworkers reported the very stable cyclic imidazol-2-ylidene carbene, $[(HCNAd)_2C:]$ (**19**) with two adjacent π-donor amino groups capped with very bulky adamantyl (-Ad) substituents.[37] These strong σ-donor imidazole-2-ylidene carbenes are also referred to as *N*-heterocyclic carbenes (NHCs) and are the most widely used carbene class in transition metal and main group chemistry.[38]

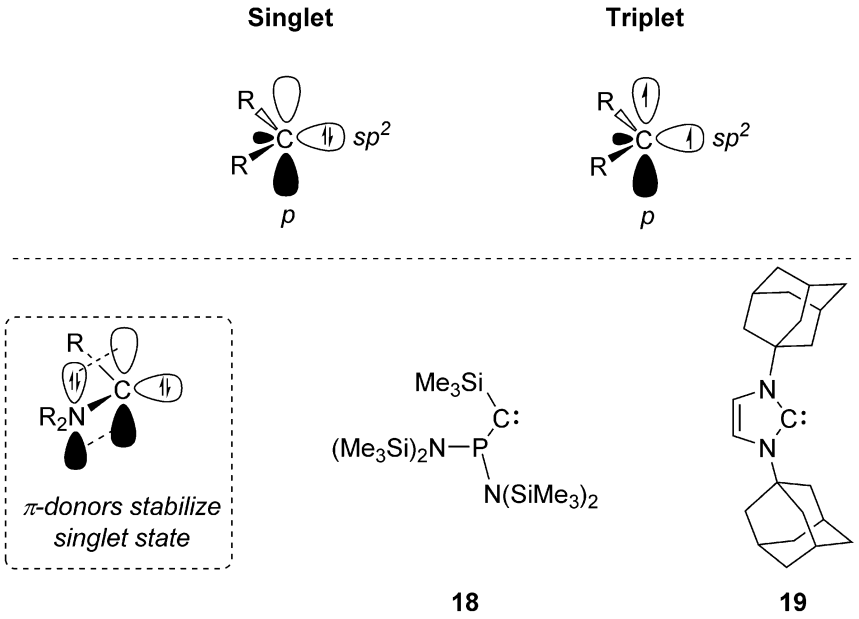

Figure 1.8. Depiction of general singlet and triple state carbenes (top); depiction of influence of adjacent π-donor stabilizing singlet state carbene (bottom left) and the first isolable carbenes **18** and **19**.

In addition to the commonly used *N*-heterocyclic carbene class, Bertrand and coworkers pioneered the development of cyclic(alkyl)amino carbenes (CAACs) which were first reported in 2005 (Figure 1.9).[39] CAACs may be viewed as NHCs where one of the amino substituents has been replaced by a quaternary carbon atom. Removing one of the electronegative nitrogen atoms renders the carbene more electron rich (superior σ-donor) while also enhancing its π-accepting properties relative to NHCs. These ligand alterations often render the chemistry of NHCs and CAACs to be strikingly different. Additionally, NHCs have been used as building blocks in the synthesis of structurally related ligands such as NHIs (*vide supra*) and *N*-heterocyclic olefins (NHOs; Figure 1.10).

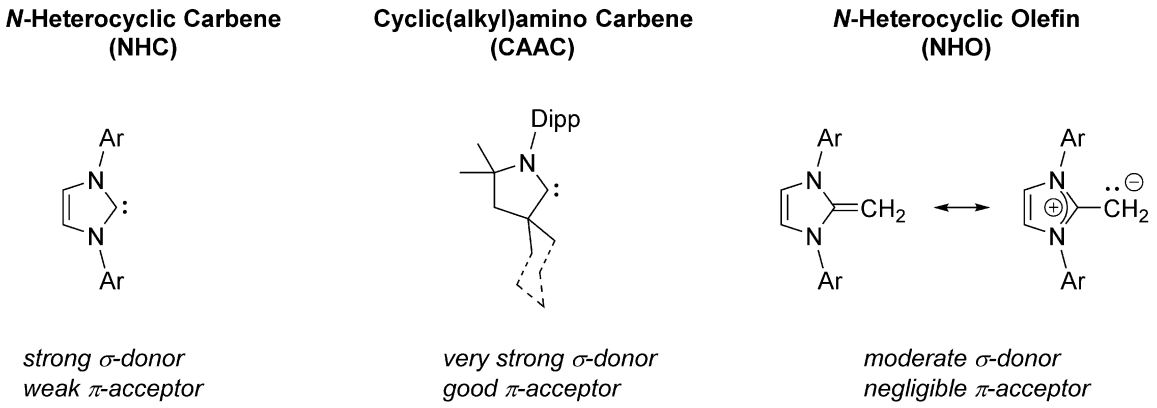

Figure 1.9. The general structures of selected neutral donor ligands with their relative σ-donor and π-acceptor properties listed.

N-heterocyclic olefins represent a compound class that formally contains an alkylidene unit terminally appended to an *N*-heterocyclic carbene framework. This molecular arrangement leads to substantial polarization of the exocyclic C=C array and a concomitant increase in nucleophilic character at the ylidic carbon atom (as shown by the canonical forms in Figure 1.9). In 1993 the Kuhn group isolated the first NHOs along with their 1:1 adducts with simple Lewis acids such as BH_3 and $Cr(CO)_5$.[40] Later these ligands were applied to main group chemistry, often providing divergent reactivity when compared to NHCs (and CAACs). When compared to carbenes, NHOs are generally more moderate σ-donor ligands with no energetically accessible π* orbitals for element-carbon backbonding.[41]

1.3.4. Low-Valent Main Group Fragments Supported by Neutral Donor Ligands

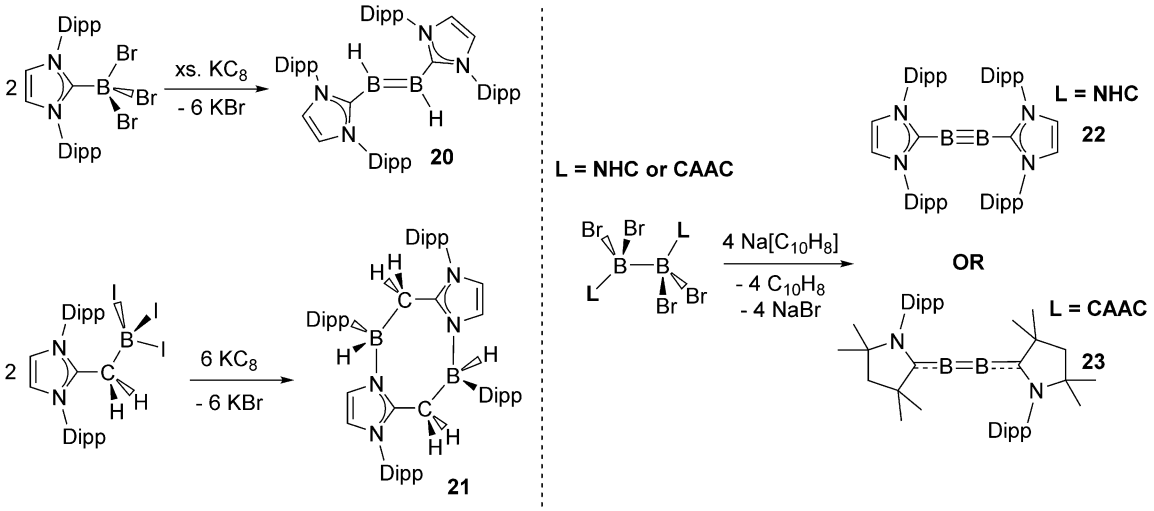

Scheme 1.2. The reduction of CAAC, NHC and NHO-supported boron halides and their divergent products.

An example of the divergent reactivity of reduced main group fragments supported CAACs, NHCs or NHOs can be seen from low-oxidation state boron compounds (Scheme 1.2). For example, Robinson and coworkers showed that when the NHC boron trihalide adduct IPr•BBr_3 (IPr = [(HCNDipp)$_2$C:]; Dipp = 2,6-*i*Pr$_2$C$_6$H$_3$) is reduced with KC_8, a base-stabilized diborene IPr•HB=BH•IPr (**20**) was formed, with the hydrogen atoms likely deriving from the solvent (Scheme 1.2).[42] When the analogous reaction was performed with the structurally related NHO, IPr=CH_2, boron insertion into a ligand C–N bond occurred along with hydrogen atom abstraction forming **21** (Scheme 1.2).[43] The poorer σ-donor strength and lack of π-accepting ability of the NHO (compared to an NHC) are likely insufficient to stabilize the HB=BH fragment. When the IPr•Br_2B–BBr_2•IPr adduct was reduced by Braunschweig and coworkers, the remarkable boron(0) adduct IPr•BB•IPr (**22**) was formed, being the first example of a B–B triple bond with a short bond length of 1.449(3) Å (Scheme 1.2).[44] When the analogous reduction was performed using a CAAC

instead of an NHC, a boron(0) adduct was again formed, but a longer B–B distance of 1.489(2) Å was observed (along with shorter C–B bonds) illustrating the enhanced π-acceptor capabilities of CAACs.[45]

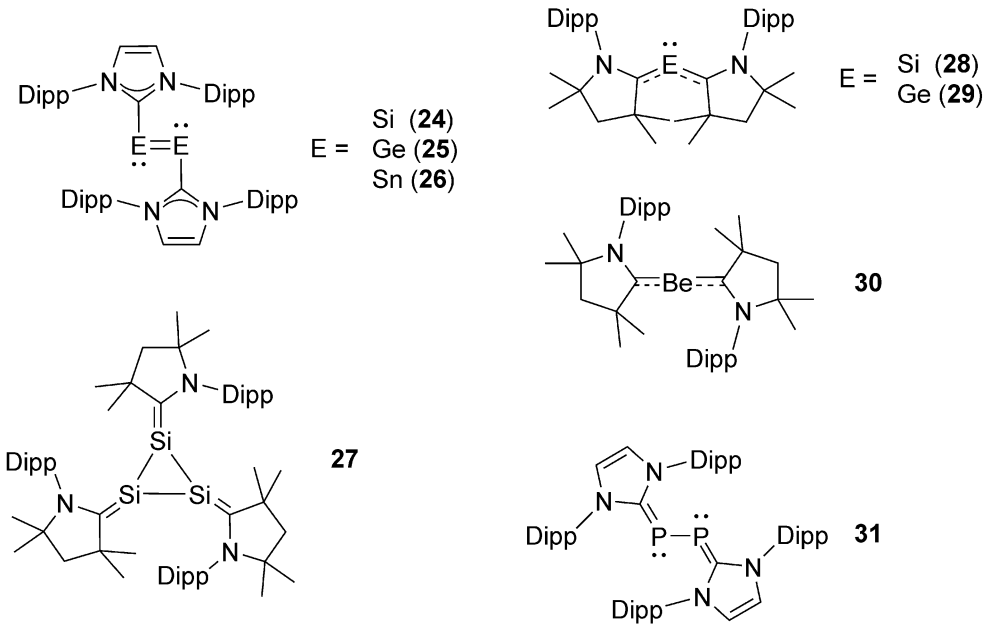

Figure 1.10. Selected NHC and CAAC adducts of main group elements in their zeroth oxidation state.

In addition to boron(0) adducts, several other zero-valent main group species have been isolated using carbene donors (Figure 1.10). For example, the Robinson group first prepared the remarkable NHC-stabilized Si_2^0 fragment[46] (**24**) in 2008 which was soon followed by the heavy Ge and Sn analogues as reported by Jones and coworkers (Figure 1.10).[47] The CAAC-supported Si_3^0 species **27** was synthesized by Roesky and coworkers in 2016 which, as in common for CAAC adducts, exhibits π-bonding between carbon and silicon.[48] In addition, CAAC-stabilized monomeric Si^0 (**28**) and Ge^0 (**29**) adducts have been reported.[49] An NHC adduct of P_2^0 was prepared using IPr as a donor (**31**),[50] and it was recently shown that even a formal beryllium(0) complex can be stabilized using two CAAC equivalents as ligands (**30**).[51]

1.4. Strong Bond Activation by Earth-Abundant Elements

As discussed in the previous sections, a wide array of main group element complexes in low oxidation states have been reported. One principle aim of molecular main group chemistry is to explore whether main group (s- or p-block) elements can replace expensive (and often more toxic) transition metals in catalysis. Many transition metal catalyzed transformations rely on M^n/M^{n+2} redox couples where a substrate oxidatively adds to a metal center, undergoes functionalization and the product is subsequently released via reductive elimination. Using some of the previously described low-oxidation state main group compounds, the oxidative addition of strong organic bonds (such as C–H, C–F and H–H) to main group centers has been found to be possible and, in some cases, the reverse (reductive elimination) may also occur.

1.4.1. Oxidative Addition to Main Group Centers

In 2005, Power and coworkers showed that digermyne ArGeGeAr (**4**) could activate H_2, giving the first indication that main group elements may indeed mimic the reactivity of transition metals (Scheme 1.3).[52] This reaction afforded a mixture of both the Ge^{III} digermane $ArH_2Ge–GeH_2Ar$ (**32**) and the Ge^{IV} germane $ArGeH_3$ (**33**) (Ar = 2,6-$Dipp_2C_6H_3$). Since this early discovery, the oxidative addition of H_2 has been extended to a variety of reduced main group centers.[53] For example, at elevated temperatures and pressures, Nikonov and coworkers reported the clean oxidative addition of H_2 to an Al^I center in (NacNac)Al: (**15**) giving a single Al^{III} product, $(NacNac)AlH_2$ (**34**).[54] Similarly, the CAAC diboron(0) adduct **23** cleanly underwent the oxidative addition of a single equivalent of H_2 to form the diborane **35** (Scheme 1.3).[55] Interestingly, a recent example

from the Inoue group showed that an *N*-heterocyclic imine supported *trans*-bent disilene **36** adds H_2 exclusively via an *anti*-addition.[56]

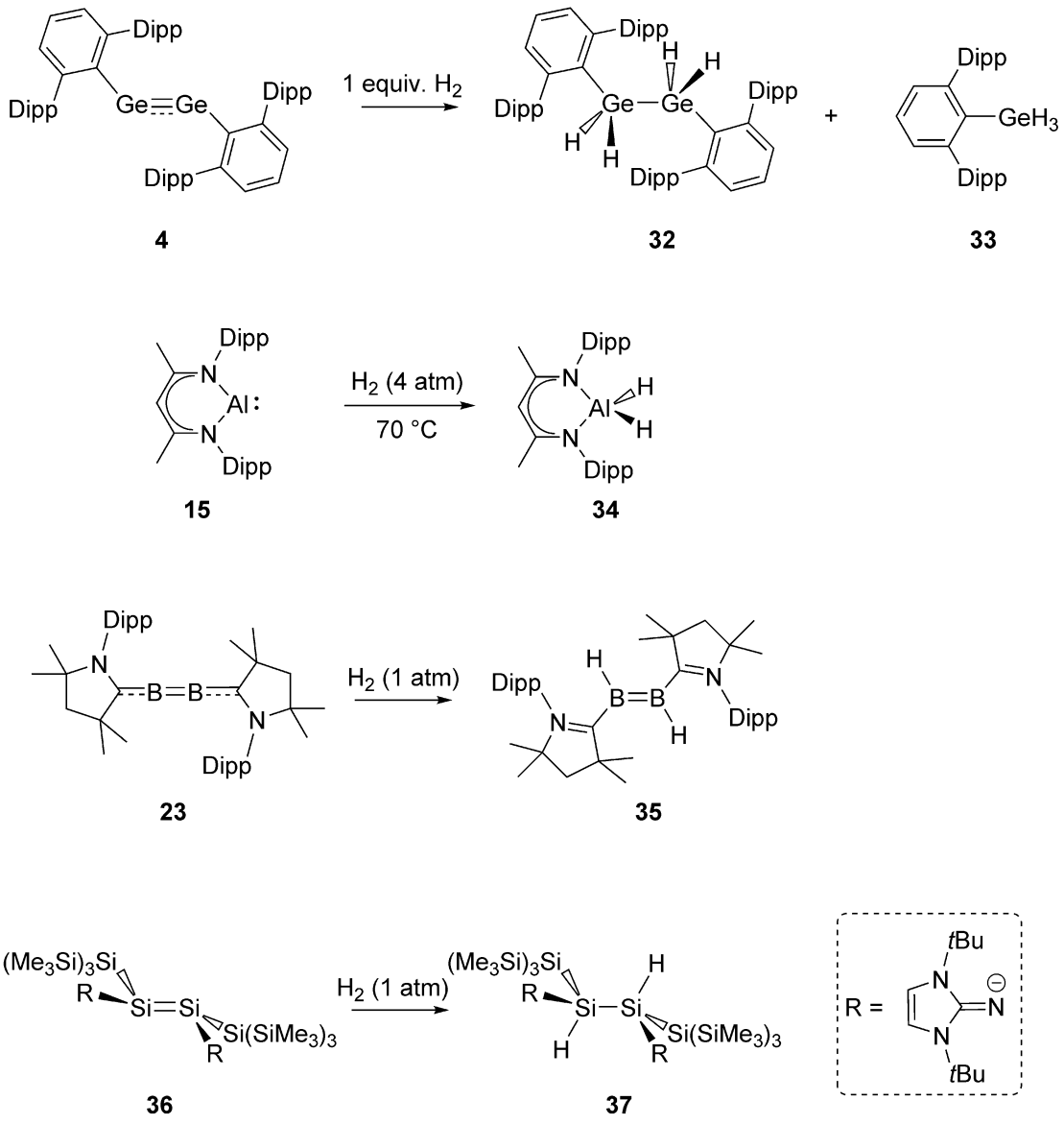

Scheme 1.3. Selected examples of H_2 oxidative addition by main group elements.

In addition to the oxidative addition of H_2, reduced main group element centers have been shown to cleave other strong σ-bonds such as C–H bonds. For example, Aldridge and coworkers demonstrated that by heating silylene **14**, an intramolecular C–H activation

occurred, forming the silicon(IV) product **38** (Scheme 1.4).[32] This example of an intramolecular C–H bond cleavage was in fact preceded by a report in 2007 where Driess and coworkers demonstrated the activation of a C–H bond of phenylacetylene using the cyclic silylene **39**.[57] Heavier Group 14 elements have also been shown to facilitate the oxidative addition of hydrocarbons. In 2011, the Power group showed that digermyne (**4**) and distannyne (**5**) reacted with cyclopentadiene to give Cp-supported tetrelenes Ar(Cp)E: (Cp = C_5H_5) **41** and **42** through a dehydroaromatization reaction.[58] Another remarkable example of main group element-promoted C–H activation was recently demonstrated by Aldridge and coworkers. Using a bis-amide ligand with a xanthene backbone, they reported the aluminum(I) anion dimer **43**.[59] Among the reactivity reported, **43** was shown to undergo the oxidative addition of a C–H bond of benzene upon mild (50 °C) heating.

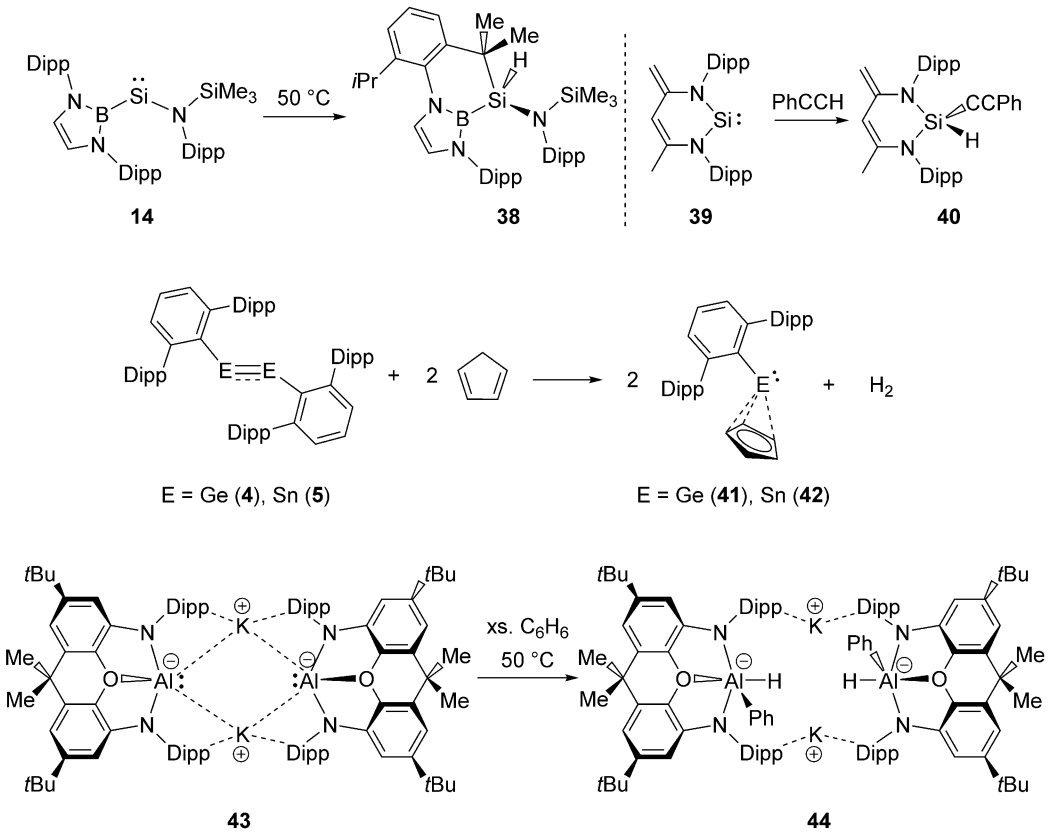

Scheme 1.4. Selected examples of C–H oxidative addition by main group elements.

While many other examples of activations of strong non-polar organic bonds are known,[53] the cleavage of very strong C–F bonds (bond dissociation energy = 536 kJ/mol) by main group elements is still rare. Most known examples of main group promoted C–F bond cleavage are limited to highly electropositive main group centers which form strong bonds with fluorine (such as magnesium, aluminum and silicon). Tacke and coworkers showed that, when combined with hexafluorobenzene, the three-coordinate silylene **45** underwent oxidative addition of an sp^2 C–F bond at room temperature, affording the fluorosilane **46** (Scheme 1.5).[60] Like with the activation of H_2 and C–H bonds, aluminum(I) is known to cleave both sp^2 and sp^3 C–F bonds. In 2015, both the groups of Crimmin[61] and Nikonov[62] independently reported that (NacNac)Al: (**15**) is capable of cleaving C–F bonds. Both the Crimmin and Nikonov groups reported that the aluminum lone pair inserts into a C–F bond of hexafluorobenzene, giving the Al^{III} product (NacNac)Al(F)C_6F_5 (**47**). In addition, Crimmin reported that fluoroalkenes can undergo a similar transformation (*cf.* **48**), while Nikonov extended the scope to a wide array of fluoroarenes. A few years later, Crimmin expanded this reactivity to include alkenes containing $–CF_3$ groups.[63] Crimmin has also shown that Jones' NacNac-stabilized magnesium(I) dimer (**50**, Scheme 1.5) activates fluoroarenes to give Grignard-type products (NacNac)Mg–Ar^F (*cf.* **52**) (Ar^F = fluoroarene) with the concomitant precipitation of [(NacNac)MgF]$_2$ (**51**).[64] It should be noted that Mg^I dimers (such as **52**) are important reducing agents in main group chemistry.[65]

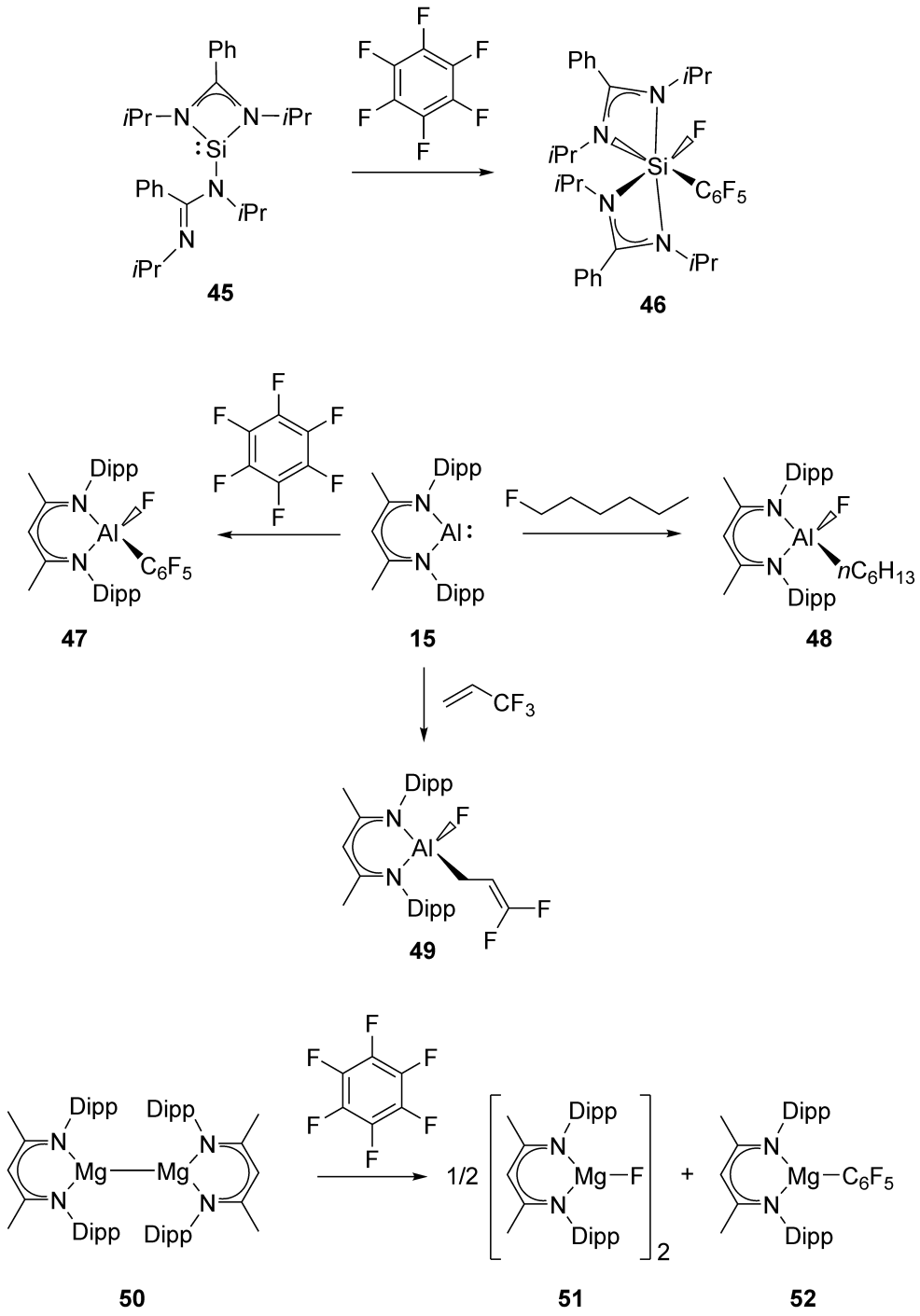

Scheme 1.5. Selected examples of C–F oxidative addition by main group elements.

In addition to the transition metal-like cleavage of strong σ-bonds, transformations which are known to be difficult for transition metals have also been investigated. For example, a recent report from Braunschweig and coworkers showed that an *in situ*

generated Lewis base stabilized borylene [:B(L)R] (L = CAAC, R = aryl substituent) was able to bind dinitrogen through synergic bonding.[66] Transition metals can bind dinitrogen in an end-on fashion where an empty *d*-orbital on the metal is capable of accepting N_2 electrons in a σ-symmetry orbital and a filled metal-based *d*-orbital can donate to an N_2 π* orbital (Scheme 1.6; top).[67] The Braunschweig group was able to mimic this cooperative binding using a CAAC-stabilized boron(I) compound (borylene) **54** which was generated *in situ* by the potassium graphite reduction of the borane precursor **53** (Scheme 1.6). In a similar manner to a transition metal, the borylene is able to accept N_2-based σ-electrons via an empty sp^2-orbital on boron, whereas the boron-based *p*-orbital lone pair is capable of donating to the N_2 π*. By reducing **53** in a dinitrogen atmosphere, the authors observed the bis-borylene N_2 complex **55**, which exhibits π delocalization across the flanking CAAC ligands.

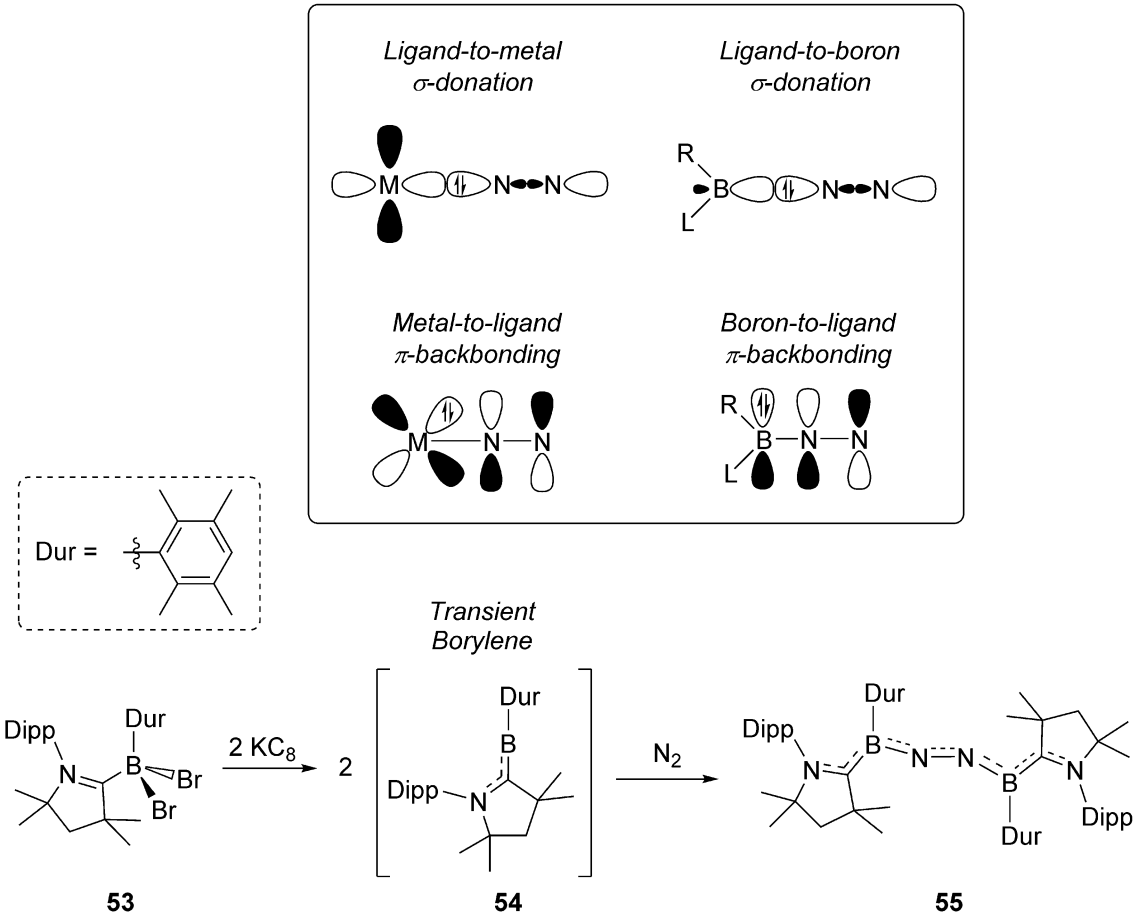

Scheme 1.6. Comparison of transition metal and base-stabilized borylene synergistic binding of N_2 (top) and bis-borylene N_2 adduct **55** from *in situ* generated borylene **54** (bottom); L = neutral donor ligand, R = anionic ligand.

1.4.2. Reductive Elimination from Main Group Centers

The abovementioned reactions are only a few examples main group-promoted activations of strong bonds and demonstrate that reduced main group elements are more than capable of performing such oxidative additions. In order to be relevant to catalytic processes, however, the microscopic reverse (reductive elimination) must also be possible. The availability of E^n/E^{n+2} main group redox couples are relatively limited, owing in part to the relative instability of the reduced state, often requiring strong reducing agents and the assistance of specialized ligands to access. Despite this drawback, examples of reductive

eliminations from main group element centers are known, including reversible oxidative addition/reductive elimination transformations (Scheme 1.7).

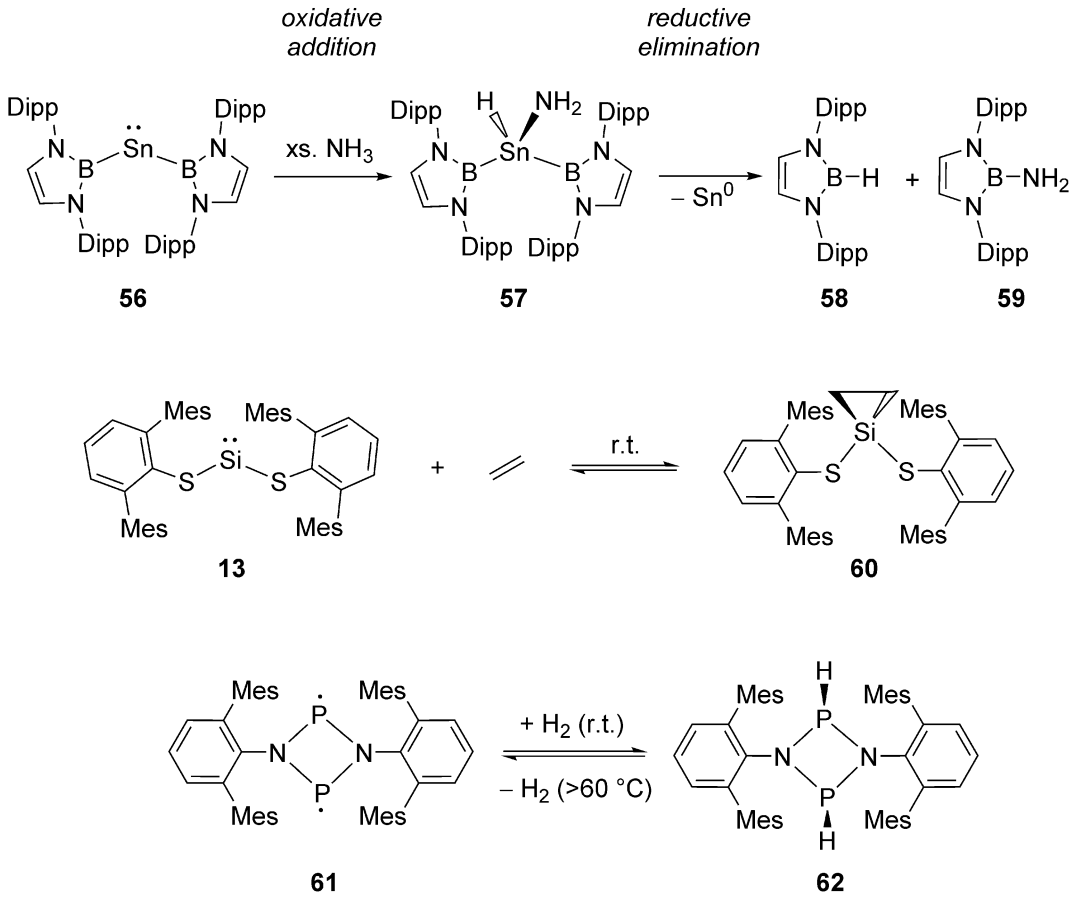

Scheme 1.7. Selected examples of main group centers which can undergo both oxidative addition and reductive elimination processes.

Aldridge and coworkers reported that the bis(borylated) stannylene **56** (Figure 1.7) was able to oxidatively add a wide array of σ-bonds including H–H, N–H, Si–H and B–H bonds.[68] In the case of ammonia, it was found that the N–H oxidative addition product **57** decomposed to the borane **58** and aminoborane **59**. The concomitant formation of metallic tin was also observed, thus representing two reductive eliminations from a Sn^{IV} center. While this process is irreversible, the reaction demonstrates that Group 14 redox couples are possible. Along these lines, the Power group has investigated the interaction

dithiolatosilylene **13** with ethylene.[69] Importantly, it was shown that the oxidative addition of ethylene to **13** was reversible at room temperature, representing a Si^{II}/Si^{IV} redox couple. Another remarkable example of reversible small molecule activation was reported by Schulz and coworkers. Using the terphenyl-protected $ArP(\mu\text{-}N)_2PAr$ singlet biradicaloid **61**, the authors observed that when H_2 was added to the system, one hydrogen atom was added to each phosphorus, forming **62**.[70] The *cis* isomer of **62** was exclusively observed, implying a concerted mechanism of H_2 addition. This single electron oxidation at phosphorus was shown to be reversible, with hydrogen extrusion demonstrated at temperatures exceeding 60 °C.

1.5. Earth-Abundant Element Catalysis

In addition to the wide array of main group molecules which promote the activation (and reductive elimination) of organic substrates, there are now several main group-based catalytic systems which sometimes rival those of the more costly d-block element complexes. Catalytic transformations promoted by abundant elements include (but are not limited to) hydrogenation, hydrodefluorination, and carbonyl reduction reactions. In this section, selected examples of prominent catalytic systems and their mechanisms will be discussed.

1.5.1. Frustrated Lewis Pairs

The first example of a metal-free system found to reversibly bind dihydrogen was reported by Stephan and coworkers in 2006.[71] When bis(mesityl)phosphine Mes_2PH was combined with the strong Lewis acid tris(pentafluorophenyl)borane $B(C_6F_5)_3$, the zwitterionic phosphonium borate **63** was formed rather than a simple Lewis acid/base adduct, owing to the high degree of steric bulk of both the phosphine and the borane (Scheme 1.8). Reacting

63 with $Me_2Si(H)Cl$ gave the phosphonium borate **64** which contains polarized $P–H^{\delta+}$ and $B–H^{\delta-}$ bonds. This polarization allowed for dehydrogenation upon heating to 100 °C and formation of the arene-linked phophine-borane **65** which contains both a Lewis basic phosphine and a Lewis acidic borane which do not coordinate to each other. This allowed for the room temperature and pressure splitting of H_2 to reform **64**. This class of compounds containing non-associated Lewis basic and Lewis acidic functionalities was later termed "frustrated Lewis pairs" (FLPs) by the Stephan group.[72]

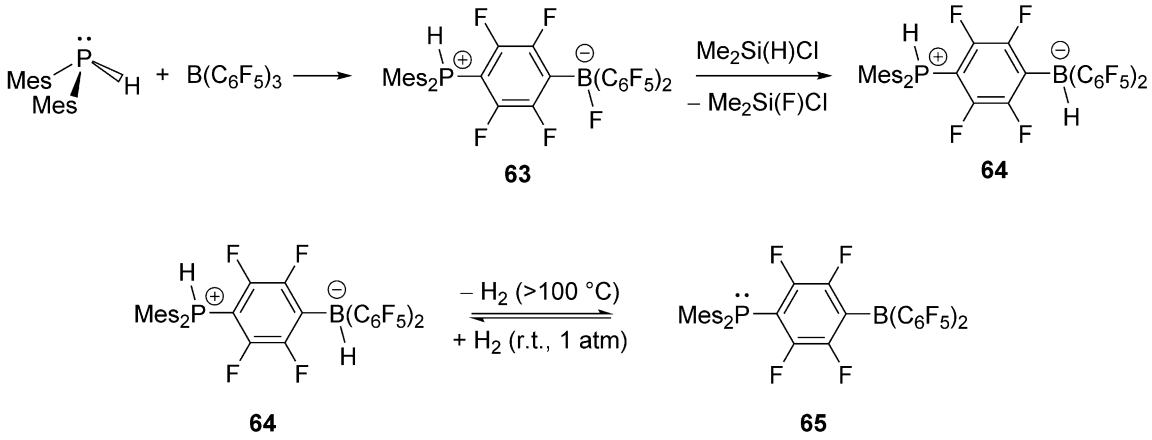

Scheme 1.8. Formation of the phosphonium borate **64** and its reversible hydrogen release generating the frustrated Lewis pair (FLP) **65**.

Shortly after their initial report, frustrated Lewis pairs were shown to catalytically hydrogenate imines.[73] By combining a substoichiometric quantity of **65** with imines in the presence of H_2, formal H_2 addition across the imine C=N bond was observed, affording the corresponding amine (Scheme 1.9). The first step of the mechanism is the FLP-promoted activation of H_2 to form **64**. The acidic phosphorus-bound hydrogen atom in **64** then protonates the imine, generating an iminium borate $[R_2C=N(H)R][H–BR_3]$ salt. The hydridic boron-based hydrogen atom can then attack the iminium carbon atom, followed by release of the amine product and regeneration of the catalyst. Following this work, it

was shown that the imine substrate [in combination with $B(C_6F_5)_3$] was sufficiently basic to activate H_2 and so $B(C_6F_5)_3$ alone could be used as a catalyst.[74] Since the first FLP-catalyzed hydrogenation of imines was reported, this reactivity has been extended to many other substrates containing unsaturated CN, CC and CO bonds.[75]

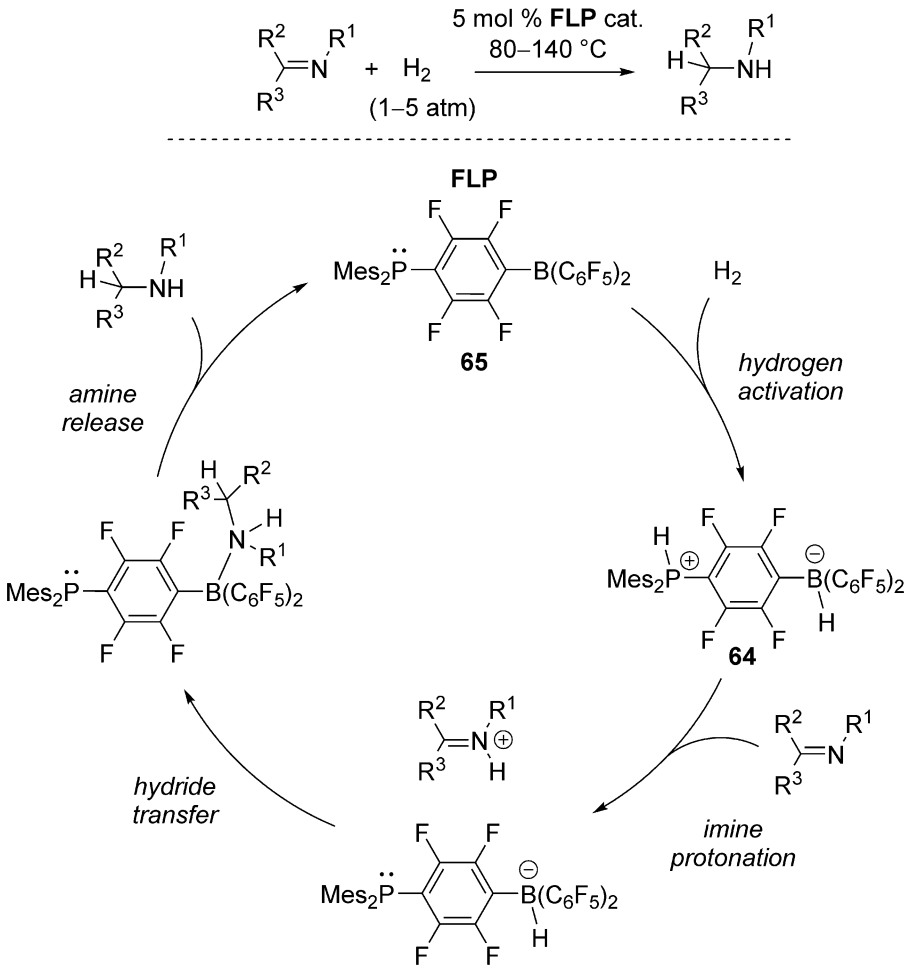

Scheme 1.9. Catalytic hydrogenation of imines using a frustrated Lewis pair catalyst.

1.5.2. Lewis Acid Catalysis

Main group Lewis acids have been used for decades in catalysis such as in Friedel-Crafts C–C bond forming reactions.[76] In fact, the advent of FLPs was preceded by related Lewis acid catalyzed reductions. Specifically, Piers and coworkers demonstrated in 1996 that $B(C_6F_5)_3$ catalyzes the hydrosilylation of aldehydes, ketones and esters.[77] Rather than

Lewis acid activation of the carbonyl moiety as conventional wisdom suggested, mechanistic studies revealed that $B(C_6F_5)_3$ instead activates the silane while the adduct $Ar(R)C{=}O\cdots B(C_6F_5)_3$ was found to inhibit product formation.[78] The coordination of $B(C_6F_5)_3$ to triphenylsilane renders the silicon more susceptible to attack from carbonyl substrates, leading the formation of an ion pair $[Ar(R)CO(SiPh_3)][HB(C_6F_5)_3]$ which is attacked by a hydride of the borate anion and results in product formation (Scheme 1.10).

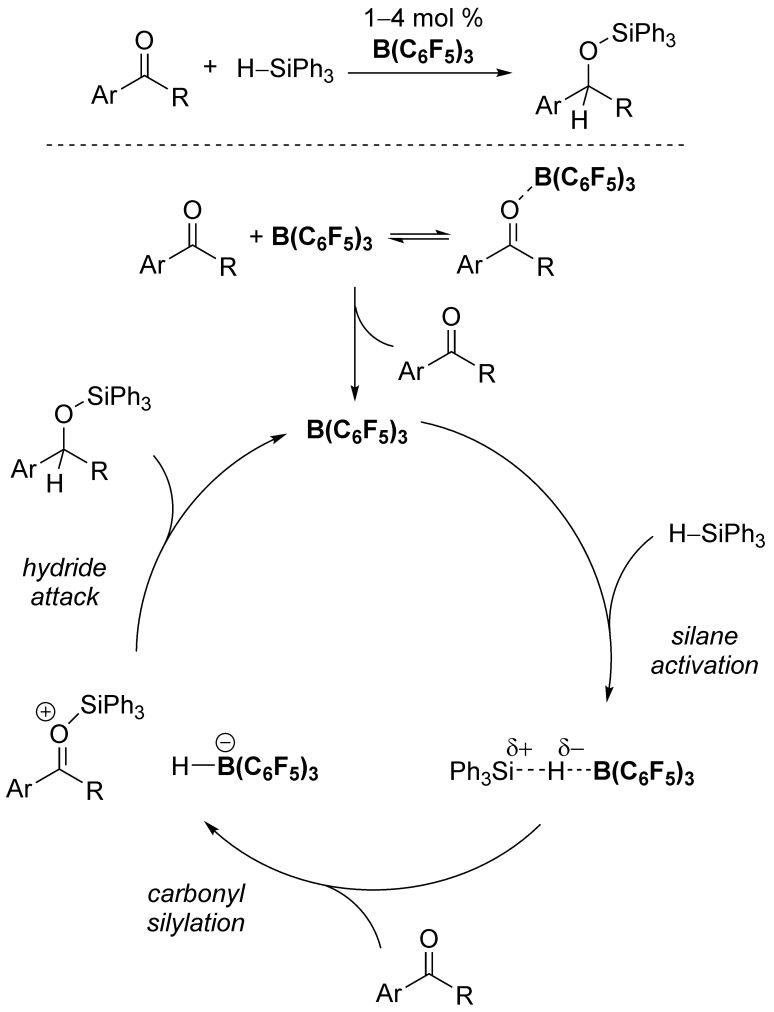

Scheme 1.10. Catalytic hydrosilylation of carbonyls using a $B(C_6F_5)_3$ Lewis acid catalyst.

In 2008, the Ozerov group reported that silylium (R_3Si^+) cations catalyze the hydrodefluorination of C–F bonds in the presence of stoichiometric amounts of

trialkylsilane (Scheme 1.11).[79] Triorganosilylium ions are relatively stable if they are partnered with an appropriate weakly coordinating anion, such as a carborane. In the presence of alkyl fluorides, the silylium cation abstracts a fluoride, generating a carbocation. The carbocation can then abstract a hydride from the trialkylsilane, thus regenerating the silylium catalyst. This process has since been investigated using both aluminum and phosphorus(V) cations as catalysts.[80] Main group catalysts are not limited to the Lewis acid/base catalysts discussed thus far. For example, catalytic reductions of organic substrates have been demonstrated using abundant element hydrides.

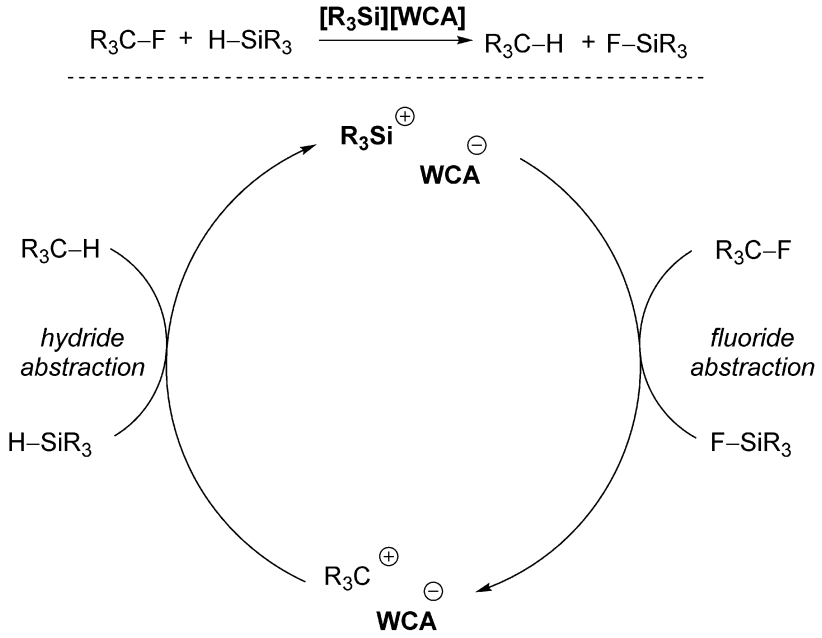

Scheme 1.11. General mechanism for the silylium-catalyzed hydrodefluorination of C–F bonds; WCA = weakly coordinating anion.

1.5.3. Carbonyl Reductions Catalyzed by s-block, p-block and Group 12 Elements

From an industrial standpoint, the reduction of carbonyl compounds is an important route to alcohols on a large scale. Typically, C=O reduction is achieved using either stoichiometric amounts of metal hydrides (such as $NaBH_4$) or transition metal-catalyzed hydrogenations.[81] Recently, there has been interest in mild-condition carbonyl reductions

which avoid the use of flammable H_2 gas. Commonly employed routes typically involve the catalyzed hydroborylation or hydrosilylation of a carbonyl, affording boryl- or silyl-ethers, which can be subsequently hydrolyzed to the corresponding alcohol. Active catalysts usually contain metal hydrides; for example, a modified version of the Shvo ruthenium hydride-based catalyst, [2,3,4,5-Ph_4(η^5-C_4COH)Ru$(CO)_2$H] was shown to catalyze ketone hydroborylation.[82] Recently, it has been found that main group (and Group 12) element hydrides can also reduce carbonyl compounds.[83]

Since the pioneering of Brown, Schlesinger and Burg in 1939 using B_2H_6 in uncatalyzed hydroborylation reactions,[84] chemists have sought to extend this concept to milder silane and borane sources as part of a catalytic cycle. An early example of a metal-free carbonyl reduction catalyst was reported in 1987 and is known as the Corey-Bakashi-Shibata (or CBS) catalyst (**66**, Scheme 1.12). This chiral catalyst was shown to hydroborylate ketones (using THF•BH_3 as the borane source), affording highly enantioenriched alcohols after aqueous workup.[85] More recently, Hill and coworkers demonstrated the hydroborylation of aldehydes and ketones using the NacNac-supported magnesium hydride catalyst **67** (Scheme 1.12) and pinacolborane (HBpin) as a mild hydride source at ambient temperatures.[86] Okuda and coworkers then reported an *N*-heterocyclic carbene adduct of zinc dihydride, [IPr•ZnH(μ-H)]$_2$ which was found to undergo CO_2 insertion into the reactive Zn–H bonds.[87] This C=O bond insertion reaction prompted Rivard and coworkers to explore zinc hydride-catalyzed ketone reductions. Specifically, the hydrido-triflate **68** (Scheme 1.12) was shown to catalyze the hydroborylation and hydrosilylation of benzophenone using pinacolborane and

methyl(phenyl)silane, respectively.[88] The Okuda group subsequently published the zinc hydride cluster **69** and explored its utility as a C=O reduction catalyst.[89]

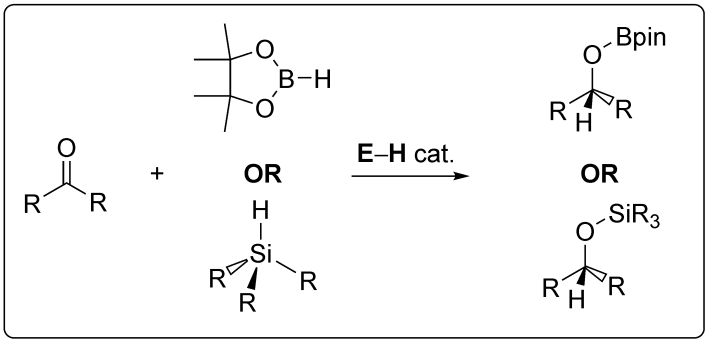

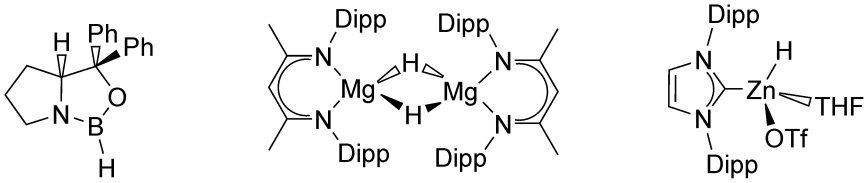

66 **67** **68**

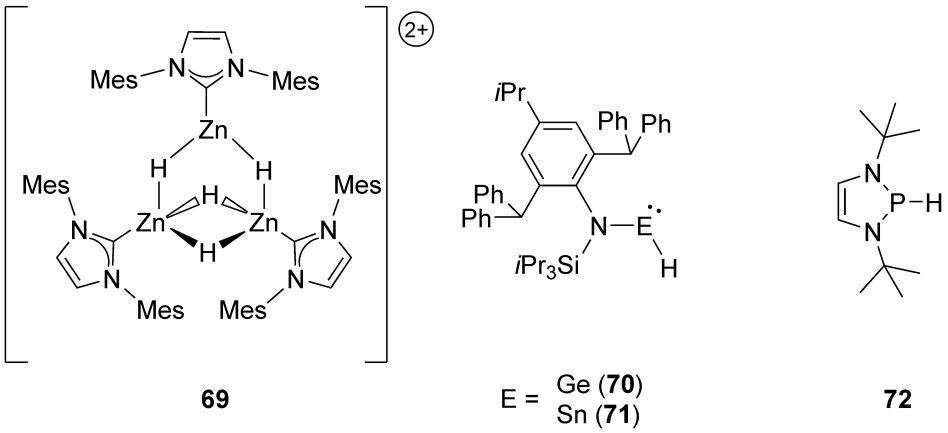

69 E = Ge (**70**) Sn (**71**) **72**

Scheme 1.12. General hydrosilylation/borylation reaction of carbonyls (top) and selected main group (and Group 12) hydride catalysts; OTf = F_3CSO_3.

Jones and coworkers employed a similar strategy using germanium and tin(II) hydrides supported by a bulky silyl amide ligand (compounds **70** and **71**; Scheme 1.12). Using HBpin, the hydroborylation of aldehydes and ketones was demonstrated with very high turnover numbers (> 13 330 h^{-1}) and low catalyst loadings (< 0.05 mol %) in some cases.[90] In 2015, Kinjo and coworkers showed that P^{III} hydrides could also catalyze

carbonyl reductions using the diazaphospholene [(HCN*t*Bu)$_2$PH] (**72**).[91] Using the same diazaphospholene framework, Speed and coworkers later substituted the amine *tert*-butyl groups for chiral alkyl groups and demonstrated the hydroborylation of imines to enantioenriched chiral 2° amines.[92]

Using their germanium and tin hydrides **70** and **71**, Jones and coworkers also investigated the mechanism of hydroborylation.[90] The stoichiometric reaction of these hydrides with diisopropyl ketone gave germanium (and tin) alkoxides, from C=O insertion into M–H bonds. An investigation of the kinetics revealed the rate to be independent of ketone concentration, while a first order rate dependence on the catalyst concentration and the concentration of HBpin was found.[90] These results suggest that the rate limiting step is σ-bond metathesis between the alkoxide intermediate, L$_n$E–OC(H)R$_2$ and HBpin (Scheme 1.13).

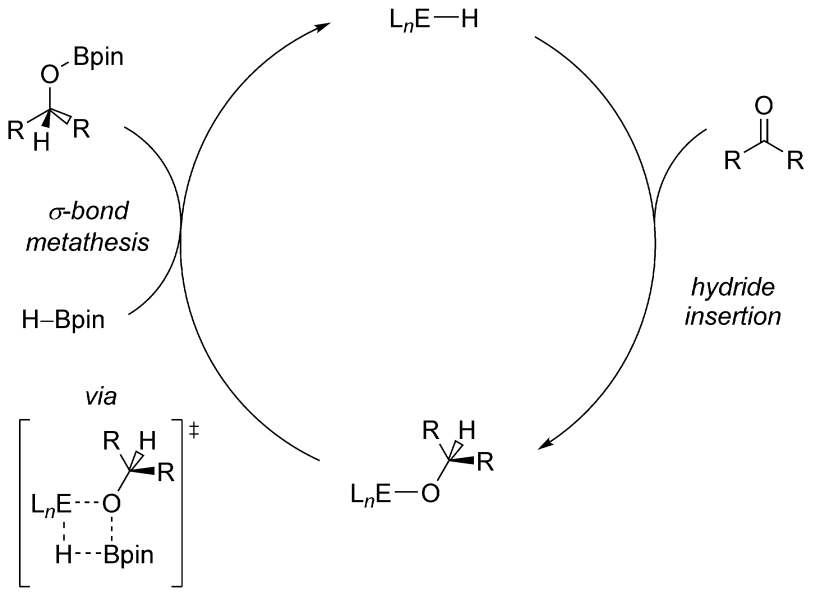

Scheme 1.13. General hydroborylation mechanism of carbonyls using E–H catalysts; L = neutral and/or anionic ligand.

The experimental portion of this thesis will demonstrate some of the abovementioned stabilization strategies in the isolation of new Group 12 and p-block element bonding environments. In several cases, new ligands were designed which allowed for the isolation of otherwise non-isolable main group species. Some of the newly reported molecules will be shown to cleave strong organic and inorganic bonds, while others were found to be catalysts (or precatalysts) in the reduction of carbonyl-containing compounds.

1.6. References

1. (a) Kealy, T. J.; Pauson, P. J. *Nature* **1951**, *168*, 1039; (b) Wilkinson, G.; Rosenblum, M.; Whiting, M. C.; Woodward, R. B. *J. Am. Chem. Soc.* **1952**, *74*, 2125.
2. (a) Vaska, L.; DiLuzio, J. W. *J. Am. Chem. Soc.* **1961**, *83*, 2784; (b) Vaska, L.; DiLuzio, J. W. *J. Am. Chem. Soc.* **1962**, *84*, 679.
3. Osborne, J. A.; Jardine, F. H.; Young, J. F.; Wilkinson, G. *J. Chem. Soc. A.* **1966**, 1711.
4. Cotton, F. A.; Wilkinson, G. *Advanced Inorganic Chemistry*, *Fourth Edition*; Wiley-Interscience, New York, 1980; pp 377.
5. Jutzi, P. *Angew. Chem. Int. Ed. Engl.* **1975**, *14*, 232.
6. West, R.; Fink, M. J. *Science* **1981**, *214*, 1343.
7. Yoshifuji, M.; Shima, I.; Inamoto, N. *J. Am. Chem. Soc.* **1981**, *103*, 4587.
8. Miller, R. D.; Michl, J. *Chem. Rev.* **1989**, *89*, 1359.
9. Drahnak, T. J.; Michl, J.; West, R. *J. Am. Chem. Soc.* **1979**, *101*, 5427.
10. Daly, J. J. *J. Chem. Soc.* **1964**, 6147.
11. (a) Davidson, P. J.; Lappert, M. F. *J. Chem. Soc., Chem. Commun.* **1973**, 317; (b) Goldberg, D. E.; Harris, D. H.; Lappert, M. F.; Thomas, K. M. *J. Chem. Soc., Chem. Commun.* **1976**, 261; (c) Hitchcock, P. B.; Lappert, M. F.; Miles, S. J.; Thorne, A. J. *J. Chem. Soc., Chem. Commun.* **1984**, 480; (d) Goldberg, D. E.; Hitchcock, P. B.; Lappert, M. F.; Thomas, K. M. *J. Chem. Soc., Chem. Commun.* **1986**, 2387.
12. Fink, M. J.; Michalczyk, M. J.; Haller, K. J.; West, R.; Michl, J. *J. Chem. Soc., Chem. Commun.* **1983**, 1010.

13. (a) Drago, R. S. *J. Phys. Chem.* **1958**, *62*, 353; (b) Schwerdtfeger, P.; Heath, G. A.; Dolg, M.; Bennett, M. A. *J. Am. Chem. Soc.* **1992**, *114*, 7518.

14. While the complete X-ray data for :Pb{CH(SiMe$_3$)$_2$}$_2$ has not been published, the structural features listed in Table 1.1 were published in reference 4c of the following manuscript: Stürmann, M.; Weidenbruch, M.; Klinkhammer, K. W.; Lissner, F.; Marsmann, H. *Organometallics* **1998**, *17*, 4425.

15. Sekiguchi, A.; Kinjo, R.; Ichinohe, M. *Science* **2004**, *305*, 1755.

16. Wedler, H. B.; Wendelboe, P.; Power, P. P. *Organometallics* **2018**, *37*, 2929.

17. Hardman, N. J.; Wright, R. J.; Phillips, A. D.; Power, P. P. *Angew. Chem. Int. Ed.* **2002**, *41*, 2842.

18. Wright, R. J.; Phillips, A. D.; Hardman, N. J.; Power, P. P. *J. Am. Chem. Soc.* **2002**, *124*, 8538.

19. Wright, R. J.; Phillips, A. D.; Hino, S.; Power, P. P. *J. Am. Chem. Soc.* **2005**, *127*, 4794.

20. Grigsby, W. J.; Power, P. P. *J. Am. Chem. Soc.* **1996**, *118*, 7981.

21. (a) Wright, R. J.; Phillips, A. D.; Power, P. P. *J. Am. Chem. Soc.* **2003**, *125*, 10784; (b) Agou, T.; Nagata, K.; Tokitoh, N. *Angew. Chem. Int. Ed.* **2013**, *52*, 10818.

22. Cowley, A. H.; Lasch, J. G.; Norman, N. C.; Pakulski, M. *J. Am. Chem. Soc.* **1983**, *105*, 5506.

23. Tokitoh, N.; Arai, Y.; Sasamori, T.; Okazaki, R.; Nagase, S.; Uekusa, H.; Oshashi, Y. *J. Am. Chem. Soc.* **1998**, *120*, 433.

24. Tokitoh, N.; Arai, Y.; Okazaki, R.; Nagase, S. *Science* **1997**, *277*, 78.

25. Mindiola, D. J.; Holland, P. J.; Warren, T. H. in: *Inorganic Syntheses, Volume 35*; John Wiley & Sons, Hoboken, NJ, 2010, pp 4–19.
26. Kays, D. L. *Chem. Soc. Rev.* **2016**, *45*, 1004.
27. Ochiai, T.; Franz, D.; Inoue, S. *Chem. Soc. Rev.* **2016**, *45*, 6327.
28. Niemeyer, M.; Power, P. P. *Inorg. Chem.* **1996**, *35*, 7264.
29. Segawa, Y.; Yamashita, M.; Nozaki, K. *Science* **2006**, *314*, 113.
30. For example, a bis(boryl)diphosphene has been reported: Asami, S.-S.; Okamoto, M.; Suzuki, K.; Yamashita, M. *Angew. Chem. Int. Ed.* **2016**, *55*, 12827.
31. Rekken, B. D.; Brown, T. M.; Fettinger, J. C.; Tuononen, H. M.; Power, P. P. *J. Am. Chem. Soc.* **2012**, *134*, 6504.
32. Protchenko, A. V.; Birjkumar, K. H.; Dange, D.; Schwarz, A. D.; Vidovic, D.; Jones, C.; Kaltsoyannis, N.; Mountford, P.; Aldridge, S. *J. Am. Chem. Soc.* **2012**, *134*, 6500.
33. Cui, C.; Roesky, H. W.; Schmidt, H.-G.; Noltemeyer, M.; Hao, H.; Cimpoesu, F. *Angew. Chem. Int. Ed.* **2000**, *39*, 4274.
34. Rit, A.; Campos, J.; Niu, H.; Aldridge, S. *Nat. Chem.* **2016**, *8*, 1022.
35. Wendel, D.; Reiter, D.; Porzelt, A.; Altmann, P. J.; Inoue, S.; Rieger, B. *J. Am. Chem. Soc.* **2017**, *139*, 17193.
36. Igau, A.; Grützmacher, H.; Baceiredo, A.; Bertrand, G. *J. Am. Chem. Soc.* **1988**, *110*, 6463.
37. Arduengo III, A. J.; Harlow, R. L.; Kline, M. *J. Am. Chem. Soc.* **1991**, *113*, 361.
38. (a) Nesterov, V.; Reiter, D.; Bag, P.; Frisch, P.; Holzner, R.; Porzelt, A; Inoue, S. *Chem. Rev.* **2018**, *118*, 9678. (b) Nolan, S. P. *N-Heterocyclic Carbenes: Effective Tools for Organometallic Synthesis*; Wiley-VCH, Weinheim, 2014.

39. Lavallo, V.; Canac, Y.; Präsang, C.; Donnadieu, B.; Bertrand, G. *Angew. Chem. Int. Ed.* **2005**, *44*, 5705.

40. (a) Kuhn, N.; Bohnen, H.; Kreutzberg, H.; Blässer, D.; Boese, R. *Chem. Commun.* **1993**, 1136; (b) Kuhn, N.; Bohnen, H.; Blässer, D.; Boese, R. *Chem. Ber.* **1994**, *127*, 1405.

41. Roy, M. M. D.; Rivard, E. *Acc. Chem. Res.* **2017**, *50*, 2017.

42. Wang, Y.; Quillian, B.; Wei, P.; Wannere, C. S.; Xie, Y.; King, R. B.; Schaefer III, H. F.; Schleyer, P. v. R.; Robinson, G. H. *J. Am. Chem. Soc.* **2007**, *129*, 12412.

43. Ghadwal, R. S.; Schürmann, C. J.; Engelhardt, F.; Steinmetzger, C. *Eur. J. Inorg. Chem.* **2014**, 4921.

44. Braunschweig, H.; Dewhurst, R. D.; Hammond, K.; Mies, J.; Radacki, K.; Vargas, A. *Science* **2012**, *336*, 1420.

45. Böhnke, J.; Braunschweig, H.; Ewing, W. C.; Hörl, C.; Kramer, T.; Krummenacher, I.; Mies, J.; Vargas, A. *Angew. Chem. Int. Ed.* **2014**, *53*, 9082.

46. Wang, Y.; Xie, Y.; Wei, P.; King, R. B.; Schaefer III, H. F.; Schleyer, P. v. R.; Robinson, G. H. *Science* **2008**, *321*, 1069.

47. (a) Sidiropoulos, A.; Jones, C.; Stasch, A.; Klein, S.; Frenking, G. *Angew. Chem. Int. Ed.* **2009**, *48*, 9701; (b) Jones, C.; Sidiropoulos, A.; Holzmann, N.; Frenking, G.; Stasch, A. *Chem. Commun.* **2012**, 9855.

48. Mondal, K. C.; Roy, S.; Dittrich, B.; Andrada, D. M.; Frenking, G.; Roesky, H. W. *Angew. Chem. Int. Ed.* **2016**, *55*, 3158.

49. (a) Mondal, K. C.; Roesky, H. W.; Schwarzer, M. C.; Frenking, G.; Niepötter, B.; Wolf, H.; Herbst-Irmer, R.; Stalke, D. *Angew. Chem. Int. Ed.* **2013**, *52*, 2963; (b) Li,

Y.; Mondal, K. C.; Roesky, H. W.; Zhu, H.; Stollberg, P.; Herbst-Irmer, R.; Stalke, D.; Andrada, D. M. *J. Am. Chem. Soc.* **2013**, *135*, 12422.

50. Wang, Y.; Xie, Y.; Wei, P.; King, B. R.; Schaefer III, H. F.; Schleyer, P. v. R.; Robinson, G. H. *J. Am. Chem. Soc.* **2008**, *130*, 14970.
51. Arrowsmith, M.; Braunschweig, H.; Celik, M. A.; Dellermann, T.; Dewhurst, R. D.; Ewing, W. C.; Hammond, K.; Kramer, T.; Krummenacher, I.; Mies, J.; Radacki, K.; Schuster, J. K. *Nat. Chem.* **2016**, *8*, 890.
52. Spikes, G. H.; Fettinger, J. C.; Power, P. P. *J. Am. Chem. Soc.* **2005**, *127*, 12232.
53. Chu, T.; Nikonov, G. I. *Chem. Rev.* **2018**, *118*, 3608.
54. Chu, T.; Korobkov, I.; Nikonov, G. I. *J. Am. Chem. Soc.* **2014**, *136*, 9195.
55. Arrowsmith, M.; Böhnke, J.; Braunschweig, H.; Celik, M. A.; Dellerman, T.; Hammond, K. *Chem. Eur. J.* **2016**, *22*, 17169.
56. Wendel, D.; Szilvási, T.; Jandl, C.; Inoue, S.; Rieger, B. *J. Am. Chem. Soc.* **2017**, *139*, 9156.
57. Yao, S.; Wüllen, C. v.; Sun, X.-Y.; Driess, M. *Angew. Chem. Int. Ed.* **2008**, *47*, 3250.
58. Summerscales, O. T.; Fettinger, J. C.; Power, P. P. *J. Am. Chem. Soc.* **2011**, *133*, 11960.
59. Hicks, J.; Vasko, P.; Goicoechea, J. M.; Aldridge, S. *Nature* **2018**, *557*, 92.
60. Junold, K.; Nutz, M.; Baus, J. A.; Burschka, C.; Guerra, C. F.; Bickelhapt, F. M.; Tacke, R. *Chem. Eur. J.* **2014**, *20*, 9319.
61. Crimmin, M. R.; Butler, M. J.; White, A. J. P. *Chem. Commun.* **2015**, *51*, 15994.
62. Chu, T.; Boyko, Y.; Korobkov, I.; Nikonov, G. I. *Organometallics* **2015**, *34*, 5363.
63. Bakewell, C.; White, A. J. P.; Crimmin, M. R. *Angew. Chem. Int. Ed.* **2018**, *57*, 6638.

64. Bakewell, C.; White, A. J. P.; Crimmin, M. R. *J. Am. Chem. Soc.* **2016**, *138*, 12763.

65. Jones, C. *Nat. Rev.* **2017**, *1*, 0059.

66. Légaré, M.-A.; Bélanger-Chabot, G.; Dewhurst, R. D.; Welz, E.; Krummenacher, I.; Engels, B.; Braunschweig, H. *Science* **2018**, *359*, 896.

67. Holland, P. L. *Dalton Trans.* **2010**, *39*, 5415.

68. Protchenko, A. V.; Bates, J. I.; Saleh, L. M. A.; Blake, M. P.; Schwarz, A. D.; Kolychev, E. L.; Thompson, A. L.; Jones, C.; Mountford, P.; Aldridge, S. *J. Am. Chem. Soc.* **2016**, *138*, 4555.

69. Lips, F.; Fettinger, J. C.; Mansikkamäki, A.; Tuonen, H. M.; Power, P. P. *J. Am. Chem. Soc.* **2014**, *136*, 634.

70. Hinz, A.; Schulz, A.; Villinger, A. *Angew. Chem. Int. Ed.* **2016**, *55*, 12214.

71. Welch, G. C.; San Juan, R. R.; Masuda, J. D.; Stephan, D. W. *Science* **2006**, *314*, 1124.

72. McCahill, J. S. J.; Welch, G. C.; Stephan, D. W. *Angew. Chem. Int. Ed.* **2007**, *46*, 4968.

73. Chase, P. A.; Welch, G. C.; Jurca, T.; Stephan, D. W. *Angew. Chem. Int. Ed.* **2007**, *46*, 8050.

74. Chase, P. A.; Jurca, T.; Stephan, D. W. *Chem. Commun.* **2008**, 1701.

75. Lam, J.; Szkop, K. M.; Mosaferi, E.; Stephan, D. W. *Chem. Soc. Rev.* **2019**, 48, 3592.

76. Frank, H. G. *Industrial Aromatic Chemistry*; Springer, Berlin, 1988.

77. Parks, D. J.; Piers, W. E. *J. Am. Chem. Soc.* **1996**, *118*, 9440.

78. Parks, D. J.; Blackwell, J. M.; Piers, W. E. *J. Org. Chem.* **2000**, *65*, 3090.

79. Douvris, C.; Ozerov, O. V. *Science* **2008**, *321*, 1188.

80. (a) Gu, W.; Haneline, M. R.; Douvris, C.; Ozerov, O. V. *J. Am. Chem. Soc.* **2009**, *131*, 11203; (b) Caputo, C. B.; Hounjet, L. J.; Dobrovetsky, R.; Stephan, D. W. *Science* **2013**, *341*, 1374.

81. Mango, J.; Dunetz, J. R. *Org. Process Res. Dev.* **2012**, *16*, 1156.

82. Koren-Selfridge, L.; Londino, H. N.; Vellucci, J. K.; Simmons, B. J.; Casey, C. P.; Clark, T. B. *Organometallics* **2009**, *28*, 2085.

83. Chong, C. C.; Kinjo, R.; *ACS Catal.* **2015**, *5*, 3238.

84. Brown, H. C.; Schlesinger, H. I.; Burg, A. B. *J. Am. Chem. Soc.* **1939**, *61*, 673.

85. (a) Corey, E. J.; Bakshi, R. K.; Shibata, S. *J. Am. Chem. Soc.* **1987**, *109*, 5551; (b) Corey, E. J.; Shibata, S.; Bakshi, R. *J. Org. Chem.* **1988**, *53*, 2861.

86. Arrowsmith, M.; Hadlington, T. J.; Hill, M. S.; Kociok-Köhn, G. *Chem. Commun.* **2012**, *48*, 4567.

87. Rit, A.; Spaniol, T. P.; Maron, L.; Okuda, J. *Angew. Chem. Int. Ed.* **2013**, *52*, 4664.

88. Lummis, P. A.; Momeni, M. R.; Lui, M. W.; McDonald, R.; Ferguson, M. J.; Miskolzie, M.; Brown, A.; Rivard, E. *Angew. Chem. Int. Ed.* **2014**, *53*, 9347.

89. Rit, A.; Zanardi, A.; Spaniol, T. P.; Maron, L.; Okuda, J. *Angew. Chem. Int. Ed.* **2014**, *53*, 13273.

90. Hadlington, T. J.; Hermann, M.; Frenking, G.; Jones, C. *J. Am. Chem. Soc.* **2014**, *136*, 3028.

91. Chong, C. C.; Hirao, H.; Kinjo, R. *Angew. Chem. Int. Ed.* **2015**, *54*, 190.

92. Adams, M. R.; Tien, C.-H.; McDonald, R.; Speed, A. H. W. *Angew. Chem. Int. Ed.* **2017**, *56*, 16660.

Chapter 2: Exploring the Catalytic Reduction of Carbonyls Promoted by Group 12 Elements

2.1. Introduction

The study of inorganic hydrides has increased dramatically recently due to the use of sterically encumbered anionic co-ligands or neutral donors to stabilize the more reactive members of this important molecular class.[1] Of particular interest to this chapter on Group 12 element hydrides, the parent binary MH_2 species (M = Zn, Cd and Hg) are reactive solids that have been known for over sixty years. The thermal stability of these metal hydrides decreases dramatically as one descends the group, with decomposition noted for ZnH_2 upon heating to 90 °C (slow decomposition at room temperature), while CdH_2 and HgH_2 decompose into their constituent elements at −20 °C and −125 °C, respectively.[2]

In 2013 Okuda and co-workers reported the *N*-heterocyclic carbene (NHC)-supported molecular zinc dihydride dimer $[IPr•ZnH(\mu\text{-}H)]_2$ (IPr = [(HCNDipp)$_2$C:]; Dipp = 2,6-*i*Pr$_2$C$_6$H$_3$).[3] This zinc dihydride complex exhibits low thermal stability as it slowly decomposes in the solid state at room temperature, and degradation was noted upon prolonged storage at −35 °C.[4] This result prompted the Rivard group to design the NHC-complex [IPr•ZnH(OTf)•THF] which contains a formal cationic zinc hydride unit $[ZnH]^+$ along with a weakly associated triflate (OTf^- = $O_3SCF_3^-$) counterion.[4,5] Notably [IPr•ZnH(OTf)•THF] is catalytically active with respect to the hydrosilylation and hydroborylation of benzophenone,[4,6] and contrary to Okuda's initial NHC-ZnH_2 adduct, the Rivard group's $[ZnH]^+$ species is monomeric and has considerable thermal stability (up to 260 °C) in the solid state. Despite the abovementioned successes with zinc hydrides,

molecular species containing Cd–H or Hg–H moieties remain extremely rare in the literature (Scheme 2.1),[1d,5] while their use in promoting catalysis has not been documented thus far.

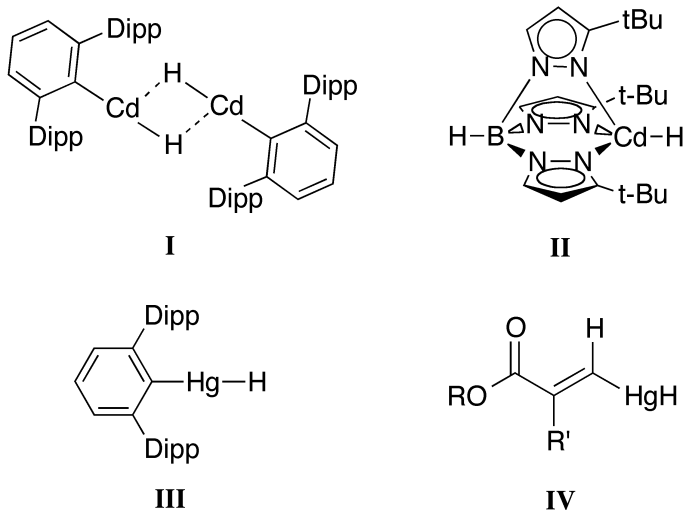

Scheme 2.1. Selected cadmium and mercury hydride complexes (Dipp = 2,6-*i*$Pr_2C_6H_3$; R = $CH_2C(CH_3)_2CH_2OH$, CH_3, *p*-$O_2NC_6H_4$; R′ = C_2H_5, H).

In this chapter, the synthesis of a series of new carbene-supported cadmium and mercury triflate compounds and the attempted preparation of their corresponding hydrides is reported; guiding computational data on the stabilities of the homologous NHC adduct series [IPr•MH_2] (M = Zn, Cd and Hg) is also provided. The central tenet driving this study is the expected enhanced reactivity of Cd and Hg hydrides due to the increased size of the Group 12 element (and increased lability of the M–H fragment) in relation to zinc hydrides, which should promote catalysis. Regarding this concept, it is shown that a Cd-containing species is far superior as a hydrosilylation/borylation precatalyst than its zinc congener, representing a promising new direction in catalysis.

2.2. Results and Discussion

In previous work[7] the Rivard group reported the attempted formation of the heavy Group 12 dihydride complexes [IPr•MH_2] (M = Cd and Hg) from their corresponding halide precursors [IPr•CdI(μ-I)]$_2$[8] and [IPr•HgI_2],[9] using Li[$HBEt_3$] (4 and 2 equivalents, respectively) as a hydride source. This reaction invariably led to the immediate liberation of Cd and Hg metal and the recovery of soluble [IPr•BEt_3] and the dihydroaminal $IPrH_2$ [$IPrH_2$ = $(HCNDipp)_2CH_2$][10] as byproducts. Given the enhanced thermal stability of [IPr•ZnH(OTf)•THF] relative to the parent dimer [IPr•ZnH(μ-H)]$_2$, the synthesis of a series of NHC-bound cadmium and mercury triflates was conducted in order to gain access to the target hydrides [IPr•MH(OTf)]$_x$ (M = Cd, Hg). Due to the apparent instability of [IPr•MH_2] complexes (M = Cd and Hg),[7] the approach taken was to first install triflate groups onto the metal, followed by hydride complex formation via OTf^-/H^- exchange.

The first stable cadmium triflato complex prepared in this study [IPr•Cd(μ-I)(OTf)]$_2$ (**1**) was generated as a colorless solid in 90 % yield by adding 2 equivalents of AgOTf to the CdI_2 adduct [IPr•CdI(μ-I)]$_2$ in CH_2Cl_2, followed by removal of the bright yellow AgI precipitate by filtration (Scheme 2.2). As shown in Figures 2.1 and 2.2, compound **1** crystallizes with two different structural arrangements in the solid state: one species features monodentate (terminal) Cd–OTf coordination mode (**1a**, Figure 2.1), while in the second molecule in the asymmetric unit (**1b**) the OTf^- ligands adopt bridging motifs spanning two Cd centers (Figure 2.2). In each structure, the iodo ligands link two Cd atoms to yield centrosymmetric Cd_2I_2 rhomboid cores.[11] Despite the presence of two structurally distinct molecules in the crystal structure of **1**, the NMR spectra of **1** in $CDCl_3$ reveal the

presence of one carbene and one OTf^- environment; thus it appears that the OTf^- groups in **1** are fluxional/mobile in solution.

When four equivalents of AgOTf were added to $[IPr•CdI(\mu\text{-}I)]_2$ the complete substitution of the iodine atoms for triflate groups transpired to yield the centrosymmetric dimer $[IPr•Cd(\mu\text{-}OTf)_2]_2$ (**2**) in a 93 % yield. X-ray crystallography (Figure 2.3) confirmed the presence of a cage-like structure for **2** derived from four symmetric OTf^- bridges that each link two formally 5-coordinate (square pyramidal) cadmium centers. Presently, there are two related structures in the literature which also exhibit triflate groups bridging two cadmium centers in a similar fashion as in **1b** and **2**.[12]

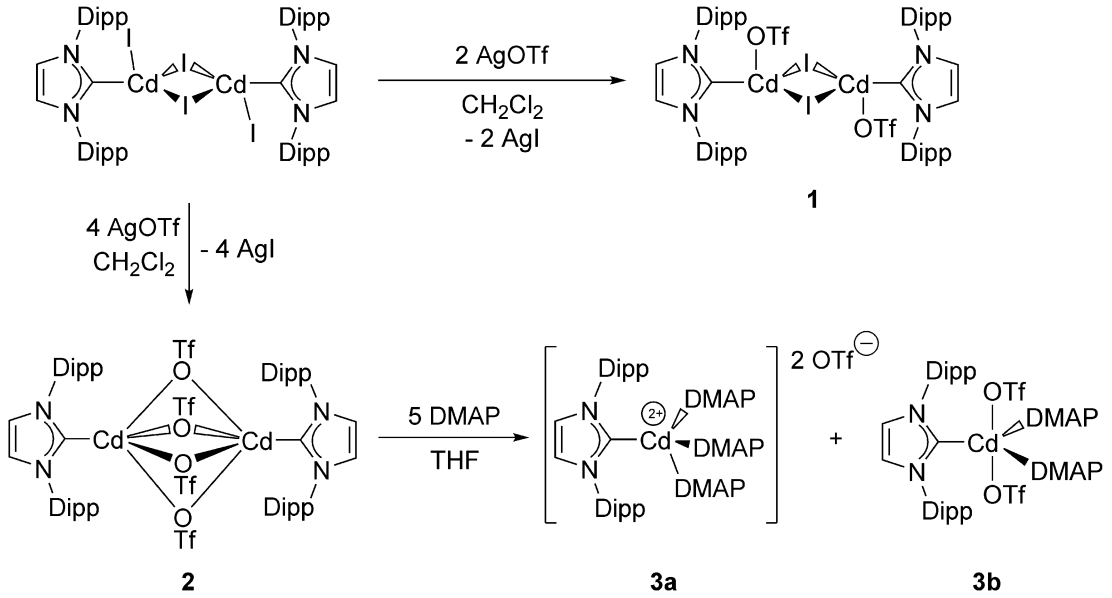

Scheme 2.2. Preparation of the NHC–Cd triflate complexes **1**–**3**.

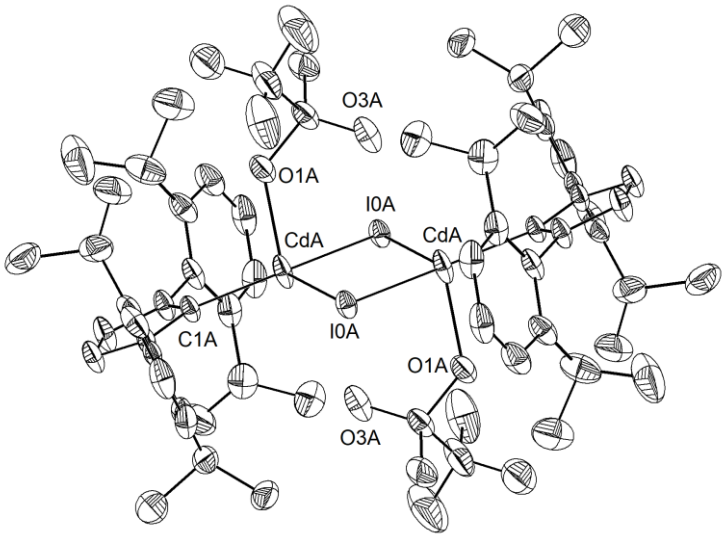

Figure 2.1. Molecular structure of **1a** with thermal ellipsoids plotted at a 30 % probability level. All hydrogen atoms, CH_2Cl_2 and Et_2O solvate molecules have been omitted for clarity. Selected bond lengths [Å] and angles [°]: C1A-CdA 2.191(4), CdA-I0A 2.7923(4), CdA-I0A 2.8204(4), CdA-O1A 2.281(4), CdA-O3A 3.276(5); CdA-I-CdA 74.709(12), I0A-CdA-I0A 105.290(12).

The bridging Cd–O bond lengths in **2** [2.270(2)–2.299(2) Å; Figure 2.3] are notably shorter than in **1b** [2.432(3) and 2.660(3) Å] and are almost the same value within experimental error as in the mixed element cluster $[(\mu\text{-OTf})Cd\{Zn_2(O\textit{i}Pr)_9\}]_2$ where Cd–O distances of 2.234(5) and 2.256(4) Å are found.[12a] Consistent with stronger average Cd–OTf interactions in $[IPr{\bullet}Cd(OTf)_2]_2$ (**2**) versus in the iodo–OTf complex $[IPr{\bullet}Cd(OTf)(\mu\text{-}I)]_2$ (**1**), a downfield shifted ^{19}F NMR resonance at −74.4 ppm (in $CDCl_3$) is found in **2**, corresponding to the presence Cd-coordinated OTf^- groups in solution.[13] The structure of **2** is notably different from the 4-coordinate monomeric zinc bis(triflato)-carbene complex, $[IMes{\bullet}Zn(OTf)_2{\bullet}THF]$[14] (IMes = $[(HCNMes)_2C:]$; Mes = 2,4,6-$Me_3C_6H_2$). When **2** is dissolved in THF and the solvent is removed *in vacuo*, the remaining product is the THF-free adduct $[IPr{\bullet}Cd(\mu\text{-}OTf)_2]_2$ (**2**) suggesting that any coordination of THF to Cd in solution is both reversible and weak in nature.

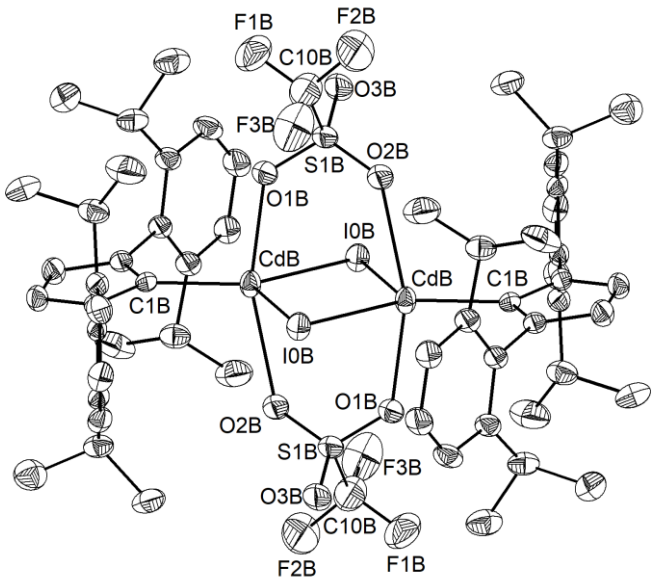

Figure 2.2. Molecular structure of **1b** with thermal ellipsoids plotted at a 30 % probability level. All hydrogen atoms, CH_2Cl_2 and Et_2O solvate molecules have been omitted for clarity. Selected bond lengths [Å] and angles [°]: C1B-CdB 2.193(4), CdB-O1B 2.432(3), CdB-O2B 2.660(3); CdB-I0B-CdB 71.273(12), I0B-CdB-I0B 108.727(12).

In order to probe the nature of **2** in solution, a diffusion-ordered spectroscopy (DOSY) NMR experiment was carried out in [D_8]THF. The diffusion coefficient of **2** was estimated to be $8.0 \times 10^{-10} m^2 s^{-2}$, corresponding to a hydrodynamic radius of 5.9 Å. This is in good agreement with the end-to-end distance of **2** in the solid state (14.3 Å), implying the dimeric nature is retained in solution.

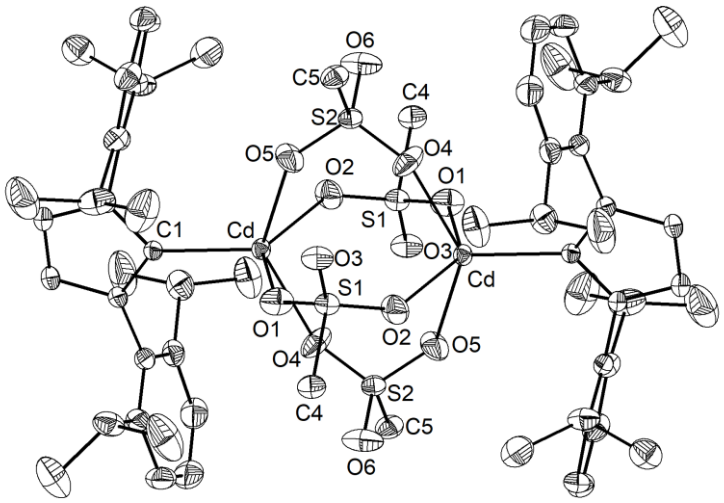

Figure 2.3. Molecular structure of **2** with thermal ellipsoids plotted at a 30 % probability level. All hydrogen atoms, OTf-containing fluorine atoms and CH_2Cl_2 solvate have been omitted for clarity. Selected bond lengths [Å] and angles [°]: C1-Cd 2.189(2), Cd-O range 2.270(2)–2.299(2); C1-Cd-O range 109.79(9)-114.04(9), "cis" O-Cd-O range 79.87(10)–82.93(10), "trans" O-Cd-O range 135.55(10)–136.15(10).

In an attempt to disrupt the persistent bridging OTf^- interactions in **2**, this complex was combined with an excess (6 equivalents) of the strong donor 4-dimethylaminopyridine (DMAP) in THF (Scheme 2.2). The crude ^1H NMR spectrum revealed the complete consumption of **2** and the presence of two distinct IPr environments, along with small amounts of the imidazolium salt [IPrH]OTf. Crystals were obtained by cooling a concentrated CH_2Cl_2 solution of the crude material to −35 °C. The resulting crystallographic structure determination identified the presence of two discrete molecules in the structure in a 1:1 ratio: [IPr•Cd(DMAP)$_3$][OTf]$_2$ (**3a**) and [IPr•Cd(DMAP)$_2$(OTf)$_2$] (**3b**; shown in Figures 2.4 2.5, respectively). Although compounds **3a** and **3b** both exhibit high solubility in CH_2Cl_2 and moderate solubility in THF, concentration of the crude reaction mixture in THF results in the exclusive initial precipitation of the dicationic cadmium salt **3a** as a pure microcrystalline solid. The remaining DMAP complex **3b** could

not be isolated in an analytically pure form due to its similar solubility as the imidazolium $[IPrH]^+$ salt byproduct. Even when the reaction of **2** is carried out with a large excess of DMAP (10 equivalents), the concomitant formation of **3b** is always observed (ca. 5 % by ^1H NMR spectroscopy).

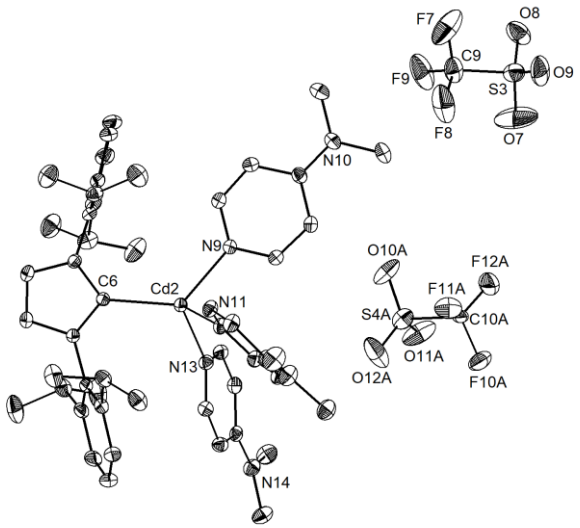

Figure 2.4. Molecular structure of **3a** with thermal ellipsoids plotted at a 30 % probability level. All hydrogen atoms and CH_2Cl_2 solvate have been omitted for clarity. Selected bond lengths [Å] and angles [°]: C6-Cd2 2.200(2), N-Cd2 2.242(2)–2.258(2); C6-Cd2-N 114.83(8)–125.81(8).

The formation of stable NHC–Hg precursors was also targeted to see if reactive Hg–H bonding environments could be obtained for subsequent catalysis. The carbene-bound mercury triflate precursors were prepared (Scheme 2.3) again by using AgOTf as a source of OTf^- groups. When one equivalent of AgOTf was combined with [IPr•HgI_2] in CH_2Cl_2, the expected iodo-triflato complex [IPr•HgI]OTf (**4**) was obtained as a colorless solid in quantitative yield.

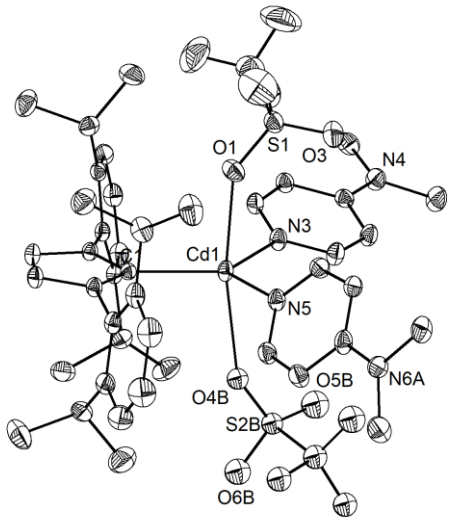

Figure 2.5. Molecular structure of **3b** with thermal ellipsoids plotted at a 30 % probability level. All hydrogen atoms and CH_2Cl_2 solvate have been omitted for clarity. Selected bond lengths [Å] and angles [°]: C(1)-Cd(1) 2.220(2), Cd(1)-O 2.449(7)–2.478(2), Cd(1)-N 2.218(2)–2.230(2); O(1)-Cd(1)-O(4 A) 163.27(18), C(1)-Cd(1)-N 120.37(8)–123.94(8).

The molecular structure of [IPr•HgI]OTf (**4**; Figure 2.6) shows a slightly bent quasi-two coordinate geometry about mercury with a C_{IPr}-Hg-I angle of 166.46(7)°. The canting of the C-Hg-I angle away from a linear arrangement is due to the presence of a pair of weak Hg–O interactions [2.679(2) and 2.880(2) Å] involving a proximal triflate group (Figure 2.6). The coordinative C_{IPr}–Hg distance is 2.075(3) Å and is the same within experimental error as the corresponding distance in the monomeric Hg^{II} halide adduct [IPr•HgI_2].[9]

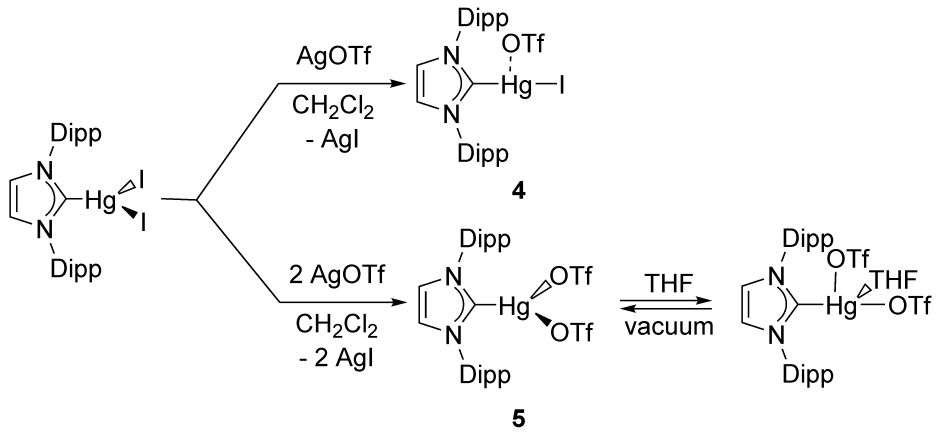

Scheme 2.3. Preparation of the NHC-mercury triflato complexes **4** and **5**.

The last member of the NHC-Group 12 element triflato series to be discussed here, [IPr•Hg(OTf)$_2$] (**5**), was synthesized by adding 2 equivalents of AgOTf to [IPr•HgI$_2$] in CH_2Cl_2. Crystals of the resulting compound were grown from a THF solution of **5** layered with hexanes and the corresponding X-ray structure was found to contain THF within the coordination sphere of mercury [IPr•Hg(OTf)$_2$•THF] (Figure 2.7).[15] The Hg center in **5**•THF adopts a rare distorted *cis*-divacant octahedral geometry wherein the ligating carbene carbon (C1), the THF oxygen atom, and one OTf-based oxygen donor (O21) all lie in an equatorial plane and form a T-shaped motif with Hg [sum of angles in this plane = 353.69(17)°]; the remaining OTf^- group forms a capping axial interaction with Hg.

The reactivity of the new iodo-triflato and bis(triflato) carbene adducts **1**–**5** with the commonly used mild hydride source K[*s*Bu$_3$BH][4,16] to possibly yield [IPr•MH(OTf)•(THF)$_x$] (M = Cd and Hg) complexes was then explored. The known zinc congener [IPr•ZnH(OTf)•THF] is an active hydrosilylation/borylation catalyst,[4] and the decreased stability of the M–H linkages (M = Cd and Hg) could accelerate the rate of catalysis.

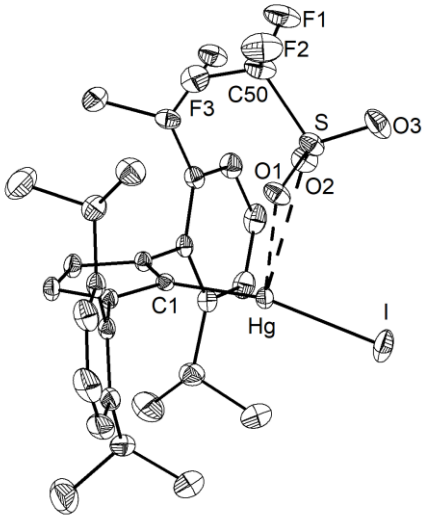

Figure 2.6. Molecular structure of **4** with thermal ellipsoids plotted at a 30 % probability level. All hydrogen atoms have been omitted for clarity. Selected bond lengths [Å] and angles [°]: C1-Hg 2.075(3), Hg-I 2.5689(3), Hg-O1 2.679(2), Hg-O2 2.880(2); C1-Hg-I 166.46(7), C1-Hg-O1 99.14(9), C1-Hg-O2 93.57(9).

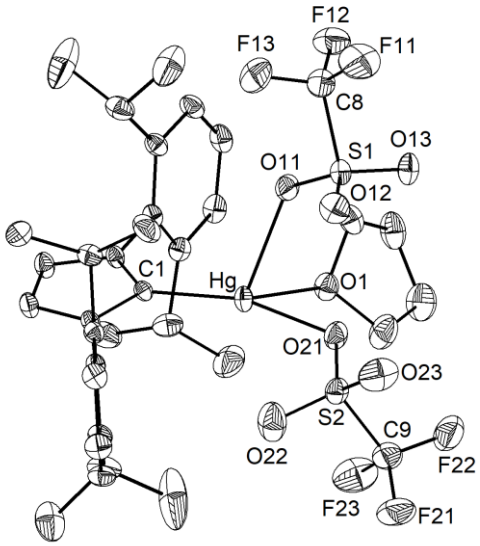

Figure 2.7. Molecular structure of **5**•THF with thermal ellipsoids plotted at a 30 % probability level. All hydrogen atoms have been omitted for clarity. Selected bond lengths [Å] and angles [°]: C1-Hg 2.049(3), Hg-O11 2.435(2), Hg-O21 2.109(2), Hg-O1 2.492(2); O1-Hg-O21 78.27(9), C1-Hg-O21 162.47(11), C1-Hg-O1 112.95(10), C1-Hg-O11 110.24(10).

However, when compounds **1**–**5** were combined with either one or two equivalents of K[*s*Bu$_3$BH] in THF at room temperature, the immediate formation of a metallic precipitate was noted in each case. ^{1}H NMR analysis revealed the formation of free IPr, minor amounts of IPrH$_2$ and multiple unidentified products (with no discernable Cd–H resonances) for the Cd compounds **1**–**3**, while the Hg analogues **4** and **5** afforded only free IPr as a soluble product. In order to get a sense of whether these reactive hydrides could be observed at lower temperatures, THF solutions of compounds **1**–**5** were first frozen in a cold well in a N$_2$ filled glove-box, and were then layered with THF solutions of K[*s*Bu$_3$BH] that were pre-cooled to −35 °C. Warming these reaction mixtures slowly to room temperature revealed the immediate formation of metallic precipitates upon thawing of the THF solutions containing the cadmium and mercury triflates; the resulting ^{1}H NMR spectra were similar to those described above. Undaunted by these unsuccessful attempts to generate stable [IPr•MH(OTf)•THF] complexes (M = Cd and Hg), it was decided to explore the catalytic activity of [IPr•Cd(OTf)$_2$]$_2$ (**2**) and [IPr•Hg(OTf)$_2$] (**5**) with respect to the hydrosilylation and hydroborylation of benzophenone (Scheme 2.4) as the *in situ* formation of M–H bonds could transpire in the presence of silane or boronic ester.

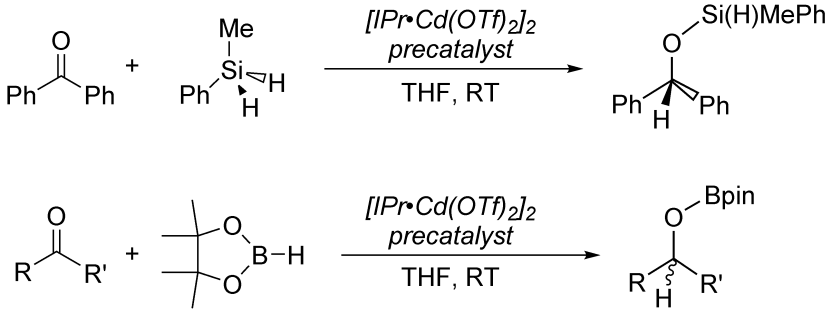

Scheme 2.4. Catalytic hydrosilylation and hydroborylation of aldehydes and/or ketones using [IPr•Cd(OTf)$_2$]$_2$ (**2**) as a precatalyst.

Following the successful ketone hydrosilylation and hydroborylation conditions used previously by the Rivard group with the active catalyst [IPr•ZnH(OTf)•THF], a THF solution containing 5 mol % of $[IPr•Cd(OTf)_2]_2$ (**2**) and benzophenone was combined with phenylmethylsilane ($PhMeSiH_2$) at room temperature. Surprisingly, given the failure at obtaining well-defined Cd–H complexes, **2** was found to be an active precatalyst, with 96 % conversion of the ketone to the corresponding hydrosilylation product $Ph_2CH–OSi(H)PhMe$[4] after 120 minutes (TOF = 10 h^{-1}), as determined by ^1H NMR spectroscopy. Using a lower catalyst loading of 1 mol % resulted in the formation of only a small amount of hydrosilylated product (7 % conversion, Table 2.1); in all cases the visible formation of Cd metal was noted.

Table 2.1. Summary of the catalytic hydrosilylation and hydroboylation of selected aldehydes and ketones (outlined in Scheme 2.4).

Cat.[a]	Cat. [mol %][b]	R/R′	Substrate	*t* [min]	Yield [%][c]	TOF [h^{-1}][d]
2	1	Ph/Ph	$PhMeSiH_2$	60	7	13
2	5	Ph/Ph	$PhMeSiH_2$	70	79	14
2	5	Ph/Ph	$PhMeSiH_2$	120	96	10
5	5	Ph/Ph	$PhMeSiH_2$	90	0	-
[Zn]	1	Ph/Ph	$PhMeSiH_2$	30	0	-
2	0.1	Ph/Ph	HBpin	10	9	526
2	1	Ph/Ph	HBpin	10	98	593
5	5	Ph/Ph	HBpin	90	0	-
[Zn]	1	Ph/Ph	HBpin	30	0	-
2	1	4-ClC_6H_4/4-ClC_6H_4	HBpin	105	32	19
2	5	4-ClC_6H_4/4-ClC_6H_4	HBpin	60	>99	20
2	1	Mes/H	HBpin	10	89	534
2	1	Mes/H	HBpin	20	>99	297
2	1	Cy/Cy	HBpin	5	58	696

[a][Zn] = [IMes•Zn(OTf)•THF]
[b][Cat.] = 0.02 M
[c]Yield determined by ^1H NMR integration in C_6D_6
[d]Calculated per mole of dimer **2**

Although the mechanism of hydrosilylation by cationic NHC zinc hydrides is unknown at this time,[4] it has been postulated that the ketone inserts into the Zn–H bond, forming a zinc alkoxy intermediate $[IPr•Zn(OCHR_2)]^+$ which in turn can react with a silane to regenerate the $[IPr•ZnH]^+$ catalyst and yield the desired hydrosilylation product in the process.[4,6] An alternate possible mechanism for hydrosilylation is a scenario where the metal complex [M] is acting like a Lewis acid, leading to a transient [M]–H–SiR_3–OCR_2 species, as is known for the $B(C_6F_5)_3$-catalyzed hydrosilylation of ketones.[17]

Preliminary investigations (*vide infra*) suggest that a transient cadmium hydride may be forming from **2** during catalytic hydrosilylation, which can then react rapidly with benzophenone to form a cadmium alkoxy intermediate. The reaction of a stoichiometric amount of **2** and $PhMeSiH_2$ was monitored by variable temperature ^{1}H NMR spectroscopy in $[D_8]$THF. Beginning at −80 °C, the temperature was slowly increased until reactivity was observed. No reaction occurred until +10 °C, where 37 % of **2** had converted into an $[IPrH]^+$ salt and a new carbene containing product in a ca. 1:1 ratio, however no Cd–H resonances were observed; the presence of H_2 was also noted in the ^{1}H NMR spectrum. The formation of the known silyltriflate PhMeSiH(OTf)[18] was observed when **2** and $PhMeSiH_2$ were combined at room temperature which can be taken as substantial evidence of $H^–/OTf^–$ exchange between **2** and $PhMeSiH_2$ to initially form a Cd–H intermediate. Compound **2** and $PhMeSiH_2$ were also combined in toluene in a 1:1 ratio, however no reaction was observed at room temperature presumably due to the insolubility of **2** in toluene.

In order to give more credence to the proposed hydride insertion mechanism, the cadmium alkoxide [IPr•CdI(O*i*Pr)] (**6**) was synthesized from $[IPr•CdI(\mu\text{-}I)]_2$ and 2

equivalents of NaO*i*Pr (Scheme 2.5). [IPr•CdI(O*i*Pr)] represents a model of the first intermediate formed in the proposed hydride insertion mechanism, and treatment of this species with $PhMeSiH_2$ afforded the expected silane PhMeSiH(O*i*Pr) via O*i*Pr/H exchange at cadmium; Cd metal formation and unidentified soluble products were also noted.

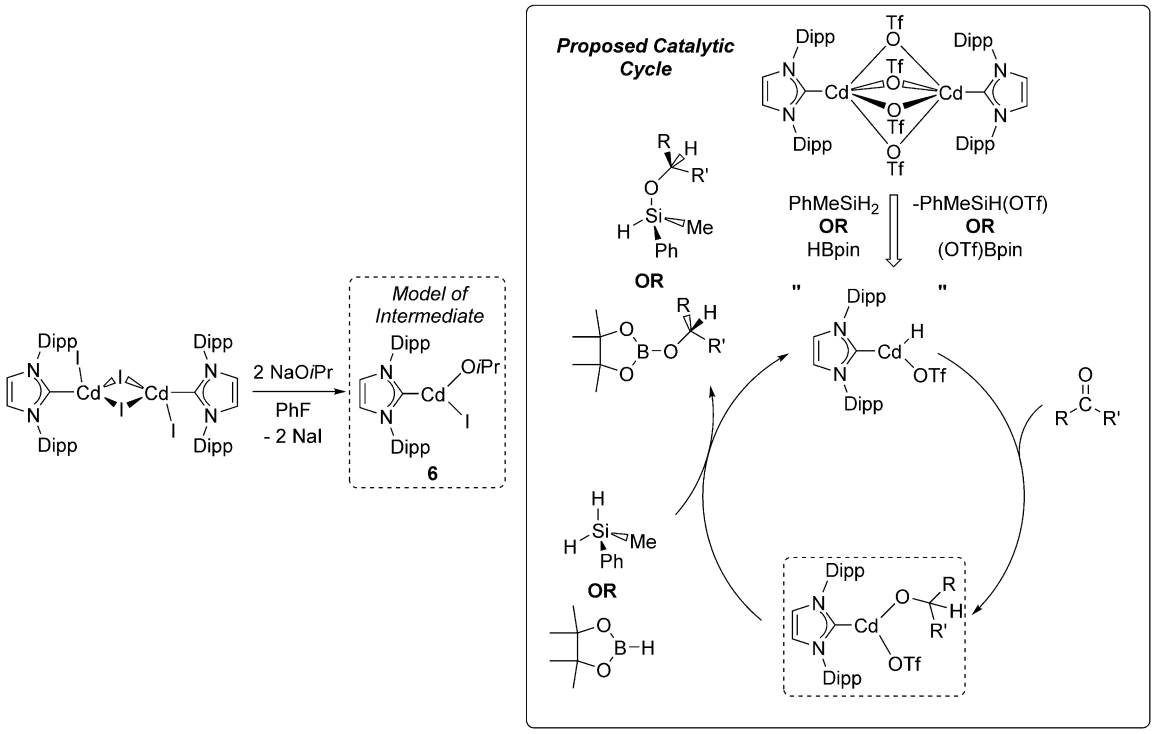

Scheme 2.5. Proposed catalytic cycle and the synthesis of the model intermediate **6**.

The hydrosilylation of benzophenone was also attempted in the presence of 5 mol % of [IPr•Hg$(OTf)_2$] (**5**) in THF. In this case, the formation of mercury metal was noted immediately upon the addition of phenylmethylsilane to the mixture of **5** and benzophenone, with no sign of benzophenone conversion after 90 min. When **5** was combined with 2 equivalents of $PhMeSiH_2$ in THF, the rapid decomposition to Hg metal occurred along with the formation of several unidentified soluble products, the known silyltriflate PhMeSiH(OTf)[18] and free IPr.

The hydroborylation of benzophenone with HBpin was explored using the Cd complex **2** as a precatalyst. The resulting catalytic hydroborylation reaction was found to be much more rapid than hydrosilylation, with the reaction going to 98 % completion after 10 minutes in the presence of a 1 mol % loading of **2** (TOF = 593 h^{-1}; Table 2.1). For comparison, **2** is more active than Jones' novel low-coordinate tin(II) hydride hydroborylation catalyst [Ar†N(Si*i*Pr$_3$)SnH] (Ar† = $C_6H_2\{CHPh_2\}_2$*i*Pr-2,6,4; TOF = 80 h^{-1}),[19] and a recently reported diazaphospholene catalyst prepared by Kinjo and co-workers (TOF = 1.8 h^{-1} at 90 °C).[20] The hydroborylation of benzophenone with 1 mol % of **2** was attempted in toluene at room temperature, however only 5 % conversion was noted after 8 hours, likely due to the insolubility of the precatalyst. When **2** was combined with 4 equivalents of HBpin, the formation of a metallic precipitate was noted along with several unidentified soluble products. Notably, the formation of pinB(OTf) was also detected by NMR spectroscopy, and the identity of this new species was confirmed by its independent synthesis from HBpin and $Me_3Si(OTf)$.

Motivated by the high hydroborylation activity observed with benzophenone, the ability of **2** to catalyze the hydroborylation of various ketones and aldehydes was investigated. Hydroborylation of 4,4′-dichlorobenzophenone occurred more slowly than benzophenone, however complete conversion to the boryl ether $(4\text{-}ClC_6H_4)_2CHOBpin$ was observed after 60 minutes (TOF = 20 h^{-1}; Table 2.1) with a 5 mol % loading of **2**. Again, this represents a more enhanced activity relative to Kinjo's catalyst (TOF = 1.7 h^{-1}, 90 °C).[20] High turnover frequencies were also maintained with more sterically hindered substrates. For example, the hydroborylation of mesitaldehyde (R/R′ = Mes/H; Table 2.1) occurred rapidly in the presence of 1 mol % **2** with 89 % of the aldehyde being converted

to the desired product after 10 minutes (TOF = 534 h^{-1}) and quantitative conversion observed after 20 minutes. Dicyclohexyl ketone was also investigated as a substrate, and it was found that 58 % of the starting ketone was converted to the hydroborylated species $Cy_2CHOBpin$ after just 5 minutes with a 1 mol % loading of **2** (TOF = 696 h^{-1}). This represents the first example of the catalytic hydroborylation of dicyclohexyl ketone. As was the case with hydrosilylation, when **5** was examined as a hydroborylation precatalyst, metal formation was observed immediately following the addition of HBpin and benzophenone, with no sign of the borylated product $Ph_2CHOBpin$ by ^1H NMR spectroscopy, likely due to inherent instability of Hg–H bonds.

The known zinc bis-triflate analogue, [IMes•$Zn(OTf)_2$•THF][14] was also evaluated as a precatalyst. In the case of both hydrosilylation and hydroborylation no catalytic activity was observed. This is likely due to the oxophilic nature of zinc relative to the soft Lewis acids cadmium and mercury which inhibits the formation of a catalytically active zinc-hydride containing species from the mild hydride sources $PhMeSiH_2$ and HBpin (via H^-/OTf^- exchange).

The observation that the IPr-bound cadmium and mercury triflates **1**–**5** did not form stable hydride complexes suggests that the carbene–metal interactions are not very strong in the target [IPr•MH_2] and [IPr•MH(OTf)] complexes (M = Cd and Hg). This prompted the study of the stability of the IPr-bound Group 12 element dihydride complexes [IPr•MH_2] computationally at the M06-2X/cc-pVTZ level of theory.

Table 2.2. Computational investigation of the formation of [IPr•MH_2] adducts.

Adduct	$\Delta_r H°$ [kcal/mol][a]	$\Delta_r G°$ [kcal/mol][a]	C–M Distance [Å]	H-M-H Angle [°]
[IPr•ZnH_2]	−23.7	−15.6	2.190	141.8
[IPr•CdH_2]	−17.7	−10.0	2.466	152.7
[IPr•HgH_2]	−9.4	−0.9	2.882	172.7

[a]Calculated for the gas-phase reaction IPr + MH_2 → [IPr•MH_2]

The formation of [IPr•ZnH_2] from the free carbene and linear ZnH_2 fragments was found to be significantly exothermic and exergonic ($\Delta_r H°$ = −23.7 kcal/mol, $\Delta_r G°$ = −15.6 kcal/mol; Table 2.2). In comparison with the heavier Group 12 element (Cd, Hg) congeners, a significant donor–acceptor interaction was present in [IPr•ZnH_2] as demonstrated by the short carbene carbon–zinc distance (2.190 Å) and significant bending of the H-Zn-H angle from linearity (141.8°). The formation of the carbene adducts of CdH_2 and HgH_2 were also evaluated computationally. Specifically, [IPr•CdH_2] formation was found to be favorable in the gas phase, however less so than the zinc dihydride complex ($\Delta_r H°$ = −17.7 kcal/mol, $\Delta_r G°$ = −10.0 kcal/mol). The carbene carbon–cadmium distance (2.466 Å) was computed to be elongated relative to the C–Zn bond in [IPr•ZnH_2] (2.190 Å), and a more linear H-M-H angle (152.7°) was present in [IPr•CdH_2], consistent with a weaker C_{IPr}–CdH_2 interaction. The formation of [IPr•HgH_2] was found to be the least favorable of the series ($\Delta_r H°$ = −9.4 kcal/mol, $\Delta_r G°$ = −0.9 kcal/mol) and a correspondingly long carbene carbon–mercury distance of 2.882 Å was found; furthermore the H-Hg-H angle in the carbene complex was only slightly bent from a linear arrangement (172.7°), illustrating the very weak nature of the C_{IPr}–Hg donor–acceptor interaction. The general trend of decreasing stability of [IPr•MH_2] down the group was further observed by second-order perturbation theory analysis of the C_{IPr}→M interactions. Of note, attempts to

compute the Cd and Hg dimers [IPr•MH(μ-H)]$_2$ (M = Cd and Hg) failed due to IPr dissociation from the M_2H_4 dimeric core during geometry optimization. In contrast, the Zn congener [IPr•ZnH(μ-H)]$_2$ was previously shown to be an energetic minimum on the potential energy surface.[4] The noted hydrosilylation and hydroborylation activity in the presence of the Cd triflate complex **2** suggests the possible formation of short-lived cadmium hydride-containing species that participate in catalysis. However, in the case of the mercury analogue **5**, if any hydrides were formed these species decompose rapidly. While target cadmium and mercury hydrides were not isolable, the robust nature of the IPr–M^{II} adducts **1**–**5** prompted the exploration of the reactivity of IPr toward the mercury(I) chloride, calomel (Hg_2Cl_2).

Mercury, unlike its lighter congeners zinc and cadmium, is stable in its +1 oxidation without the aid of stabilizing co-ligands. Mercury(I) compounds exclusively form an Hg–Hg bond within a formal $[Hg_2]^{2+}$ fragment, with common examples being complexes with either halide or nitrate counterions. Typically, such mercury(I) species undergo disproportionation in the presence of common neutral donor ligands.[21] Despite the advanced stage of *N*-heterocyclic carbene (NHC) complexation in the main group,[22] well-defined carbene-mercury coordination chemistry remains underdeveloped and examples are typically limited to [NHC→HgX_2]$_{1\ or\ 2}$ adducts (X = Cl, I)[9] or mercury triflates (compounds **4** and **5**). It was therefore decided to investigate whether NHC–mercury(I) complexes could be isolated or if disproportionation chemistry would occur.

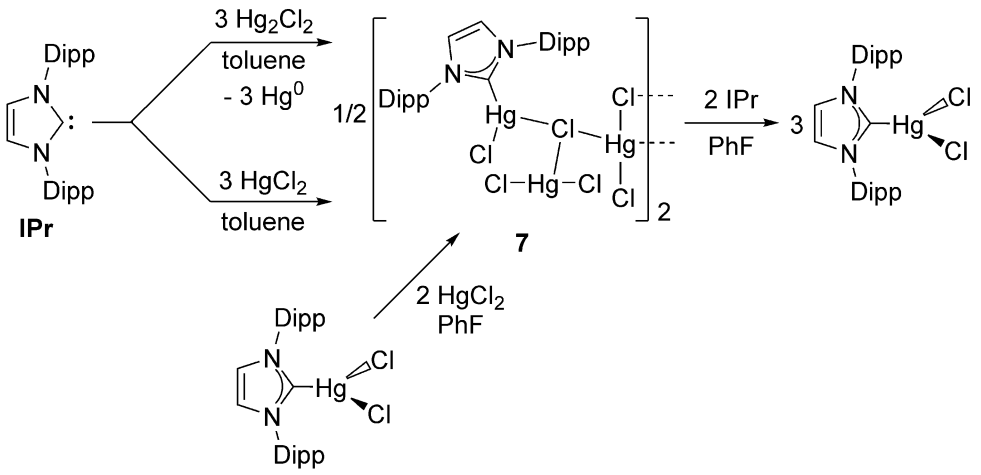

Scheme 2.6. Preparation of **7** through disproportionation of Hg_2Cl_2 (or addition of $HgCl_2$ to IPr or [IPr•$HgCl_2$]) and subsequent regeneration of IPr•$HgCl_2$.

Attempts to generate an unprecedented NHC–Hg^I complex by combining the commercially available mercurous chloride (Hg_2Cl_2) and the *N*-heterocyclic carbene IPr in toluene invariably led to disproportionation, as evidenced by the production of mercury metal. Somewhat surprisingly, the known Hg(II) dichloride adduct [IPr•$HgCl_2$][9] was not the product recovered. In addition to affording new ^{1}H and $^{13}C\{^1H\}$ NMR carbene resonances, the isolated product gave a $^{199}Hg\{^1H\}$ spectrum (Figure 2.8) with two distinct signals (1:2 ratio) suggesting the retention of a polymercury halide entity in solution. The presence of diagnostic flanking satellites about the olefinic carbene backbone singlet resonance in the ^{1}H NMR spectrum also suggested an intact C_{IPr}–Hg bond in the product; the value of the resulting $^4J_{H–Hg}$ coupling constant (33 Hz) in the new species compares well with that in [IPr•$HgCl_2$] ($^4J_{H–Hg}$ = 31 Hz).[9]

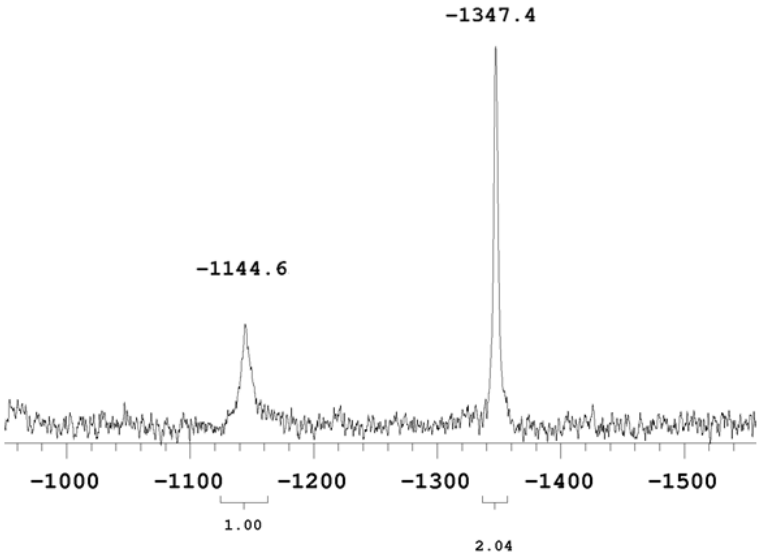

Figure 2.8. $^{199}Hg\{^{1}H\}$ NMR spectrum of **7** illustrating two Hg environments in solution.

Dissolution of the abovementioned disproportionation product in fluorobenzene and allowing the slow diffusion of hexane vapor into the solution, resulted in the formation of colorless needles of $[IPr{\bullet}Hg_3Cl_6]_2$ (**7**) in a 47 % yield according to the equation in Scheme 2.6. X-ray analysis identified the presence of three crystallographically distinct mercury environments[23,24,25] in **7** (Figure 2.9) and represents a new bonding motif for coordinated mercury dichloride. IPr binds to Hg1 with a typical C_{NHC}–Hg bond length of 2.066(3) Å {e.g. 2.090(4) Å in $IPr{\bullet}HgCl_2$]}[9] and an Hg–Cl bond of 2.3100(10) Å [Hg1–Cl1] to the terminal chloride. The arrangement about Hg1 can be described as distorted T-shaped [C1-Hg1-Cl1 = 160.27(10); C1-Hg1-Cl2 = 108.22(10)°]. The three mercury atoms are all bridged by Cl2 with Cl–Hg distances in the range of 2.7657(10) to 2.7985(10) Å. The Hg2 and Hg3 atoms are also each bound to a pair of terminal chlorides with similar bond lengths [2.289(2)–2.309(2) Å] to that of Hg1–Cl1. Both Hg2 and Hg3 possess Cl-Hg-Cl angles that are slightly bent away from linearity [Cl3-Hg2-Cl4 = 168.60(7)°, Cl5-

Hg3-Cl6 = 166.12(5)°]. Compound **7** may also be viewed as a dimer in the solid state, possessing a long Hg3–Cl5 bonding interaction of 3.120(1) Å (sum of the van der Waals radii for Hg and Cl = 3.30 Å) linking two [IPr•Hg_3Cl_6] subunits.

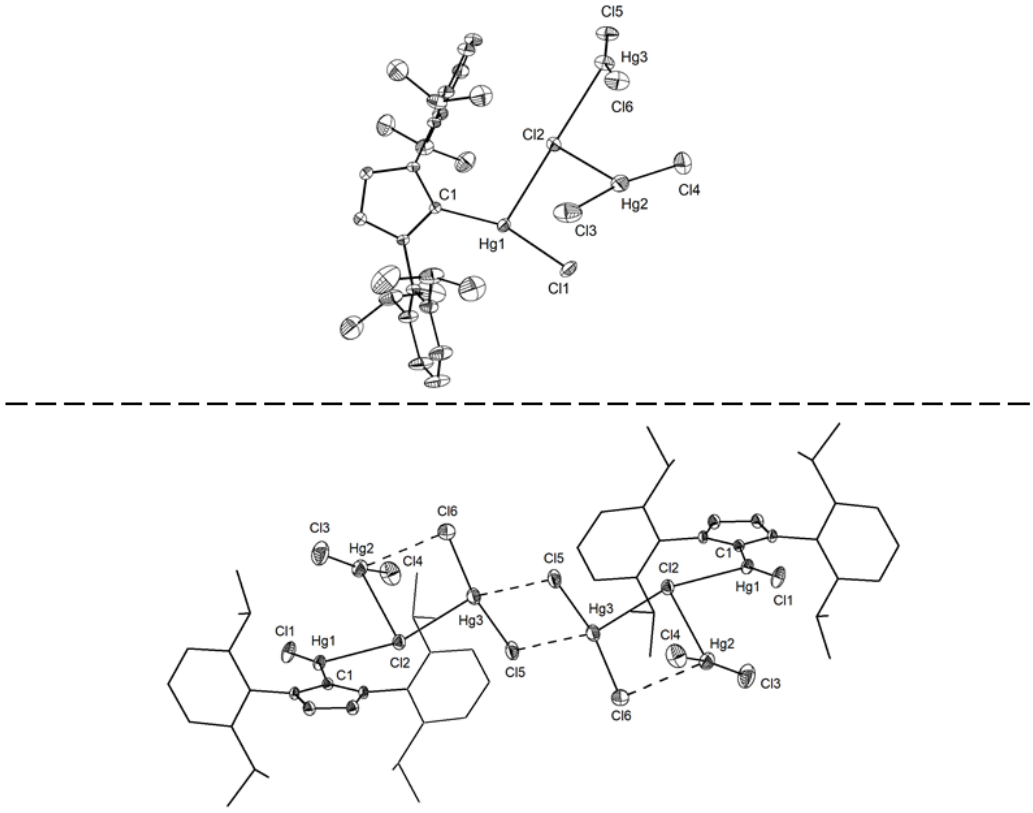

Figure 2.9. Molecular structure of **7** with thermal ellipsoids plotted at a 30 % probability level. Both the monomer unit (above) and dimer (below) of **7** are show. All hydrogen atoms are omitted and the Dipp groups presented as wireframes (below) for clarity. Selected bond lengths [Å] and angles [°]: C1–Hg1 2.066(3), Hg1–Cl1 2.3110(10), Hg1–Cl2 2.7657(10), Cl2–Hg2 2.7918(10), Cl2–Hg3 2.7985(10), Hg3–Cl5 3.120(1); C1-Hg1-Cl1 160.27(10), Hg1-Cl2-Hg3 161.03(4), Cl3-Hg2-Cl4 168.60(7), Cl5-Hg3-Cl6 166.12(5).

To see if the $(HgCl_2)_3$ array in **7** could be cleaved by an exogenous Lewis base, a fluorobenzene solution of IPr was added to **7** which led to the formation of a colorless precipitate. This was later identified as [IPr•$HgCl_2$] by NMR spectroscopy (quantitative yield; Scheme 2.6). Interestingly, it was discovered that **7** can also be generated in good yield directly from the commercially available mercury(II) source, $HgCl_2$. Specifically, the

addition of IPr to 3 equivalents of $HgCl_2$ led to the formation of **7** in 75 % yield. Furthermore, **7** can be formed in a high yield of 93 % by the addition of two equivalents of $HgCl_2$ to [IPr•$HgCl_2$] (Scheme 2.6). The generation of the complex structure of **7** via multiple routes is, in itself, noteworthy.

2.3. Conclusions

A series of IPr-supported cadmium and mercury triflates were synthesized and used as precursors in the attempted formation of cadmium and mercury hydrides. It was found that the target metal hydride complexes [IPr•MH(OTf)•THF] (M = Cd or Hg) could not be prepared, and rapid decomposition into free carbene and Cd or Hg metal was noted. Computations reveal the stability of IPr-bound Group 12 element hydrides [IPr•MH_2] (M = Zn, Cd and Hg) decreases drastically down the group, which is in agreement with our experimental observations. [IPr•$Cd(OTf)_2$]$_2$ (**2**) was found to be an active precatalyst for the hydrosilylation and hydroborylation of hindered aldehydes and ketones. In contrast, [IMes•$Zn(OTf)_2$•THF] is completely inactive as a hydrosilylation/borylation precatalyst; thus the larger size and decreased bond enthalpy of the Cd–O (and putative Cd–H bonds formed during the use of **2** as a catalyst) is in line with the increase in catalytic activity expected for heavier Group 12 element complexes. Additionally, the formation of a new bonding motif of mercury dichloride has been described which was obtained via a carbene-induced disproportionation of mercury(I) chloride. The exclusive formation of [IPr•Hg_3Cl_6]$_2$ (**7**) rather than the known adduct [IPr•$HgCl_2$] demonstrates that NHC-aided disproportionation of reduced element halide precursors should be an ongoing and very useful general strategy in accessing new main group bonding environments.[25] Future work

will include the extension of the presented concept of using heavy (low oxophilicity) elements in catalysis to include more environmentally benign systems.

2.4. Experimental Details

2.4.1. General

All reactions were performed in an inert atmosphere glovebox (Innovative Technology, Inc.) and were manipulated in the absence of light until the products were isolated as solids. Solvents were dried using a Grubbs-type solvent purification system[26] manufactured by Innovative Technologies, Inc., degassed (freeze-pump-thaw method), and stored under an atmosphere of nitrogen prior to use. CdI_2, HgI_2, $HgCl_2$, Hg_2Cl_2, K[*s*Bu_3BH] (1.0 M solution in THF), dicyclohexyl ketone, 4,4′-dichlorobenzophenone, trimethylsilyl triflate, sodium isopropoxide, and $PhMeSiH_2$ were purchased from Aldrich and used as received. AgOTf and HBpin were purchased from Matrix Scientific and used as received. Mesitaldehyde was purchased from Tokyo Chemical Industry and used as received. IPr,[27] [IMes•Zn$(OTf)_2$•THF],[14] [IPr•CdI(μ-I)]$_2$,[8] and [IPr•HgI_2][9] were prepared according to literature procedures. ^{1}H, ^{11}B{^{1}H}, ^{13}C{^{1}H} and ^{19}F NMR spectra were recorded on 400, 500, 600 or 700 MHz Varian Inova instruments and were referenced externally to $SiMe_4$ (^{1}H, ^{13}C{^{1}H}), $CFCl_3$ (^{19}F) or BF_3•Et_2O (^{11}B{^{1}H}). The ^{199}Hg{^{1}H} spectrum was recorded with a 400 MHz Varian Inova instrument and referenced externally to $Hg(NO_3)_2$ [ppm scale relative to δ = 0.0 ppm for $Hg(CH_3)_2$]. Elemental analyses were performed by the Analytical and Instrumentation Laboratory at the University of Alberta. Melting points were measured in sealed glass capillaries under nitrogen by using a MelTemp melting point apparatus and are uncorrected. Diffusion-ordered spectroscopy (DOSY) experiments were performed on Varian 500 and 600 MHz instruments equipped with a Z-gradient broadband

probe capable of outputting 61.6 G cm^{-1} of gradient strength. All measurements were carried out non-spinning and at a calibrated temperature of 27 °C using the Oneshot45 pulse sequence.[28,29] For all DOSY experiments a spectral window of 6 kHz was used with a 3 s acquisition time and a 2 s S4 relaxation delay with 8 scans for each gradient increment. Pulse widths and gradient strengths were optimized for each sample. For both solvent systems a diffusion delay of 50 ms and a diffusion gradient length of 2 ms was used. Gradient strengths of 1.9 to 47.1 G cm^{-1} incremented in 20 steps were used for the toluene solutions and gradient strengths of 1.9 to 37.6 G cm^{-1} also incremented in 20 steps were used for the THF solutions. The spectra were Fourier transformed and baseline corrected prior to discrete processing, fitting the data to a double exponential fit and applying corrections for non-uniform gradients.[30] The diffusion dimension was zero filled to 1024 data points and the directly detected dimension was zero filled to 128K data points.

2.4.2. X-ray Crystallography

Crystals for X-ray diffraction studies were removed from a vial (in a glovebox) and immediately coated with a thin layer of hydrocarbon oil (Paratone-N). A suitable crystal was then mounted on a glass fiber and quickly placed in a low temperature stream of nitrogen on the X-ray diffractometer.[31] All data were collected using a Bruker APEX II CCD detector/D8 or PLATFORM diffractometer using Mo K_α or Cu K_α radiation, with the crystals cooled to −80 °C or −100 °C. The data were corrected for absorption through Gaussian integration from the indexing of the crystal faces. Crystal structures were solved using intrinsic phasing (SHELXT)[32] and refined using SHELXL-2014.[33] The assignment of hydrogen atom positions was based on the sp^2 or sp^3 hybridization geometries of their

attached carbon atoms and were given thermal parameters 20 % greater than those of their parent atoms.

Special refinement conditions. Compound **3**•0.5 CH_2Cl_2: Attempts to refine peaks of residual electron density as disordered or partial-occupancy solvent dichloromethane chlorine or carbon atoms were unsuccessful. The data were corrected for disordered electron density through use of the SQUEEZE procedure as implemented in PLATON.[34] A total solvent-accessible void volume of 170 $Å^3$ with a total electron count of 49 (consistent with 1 molecule of solvent dichloromethane) was found in the unit cell. The N–C distance was restrained to be 1.450(2) Å for the following pairs of atoms: N6A–C48A, N6A–C49A, N6B–C48B, N6B–C49B. Additionally, an anti-bumping restraint (2 Å) was applied to H44···H48C.

2.4.3. Computational Methods

All calculations were carried out using the Gaussian 09, Rev. D.01, software package.[35] Input structures were optimized using the B3LYP[36] functional and 6–31G(d,p)[37] basis set in the gas phase. The structures were then optimized using the M06–2X[38] functional and cc-pVTZ[39] basis set in the gas phase with "very tight" convergence criteria and an ultrafine integration grid. A 28 electron, fully relativistic effective core potential (ECP28MDF)[40] was employed for cadmium with the cc-pVTZ-PP[41] basis set and a 60 electron, fully relativistic effective core potential (ECP60MDF)[40] was utilized for mercury with the same cc-pVTZ-PP[41] basis set. All optimized structures were then confirmed to be local energy minima on the potential energy surface by frequency analysis.

2.4.4. Synthetic Procedures

Synthesis of [IPr•Cd(OTf)(μ-I)]$_2$ (1). To a vial charged with [IPr•Cd(I)(μ-I)]$_2$ (0.174 g, 0.115 mmol) and AgOTf (0.059 g, 0.21 mmol) was added 5 mL of CH_2Cl_2 which resulted in the immediate formation of a yellow precipitate. The resulting mixture was stirred for 2 h, filtered and the solid was discarded. The solvent was removed from the colorless filtrate under vacuum affording [IPr•Cd(OTf)(μ-I)]$_2$ as a colorless solid (0.140 g, 90 %). Crystals of **1** suitable for X-ray crystallographic analysis were obtained by storing a solution of the product in CH_2Cl_2 layered with Et_2O at −35 °C, overnight. ^{1}H NMR ($CDCl_3$, 400.0 MHz): δ 7.61 (broad s, 4H, NC*H*), 7.49 (t, 4H, $^3J_{HH}$ = 7.6 Hz, *p*-Ar*H*), 7.27 (d, 8H, $^3J_{HH}$ = 7.6 Hz, *m*-Ar*H*), 2.33 (septet, 8H, $^3J_{HH}$ = 7.2 Hz, C*H*(CH_3)$_2$), 1.16 (d, 24H, $^3J_{HH}$ = 8.0 Hz, CH(C*H*$_3$)$_2$), 1.14 (d, 24H, $^3J_{HH}$ = 7.2 Hz, CH(C*H*$_3$)$_2$). ^{13}C{^{1}H} NMR ($CDCl_3$, 125.7 MHz): δ 145.3 (N*C*H), 132.8 (Ar*C*), 131.8 (Ar*C*), 126.7 (Ar*C*), 124.8 (Ar*C*), 28.9 (*C*H(CH_3)$_2$), 25.5 (CH(*C*H$_3$)$_2$), 23.4 (CH(*C*H$_3$)$_2$). N*C*N and OTf resonances were not observed. ^{19}F NMR ($CDCl_3$, 376.3 MHz): δ −77.9. Anal. Calcd. for $C_{56}H_{72}Cd_2F_6I_2N_4O_6S_2$: C 43.28, H 4.67, N 3.61, S 4.13. Found: C 43.54, H 4.68, N 3.60, S 3.92. M.p. 280 °C (decomp.)

Synthesis of [IPr•Cd(μ-OTf)$_2$]$_2$ (2). To a vial charged with [IPr•Cd(I)(μ-I)]$_2$ (0.181 g, 0.120 mmol) and AgOTf (0.127 g, 0.49 mmol) was added about 5 mL of CH_2Cl_2, which resulted in the immediate formation of a yellow precipitate. The resulting mixture was stirred for 2 h, filtered and the solid was discarded. The solvent was removed from the colorless filtrate under vacuum affording [IPr•Cd(OTf)$_2$]$_2$ as a colorless solid (0.178 g, 93 %). Crystals of **2** suitable for X-ray crystallographic analysis were obtained by storing a solution of the product in CH_2Cl_2 layered with hexanes in a −35 °C freezer for two days. ^{1}H NMR ($CDCl_3$, 498.1 MHz): δ 7.44 (t, 4H, $^3J_{HH}$ = 8.0 Hz, *p*-Ar*H*), 7.25 (d, 8H, $^3J_{HH}$ =

8.0 Hz, *m*-Ar*H*), 7.21 (s, 4H, satellites: $^{4}J_{H–Cd}$ = 9.7 Hz, NC*H*), 2.42 (septet, 8H, $^{3}J_{HH}$ = 7.0 Hz, C*H*(CH_3)$_2$), 1.24 (d, 24H, $^{3}J_{HH}$ = 7.0 Hz, CH(C*H*$_3$)$_2$), 1.08 (d, 24H, $^{3}J_{HH}$ = 7.0 Hz, C*H*(CH_3)$_2$). $^{13}C\{^{1}H\}$ NMR ($CDCl_3$, 125.7 MHz): δ 175.3 (N*C*N), 145.1 (Ar*C*), 133.1 (Ar*C*), 131.4 (N*C*H), 125.7 (Ar*C*), 124.3 (Ar*C*), 28.9 (*C*H(CH_3)$_2$), 25.3 (CH(*C*H$_3$)$_2$), 22.6 (CH(*C*H$_3$)$_2$). A resonance for the OTf groups was not observed. ^{19}F NMR ($CDCl_3$, 468.7 MHz): δ –74.4. Anal. Calcd. for $C_{58}H_{72}Cd_2F_{12}N_4O_{12}S_4$: C 43.59, H 4.54, N 3.51, S 8.02. Found: C 43.87, H 4.69, N 3.45, S 7.77. M.p. >300 °C (stable).

Synthesis of [IPr•Cd(DMAP)$_3$][OTf]$_2$ (3a). A solution of 4-dimethylaminopyridine (DMAP) (0.146 g, 1.20 mmol) in ca. 8 mL of THF was added to a ca. 8 mL THF solution of [IPr•Cd(OTf)$_2$]$_2$ (0.330 g, 0.206 mmol). The reaction mixture was stirred, overnight, yielding a white precipitate. The mixture was concentrated to a volume of 4 mL under vacuum, and the supernatant was decanted. The resulting white precipitate was washed with 3×5 mL portions of hexanes and dried under vacuum, affording [IPr•Cd(DMAP)$_3$][OTf]$_2$ (**3a**) as a colorless solid (0.416 g, 90 %). Data for **3a**: ^{1}H NMR ($CDCl_3$, 498.1 MHz): δ 7.61 (t, 2H, $^{3}J_{HH}$ = 7.9 Hz, *p*-Ar*H*), 7.54 (broad s, 2H, NC*H*), 7.41 (broad s, 6H, DMAP Ar*H*), 7.36 (d, 4H, $^{3}J_{HH}$ = 7.9 Hz, *m*-Ar*H*), 6.41 (d, 6H, $^{3}J_{HH}$ = 7.0 Hz, DMAP Ar*H*), 3.01 (s, 18H, DMAP N-C*H*$_3$), 2.61 (septet, 4H, $^{3}J_{HH}$ = 6.8 Hz, C*H*(CH_3)$_2$), 1.19 (d, 12H, $^{3}J_{HH}$ = 6.8 Hz, CH(C*H*$_3$)$_2$), 1.13 (d, 12H, $^{3}J_{HH}$ = 6.8 Hz, CH(C*H*$_3$)$_2$). $^{13}C\{^{1}H\}$ NMR ($CDCl_3$, 125.7 MHz): δ 155.1 (N*C*H), 148.9 (Ar*C*), 145.9 (Ar*C*), 134.0 (Ar*C*), 131.8 (Ar*C*), 125.1 (Ar*C*), 107.1 (Ar*C*), 39.2 (DMAP N-*C*H$_3$), 29.0 (*C*H(CH_3)$_2$), 25.4 (CH(*C*H$_3$)$_2$), 23.0 (CH(*C*H$_3$)$_2$). An N*C*N resonance was not observed. A resonance for the OTf groups was not observed. ^{19}F NMR ($CDCl_3$, 468.7 MHz): δ −77.9.

Anal. Calcd. for $C_{50}H_{66}CdF_6N_8O_6S_2$: C 51.52, H 5.71, N 9.61, S 5.50. Found: C 50.60, H 5.62, N 8.87, S 5.58. M.p. 187 °C (decomp.).

The supernatant of the above synthesis (**3a**) was dried under vacuum, affording a colorless solid (0.051 g). The solid was found by ^{1}H NMR spectroscopy to contain **3a** (39 %), **3b** (39 %) and [IPrH]OTf (21 %).[7,27]

NMR data for [IPr•Cd(DMAP)$_2$(OTf)$_2$] (3b). ^{1}H NMR ($CDCl_3$, 498.1 MHz): δ 7.54 (broad s, 4H, DMAP-Ar*H*), 7.46 (t, 2H, $^3J_{HH}$ = 8.0 Hz, *p*-Ar*H*), 7.13 (d, 4H, $^3J_{HH}$ = 8.0 Hz, *m*-Ar*H*), 6.41 (d, 4H, $^3J_{HH}$ = 7.0 Hz, DMAP-Ar*H*), 3.01 (s, 12H, DMAP N-CH_3), 2.25 (septet, 4H, $^3J_{HH}$ = 7.0 Hz, C*H*(CH_3)$_2$), 1.06 (d, 12H, $^3J_{HH}$ = 7.0 Hz, CH(CH_3)$_2$), 0.77 (d, 12H, $^3J_{HH}$ = 7.0 Hz, CH(CH_3)$_2$). An NC*H* resonance was not observed. A single ^{19}F signal was observed for the mixture; ^{19}F NMR ($CDCl_3$, 468.7 MHz): δ −78.0 ppm.

When the above reaction was repeated and the crude product containing both **3a** and **3b** was crystallized from CH_2Cl_2 (−35 °C; one week), colorless crystals were obtained which contained a 1:1 mixture of **3a** [IPr•Cd(DMAP)$_3$][OTf]$_2$ and **3b** [IPr•Cd(DMAP)$_2$(OTf)$_2$] in the lattice. Attempts to form **3b** exclusively by reacting 4 equivalents of DMAP with [IPr•Cd(OTf)$_2$]$_2$ were unsuccessful as **3a** remained as the major product (74 % by ^{1}H NMR spectroscopy), along with the formation of **3b** (14 % by ^{1}H NMR spectroscopy) and [IPrH]OTf (12 % by ^{1}H NMR spectroscopy). Attempts to separate **3b** and [IPrH]OTf by crystallization from CH_2Cl_2/hexanes and THF/hexanes solvent mixtures were unsuccessful.

Synthesis of [IPr•HgI][OTf] (4). To a vial charged with [IPr•HgI_2] (0.105 g, 0.125 mmol) and AgOTf (0.031 g, 0.12 mmol) was added ca. 5 mL of CH_2Cl_2, which resulted in the immediate formation of a yellow precipitate. The resulting mixture was stirred for 2 h,

filtered and the solid was discarded. The solvent was removed from the colorless filtrate under reduced pressure, affording [IPr•HgI][OTf] as a white solid (0.103 g, quantitative yield). Crystals of **4** suitable for X-ray crystallographic analysis were obtained by storing a concentrated solution of the product in THF layered with hexanes in a −35 °C freezer for three days; ^{1}H NMR ($CDCl_3$, 499.8 MHz): δ 7.66 (s, 2H, satellites: $^{4}J_{H–Hg}$ = 28.5 Hz, NC*H*), 7.56 (t, 2H, $^{3}J_{HH}$ = 7.5 Hz, *p*-Ar*H*), 7.34 (d, 4H, $^{3}J_{HH}$ = 7.5 Hz, *m*-Ar*H*), 2.42 (septet, 4H, $^{3}J_{HH}$ = 6.5 Hz, C*H*(CH_3)$_2$), 1.29 (d, 12H, $^{3}J_{HH}$ = 6.5 Hz, CH(C*H*$_3$)$_2$), 1.18 (d, 12H, $^{3}J_{HH}$ = 6.5 Hz, CH(C*H*$_3$)$_2$). ^{13}C{^{1}H} NMR ($CDCl_3$, 125.7 MHz): δ 145.5 (N*C*H), 132.4 (Ar*C*), 131.6 (Ar*C*), 127.0 (Ar*C*), 125.2 (Ar*C*), 29.0 (*C*H(CH_3)$_2$), 25.3 (CH(*C*H$_3$)$_2$), 23.6 (CH(*C*H$_3$)$_2$). An N*C*N resonance was not observed. A resonance for the OTf group was not observed. ^{19}F NMR ($CDCl_3$, 376.7 MHz): δ −78.0. Anal. Calcd. for $C_{28}H_{36}F_3HgIN_2O_3S$: C 38.87, H 4.19, N 3.24, S 3.71. Found: C 38.98, H 4.19, N 3.22, S 3.64. M.p. >260 °C (stable).

Synthesis of [IPr•Hg(OTf)$_2$] (5). To a vial charged with [IPr•HgI_2] (0.079 g, 0.094 mmol) and AgOTf (0.054 g, 0.21 mmol) was added ca. 5 mL of CH_2Cl_2, which resulted in the immediate formation of a yellow precipitate. The resulting mixture was stirred for 2 h and filtered. The solvent was removed from the colorless filtrate under reduced pressure, yielding [IPr•Hg(OTf)$_2$] as a colorless solid (0.079 g, 95 %). Crystals of the THF adduct, [IPr•Hg(OTf)$_2$•THF], suitable for X-ray crystallographic analysis[15] were obtained by storing a concentrated solution of the product in THF layered with hexanes in a −35 °C freezer, overnight. ^{1}H NMR ($CDCl_3$, 699.8 MHz): δ 7.72 (broad s, 2H, NC*H*), 7.58 (t, 2H, $^{3}J_{HH}$ = 8.0 Hz, *p*-Ar*H*), 7.35 (d, 4H, $^{3}J_{HH}$ = 7.8 Hz, *m*-Ar*H*), 2.35 (sept, 4H, $^{3}J_{HH}$ = 7.0 Hz, C*H*(CH_3)$_2$), 1.24 (d, 12H, $^{3}J_{HH}$ = 6.9 Hz, CH(C*H*$_3$)$_2$), 1.18 (d, 12H, $^{3}J_{HH}$ = 6.9 Hz,

CH(CH_3)$_2$). ^{13}C{^{1}H} NMR ($CDCl_3$, 176.0 MHz): δ 188.6 (N*C*N), 145.3 (N*C*H), 132.1 (Ar*C*), 131.6 (Ar*C*), 127.6 (Ar*C*), 125.0 (Ar*C*), 29.1 (*C*H(CH$_3$)$_2$), 25.1 (CH(*C*H$_3$)$_2$), 23.4 (CH(*C*H$_3$)$_2$). A resonance for the OTf groups was not observed. ^{19}F NMR ($CDCl_3$, 376.1 MHz): δ −77.1. Elemental analyses were performed on three different crystalline samples. In all cases the CHNS values were systematically low.

Synthesis of [IPr•Hg$_3$Cl$_6$]$_2$ (7). A toluene (ca. 6 mL) solution of IPr (0.060 g, 0.15 mmol) was quickly added to a vial containing a toluene slurry (ca. 2 mL) of Hg_2Cl_2 (0.220 g, 0.466 mmol). A colorless precipitate immediately began to form. The reaction mixture was allowed to stir for 6.5 h, after which the precipitate was left to settle. The toluene supernatant was decanted and the precipitate dried *in vacuo*. The dried precipitate was extracted with fluorobenzene (ca. 15 mL) and filtered. The filtrate was concentrated to a volume of ca. 2 mL, layered with hexanes (2 mL), and placed in a –35 °C freezer overnight. Colorless blocks of **6** were recovered by decanting the mother liquor and washing the solid with hexanes (3×3 mL). The volatiles were removed *in vacuo* yielding [IPr•Hg$_3$Cl$_6$]$_2$ (**6**) as a colorless solid (0.088 g, 47 %). Crystals of **6** suitable for X-ray crystallographic analysis were obtained by allowing hexane vapors to slowly diffuse into a fluorobenzene solution of **6** for one day at room temperature. ^{1}H NMR ($CDCl_3$, 400.0 MHz): δ 7.61 (t, 2H, $^3J_{HH}$ = 7.8 Hz, *p*-Ar*H*), 7.52 (s, 2H, satellites: $^4J_{H–Hg}$ = 33.6 Hz, NC*H*), 7.37 (d, 4H, $^3J_{HH}$ = 7.8 Hz, *m*-Ar*H*), 2.46 (sept, 4H, $^3J_{HH}$ = 6.8 Hz, C*H*(CH$_3$)$_2$), 1.36 (d, 12H, $^3J_{HH}$ = 6.8 Hz, CH(C*H*$_3$)$_2$), 1.21 (d, 12H, $^3J_{HH}$ = 6.8 Hz, CH(C*H*$_3$)$_2$). ^{13}C{^{1}H} NMR ($CDCl_3$, 125.7 MHz): δ 176.9 (N*C*N), 145.4 (Ar*C*), 132.5 (Ar*C*), 131.8 (Ar*C*), 126.2 (Ar*C*), 125.3 (Ar*C*), 29.2 (CH(*C*H$_3$)$_2$), 25.3 (CH(*C*H$_3$)$_2$), 23.6 (*C*H(CH$_3$)$_2$). ^{1}H NMR ([D$_6$]DMSO, 400.0 MHz): δ 8.43 (s, 2H, satellites: $^4J_{H–Hg}$ = 32.5 Hz, NC*H*), 7.64 (t, 2H, $^3J_{HH}$ = 7.6 Hz, *p*-Ar*H*), 7.45 (d,

4H, $^{3}J_{HH}$ = 7.6 Hz, *m*-Ar*H*), 2.35 (sept, 4H, $^{3}J_{HH}$ = 6.8 Hz, C*H*(CH_3)$_2$), 1.25 (d, 12H, $^{3}J_{HH}$ = 6.8 Hz, CH(C*H*$_3$)$_2$), 1.16 (d, 12H, $^{3}J_{HH}$ = 6.8 Hz, CH(C*H*$_3$)$_2$). $^{13}C\{^{1}H\}$ NMR ([D_6]DMSO, 125.7 MHz): δ 145.2 (Ar*C*), 132.6 (Ar*C*), 131.2 (Ar*C*), 127.6 (Ar*C*), 124.3 (Ar*C*), 28.4 (CH(*C*H$_3$)$_2$), 24.6 (CH(*C*H$_3$)$_2$), 22.9 (*C*H(CH$_3$)$_2$). An NCN resonance was not observed. $^{199}Hg\{^{1}H\}$ NMR ([D_6]DMSO, 71.5 MHz): δ –1144.6 (1Hg), –1347.5 (2Hg). Anal. Calcd. for $C_{54}H_{72}Cl_{12}Hg_6N_4$: C 26.96, H 3.02, N 2.33. Found: C 27.00, H 3.02, N 2.24. M.p. 164 °C (decomp.)

Synthesis of 7 from IPr and $HgCl_2$. A toluene solution (ca. 5 mL) of IPr (0.075 g, 0.19 mmol) was added to a vial containing a toluene slurry (ca. 1 mL) of $HgCl_2$ (0.157 g, 0.58 mmol). A colorless precipitate immediately began to form. The reaction mixture was allowed to stir overnight, after which the precipitate was left to settle. The toluene supernatant was decanted and the precipitate dried *in vacuo* yielding **6** as a colorless solid (0.175 g, 75%).

Synthesis of 7 from [IPr•$HgCl_2$] and $HgCl_2$. To a vial loaded with [IPr•$HgCl_2$] (0.171 g, 0.259 mmol) and $HgCl_2$ (0.139 g, 0.512 mmol) was added fluorobenzene (ca. 15 mL), forming a colorless slurry. The reaction mixture was allowed to stir for 2 d, after which the volatiles were removed *in vacuo* yielding **6** as a colorless solid (0.286 g, 93%).

Reaction of 7 with 2 equivalents of IPr. A fluorobenzene solution (ca. 2 mL) of IPr (0.014 g, 0.036 mmol) was added to a vial containing a toluene solution (ca. 4 mL) of 1 (0.022, 0.009 mmol). A colorless precipitate immediately formed upon addition. The reaction mixture was allowed to stir for 1 h, after which an aliquot of the slurry was removed for NMR spectroscopic analysis. The ^{1}H NMR spectrum revealed the quantitative conversion of **7** to [IPr•$HgCl_2$].[9]

Alternative Synthesis of [IPr•$HgCl_2$]. A THF solution (ca. 18 mL) of IPr (0.792 g, 2.04 mmol) was added to a vial containing $HgCl_2$ (0.555 g, 2.04 mmol) leading to the immediate formation of a colorless precipitate. The reaction mixture was stirred overnight, after which the precipitate was left to settle. The THF supernatant was decanted and the precipitate dried *in vacuo* yielding [IPr•$HgCl_2$] as a colorless solid (1.220 g, 91%). Data for [IPr•$HgCl_2$] is consistent with the literature.[9]

Synthesis of [IPr•CdI(O*i*Pr)] (6). To a vial charged with [IPr•Cd(I)(μ-I)]$_2$ (0.160 g, 0.106 mmol) and NaO*i*Pr (0.018 g, 0.22 mmol) was added ca. 10 mL of fluorobenzene leading to the immediate formation of a white slurry. The reaction mixture was stirred for 1.5 h and filtered. The solvent was removed from the colorless filtrate under reduced pressure, yielding a colorless solid (0.135 g). The ^{1}H NMR spectrum identified [IPr•CdI(O*i*Pr)] as the major product (84 %) along with about 3 % free IPr and another minor carbene containing product (ca. 13 %). Data for [IPr•CdI(O*i*Pr)]: ^{1}H NMR (C_6D_6, 399.9 MHz): δ 7.18 (t, 2H, $^3J_{HH}$ = 8.0 Hz, *p*-Ar*H*), 7.06 (d, 4H, $^3J_{HH}$ = 8.0Hz, *m*-Ar*H*), 6.40 (s, 2H, satellites: $^4J_{H–Cd}$ = 6.0 Hz, NC*H*), 2.99–2.66 (broad m, 5H, C*H*$(CH_3)_2$), 1.57 (broad d, 12H, $^3J_{HH}$ = ca. 8 Hz, CH(C*H*$_3)_2$), 1.01–0.96 (broad m, 3H, OCH(C*H*$_3)_2$), 0.93 (broad d, 12H, $^3J_{HH}$ = ca. 8 Hz, CH(C*H*$_3)_2$), 0.70–0.39 (broad m, 3H, OCH(C*H*$_3)_2$).

Catalytic hydrosilylation of benzophenone. To a vial charged with [IPr•Cd(OTf)$_2$]$_2$ (0.014 g, 0.0088 mmol, 5 mol %) and benzophenone (0.033 g, 0.18 mmol) was added 1 mL of THF which formed a colorless solution. Phenylmethylsilane (24 μL, 0.18 mmol) was then immediately added to the reaction mixture. The mixture was allowed to stir for 40 min at which time a 0.2 mL aliquot was taken from the reaction mixture and the volatiles were removed under vacuum. ^{1}H NMR analysis in C_6D_6 revealed that the reaction had

proceeded to 42 % completion (TON = 8, TOF = 13 h^{-1}). In a similar manner, 0.2 mL aliquots were removed from the reaction mixture after 70 and 120 min, revealing 79 % completion (TON = 16, TOF = 14 h^{-1}) and 96 % completion (TON = 19, TOF = 10 h^{-1}), respectively. Data for $Ph_2C(H)OSi(H)MePh$ are consistent with the literature.[4]

Representative catalytic hydroborylation procedure. To a vial charged with $[IPr•Cd(OTf)_2]_2$ (0.015 g, 0.0094 mmol, 5 mol %) and benzophenone (0.035 g, 0.19 mmol) was added 1 mL of THF which afforded a colorless solution. HBpin (28 μL, 0.19 mmol) was then immediately added to the reaction mixture. The reaction mixture was allowed to stir for 10 min at which time a 0.2 mL aliquot was taken from the reaction mixture and the volatiles were removed under vacuum. ^{1}H NMR analysis in C_6D_6 revealed that the reaction had proceeded to completion (TON = 21, TOF = 124 h^{-1}). In a similar manner, the reaction was conducted with a 1 mol % loading of $[IPr•Cd(OTf)_2]_2$ (0.008 g, 0.005 mmol), benzophenone (0.092 g, 0.51 mmol), HBpin (73 μL, 0.51 mmol) in 2 mL of THF. The reaction was also conducted with a 0.1 mol % loading of $[IPr•Cd(OTf)_2]_2$ (0.006 g, 0.004 mmol), benzophenone (0.681 g, 3.74 mmol), HBpin (542 μL, 3.74 mmol) and 5 mL of THF. Relevant data are presented in Table 2.1. Data for $Ph_2C(H)OBpin$ are consistent with the literature.[42]

The abovementioned general procedure was followed for the hydroborylation of 4,4′-dichlorobenzophenone, mesitaldehyde and dicyclohexyl ketone. Data for $(4\text{-}ClC_6H_4)_2CHOBpin$[20] and $MesCH_2OBpin$[42] were consistent with the literature.

NMR data for $Cy_2C(H)OBpin$. ^{1}H NMR (C_6D_6, 498.1MHz): δ 3.83 (m, 1H, OC*H*$(Cy)_2$), 1.92–1.86 (m, 2H, Cy*H*), 1.76–1.67 (m, 4H, Cy*H*), 1.66–1.51 (m, 6H, Cy*H*), 1.32–1.11 (m, 10H, Cy*H*), 1.10 (s, 12H, Bpin). $^{13}C\{^1H\}$ NMR (C_6D_6, 126.7 MHz): δ 82.8 (*C*-CH_3 in

Bpin), 82.1 (O*C*H), 39.6 (Cy-*C*H), 30.1 (Cy-*C*H_2), 27.6 (Cy-*C*H_2), 26.9 (Cy-*C*H_2), 26.7 (Cy-*C*H_2), 26.5 (Cy-*C*H_2), 24.6 (C-*C*H_3 in Bpin). $^{11}B\{^1H\}$ NMR (C_6D_6, 159.8 MHz): δ 22.6.

Stoichiometric reaction of 2 with $PhMeSiH_2$. A J-Young NMR tube was loaded with **2** (0.006 g, 0.004 mmol) in 400 μL of [D_8]THF in a glovebox and the mixture was frozen in a cold well. A 0.3 M solution of $PhMeSiH_2$ in [D_8]THF (25 μL, 0.008 mmol) was then added to the J-Young NMR tube and the total volume was increased to 700 μL with [D_8]THF and frozen in the cold well. The J-Young tube was removed from the glovebox and transported to the NMR instrument in a liquid nitrogen dewar. The NMR tube was quickly inserted into the NMR instrument and let warm to −80 °C. A ^1H NMR spectrum was recorded every 20 min. After 1 h the temperature was increased by 20 °C. This was repeated until a temperature of 0 °C was reached. The temperature was then increased in increments of 5 °C. No reaction was observed until a temperature of +10 °C was reached. After monitoring the reaction for 1 h at +10 °C, 37 % of **2** had been consumed and converted to an $[IPrH]^+$ salt and a new carbene containing product in an approximate 1:1 ratio, however no Cd–H resonances or $^4J_{H–Cd}$ satellites were observed. The presence of H_2 was also confirmed by ^1H NMR spectroscopy and a metallic precipitate was observed in the NMR tube after completion of the experiment.

Reaction of 2 with $PhMeSiH_2$ in toluene. To a vial charged with [IPr•Cd(μ-OTf)$_2$]$_2$ (**2**) (0.010 g, 0.013 mmol) was added ca. 3 mL of toluene forming an insoluble slurry. An aliquot of a freshly prepared 1.0 M toluene solution of $PhMeSiH_2$ (12.5 μL, 0.0125 mmol) was added to the slurry and the reaction mixture was let stir for 6 h after which time an

aliquot was removed for NMR analysis. ^{1}H and ^{19}F NMR revealed that no reaction had occurred.

Reaction of 2 with 2 equivalents of PhMeSiH$_2$. To a vial charged with [IPr•Cd(μ-OTf)$_2$]$_2$ (**2**) (0.035 g, 0.022 mmol) was added about 3 mL THF, forming a colorless solution. PhMeSiH$_2$ (12 μL, 0.087 mmol) was added to the solution. After 1.5 h, the formation of a metallic precipitate was observed and an aliquot was removed and filtered for NMR analysis. The ^{1}H NMR spectrum revealed the partial consumption of **2** (68 %) and the formation of PhMeSiH(OTf)[18] along with several other unidentified soluble products. No Cd–H resonances or $^{4}J_{H–Cd}$ satellites were observed. The ^{19}F spectrum revealed two peaks corresponding to **2** and PhMeSiH(OTf).

Reaction of 2 with 2 equivalents of HBpin. To a vial charged with [IPr•Cd(μ-OTf)$_2$]$_2$ (0.028 g, 0.018 mmol) was added about 3 mL of THF, leading to a colorless solution. HBpin (10 μL, 0.070 mmol) was added to the solution and the formation of a metallic precipitate was observed after 5 min. After 1.5 h an aliquot was removed and filtered for NMR analysis. The ^{1}H NMR spectrum revealed the complete consumption of **2** and the formation of pinB(OTf) (see below for independent synthesis) along with several other unidentified soluble products. No Cd–H resonances or $^{4}J_{H–Cd}$ satellites were observed. The ^{11}B{^{1}H} and ^{19}F spectra were consistent with that of pinB(OTf).

Independent synthesis of pinB(OTf). To a vial containing HBpin (100 μL, 0.689 mmol) and ca. 1 mL of toluene was added Me$_3$Si(OTf) (125 μL, 0.689 mmol). Bubbling was noted upon addition. After 1 h, an aliquot was removed from the reaction mixture revealing the formation of pinB(OTf). ^{1}H NMR (C$_6$D$_6$, 400.0 MHz): δ 1.01 (s, 12H, Bpin). ^{11}B{^{1}H} NMR (C$_6$D$_6$, 128.3 MHz): δ 21.9. ^{19}F NMR (C$_6$D$_6$, 376.3 MHz): δ −78.0. ^{13}C{^{1}H} NMR

(C_6D_6): δ 82.9 (*C*-CH_3), 24.6 (C-*C*H_3). A $^{13}C\{^1H\}$ resonance for the OTf group was not located.

Reaction of 5 with 2 equivalents of PhMeSiH$_2$. To a vial charged with [IPr•Hg(OTf)$_2$] (0.056 g, 0.063 mmol) was added ca. 3 mL of THF, forming a colorless solution. $PhMeSiH_2$ (17 μL, 0.13 mmol) was added to the solution and the formation of a metallic precipitate was immediately observed. After 45 min, a ca. 1 mL aliquot was filtered through diatomaceous earth for NMR analysis. The ^1H NMR spectrum revealed the complete consumption of **5** and the formation of PhMeSiH(OTf)[18] and free IPr, along with several other unidentified soluble products. No Hg–H resonances or $^4J_{H–Hg}$ satellites were observed. The ^{19}F spectrum revealed a single peak corresponding to PhMeSiH(OTf).

Reaction of 6 with PhMeSiH$_2$. To a vial containing [IPr•CdI(O*i*Pr)] (0.047 g, 0.068 mmol) was added ca. 2 mL of fluorobenzene, forming a colorless solution. To the solution was added $PhMeSiH_2$ (9.4 μL, 0.068 mmol) and the reaction mixture was allowed to stir, overnight. Slow formation of a metallic precipitate was observed over the course of the reaction. An aliquot was removed from the reaction mixture and filtered for NMR analysis revealing the formation of PhMeSiH(O*i*Pr)[43] and several unidentified soluble products.

2.5. Crystallographic Data

Table 2.3. Crystallographic data for compounds **1** and **2**.

Compound	**1**•Et_2O•0.5 CH_2Cl_2	**2**•2 CH_2Cl_2
formula	$C_{60.5}H_{83}Cd_2ClF_6I_2N_4O_7S_2$	$C_{60}H_{76}Cd_2Cl_4F_{12}N_4O_{12}S_4$
formula weight	1670.47	1768.08
crystal system	triclinic	monoclinic
space group	$P\overline{1}$	$P2_1/n$
a [Å]	13.1534(7)	12.2026(4)
b [Å]	15.6813(9)	16.7035(6)
c [Å]	17.5468(10)	19.8733(7)
α [°]	85.7770(7)	90
β [°]	83.8400(7)	104.6639
γ [°]	80.8984(7)	90
V [Å^3]	3547.1(3)	3918.8(2)
Z	2	2
ρ_{calcd} [g/cm^3]	1.564	1.498
μ [mm^{-1}]	1.631	0.869
T [°C]	−100	−100
$2\theta_{max}$ [°]	56.67	56.66
total data collected	33352	35890
unique data (R_{int})	17215 (0.0223)	9669 (0.0310)
obs data [$I \geq 2\sigma(I)$]	12990	9669
params	766	442
R_1 [$I \geq 2\sigma(I)$][a]	0.0483	0.0407
wR_2 [all data][a]	0.1424	0.1120
max/min $\Delta\rho$ [e/Å^3]	3.233/−1.618	1.325/−0.923

[a] $R_1 = \sum||F_o| - |F_c||/\sum|F_o|$; $wR_2 = [\sum w(F_o^2 - F_c^2)^2/\sum w(F_o^4)]^{1/2}$

Table 2.4. Crystallographic data for compounds **3** and **4**.

Compound	**3**•0.5 CH_2Cl_2	**4**
formula	$C_{93.5}H_{123}Cd_2ClF_{12}N_{14}O_{12}S_4$	$C_{28}H_{36}F_3HgIN_2O_3S$
formula weight	2251.54	865.14
crystal system	triclinic	monoclinic
space group	$P\bar{1}$	$P2_1/n$
a [Å]	12.5764(3)	10.7437(5)
b [Å]	17.6794(3)	16.3258(8)
c [Å]	24.7608(5)	18.7565(8)
α [°]	75.0092(9)	90
β [°]	86.3747(12)	94.4218(6)
γ [°]	79.7883(10)	90
V [Å^3]	5232.92(19)	3280.1(3)
Z	2	4
ρ_{calcd} [g/cm^3]	1.429	1.752
μ [mm^{-1}]	4.955	5.743
T [°C]	−100	−80
$2\theta_{max}$ [°]	144.59	55.11
total data collected	36769	18532
unique data (R_{int})	19913 (0.0229)	7466 (0.0256)
obs data [$I \geq 2\sigma(I)$]	17928	6334
params	1335	352
R_1 [$I \geq 2\sigma(I)$][a]	0.0344	0.0253
wR_2 [all data][a]	0.0883	0.0555
max/min $\Delta\rho$ [e/Å^3]	0.992/−0.583	0.859/−0.624

[a] $R_1 = \sum||F_o| - |F_c||/\sum|F_o|$; $wR_2 = [\sum w(F_o^2 - F_c^2)^2/\sum w(F_o^4)]^{1/2}$

Table 2.5. Crystallographic data for compounds **5** and **6**.

Compound	**5**•THF	**6**
formula	$C_{33}H_{44}F_6HgN_2O_7S_2$	$C_{54}H_{72}Cl_{12}Hg_6N_4$
formula weight	959.41	2406.10
crystal system	triclinic	monoclinic
space group	$P\bar{1}$	$P2_1/c$
a [Å]	10.2688(3)	21.5079(5)
b [Å]	10.8702(4)	10.8621(2)
c [Å]	18.4876(6)	16.2226(3)
α [°]	84.7868(4)	90
β [°]	87.1979(4)	108.8150(9)
γ [°]	71.4505(4)	90
V [Å^3]	1947.92(11)	3587.41(13)
Z	2	2
ρ_{calcd} [g/cm^3]	1.636	2.227
μ [mm^{-1}]	4.132	26.83
T [°C]	−80	−100
$2\theta_{max}$ [°]	55.10	148.35
total data collected	17780	24858
unique data (R_{int})	8952 (0.0151)	7282 (0.0378)
obs data [$I \geq 2\sigma(I)$]	8357	6719
params	460	343
R_1 [$I \geq 2\sigma(I)$][a]	0.0275	0.0283
wR_2 [all data][a]	0.0701	0.0736
max/min $\Delta\rho$ [e/Å^3]	2.628/−0.592	1.531/−2.008

[a] $R_1 = \sum||F_o| - |F_c||/\sum|F_o|$; $wR_2 = [\sum w(F_o^2 - F_c^2)^2/\sum w(F_o^4)]^{1/2}$

2.6. References

1. (a) Aldridge, S.; Downs, A. J. *Chem. Rev.* **2001**, *101*, 3305; (b) Ding, Y.; Hao, H.; Roesky, H. W.; Noltemeyer, M.; Schmidt, H.-G. *Organometallics* **2001**, *20*, 4806; (c) Mankad, N.P.; Laitar, D. S.; Sadighi, J. P. *Organometallics* **2004**, *23*, 3369; (d) Zhu, Z.; Brynda, M.; Wright, R. J.; Fischer, R. C.; Merrill, W. A.; Rivard, E.; Wolf, R.; Fettinger, J. C.; Olmstead, M. M.; Power, P. P. *J. Am. Chem. Soc.* **2007**, *129*, 10847; (e) Rivard, E. *Dalton Trans.* **2014**, *43*, 8577; (f) Marquardt, C.; Jurca, T.; Schwan, K.-C.; Stauber, A.; Virovets, A. V.; Whittell, G. R.; Manners, I.; Scheer, M. *Angew. Chem. Int. Ed.* **2015**, *54*, 13469; (g) Rivard, E. *Chem. Soc. Rev.* **2016**, *45*, 989; (h) Pagano, J. K.; Dorhout, J. M.; Czerwinski, K. R.; Morris, D. E.; Scott, B. L.; Waterman, R.; Kiplinger, J. L. *Organometallics* **2016**, *35*, 617, and references therein.
2. (a) Finholt, A. E.; Bond Jr., A. C.; Schlesinger, H. I. *J. Am. Chem. Soc.* **1947**, *69*, 1199; (b) Barbaras, G. D.; Dillard, C.; Finholt, A. E.; Wartik, T.; Wilzbach, K. E.; Schlesinger, H. I. *J. Am. Chem. Soc.* **1951**, *73*, 4585; (c) Shayesteh, A.; Yu, S.; Bernath, P. F. *Chem. Eur. J.* **2005**, *11*, 4709.
3. Rit, A.; Spaniol, T. P.; Maron, L.; Okuda, J. *Angew. Chem. Int. Ed.* **2013**, *52*, 4664.
4. Lummis, P. A.; Momeni, M. R.; Lui, M. W.; McDonald, R.; Ferguson, M. J.; Miskolzie, M.; Brown, A.; Rivard, E. *Angew. Chem. Int. Ed.* **2014**, *53*, 9347.
5. For selected examples of molecular cadmium and mercury hydrides, see: (a) Reger, D. L.; Mason, S. S.; Rheingold, A. L. *J. Am. Chem. Soc.* **1993**, *115*, 10406; (b) Dowling, C. M.; Parkin, G. *Polyhedron* **2001**, *20*, 285; (c) Nakamura, E.; Yu, Y.; Mori, S.; Yamago, S. *Angew. Chem. Int. Ed. Engl.* **1997**, *36*, 374.

6. For related studies and review articles, see: (a) Rit, A.; Zanardi, A.; Spaniol, T. P.; Maron, L.; Okuda, J. *Angew. Chem. Int. Ed.* **2014**, *53*, 13273; (b) Wiegand, A.-K.; Rit, A.; Okuda, J. *Coord. Chem. Rev.* **2016**, *314*, 71; (c) Revunova, K.; Nikonov, G. I. *Dalton Trans.* **2015**, *44*, 840; (d) Chong, C. C.; Kinjo, R. *ACS Catal.* **2015**, *5*, 3238; (e) Marinos, N. A.; Enthaler, S.; Driess, M. *ChemCatChem* **2010**, *2*, 846; (f) Mukherjee, D.; Ellern, A.; Sadow, A. D. *J. Am. Chem. Soc.* **2010**, *132*, 7582; (g) Bendt, G.; Schulz, S.; Spielmann, J.; Schmidt, S.; Bläser, D.; Wölper, C. *Eur. J. Inorg. Chem.* **2012**, 3725; (h) Jochmann, P.; Stephan, D. W. *Angew. Chem. Int. Ed.* **2013**, *52*, 9831; (i) Roberts, A. J.; Clegg, W.; Kennedy, A. R.; Probert, M. R.; Robertson, S. D.; Hevia, E. *Dalton Trans.* **2015**, *44*, 8169; (j) Sattler, W.; Ruccolo, S.; Chaijan, M. R.; Allah, T. N.; Parkin, G. *Organometallics* **2015**, *34*, 4717; (k) Bagherzadeh, S.; Mankad, N. P. *Chem. Commun.* **2016**, *52*, 3844; (l) Dawkins, M. J. C.; Middleton, E.; Kefalidis, C. E.; Dange, D.; Juckel, M. M.; Maron, L.; Jones, C. *Chem. Commun.* **2016**, *52*, 10490.

7. Al-Rafia, S. M. I.; Lummis, P. A.; Swarnakar, A. K.; Deutsch, K. C.; Ferguson, M. J.; McDonald, R.; Rivard, E. *Aust. J. Chem.* **2013**, *66*, 1235.

8. Ma, M.; Sidiropoulos, A.; Ralte, L.; Stasch, A.; Jones, C. *Chem. Commun.* **2013**, *49*, 48.

9. Pelz, S.; Mohr, F. *Organometallics* **2011**, *30*, 383.

10. Al-Rafia, S. M. I.; Malcolm, A. C.; Liew, S. K.; Ferguson, M. J.; Rivard, E. *J. Am. Chem. Soc.* **2011**, *133*, 777.

11. Halide bridging to form M_2I_2 rings is a common structural arrangement within Group 12 element chemistry: He, G.; Shynkaruk, O.; Lui, M. W.; Rivard, E. *Chem. Rev.* **2014**, *114*, 7815.

12. (a) Hegemann, C.; Tyrra, W.; Neudörfl, J.-M.; Marthur, S. *Organometallics* **2013**, *32*, 1654; (b) Gan, Q.; Ronson, T. K.; Vosburg, D. A.; Thoburn, J. D.; Nitschke, J. R. *J. Am. Chem. Soc.* **2015**, *137*, 1770.

13. Ruiz, D. A.; Melaimi, M.; Bertrand, G. *Chem. Commun.* **2014**, *50*, 7837.

14. Wang, D.; Wurst, K.; Buchmeiser, M. R. *J. Organomet. Chem.* **2004**, *689*, 2123.

15. Although THF is present within the coordination sphere of Hg in the X-ray structure of **5**•THF, coordinated THF was not observed in the ^{1}H NMR spectrum of **5** after this compound was dissolved in THF and stirred for one hour, followed by removal of the solvent under vacuum.

16. Richards, A. F.; Phillips, A. D.; Olmstead, M. M.; Power, P. P. *J. Am. Chem. Soc.* **2003**, *125*, 3204.

17. (a) Parks, D. J.; Blackwell, J. M.; Piers, W. E. *J. Org. Chem.* **2000**, *65*, 3090; (b) Oestreich, M.; Hermeke, J.; Mohr, J. *Chem. Soc. Rev.* **2015**, *44*, 2202.

18. Uhlig, W. *Chem. Ber.* **1992**, *125*, 47.

19. Hadlington, T. J.; Hermann, M.; Frenking, G.; Jones, C. *J. Am. Chem. Soc.* **2014**, *136*, 3028.

20. Chong, C. C.; Hirao, H.; Kinjo, R. *Angew. Chem. Int. Ed.* **2015**, *54*, 190.

21. (a) Cotton, F. A.; Wilkinson, G. in: *Advanced Inorganic Chemistry*, *4th ed.*, Wiley-Interscience, New York, **1980**, pp. 593–597; For selected examples of well-defined R*MM*R complexes (*M* = group 12 element), see: (b) Resa, I.; Carmona, E.; Gutierrez-

Puebla, E.; Monge, A. *Science* **2004**, *305*, 1136; (c) Zhu, Z.; Wright, R. J.; Olmstead, M. M.; Rivard, E.; Brynda, M.; Power, P. P. *Angew. Chem. Int. Ed.* **2006**, *45*, 5807; (d) Hicks, J.; Underhill, E. J.; Kefalidis, C. E.; Maron, L.; Jones, C. *Angew. Chem. Int. Ed.* **2015**, *54*, 10000.

22. (a) Jones, C. *Chem. Commun.* **2001**, 2293; (b) Kuhn, N.; Al-Sheikh, A. *Coord. Chem. Rev.* **2005**, *249*, 829; (c) Prabusankar, G.; Sathyanarayana, A.; Suresh, P.; Babu, C. N.; Srinivas, K.; Metla, B. P. R. *Coord. Chem. Rev.* **2014**, *269*, 829; (d) Wang, Y.; Robinson, G. H. *Inorg. Chem.* **2014**, *53*, 11815.
23. Baker, R. J.; Farley, R. D.; Jones, C. Kloth, M.; Murphy, D. M. *Chem. Commun.* **2002**, 1196.
24. For selected examples of mercury halide motifs with ≥ 3 Hg atoms (e.g. $[Hg_5Cl_{11}]^-$), see: (a) Brodersen, K.; Jensen, K.-P.; Thiele, G. *Z. Naturforsch.* **1980**, *35b*, 253; (b) Polyakova, N. I.; Poznyak, A. L.; Segienko, V. S. *Zh. Neorg. Khim.* **2000**, *45*, 1992; (c) Herler, S.; Mayer, P.; Nöth, H.; Schulz, A.; Suter, M.; Vogt, M. *Angew. Chem. Int. Ed.* **2001**, *40*, 3173; (d) Nockemann, P.; Pantenburg, I.; Meyer, G. *Z. Anorg. Allg. Chem.* **2007**, *633*, 814.
25. Baker, R. J.; Bettentrup, H.; Jones, C. *Eur. J. Inorg. Chem.* **2003**, 2446.
26. Pangborn, A. B.; Giardello, M. A.; Grubbs, R. H.; Rosen, R. K.; Timmers, F. J. *Organometallics* **1996**, *15*, 1518.
27. Jafarpour, L.; Stevens, E. D.; Nolan, S. P. *J. Organomet. Chem.* **2000**, *606*, 49.
28. Pelta, M. D.; Morris, G. A.; Stchedroff, M. J.; Hammond, S. J. *Magn. Reason. Chem.* **2002**, *40*, S147.
29. Botana, A.; Aguilar, J. A.; Nilsson, M.; Morris, G. A. *J. Magn. Reson.* **2011**, *208*, 270.

30. Connell, M. A.; Bowyer, P. J.; Bone, P. A.; Davis, A. L.; Swanson, A. G.; Nilsson, M.; Morris, G. A. *J. Magn. Reson.* **2009**, *198*, 121.

31. Hope, H. *Prog. Inorg. Chem.* **1994**, *41*, 1.

32. Sheldrick, G. M. *Acta. Crystallogr. Sect. A* **2015**, *71*, 3.

33. Sheldrick, G. M. *Acta. Crystallogr. Sect. C* **2015**, *71*, 3.

34. Spek, L. *Acta. Crystallogr. Sect. C* **2015**, *71*, 9.

35. Gaussian 9, Revision D.01, Frisch, M. J.; Trucks, G. W.; Schlegel, H. B.; Scuseria, G. E.; Robb, M. A.; Cheeseman, J. R.; Scalmani, G.; Barone, V.; Mennucci, B.; Petersson, G. A.; Nakatsuji, H.; Caricato, M.; Li, X.; Hratchian, H. P.; Izmaylov, A. F.; Bloino, J.; Zheng, G.; Sonnenberg, J. L.; Hada, M.; Ehara, M.; Toyota, K.; Fukuda, R.; Hasegawa, J.; Ishida, M.; Nakajima, T.; Honda, Y.; Kitao, O.; Nakai, H.; Vreven, T.; Montgomery, J. A.; Peralta, J. E.; Ogliaro, F.; Bearpark, M.; Heyd, J. J.; Brothers, E.; Kudin, K. N.; Staroverov, V. N.; Kobayashi, R.; Normand, J.; Raghavachari, K.; Rendell, A.; Burant, J. C.; Iyengar, S. S.; Tomasi, J.; Cossi, M.; Rega, N.; Millam, J. M.; Klene, M.; Knox, J. E.; Cross, J. B.; Bakken, V.; Adamo, C.; Jaramillo, J.; Gomperts, R.; Stratmann, R. E.; Yazyev, O.; Austin, A. J.; Cammi, R.; Pomelli, C.; Ochterski, J. W.; Martin, R. L.; Morokuma, K.; Zakrzewski, V. G.; Voth, G. A.; Salvodor, P.; Dannenberg, J. J.; Dapprich, S.; Daniels, A. D.; Farkas, Ö.; Foresman, J. B.; Ortiz, J. V.; Cioslowski, J.; Fox, D. J. Gaussian, Inc., Wallingford CT, **2009**.

36. (a) Lee, C.; Yang, W.; Parr, R. G. *Phys. Rev. B* **1988**, *37*, 785; (b) Becke, A. D. *Phys. Rev. A* **1988**, *38*, 3098; (c) Stephens, P. J.; Devlin, F. J.; Chabalowski, C. F.; Frisch, M. J. J. *Phys. Chem.* **1994**, *98*, 11623.

37. (a) Hariharan, P. C.; Pople, J. A. *Theor. Chim. Acta* **1973**, *28*, 213; (b) Francl, M. M.; Pietro, W. J.; Hehre, W. J.; Binkley, J. S.; Gordon, M. S.; DeFrees, D. J.; Pople, J. A. *J. Chem. Phys.* **1982**, *77*, 3654.
38. Zhao, Y.; Truhlar, D. G. *Theor. Chem. Acc.* **2008**, *120*, 215.
39. Kendall, R. A.; Dunning Jr., T. H.; Harrison, R. J. *J. Chem. Phys.* **1992**, *96*, 6796.
40. Figgen, D.; Rauhut, G.; Dolg, M.; Stoll, H. *Chem. Phys.* **2005**, *311*, 227.
41. Peterson, K. A.; Puzzarini, C. *Theor. Chem. Acc.* **2005**, *114*, 283.
42. Arrowsmith, M.; Hadlington, T. J.; Hill, M. S. Kociok-Köhn, G. *Chem. Commun.* **2012**, *48*, 4567.
43. Chakraborty, S.; Blacque, O.; Fox, T.; Berke, H. *ACS Catal.* **2013**, *3*, 2208.

Chapter 3: An *N*-Heterocyclic Carbene Supported Dichlorophosphine Azide and its Reactivity

3.1. Introduction

Originally referred to as "inorganic rubber", poly(dichlorophosphazene) $[Cl_2P{=}N]_n$ was first reported by Stokes in 1895.[1] This inorganic polymer was initially synthesized by the ring-opening polymerization (ROP) of hexachlorophosphazene $[Cl_2P{=}N]_3$, however it was of little practical importance at first due to its propensity to undergo hydrolysis. Later, Allcock and coworkers pioneered the synthesis of well-defined, air-stable polyphosphazenes $[R_2P{=}N]_n$ via the substitution of main chain chlorine atoms in poly(dichlorophosphazene) with various alkoxides, aryloxides, and amides.[2] During the search for alternate paths to polyphosphazenes and to gain insight into the ROP mechanism,[3] the reactivity of hexachlorophosphazene with Lewis acids[4] and Lewis bases[5] has been explored. Notably, when reacted with Lewis acids and bases, the cyclic nature of $[Cl_2P{=}N]_3$ is generally maintained with the phosphorus centers behaving as electron acceptors and the nitrogen atoms behaving as electron donors. Because of this, the synthesis of a dichlorophosphazene monomer $[Cl_2P{=}N]$ through a bottom-up approach was targeted. Such a species may allow for the controlled delivery of the $[Cl_2P{=}N]$ unit for materials synthesis; this work gains added inspiration from the selective construction of P–N chains via condensation chemistry[6] and the impressive recent isolation of monomeric phosphazenes R_2PN (R = bulky anionic substituent) via kinetic stabilization.[7]

The Rivard group has utilized a donor–acceptor concept to isolate various reactive main group species, typically relying on *N*-heterocyclic carbenes (NHCs) or *N*-heterocyclic

olefins (NHOs) as ligands.[8,9] Perhaps most relevant to the work described in this chapter, the Rivard group has observed that the inorganic acetylene complexes (NHC)HB=NH(LA); (LA = Lewis acid) can be synthesized by thermolysis of carbene-supported azidoboranes (NHC)BH_2N_3 in the presence of an appropriately bulky Lewis acid (Scheme 3.1).[10] A similar approach may therefore yield (NHC)Cl_2P=N(LA), a masked source of [Cl_2P=N], via dinitrogen extrusion.[11] Although the formation of the desired species was unsuccessful, an interesting NHC-supported phosphine azide adduct was synthesized,[12] (IPr)PCl_2N_3 [IPr = $(HCNDipp)_2C$:; Dipp = 2,6-*i*$Pr_2C_6H_3$], and its subsequent thermal rearrangement to the monomeric iminophosphine (IPr=N)PCl_2 was observed. Notably, (IPr=N)PCl_2 is a potential precursor to a wide range of strongly electron donating ligands of the general form (IPr=N)PR_2.[13] The latter transformation represents an example of a Staudinger reaction at a carbene-carbon center in preference over a proximal phosphine, and the energetics of this rearrangement were studied computationally. The Lewis basicity of the resulting iminophosphine was demonstrated by the synthesis of the stable phosphine-borane adduct (IPr=N)PCl_2•BH_3.

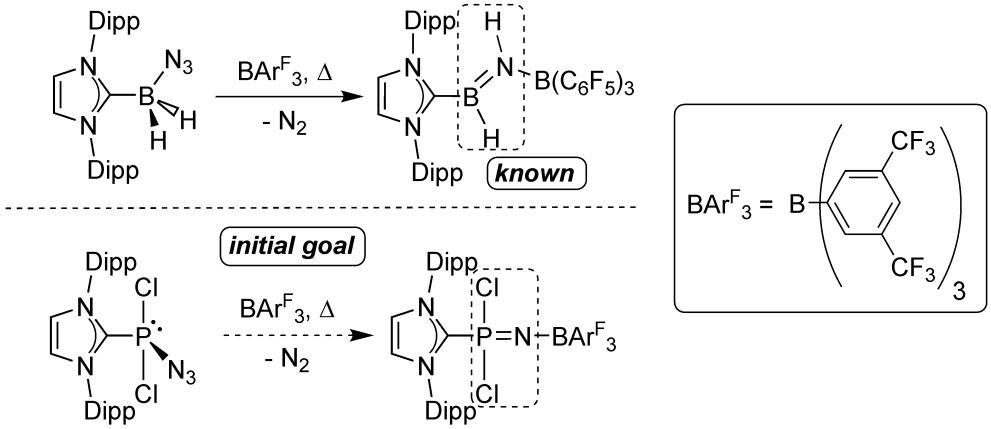

Scheme 3.1. Previous synthesis of an HBNH monomer and postulated route to a dichlorophosphazene monomer.

3.2. Results and Discussion

With the goal of forming the [Cl_2P=N] donor–acceptor species (IPr)Cl_2P=N(BAr^F_3), the soluble azide source [$n$$Bu_4N$]$N_3$ was first combined with BAr^F_3 (Ar^F = 3,5-$(CF_3)_2C_6H_3$) in fluorobenzene, leading to the *in situ* formation of the azidoborate [$n$$Bu_4N$][$N_3$–$BAr^F_3$] after one hour [broad $^{11}B\{^1H\}$ resonance at −0.6 ppm and a ^{19}F resonance at −62.2 ppm in C_6D_6].[14] Then, [$n$$Bu_4N$][$N_3$–$BAr^F_3$] was added to the known complex (IPr)PCl_3[15] with the intention of yielding (IPr)Cl_2P=N(BAr^F_3) in a one-pot fashion (via initial Cl^-/N_3^- exchange) to yield the intermediate (IPr)Cl_2P=N_3(BAr^F_3)[10] accompanied by the loss of N_2 (Scheme 3.2). The ^1H NMR spectrum of the product mixture after 90 minutes of stirring at room temperature revealed several species including unreacted (IPr)PCl_3, a highly soluble [$n$$Bu_4N$]$^+$ salt, and a new IPr-containing product. Crystallization of the reaction mixture afforded crystals of the new azidophosphine adduct (IPr)PCl_2N_3 (**1**), which was contaminated with ca. 50 % of co-crystallized (IPr)PCl_3; in the case of **1**, substitution of an equatorially bound chloride by azide transpired, with an overall seesaw geometry at phosphorus (*cf.* Figure 3.1). Although this direct approach did not afford the target species (as it did for previously reported HB=NH adducts),[10] the synthesis of **1** was conducted in an alternate fashion. As such, when Me_3Si–N_3 was added to a toluene slurry of (IPr)PCl_3 and the mixture stirred for one hour, **1** was obtained as a colorless solid in 94 % yield (Scheme 3.3) with ^1H and $^{31}P\{^1H\}$ NMR spectra which matched those of the major product formed in the above reaction between (IPr)PCl_3 and [$n$$Bu_4N$][$N_3$–$BAr^F_3$] (Scheme 3.2). From this reaction mixture, pure crystals of **1** were obtained and the structure of **1** was determined by single-crystal X-ray crystallography (Figure 3.1).

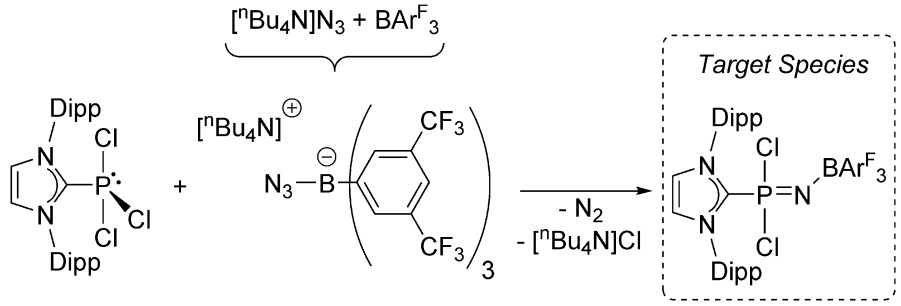

Scheme 3.2. Possible synthetic route to the target species (IPr)Cl_2P=N(BAr^F_3).

The molecular structure of **1** shows an expected distorted seesaw geometry, corresponding to an overall AEX_4 VSEPR arrangement,[15] indicating the presence of a stereochemically active phosphorus lone pair. The C_{NHC}–P distance in **1** [1.8762(15) Å] compares well with that of (IPr)PCl_3 [1.871(11) Å].[16] To determine whether thermolysis of **1** would yield an NHC-supported phosphinonitrene (R_2PN) or dichlorophosphazene oligomers via N_2 loss, compound **1** was heated to 80 °C in toluene for one hour (**Caution!**). As expected, the visible release of a gas from solution was noted, and $^{31}P\{^1H\}$ NMR analysis of the resulting pale orange slurry revealed the complete disappearance of **1** (δ 6.7 ppm) along with the formation of a new product with a downfield shifted $^{31}P\{^1H\}$ NMR resonance of 166.4 ppm; the latter resonance is in the range normally seen for monosubstituted phosphorus(III) dihalides $RPCl_2$,[17] suggesting that a Staudinger-type oxidation at phosphorus to yield a P^V species did not occur.[18] However, X-ray analysis of crystals of this product *did* show that a Staudinger reaction transpired, however via oxidation of the *N*-heterocyclic carbene ligand (and concomitant loss of N_2) to yield the new *N*-heterocyclic imine-substituted[19] phosphine (IPr=N)PCl_2 (**2**) in an 88 % yield (Scheme 3.3). Bertrand and coworkers have prepared the related backbone-saturated iminophosphine (SIPr=N)PCl_2 [SIPr = $(H_2CNDipp)_2C$:] by combining the lithiated imide [SIPr=N]Li with PCl_3.[20] As an alternative, it was shown that **2** can be synthesized directly

from IPr=N-SiMe$_3$ and PCl$_3$, with a slightly higher overall yield of 93 % versus the thermal-rearrangement route mentioned above.

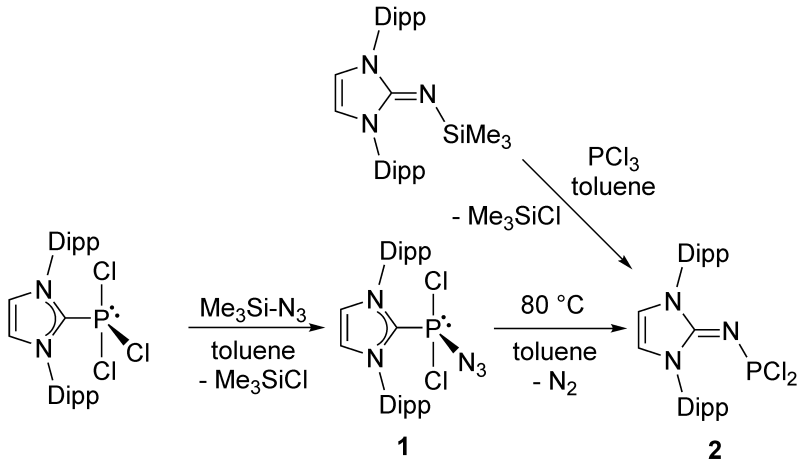

Scheme 3.3. Synthesis of (IPr)PCl$_2$N$_3$ (**1**) and its thermally induced rearrangement to (IPr=N)PCl$_2$ (**2**).

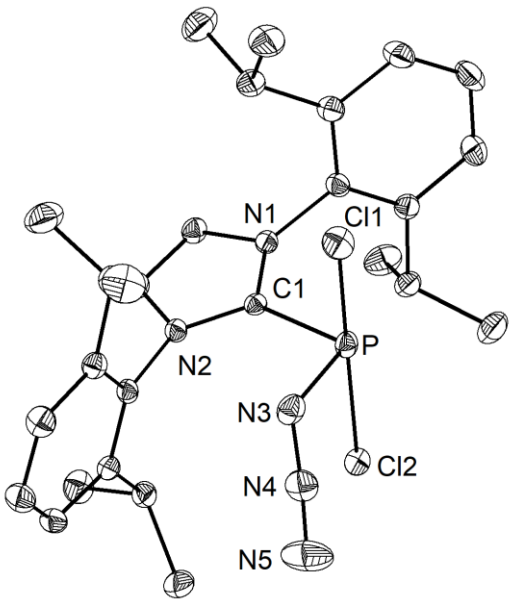

Figure 3.1. Molecular structure of (IPr)PCl$_2$N$_3$ (**1**) with thermal ellipsoids plotted at a 30 % probability level. All hydrogen atoms and fluorobenzene solvent have been omitted for clarity. Selected bond lengths [Å] and angles [°]: C1–P 1.8762(15), P–Cl1 2.1950(6), P–Cl2 2.5263(6), P–N3 1.7426(16), N3–N4 1.225(2), N4–N5 1.126(3); Cl1–P–Cl2 179.52(2), Cl1–P–N3 89.57(6), Cl1–P–C1 93.20(5), C1–P–N3 98.34(7).

The structure of **2** (Figure 3.2) shows metrical parameters consistent with the molecular structure drawn in Scheme 3.3, with a P–N single bond length of 1.6023(17) Å that is shorter than the P–N bond distance of 1.7426(16) Å found in the azido-phosphine adduct (IPr)PCl_2N_3 (**1**). Moreover, the internal IPr=N imine C=N double bond adopts a distance of 1.319(3) Å, in line with the retention of substantial double bond character, whereas the C_{IPr}=N–P bond angle is 127.64(15)°, consistent with the presence of sp^2 hybridization at nitrogen.

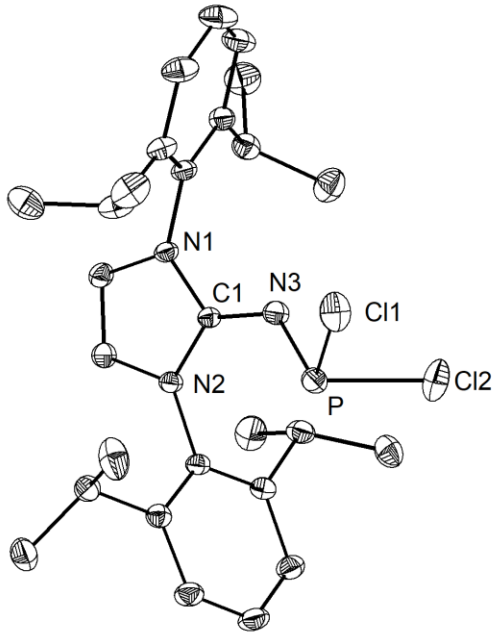

Figure 3.2. Molecular structure of (IPr=N)PCl_2 (**2**) with thermal ellipsoids plotted at a 30 % probability level. All hydrogen atoms have been omitted for clarity. Selected bond lengths [Å] and angles [°]: C1–N3 1.319(3), N3–P 1.6023(17), P–Cl1 2.1383(9), P–Cl2 2.1077(8); C1–N3–P 127.64(15), Cl1–P–Cl2 95.01(3), Cl1–P–N3 100.30(7), Cl2–P–N3 101.90(7).

The lone pair at the phosphorus(III) center in **2** was found to be chemically active, as evidenced by the reaction between **2** and $Me_2S{\bullet}BH_3$ (Scheme 3.4). The resulting stable dihalophosphine-borane adduct (IPr=N)$PCl_2{\bullet}BH_3$ (**3**) was generated in a nearly

quantitative yield (95 %) and the associated $^{1}H\{^{11}B\}$ NMR spectrum in C_6D_6 showed a doublet resonance ($^{2}J_{HP}$ = 11.0 Hz, P–BH_3), along with a broad doublet signal in the $^{311}B\{^{1}H\}$ NMR spectra arising from discernable $^{1}J_{PB}$ coupling (ca. 67 Hz). The structure of **3** was further confirmed by X-ray crystallography (Figure 3.3). Upon –BH_3 coordination, the IPr=N bond length remained nearly identical to **2** [1.324(2) Å] and a significant widening of the C1–N3–P angle was observed [143.70(14)° in **3** versus 127.64(15)° in **2**].

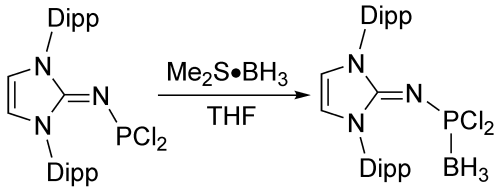

2 **3**

Scheme 3.4. Synthesis of (IPr=N)PCl_2•BH_3 (**3**) from (IPr=N)PCl_2 (**2**) and Me_2S•BH_3.

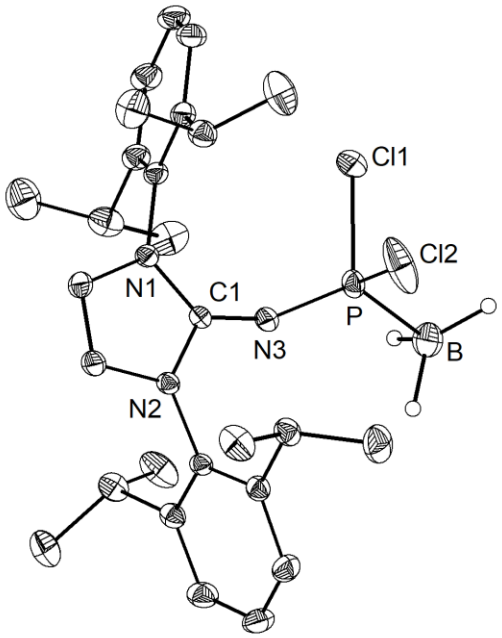

Figure 3.3. Molecular structure of (IPr=N)PCl_2•BH_3 (**3**) with thermal ellipsoids plotted at a 30 % probability level. All carbon-bound hydrogen atoms and fluorobenzene solvent have been omitted for clarity. Selected bond lengths [Å] and angles [°]: C1–N3 1.324(2), N3–P 1.5502(15), P–Cl1 2.0604(7), P–Cl2 2.0652(8), P–B 1.890(3), C1–N3–P 143.70(14), Cl1–P–N3 112.32(6), Cl2–P–N3 108.65(7), N3–P–B 117.51(13).

To probe the energetics associated with the thermal rearrangement of **1** into **2**, the dissociation of **1** was computed (Scheme 3.5). As expected, rupture of the dative C_{NHC}–P linkage was found to be both endothermic (Δ_rH = 17.6 kcal/mol) and endergonic (Δ_rG = 2.1 kcal/mol). The subsequent formation of **2** from free IPr and PCl_2N_3 was computed to be significantly exothermic (Δ_rH = −88.8 kcal/mol) and exergonic (Δ_rG = −86.1 kcal/mol) and driven by the formation of N_2. This resulted in an overall exothermic (Δ_rH = −71.2 kcal/mol) and exergonic (Δ_rG = −84.0 kcal/mol) process for the transformation of **1** into **2**.

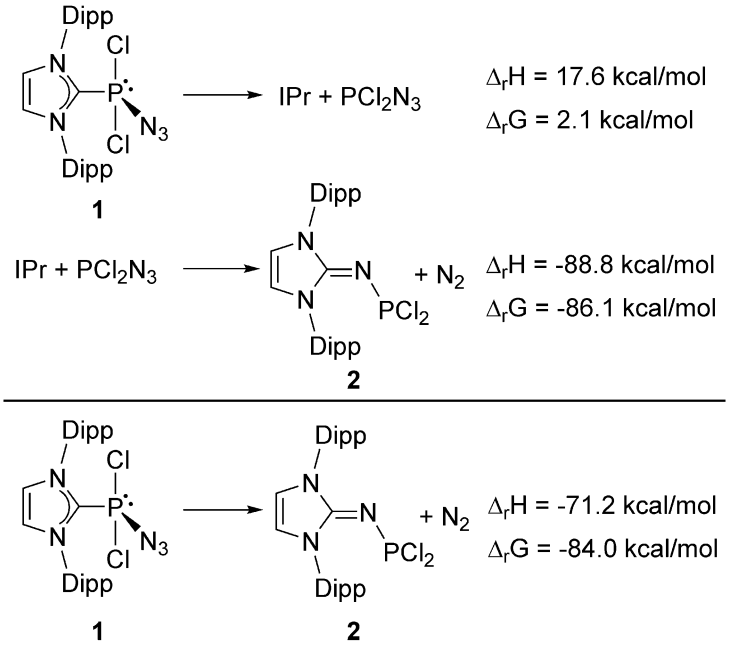

Scheme 3.5. Energetics of the thermal rearrangement of **1** into **2** via dissociation of carbene-phosphine adduct at the B3LYP/6-31G(d,p) level of theory.

The reactivity of **1** was then explored further to see whether Lewis acids would coordinate to the phosphorus-pendent azide group and induce the formation of donor–acceptor complexes of $[Cl_2P{=}N]$. Initially, BEt_3 was combined with **1** in toluene (Scheme 3.5); however, rather than azide coordination, the exclusive formation of $(IPr)BEt_3$ was observed,[21] presumably with the loss of the potentially volatile PCl_2N_3 (**Caution!**). Given

the possible risks[22] associated with the liberation of PCl_2N_3, this line of reactivity was not investigated further with BEt_3.

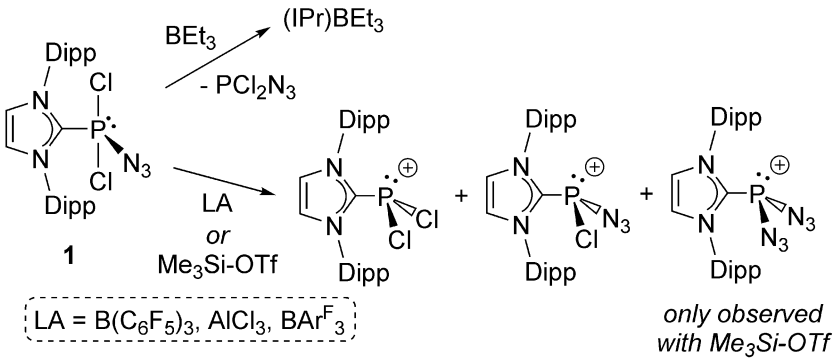

Scheme 3.6. The reactivity of $(IPr)PCl_2N_3$ (**1**) toward various Lewis acids (LA) and Me_3Si–OTf.

When compound **1** was combined with the strong Lewis acids $AlCl_3$, $B(C_6F_5)_3$, or BAr^F_3, intractable mixtures containing several unidentified species were formed, tentatively assigned as the salts $[(IPr)PCl_2]^+$ and $[(IPr)PCl(N_3)]^+$ (Scheme 3.6). For example, a $^{31}P\{^1H\}$ NMR spectrum from the reaction of **1** with $B(C_6F_5)_3$ showed the complete consumption of **1** and the formation of several products, including two major products with signals at δ 112.9 ppm (ca. 27 %) and δ 100.7 ppm (ca. 68 %), that closely match those found for the known compounds $[(IPr)PCl_2]OTf$[12a] (δ 113.7 ppm) and $[(IPr)PCl(N_3)]OTf$[12b] (δ 104.0 ppm), respectively. Similar observations were noted for the reaction of **1** with either $AlCl_3$ or BAr^F_3. All attempts to obtain pure products via fractional crystallization yielded poorly diffracting crystals consisting of co-crystallized $[(IPr)PCl(N_3)]^+$ and $[(IPr)PCl_2]^+$ cations with $Cl^-/[N_3–LA]^-$ anions [LA = $AlCl_3$, $B(C_6F_5)_3$ and BAr^F_3] resulting from concurrent chloride and azide abstraction from **1**. Next, **1** was combined with one equivalent of the electrophile Me_3Si–OTf to form $[(IPr)PCl(N_3)]^+$ in a controlled fashion. The $^{31}P\{^1H\}$ NMR spectrum in CD_3CN revealed the formation of

[(IPr)PCl_2]OTf[12a] (δ 113.7 ppm, ca. 17 %), along with the previously reported compound [(IPr)$P(N_3)_2$]OTf[12b] (δ 104.0 ppm, ca. 16 %) and the tentatively assigned species [(IPr)$PCl(N_3)$]OTf (δ 103.5 ppm, 67 %), again indicating that both chloride and azide abstraction were occurring.

3.3. Conclusions

Although preparation of the target dichlorophosphazene complex (NHC)Cl_2P=N(LA) was not achieved, a new NHC-bound azidophosphine (IPr)PCl_2N_3 (**1**) was prepared as a room-temperature stable solid. The reactivity of **1** toward a variety of Lewis acids and Me_3Si–OTf was explored, giving evidence of nonselective chloride and azide ion abstraction. Heating compound **1** afforded (IPr=N)PCl_2 (**2**) in high yield via a Staudinger-type reaction, which favors azide coupling (nitrene addition) to a carbene-carbon center over a phosphorus(III) site. Compound **2** is a promising ligand precursor to *N*-heterocyclic imine-supported phosphines, which have been shown to be strong donors in the past.[13b] Future work will involve the use of non-azide routes to accomplish nitrogen atom delivery[23] in the main group.

3.4. Experimental Details

3.4.1. General

All reactions were performed in an inert atmosphere glovebox (Innovative Technology, Inc.). Solvents were dried using a Grubbs-type solvent purification system[24] manufactured by Innovative Technologies, Inc., degassed (freeze–pump–thaw method), and stored under an atmosphere of nitrogen prior to use. PCl_3 was purchased from Sigma-Aldrich and distilled under nitrogen prior to use. Me_3Si–N_3 was purchased from Alfa Aesar and used

as received. $AlCl_3$ was purchased from Sigma-Aldrich and sublimed under dynamic vacuum (ca. 10^{-3} torr; 1 torr = 133.322 Pa) prior to use. $Me_2S{\bullet}BH_3$ was purchased as a 2.0 M solution in THF from Sigma-Aldrich and used as received. $(IPr)PCl_3$,[15] $(IPr{=}N)SiMe_3$,[25] $B(C_6F_5)_3$[3,26] and $BAr^F{}_3$ (Ar^F = 3,5-$(F_3C)_2C_6H_3$))[27] were prepared according to literature procedures. ^1H, $^{13}C\{^1H\}$, $^{11}B\{^1H\}$, ^{19}F and $^{31}P\{^1H\}$ NMR spectra were recorded on 400, 500, 600, or 700 MHz Varian Inova instruments and were referenced externally to $SiMe_4$ (^1H, $^{13}C\{^1H\}$), 85 % H_3PO_4 ($^{31}P\{^1H\}$), $ClCF_3$ (^{19}F) or $F_3B{\bullet}OEt_2$ ($^{11}B\{^1H\}$). Elemental analyses were performed by the Analytical and Instrumentation Laboratory at the University of Alberta. Melting points were measured in sealed glass capillaries under nitrogen by using a MelTemp apparatus.

3.4.2. X-ray Crystallography

Crystals for X-ray diffraction studies were removed from a vial (in a glovebox) and immediately coated with a thin layer of hydrocarbon oil (Paratone-N). A suitable crystal was then mounted on a glass fiber and quickly placed in a low temperature stream of nitrogen on the X-ray diffractometer.[28] All data were collected using a Bruker APEX II CCD detector/D8 or PLATFORM diffractometer using Mo K_α or Cu K_α radiation, with the crystals cooled to −100 °C. The data were corrected for absorption through Gaussian integration from the indexing of the crystal faces. Crystal structures were solved using intrinsic phasing (SHELXT)[29] and refined using SHELXL-2014.[29] The assignment of hydrogen atom positions were based on the sp^2 or sp^3 hybridization geometries of their attached carbon atoms and were given thermal parameters 20 % greater than those of their parent atoms.

Special refinement conditions. Compound **2**: The crystal used for data collection was found to display non-merohedral twinning. Both components of the twin were indexed with the program *CELL_NOW* (Bruker AXS Inc., Madison, WI, 2004). The second twin component can be related to the first component by 180º rotation about the [1 0 0] axis in real space and about the [1 $-1/2$ 0] axis in reciprocal space. Integrated intensities for the reflections from the two components were written into a *SHELXL-2014* HKLF 5 reflection file with the data integration program *SAINT* (version 8.37A), using all reflection data (exactly overlapped, partially overlapped and non-overlapped). The refined value of the twin fraction (*SHELXL-2014* BASF parameter) was 0.2012(13).

3.4.3. Computational Methods

The energetics of the thermal rearrangement: $(IPr)PCl_2N_3 \rightarrow (IPr{=}N)PCl_2 + N_2$ were computed using the Gaussian 09, Rev. D.01 software package.[30] Input structures were taken from X-ray crystallographic data (when possible) and optimized using the B3LYP[31] functional and 6-31G(d,p)[32] basis set in the gas phase. The optimized geometries were confirmed to be minima on the potential energy surface using frequency analysis.

3.4.4. Synthetic Procedures

Synthesis of $(IPr)PCl_2N_3$ (1). To a vial containing a slurry of $(IPr)PCl_3$ (0.291 g, 0.552 mmol) in 15 mL of toluene was added $Me_3Si{-}N_3$ (73.4 µL, 0.553 mmol). The reaction mixture was stirred for 1 hour and the volatiles were removed from the colorless slurry *in vacuo* to afford **1** as a colorless solid (0.278 g, 94 %). Colorless crystals suitable for X-ray crystallographic analysis were obtained by layering a fluorobenzene solution of **1** with hexanes and storing in a −30 °C freezer for 2 days. ^{1}H NMR ([D_8]THF, 498.1 MHz): δ

7.82 (s, 2H, NC*H*), 7.53 (t, 2H, $^{3}J_{HH}$ = 8.0 Hz, *p*-Ar*H*), 7.39 (d, 4H, $^{3}J_{HH}$ = 8.0 Hz, *m*-Ar*H*), 3.17 (broad septet, 4H, $^{3}J_{HH}$ = 6.5 Hz, C*H*(CH_3)$_2$), 1.42 (d, 12H, $^{3}J_{HH}$ = 6.5 Hz, CH(C*H*$_3$)$_2$), 1.11 (d, 12H, $^{3}J_{HH}$ = 6.5 Hz, CH(C*H*$_3$)$_2$). $^{13}C\{^{1}H\}$ NMR ([D_8]THF, 125.3 MHz): δ 147.4 (N*C*H), 132.1 (Ar*C*), 126.9 (Ar*C*), 125.0 (Ar*C*), 124.8 (Ar*C*), 29.9 (*C*H(CH_3)$_2$), 26.2 (CH(*C*H$_3$)$_2$), 23.1 (CH(*C*H$_3$)$_2$). An N*C*N resonance was not found. $^{31}P\{^{1}H\}$ NMR ([D_8]THF, 201.6 MHz): δ 11.3. M.p. 153 °C (decomp.) IR (Nujol, cm^{-1}): 2132 (m, ν-N_3). Elemental analyses were performed on three different samples. In all cases, the CHN values were systematically high in carbon content.

Synthesis of (IPr=N)PCl_2 (2).

Route A: A thick-walled Schlenk flask was loaded with a slurry of **1** (0.153 g, 0.287 mmol) in ca. 18 mL of toluene, partially evacuated, and sealed with a J Young valve. The flask was then heated to 80 °C for 1 hour (**Caution!**) where bubbling was observed, leading to the formation of a pale orange slurry. The slurry was then returned to the glovebox and transferred to a vial where the volatiles were removed *in vacuo* yielding **2** as an off-white solid (0.128 g, 88 %). Colorless crystals suitable for X-ray crystallographic analysis were obtained by storing a fluorobenzene solution of **2** in a −30 °C freezer overnight.

Route B: To a vial containing a solution of (IPr=N)$SiMe_3$ (0.396 g, 0.831 mmol) in 15 mL toluene was added PCl_3 (72.8 μL, 0.832 mmol). The resulting slurry was stirred for 1 hour and the volatiles were removed *in vacuo* yielding **2** as an off-white solid (0.390 g, 93 %).

Analytical data for 2: ^{1}H NMR (C_6D_6, 399.8 MHz): δ 7.17 (t, 2H, $^{3}J_{HH}$ = 8.0 Hz, *p*-Ar*H*), 7.06 (d, 4H, $^{3}J_{HH}$ = 8.0 Hz, *m*-Ar*H*), 5.94 (s, 2H, NC*H*), 2.88 (septet, 4H, $^{3}J_{HH}$ = 6.8 Hz, C*H*(CH_3)$_2$), 1.40 (broad d, 12H, $^{3}J_{HH}$ = 6.8 Hz, CH(C*H*$_3$)$_2$), 1.07 (broad d, 12H, $^{3}J_{HH}$ = 6.8 Hz, CH(C*H*$_3$)$_2$). $^{13}C\{^{1}H\}$ NMR (C_6D_6, 125.7 MHz): δ 147.0 (Ar*C*), 132.2 (Ar*C*), 131.0

(Ar*C*), 124.6 (Ar*C*), 116.8 (N*C*H), 29.3 (*C*H(CH_3)$_2$), 24.7 (CH(*C*H_3)$_2$), 23.4 (CH(*C*H_3)$_2$). An N*C*N resonance was not observed. $^{31}P\{^1H\}$ NMR (C_6D_6, 161.8 MHz): δ 166.4. M.p. 221 °C (decomp.) Anal. Calcd. for $C_{27}H_{36}Cl_2N_3P$: C 64.28, H 7.19, N 8.33. Found: C 63.76, H 7.21, N 7.53.

Synthesis of (IPr=N)PCl_2•BH_3 (3). To a vial containing a 15 mL THF slurry of **2** (0.231 g, 0.457 mmol) was added a 2.0 M THF solution of Me_2S•BH_3 (228.8 µL, 0.458 mmol). The reaction mixture was stirred for 1 hour and the resultant slurry was concentrated to dryness *in vacuo* affording **3** as an off-white solid (0.225 g, 95 %). Colorless crystals suitable for X-ray crystallographic analysis were obtained by storing a fluorobenzene solution of **3** in a −30 °C freezer for 3 days. $^1H\{^{11}B\}$ NMR (C_6D_6, 498.1 MHz): δ 7.17 (t, 2H, $^3J_{HH}$ = 8.0 Hz, *p*-Ar*H*), 7.05 (d, 4H, $^3J_{HH}$ = 8.0 Hz, *m*-Ar*H*), 6.04 (s, 2H, NC*H*), 2.79 (septet, 4H, $^3J_{HH}$ = 6.5 Hz, C*H*(CH_3)$_2$), 2.02 (d, 3H, $^2J_{HP}$ = 11.0 Hz, P-B*H*$_3$), 1.41 (d, 12H, $^3J_{HH}$ = 6.5 Hz, CH(C*H*$_3$)$_2$), 1.03 (d, 12H, $^3J_{HH}$ = 7.0 Hz, CH(C*H*$_3$)$_2$). $^{13}C\{^1H\}$ NMR (C_6D_6, 125.7 MHz): δ 146.6 (Ar*C*), 131.5 (Ar*C*), 131.2 (Ar*C*), 124.7 (Ar*C*), 117.8 (N*C*H), 29.3 (*C*H(CH_3)$_2$), 25.2 (CH(*C*H_3)$_2$), 23.2 (CH(*C*H_3)$_2$). $^{31}P\{^1H\}$ NMR (C_6D_6, 201.6 MHz): δ 85.6 (broad d, $^1J_{PB}$ = 66.5 Hz). $^{11}B\{^1H\}$ NMR (C_6D_6, 159.8 MHz): δ −24.9 (broad d, $^1J_{PB}$ = 49.1 Hz). M.p. 165 °C (decomp.) Anal. Calcd. for $C_{27}H_{39}BCl_2N_3P$: C 62.57, H 7.58, N 8.11. Found: C 63.42, H 7.83, N 7.55.

Reaction of 1 with Me_3Si–OTf. To a vial containing a ca. 10 mL toluene slurry of (IPr)PCl_2N_3 (0.134 g, 0.252 mmol) was added Me_3Si–OTf (45.4 µL, 0.251 mmol) and the resulting colorless slurry was stirred for 1 hour. A ca. 1 mL aliquot was removed from the reaction mixture and the volatiles were removed *in vacuo* yielding a colorless solid. A $^{31}P\{^1H\}$ NMR assay of the solid revealed the complete consumption of (IPr)PCl_2N_3 and

the formation of the known products $[(IPr)PCl_2]OTf$[12a] and $[(IPr)P(N_3)_2]OTf$[12b] and a new signal tentatively assigned to $[(IPr)PCl(N_3)]OTf$. $^{31}P\{^1H\}$ NMR (CD_3CN, 161.8 MHz): δ 113.7 (17 %, $[(IPr)PCl_2]OTf$), 104.0 (16 %, $[(IPr)P(N_3)_2]OTf$), 103.5 (67 %, $[(IPr)PCl(N_3)]OTf$). Attempts to isolate the major product by crystallization from toluene, THF, or fluorobenzene were unsuccessful.

3.5. Crystallographic Data

Table 3.1. Crystallographic data for compounds **1**–**3**.

Compound	**1**•C_6H_5F	**2**	**3**•0.5 C_6H_5F
formula	$C_{33}H_{41}Cl_2FN_5P$	$C_{27}H_{36}Cl_2N_3P$	$C_{30}H_{41.5}BCl_2F_{0.5}N_3P$
formula weight	628.58	504.46	566.34
crystal system	monoclinic	triclinic	monoclinic
space group	$P2_1/c$	$P\bar{1}$	$P2_1/n$
a [Å]	21.3900(4)	9.2023(3)	10.9329(2)
b [Å]	10.7667(2)	9.4927(3)	18.7403(4)
c [Å]	15.4357(3)	17.3362(5)	15.6449(3)
α [°]	90	90.4763(16)	90
β [°]	109.7132(7)	91.8703(14)	95.5863(9)
γ [°]	90	116.5497(14)	90
V [Å^3]	3346.50(11)	1353.53(7)	3190.19(11)
Z	4	2	4
ρ_{calcd} [g/cm^3]	1.248	1.238	1.179
μ [mm^{-1}]	2.476	2.856	2.494
T [°C]	−100	−100	−100
$2\theta_{max}$ [°]	144.71	140.58	148.00
total data collected	22726	83614	22375
unique data (R_{int})	6622 (0.0188)	4968 (0.0597)	6463 (0.0190)
obs data [$I \geq 2\sigma(I)$]	6302	4643	6158
params	367	299	382
R_1 [$I \geq 2\sigma(I)$][a]	0.0417	0.0421	0.0497
wR_2 [all data][a]	0.1151	0.1157	0.1325
max/min $\Delta\rho$ [e/Å^3]	0.628/−0.546	0.968/−0.427	1.259/−1.275

[a] $R_1 = \sum||F_o| - |F_c||/\sum|F_o|$; $wR_2 = [\sum w(F_o^2 - F_c^2)^2/\sum w(F_o^4)]^{1/2}$

3.6. References

1. (a) Stokes, H. N. *Am. Chem. J.* **1895**, *17*, 275; (b) Stokes, H. N. *Am. Chem. J.* **1896**, *18*, 629.
2. (a) Allcock, H. R.; Kugel, R. L. *J. Am. Chem. Soc.* **1965**, *87*, 4216; (b) Allcock, H. R.; Kugel, R. L.; Valan, K. J. *Inorg. Chem.* **1966**, *5*, 1709; (c) Allcock, H. R.; Kugel, R. L. *Inorg. Chem.* **1966**, 5, 1716; For selected review articles, see: (d) Neilson, R. H.; Wisian-Neilson, P. *Chem. Rev.* **1988**, *88*, 541; (e) Allen, C. W. *Coord. Chem. Rev.* **1994**, *130*, 137; (f) Manners, I. *Angew. Chem., Int. Ed. Engl.* **1996**, *35*, 1602; (g) Priegert, A. M.; Rawe, B. W.; Serin, S. C.; Gates, D. P. *Chem. Soc. Rev.* **2016**, *45*, 922.
3. (a) Lund, L. G.; Paddock, N. L.; Proctor, J. E.; Searle, H. T. *J. Chem. Soc.* **1960**, 2542; (b) Chandrasekhar, V.; Thilagar, P.; Murugesa Pandian, B. *Coord. Chem. Rev.* **2007**, *251*, 1045; (c) Zhang, Y.; Huynh, K.; Manners, I.; Reed, C. A. *Chem. Commun.* **2008**, 494.
4. Tun, Z.-M.; Heston, A. J.; Panzner, M. J.; Medvetz, D. A.; Wright, B. D.; Savant, D.; Dudipala, V. R.; Banerjee, D.; Rinaldi, P. L.; Youngs, W. J.; Tessier, C. A. *Inorg. Chem.* **2011**, *50*, 8937 and references therein.
5. (a) Boomishankar, R.; Ledger, J.; Guilbaud, J.-B.; Campbell, N. L.; Bacsa, J.; Bonar-Law, R.; Khimyak, Y. Z.; Steiner, A. *Chem. Commun.* **2007**, 5152; (b) Al-Rafia, S. M. I.; Ferguson, M. J.; Rivard, E. *Inorg. Chem.* **2011**, *50*, 10543.
6. (a) Honeyman, C. H.; Manners, I.; Morrissey, C. T.; Allcock, H. R. *J. Am. Chem. Soc.* **1995**, *117*, 7035; (b) Rivard, E.; Lough, A. J.; Manners, I. *Inorg. Chem.* **2004**, *43*, 2765; (c) Rivard, E.; Huynh, K.; Lough, A. J.; Manners, I. *J. Am. Chem. Soc.* **2004**,

126, 2286; (d) Huynh, K.; Lough, A. J.; Forgeron, M. A. M.; Bendle, M.; Soto, A. P.; Wasylishen, R. E.; Manners, I. *J. Am. Chem. Soc.* **2009**, *131*, 7905.

7. (a) Dielmann, F.; Back, O.; Henry-Ellinger, M.; Jerabek, P.; Frenking, G.; Bertrand, G. *Science* **2012**, *337*, 1526; (b) Dielmann, F.; Bertrand, G. *Chem. Eur. J.* **2015**, *21*, 191.
8. For relevant review articles, see: (a) Rivard, E. *Dalton Trans.* **2014**, *43*, 8577; (b) Rivard, E. *Chem. Soc. Rev.* **2016**, *45*, 989; (c) Roy, M. M. D.; Rivard, E. *Acc. Chem. Res.* **2017**, *50*, 2017.
9. For the use of Lewis bases to stabilize reactive phosphorus-based species, see the following selected references: (a) Gray, P. A.; Burford, N. *Coord. Chem. Rev.* **2016**, *324*, 1; (b) Burford, N.; Cameron, T. S.; Ragogna, P. J.; Ocando-Mavarez, E.; Gee, M.; McDonald, R.; Wasylishen, R. E. *J. Am. Chem. Soc.* **2001**, *123*, 7947; (c) Schwedtmann, K.; Hennersdorf, F.; Bauzá, A.; Frontera, A.; Fischer, R.; Weigand, J. J. *Angew. Chem., Int. Ed.* **2017**, *56*, 6218; (d) Macdonald, C. L. B.; Binder, J. F.; Swidan, A.; Nguyen, J. H.; Kosnik, S. C.; Ellis, B. D. *Inorg. Chem.* **2016**, *55*, 7152; (e) Dube, J. W.; Macdonald, C. L. B.; Ragogna, P. J. *Angew. Chem., Int. Ed.* **2012**, *51*, 13026; (f) Graham, C. M. E.; Pritchard, T. E.; Boyle, P. D.; Valjus, J.; Tuononen, H. M.; Ragogna, P. J. *Angew. Chem., Int. Ed.* **2017**, *56*, 6236; (g) Price, A. N.; Nichol, G. S.; Cowley, M. J. *Angew. Chem., Int. Ed.* **2017**, *56*, 9953; (h) Wang, Y.; Hickox, H. P.; Xie, Y.; Wei, P.; Cui, D.; Walter, M. R.; Schaefer, H. F., III; Robinson, G. H. *Chem. Commun.* **2016**, *52*, 5746; (i) Majhi, P. K.; Chow, K. C. F.; Hsieh, T. H. H.; Bowes, E. G.; Schnakenburg, G.; Kennepohl, P.; Streubel, R.; Gates, D. P. *Chem.*

Commun. **2016**, *52*, 998; (j) Graham, C. M. E.; Millet, C. R. P.; Price, A. N.; Valjus, J.; Cowley, M. J.; Tuononen, H. M.; Ragogna, P. J. *Chem. Eur. J.* **2018**, *24*, 672.

10. (a) Swarnakar, A. K.; Hering-Junghans, C.; Nagata, K.; Ferguson, M. J.; McDonald, R.; Tokitoh, N.; Rivard, E. *Angew. Chem., Int. Ed.* **2015**, *54*, 10666; (b) Swarnakar, A. K.; Hering-Junghans, C.; Ferguson, M. J.; McDonald, R.; Rivard, E. *Chem. Sci.* **2017**, *8*, 2337.
11. The Rivard group has also shown that donor-acceptor complexes can effectively release their trapped molecular cargo, as evidenced by the use of GeH_2 complexes to yield luminescent germanium nanoparticles: (a) Purkait, T. K.; Swarnakar, A. K.; De Los Reyes, G. B.; Hegmann, F. A.; Rivard, E.; Veinot, J. G. C. *Nanoscale* **2015**, *7*, 2241; (b) Thimer, K. C.; Al-Rafia, S. M. I.; Ferguson, M. J.; McDonald, R.; Rivard, E. *Chem. Commun.* **2009**, 7119.
12. For related examples of NHC-stabilized P^{III}-azides and chlorides, see: (a) Henne, F. D.; Schnöckelborg, E.-M.; Feldmann, K.-O.; Grunenberg, J.; Wolf, R.; Weigand, J. J. *Organometallics* **2013**, *32*, 6674; (b) Henne, F. D.; Dickschat, A. T.; Hennersdorf, F.; Feldmann, K.-O.; Weigand, J. J. *Inorg. Chem.* **2015**, *54*, 6849.
13. (a) Dumrath, A.; Lübbe, C.; Neumann, H.; Jackstell, R.; Beller, M. *Chem. Eur. J.* **2011**, *17*, 9599; (b) Wünsche, M. A.; Mehlmann, P.; Witteler, T.; Buß, F.; Rathmann, P.; Dielmann, F. *Angew. Chem., Int. Ed.* **2015**, *54*, 11857; (c) Paisley, N. R.; Lui, M. W.; McDonald, R.; Ferguson, M. J.; Rivard, E. *Dalton Trans.* **2016**, *45*, 9860; (d) Lui, M. W.; Shynkaruk, O.; Oakley, M. S.; Sinelnikov, R.; McDonald, R.; Ferguson, M. J.; Meldrum, A.; Klobukowski, M.; Rivard, E. *Dalton Trans.* **2017**, *46*, 5946.

14. For the related use of $[N_3–BR_3]^-$ anions to yield Lewis acid coordinated uranium nitrides (after N_2 loss), see: Fox, A. R.; Arnold, P. L.; Cummins, C. C. *J. Am. Chem. Soc.* **2010**, *132*, 3250.

15. Gillespie, R. J. *Coord. Chem. Rev.* **2008**, *252*, 1315.

16. Wang, Y.; Xie, Y.; Abraham, M. Y.; Gilliard, R. J., Jr.; Wei, P.; Schaefer, H. F., III; Schleyer, P. v. R.; Robinson, G. H. *Organometallics* **2010**, *29*, 4778.

17. Burford, N.; Cameron, T. S.; Conroy, K. D.; Ellis, B.; Macdonald, C. L. B.; Ovans, R.; Phillips, A. D.; Ragogna, P. J.; Walsh, D. *Can. J. Chem.* **2002**, 80, 1404.

18. Gololobov, Y. G.; Kasukhin, L. F. *Tetrahedron* **1992**, *48*, 1353.

19. For reviews of N-heterocyclic imines in main group chemistry, see: (a) Ochiai, T.; Franz, D.; Inoue, S. *Chem. Soc. Rev.* **2016**, *45*, 6327; (b) Todd, A. D. K.; McClennan, W. L.; Masuda, J. D. *RSC Adv.* **2016**, *6*, 69270.

20. Kinjo, R.; Donnadieu, B.; Bertrand, G. *Angew. Chem., Int. Ed.* **2010**, *49*, 5930.

21. (a) Monot, J.; Brahmi, M. M.; Ueng, S.-H.; Robert, C.; Murr, M. D.-E.; Curran, D. P.; Malacria, M.; Fensterbank, L.; Lacôte, E. *Org. Lett.* **2009**, *11*, 4914; (b) Al-Rafia, S. M. I.; Lummis, P. A.; Swarnakar, A. K.; Deutsch, K. C.; Ferguson, M. J.; McDonald, R.; Rivard, E. *Aust. J. Chem.* **2013**, *66*, 1235.

22. Dillon, K. B.; Platt, A. W. G.; Waddington, T. C. J. *Chem. Soc., Dalton Trans.* **1980**, 1036.

23. Betley, T. A.; Peters, J. C. *J. Am. Chem. Soc.* **2004**, *126*, 6252.

24. Pangborn, A. B.; Giardello, M. A.; Grubbs, R. H.; Rosen, R. K.; Timmers, F. J. *Organometallics* **1996**, *15*, 1518.

25. Tamm, M.; Randoll, S.; Herdtweck, E.; Kleigrewe, N.; Kehr, G.; Erker, G.; Rieger, B. *Dalton Trans.* **2006**, 459.

26. (a) Kuprat, M.; Lehmann, M.; Schulz, A.; Villinger, A. *Organometallics* **2010**, *29*, 1421; (b) Massey, A. G.; Park, A. J. *J. Organomet. Chem.* **1964**, *2*, 245.

27. Kolychev, E. L.; Bannenberg, T.; Freytag, M.; Daniliuc, C. G.; Jones, P. G.; Tamm, M. *Chem. Eur. J.* **2012**, *18*, 16938.

28. Hope, H. *Prog. Inorg. Chem.* **1994**, *41*, 1.

29. (a) Sheldrick, G. M. *Acta Crystallogr. Sect. A* **2015**, *71*, 3; (b) Sheldrick, G. M. *Acta. Crystallogr. Sect. C* **2015**, *71*, 3.

30. Gaussian 9, Revision D.01, Frisch, M. J.; Trucks, G. W.; Schlegel, H. B.; Scuseria, G. E.; Robb, M. A.; Cheeseman, J. R.; Scalmani, G.; Barone, V.; Mennucci, B.; Petersson, G. A.; Nakatsuji, H.; Caricato, M.; Li, X.; Hratchian, H. P.; Izmaylov, A. F.; Bloino, J.; Zheng, G.; Sonnenberg, J. L.; Hada, M.; Ehara, M.; Toyota, K.; Fukuda, R.; Hasegawa, J.; Ishida, M.; Nakajima, T.; Honda, Y.; Kitao, O.; Nakai, H.; Vreven, T.; Montgomery, J. A.; Peralta, J. E.; Ogliaro, F.; Bearpark, M.; Heyd, J. J.; Brothers, E.; Kudin, K. N.; Staroverov, V. N.; Kobayashi, R.; Normand, J.; Raghavachari, K.; Rendell, A.; Burant, J. C.; Iyengar, S. S.; Tomasi, J.; Cossi, M.; Rega, N.; Millam, J. M.; Klene, M.; Knox, J. E.; Cross, J. B.; Bakken, V.; Adamo, C.; Jaramillo, J.; Gomperts, R.; Stratmann, R. E.; Yazyev, O.; Austin, A. J.; Cammi, R.; Pomelli, C.; Ochterski, J. W.; Martin, R. L.; Morokuma, K.; Zakrzewski, V. G.; Voth, G. A.; Salvodor, P.; Dannenberg, J. J.; Dapprich, S.; Daniels, A. D.; Farkas, Ö.; Foresman, J. B.; Ortiz, J. V.; Cioslowski, J.; Fox, D. J. Gaussian, Inc., Wallingford CT, **2009**.

31. (a) Lee, C.; Yang, W. Parr, R. G. *Phys. Rev. B*,**1988**, *37*, 785; (b) Becke, A. D. *Phys. Rev. A* **1988**, *38*, 3098; (c) Stephens, P. J.; Devlin, F. J.; Chabalowski, C. F.; Frisch, M. J.; *J. Phys. Chem.* **1994**, *98*, 11623.

32. (a) Hariharan, P. C.; Pople, J. A. *Theor. Chim. Acta* **1973**, *28*, 213; (b) Francl, M. M.; Pietro, W. J.; Hehre, W. J.; Binkley, J. S.; Gordon, M. S.; DeFrees, D. J.; Pople, J. A. *J. Chem. Phys.*, **1982**, *77*, 3654.

Chapter 4: The Design of an Extremely Bulky *N*-Heterocyclic Carbene and its Stabilization of Low-Valent Inorganic Fragments

4.1. Introduction

The isolation of increasingly reactive low-coordinate species with hitherto unknown bonding motifs generally relies upon new ligands and synthetic methods (Scheme 4.1).[1] Such studies have led to the important discovery that Earth-abundant main group elements in low-coordination environments can display transition metal-like reactivity, such as the mild activation of H_2.[2] Within this research theme, *N*-heterocyclic carbene (NHC) ligands hold a prominent position due to their ease of synthesis, strong donor ability, and high level of structural tunability.[3] In this chapter, the extremely hindered carbene ITr is introduced, bearing flanking trityl (CPh_3) groups (ITr = [$(HCNCPh_3)_2C$:]) with the highest percent buried volume (%V_{bur}) reported to date (Scheme 4.1).[4] This ligand supports a thermally stable quasi one-coordinate Tl^I cation $[(ITr)Tl]^+$, a versatile transmetalation/ligation agent for the further preparation of cationic inorganic species previously inaccessible via known strategies. Additionally, ITr was found to stabilize low-coordinate Ag^I environments as weak solvates $[(ITr)Ag(sol)]^+$ (sol = PhF, MesH or CH_2Cl_2) and as a solvent-free dimer $[(ITr)Ag]_2^{2+}$.

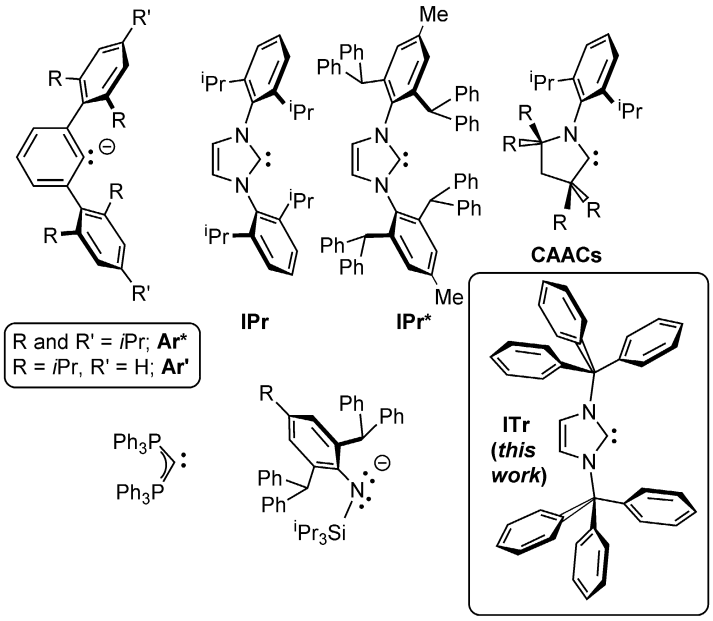

Scheme 4.1. Representative sterically encumbered monodentate ligands used to access/stabilize low-coordinate inorganic centers.

4.2. Results and Discussion

The trityl-based carbene ITr was readily prepared by two efficient steps (Scheme 4.2): first, the commercially available 1-tritylimidazole was combined with Ph_3C–OTf to give the precursor imidazolium salt [ITrH]OTf (**1**) in a 78 % yield. The target trityl-functionalized carbene ITr (**2**) was then prepared in 89 % yield by deprotonation of **1** with $K[N(SiMe_3)_2]$ in toluene. As expected for an NHC, a significantly deshielded carbene $^{13}C\{^1H\}$ NMR resonance was found in ITr (225.8 ppm in C_6D_6), while this encumbered NHC (Figure 4.1) is stable up to approximately 164 °C under nitrogen atmosphere.

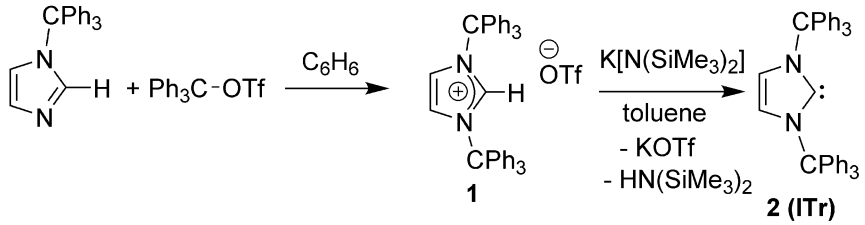

Scheme 4.2. Facile two-step synthesis of the extremely bulky carbene ITr (**2**).

The steric shielding caused by the flanking trityl groups is evident when one examines the structure of ITr and its 1:1 adduct with AuCl, [(ITr)AuCl] (**3**) (Figure 4.2; Scheme 4.3). Recently, the percent buried volume (%V_{bur}) has been used to quantify the bulk provided by NHC or phosphine ligands.[4] Accordingly, the %V_{bur} about the gold atom afforded by the ITr donor in **3** is an impressive 57.3 %. This represents the most sterically encumbering NHC to date and for comparison, the %V_{bur} for the AuCl complexes of the widely used bulky NHCs IPr and IPr* (Scheme 4.1) are 45.4 and 50.4 %, respectively.[5]

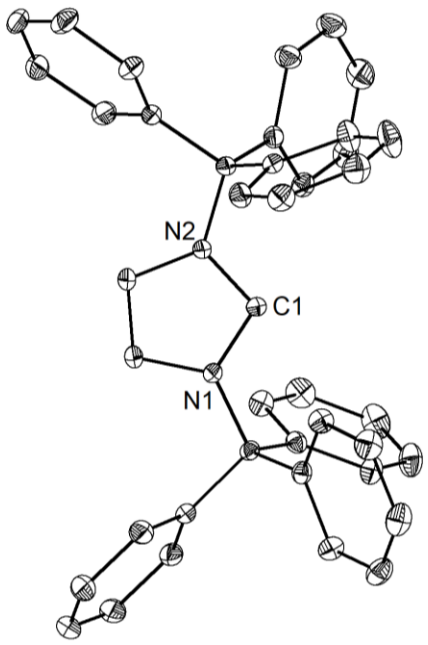

Figure 4.1. Molecular structure of ITr (**2**) with thermal ellipsoids plotted at a 30 % probability level. All hydrogen atoms have been omitted for clarity. Selected bond lengths [Å] and angles [°]: C1–N1 1.3663(18), C1–N2 1.3667(17); N1-C1-N2 102.66(11).

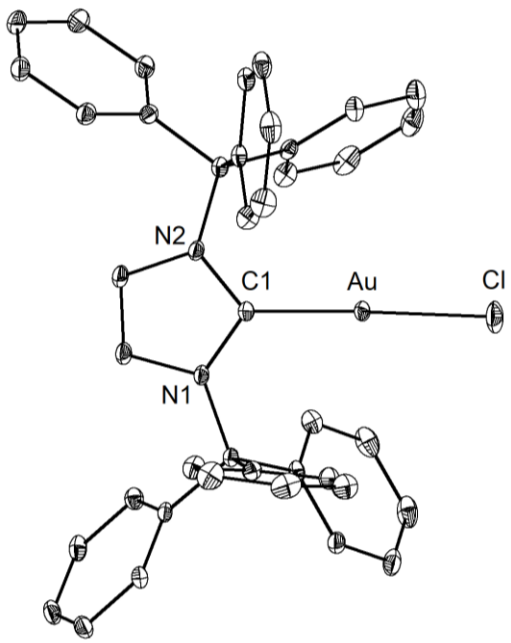

Figure 4.2. Molecular structure of [(ITr)AuCl] (**3**) with thermal ellipsoids plotted at a 30 % probability level. All hydrogen atoms have been omitted for clarity. Selected bond lengths [Å] and angles [°]: C1–Au 1.996(2), Au–Cl 2.2774(7); C1-Au-Cl 175.91(8).

The coordination profile of ITr was investigated by the synthesis of a variety of 1:1 adducts (**3**–**5**), as summarized in Scheme 4.3. The CuI adduct [(ITr)CuI] (**4**) demonstrates the steric influence of the ligand, showing a severely canted C_{ITr}-Cu-I angle [165.91(9)°] from its ideal linear geometry (Figure 4.3). The Rh^{I} carbonyl complex [(ITr)Rh(CO)$_2$Cl] (**5**) was used to extract an estimated donor strength of ITr relative to previously reported carbenes by determination of the Tolman electronic parameter (TEP).[6] Specifically, two IR ν(CO) stretches in **5** were observed at 2055 and 1980 cm^{-1}, leading to a TEP of 2034 cm^{-1}; this low value implies a remarkable donor strength in ITr that exceeds those found in benchmark NHCs (e.g., IPr: 2052 cm^{-1}) and in many cyclic(alkyl)amino carbenes, CAACs (as low as 2042 cm^{-1}).[6] The X-ray structure of [(ITr)Rh(CO)$_2$Cl] (**5**) along with computational studies provided insight into the surprisingly high estimated donor strength

of the ITr ligand (Figure 4.4). In this Rh complex, a set of flanking phenyl groups (one from each CPh_3 unit) form close Rh–C_{aryl} contacts, approaching 2.93(1) Å.

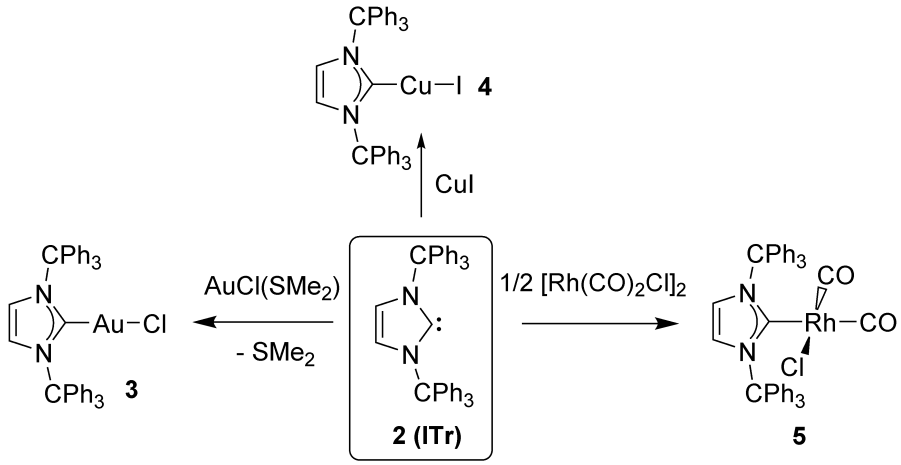

Scheme 4.3. Initially explored coordination chemistry involving ITr.

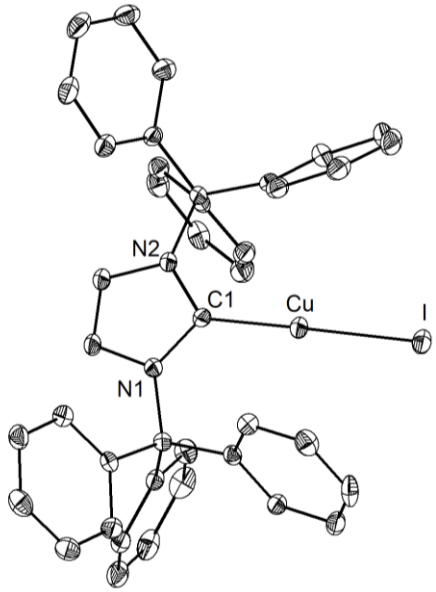

Figure 4.3. Molecular structure of [(ITr)CuI] (**4**) with thermal ellipsoids plotted at a 30 % probability level. All hydrogen atoms and toluene solvate have been omitted for clarity. Selected bond lengths [Å] and angles [°]: C1–Cu 1.917(3), Cu–I 2.4336(4); C1-Cu-I 165.91(9).

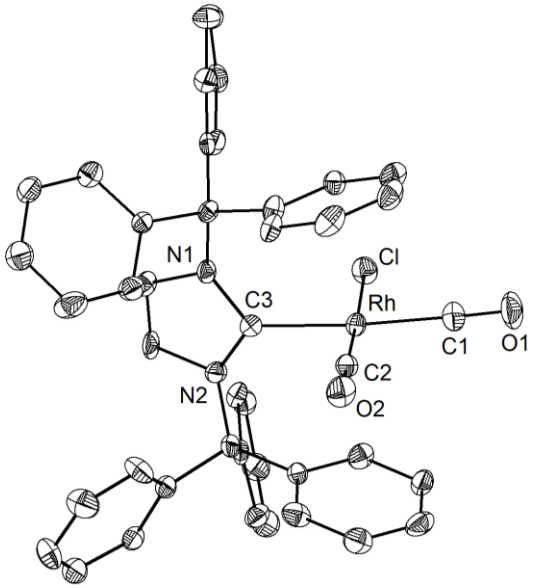

Figure 4.4. Molecular structure of [(ITr)Rh(CO)$_2$Cl] (**5**) with thermal ellipsoids plotted at a 30 % probability level. All hydrogen atoms and dichloromethane solvate have been omitted for clarity. Selected bond lengths [Å] and angles [°]: C3–Rh 2.068(9), Rh–Cl 2.389(3), Rh–C1 1.904(10), Rh–C2 1.827(10), C1–O1 1.138(11), C2–O2 1.151(10); C3-Rh-C1 85.2(2), C2- Rh-C3 93.3(4), C1-Rh-C2 92.8(4), Cl-Rh-C1 88.8(3).

The computed MOs of **5** contain various occupied orbital sets that feature the same η^2 or η^3 arene–Rh interactions (Figure 4.5), whereas second-order perturbation analysis also uncovered electron donation from the CPh$_3$ aryl groups to Rh. Thus, the combination of direct C_{NHC}–Rh σ-ligation along with accompanying arene to Rh donation places additional electron density at the metal, affording a lower TEP value than expected. The gas-phase proton affinities (PA) were also computed for IPr, Im*i*Pr$_2$ [Im*i*Pr$_2$ = (HCN*i*Pr)$_2$C:], and ITr and it was found that the trityl-capped carbene ITr has the most exothermic binding of H^+ amongst the compound series: PA = 283.6 kcal/mol versus 275.6 kcal mol^{-1} in IPr and 272.8 kcal/mol in Im*i*Pr$_2$.

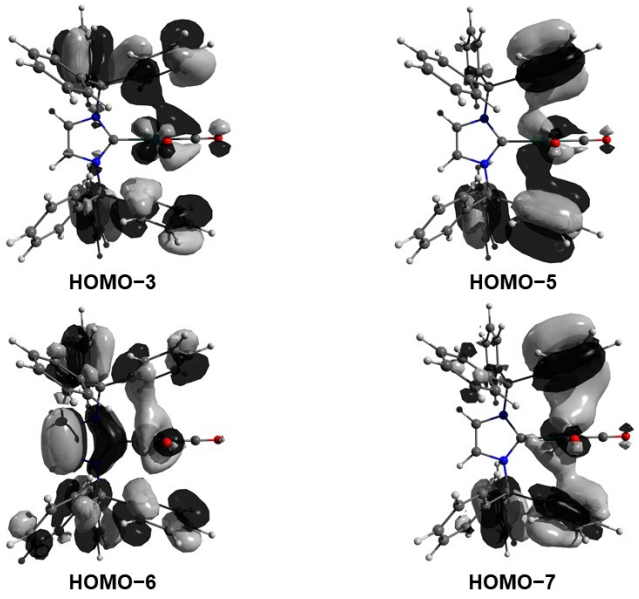

Figure 4.5. Selected molecular orbitals of [(ITr)Rh(CO)$_2$Cl] (**5**) demonstrating π_{arene}-to-metal donation from flanking aryl groups.

The steric shield and added flanking aryl interactions of the ITr donor were utilized in order to gain access to elusive main group cations not typically isolable using known ligands/strategies. The ultimate goal would be to obtain new low-coordinate main group and transition metal element entities as active catalysts[2] and as reactive precursors for advanced materials synthesis.[7]

Motivated by the substantial challenges associated with isolating thallium–carbene complexes,[8,9] the synthesis of quasi one-coordinate thallium(I) cations supported by ITr was investigated. The first member of this structural series [(ITr)Tl]OTf (**6**) was readily obtained as a remarkably thermally stable solid [M.p. 130 °C (decomp.)] from ITr and Tl[OTf] (OTf = $O_3SCF_3^-$) in THF (Scheme 4.4). X-ray crystallography (Figure 4.6) revealed that the Tl^I center in **6** is nestled into a steric pocket created by the two CPh_3 groups with a long Tl–OTf distance of 2.679(7) Å (sum of covalent radii for Tl and O: 2.18 Å).[10]

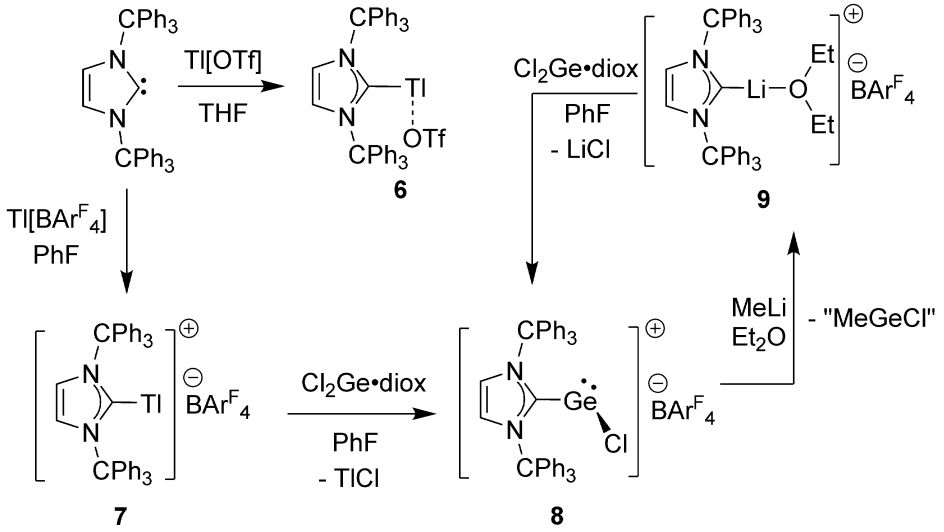

Scheme 4.4. Preparation of the ITr-supported thallium(I), lithium and germanium(II) cations **6**–**9**.

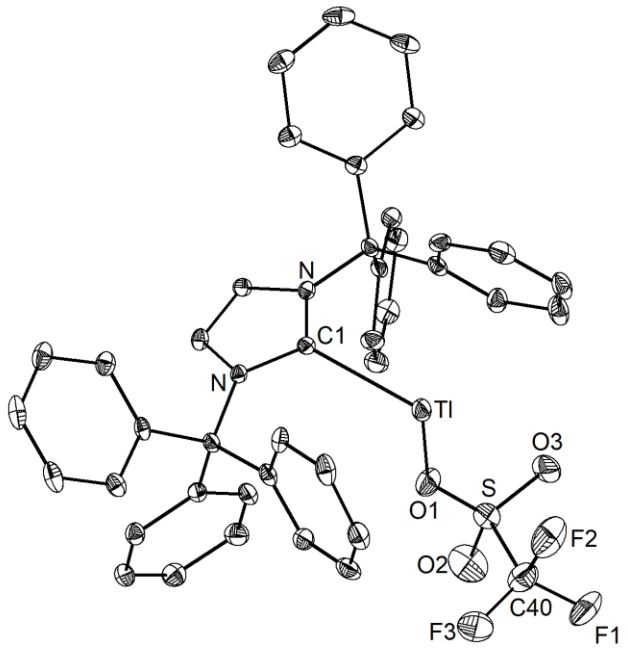

Figure 4.6. Molecular structure of [(ITr)Tl]OTf (**6**) with thermal ellipsoids plotted at a 30 % probability level. All hydrogen atoms have been omitted for clarity and flanking. Selected bond lengths [Å] and angles [°]: C1–Tl 2.679(7), Tl–O1 2.769(7); C1-Tl-O1 84.3(2).

By replacing OTf^- in **6** with the more weakly coordinating borate anion $[BAr^F{}_4]^-$ (Ar^F = 3,5-$(F_3C)_2C_6H_3$), an ion-separated pair containing a quasi monocoordinate Tl^I cation, $[(ITr)Tl][BAr^F{}_4]$ (**7**) was obtained (Scheme 4.4; Figure 4.7). The Tl–C_{NHC} distance in **7** [2.559(3) Å] is substantially shorter than in **6** [2.679(7) Å], and is the shortest Tl^I–C_{NHC} interaction reported to date.[8] For comparison, the Tl–C distance within Power's landmark one-coordinate aryl–thallium species Ar*Tl (Ar* = 2,6-$Trip_2C_6H_3$; Trip = 2,4,6-*i*$Pr_3C_6H_2$) is 2.34(1) Å.[11a] Flanking arene–Tl interactions are also present in **7**, and lie within the range of 3.13 to 3.73 Å; related Tl–arene interactions of 3.19(1) to 3.58(1) Å can be found in Aldridge's pyridine–Tl complex $[(2,6\text{-}Mes_2C_4N)Tl(PhF)_2][BAr^F{}_4]$ (Mes = 2,4,6-$Me_3C_6H_2$).[12]

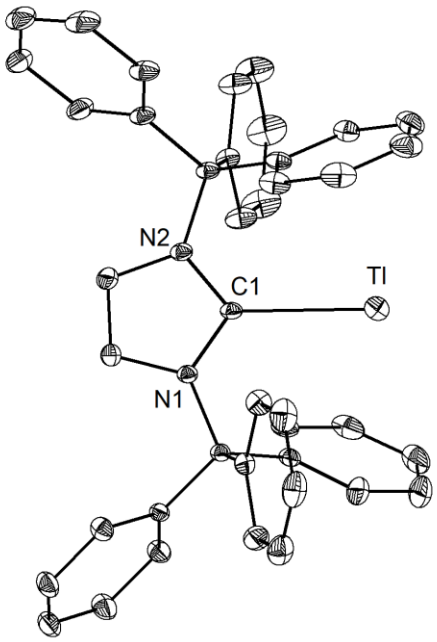

Figure 4.7. Molecular structure of $[(ITr)Tl][BAr^F{}_4]$ (**7**) with thermal ellipsoids plotted at a 30 % probability level. All hydrogen atoms and the $[BArF]^-$ counterion have been omitted for clarity. Selected bond lengths [Å] and angles [°]: C1–Tl 2.559(3), N1–C1 1.358(4), N2–C2 1.363(4); Tl-C1-N1 125.6(2), Tl-C1-N2 129.5(2), N1-C1-N2 104.8(3).

Next, the use of [(ITr)Tl][BAr^F_4] (**7**) as a concurrent halide abstractor (via the Tl^I cation) and source of ligating ITr was investigated to generate new main group element cations. For example, [(ITr)Tl][BAr^F_4] (**7**) rapidly and cleanly reacted with Cl_2Ge•dioxane in fluorobenzene solvent to give the stable $[GeCl]^+$ complex [(ITr)GeCl][BAr^F_4] (**8**) (Figure 4.8); the insoluble TlCl byproduct could be easily removed by filtration. The C_{NHC}–Ge distance in **8** [2.110(4) Å] compares well with the corresponding distance in the stable Ge^{II} adduct (IPr)$GeCl_2$ [2.112(2) Å].[13] The steric influence of the ITr ligand is manifest in the position of the Ge–Cl bond, which is nearly perpendicular to the central imidazolium ring in the carbene donor [N1A-C1A-Ge1A-Cl1A torsion angle 85.0(4)°]. The successful formation of **8** is noteworthy as attempts to directly prepare the related cation $[(IPr)GeCl]^+$ via halide abstraction from the less hindered Ge^{II} adduct (IPr)$GeCl_2$[13] were unsuccessful.[14]

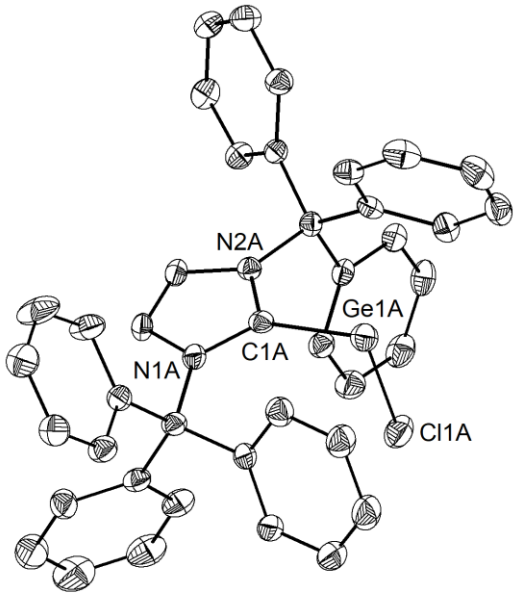

Figure 4.8. Molecular structure of [(ITr)GeCl][BAr^F_4] (**8**) with thermal ellipsoids plotted at a 30 % probability level. All hydrogens atoms and the $[BAr^F]^-$ counterion have been omitted for clarity. Selected bond lengths [Å] and angles [°]: C1A–Ge1A 2.110(4), Ge1A–Cl1A 2.2171(13); C1A-Ge1A-Cl1A 92.81(11), N1A-C1A-Ge1A-Cl1A 85.0(4).

[(ITr)GeCl][BAr^F_4] (**8**) was then combined with MeLi in Et_2O with the goal of generating the alkyl germanium(II) cation $[(ITr)GeMe]^+$. As was expected, a colorless precipitate was observed, however no resonance could be located for the CH_3 group in the ^1H NMR spectrum of the soluble product, whereas a singlet resonance at −2.3 ppm (in $CDCl_3$ solvent) was recorded by $^7Li\{^1H\}$ NMR spectroscopy. X-ray crystallography identified the species as the carbene-ligated lithium salt [(ITr)Li(OEt_2)][BAr^F_4] (**9**; Scheme 4.4). Significant arene–Li interactions were present in the solid state, as was evidenced by notable canting from linearity of the C_{NHC}-Li-O angle [151.4(4) Å] and short C_{arene}–Li contacts in the range of 2.57–3.43 Å (Figure 4.9). Moreover, [(ITr)Li(OEt_2)][BAr^F_4] (**9**) is a low-toxicity synthetic analogue of **7**,[15] as the reaction between **9** and Cl_2Ge•dioxane also gave the Ge^{II} complex **8** in quantitative yield (Scheme 4.4).

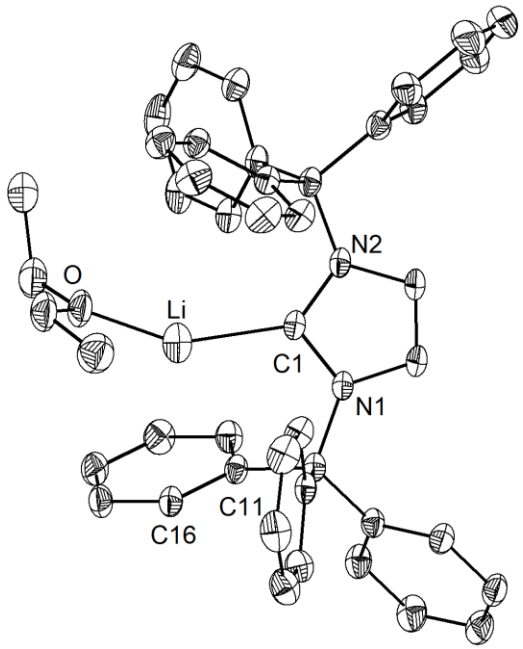

Figure 4.9. Molecular structure of [(ITr)Li(OEt$_2$)][BAr$^F{}_4$] (**9**) with thermal ellipsoids plotted at a 30 % probability level. All hydrogen atoms and the [BAr$^F{}_4$]$^-$ counterion have been omitted for clarity. Selected bond lengths [Å] and angles [°]: C1–Li 2.076(6), Li–O 1.815(6), C11–Li 2.572(7), C16–Li 2.771(8); O-Li-C1 151.4(4).

Given the successful formation of the stable, low-coordinate inorganic cations **6**–**9**, the isolation of a monocoordinate silver(I) cation was attempted. Group 11 elements in +1 oxidation states are widely used as catalysts to activate carbon–carbon multiple bonds.[16] In many instances the active species in these transformations is presumed to be a monocoordinate ligand-stabilized metal cation, [L–M]$^+$ [L = phosphine or *N*-heterocyclic carbene (NHC); M = Cu, Ag or Au],[16d] yet truly monocoordinate coinage metal cations have not yet been observed. Recently, several research groups have attempted to synthesize monocoordinate cations of the general form [NHC–M]$^+$ supported by very hindered NHCs such as IPr** [IPr** = (HCNAr**)$_2$C:] (Scheme 4.5). Arguably, the closest approach to monocoordination amongst the coinage metals was achieved by Straub and coworkers with

their toluene adduct [(IPr**)Au(PhMe)]$^{+}$, prepared from [(IPr**)AuCl] and Na[SbF_6].[17] Replacement of the [SbF_6]$^{-}$ counterion by the less coordinating [$BAr^F{}_4$]$^{-}$ anion led to Ar^F abstraction by gold to yield the Au^I aryl complex [(IPr**)Au(Ar^F)].[18] Attempts to obtain low-coordinate M^I species via hydride abstraction from metastable [(NHC)MH]$_{1,2}$ complexes afforded the aryl gold species [(NHC)Au(C_6F_5)][19] or hydride-bridged products such as [(NHC)M(μ-H)B(C_6F_5)$_3$] where M = copper[20] and silver.[21] The electrophilic nature of silver(I) ions has also been demonstrated by the coordination of the unsaturated substrates ethylene, acetylene and carbon monoxide.[22] Furthermore, the large size of Ag^I often leads to coordination of multiple NHC equivalents (i.e. in [(NHC)$_2$Ag][AgX_2] or [(NHC)$_2$$Ag_2$(μ-X)]X; X = halide or triflate) rather than simple [(NHC)Ag–X] adducts.[23]

Looking to form a suitable [(ITr)AgX] precursor for this study, the free ligand ITr was combined with AgOTf in toluene to yield [(ITr)Ag(OTf)] (**10**) as an analytically pure solid in 93 % yield; this compound can be stored under ambient lighting (under N_2) for weeks without noticeable decomposition [M.p. = 187 °C (decomp.)], again highlighting the stabilizing influence of the ITr ligand. X-ray crystallography (Figure 4.10) shows the presence of a Ag–OTf interaction [Ag–O bond length = 2.172(4) Å; *cf.* 2.137(2) Å in (SIPr)AgOTf;[23b] SIPr = (H_2CNDipp)$_2$C:] and a significantly distorted C_{NHC}–Ag–OTf angle of 162.31(13)°, similar to what was found in [(ITr)CuI] (**4**).

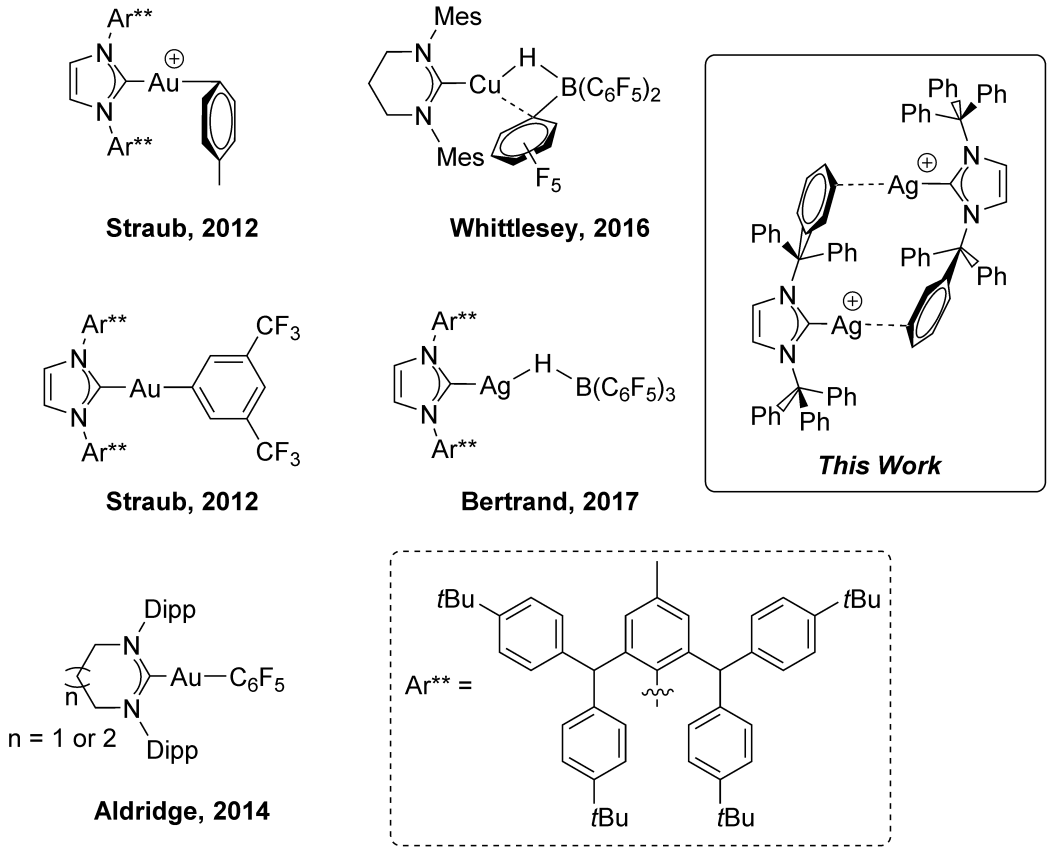

Scheme 4.5. Examples of NHC-supported Group 11 species generated during the attempted synthesis of monocoordinate [NHC–M]$^+$ compounds.

With [(ITr)Ag(OTf)] (**10**) in hand, formation of the potentially one-coordinate [(ITr)Ag]$^+$ cation (**11**) was targeted via triflate abstraction. When **10** and Na[BAr$^F{}_4$] were combined in fluorobenzene, the yellow crystalline fluorobenzene adduct, [(ITr)Ag(η^2-PhF)][BAr$^F{}_4$] (**12**) was formed (Figure 4.11). The η^2-coordination of C_6H_5F to Ag^I shows long Ag–C contacts [2.381(4) and 2.435(4) Å] which compare well with known Ag–C_6H_6 adducts[24] and are significantly longer than the coordinative C_{NHC}–Ag bond in **12** [2.115(3) Å].

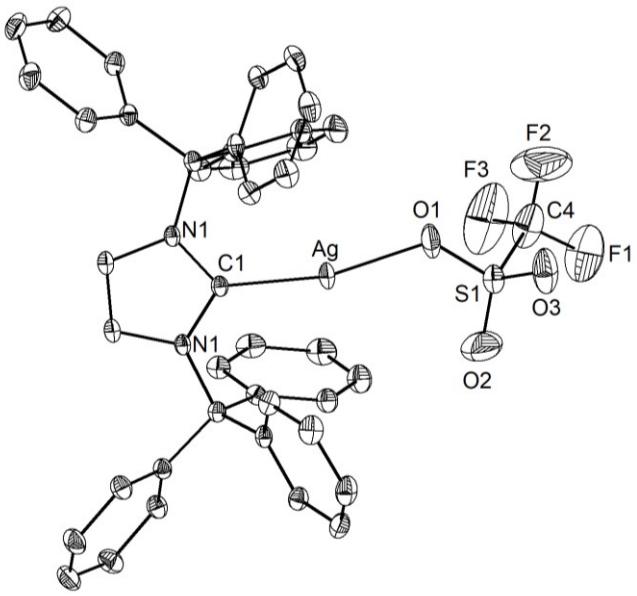

Figure 4.10. Molecular structure of [(ITr)Ag(OTf)] (**10**) with thermal ellipsoids plotted at a 30 % probability level. All hydrogen atoms have been omitted for clarity. Selected bond lengths [Å] and angles [°]: C1–Ag 2.097(3), Ag–O1 2.172(4); C1-Ag-O1 162.31(13).

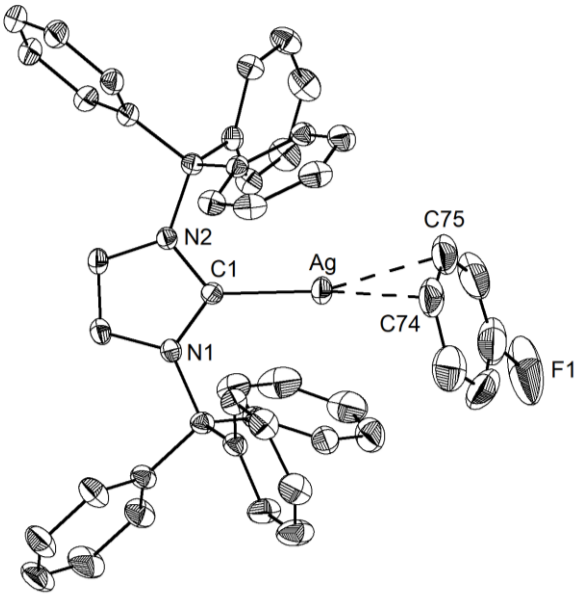

Figure 4.11. Molecular structure of [(ITr)Ag(PhF)][BAr^F_4] (**12**) with thermal ellipsoids plotted at a 30 % probability level. All hydrogen atoms and the [BAr^F_4]$^-$ counterion have been omitted for clarity. Selected bond lengths [Å] and angles [°]: C1–Ag 2.115(3), Ag–C74 2.381(4), Ag–C75 2.435(4); C1-Ag-C74, 159.33(16), C1-Ag-C75 163.92(16).

Additionally, the affinity of $[(NHC)Ag]^+$ for fluorobenzene was estimated by determination of the enthalpy of the following reaction: $[(IMe)Ag]^+ + PhF \rightarrow [(IMe)Ag(PhF)]^+$ ($\Delta_rH = -111$ kJ/mol) using a truncated model [IMe = $(HCNCH_3)_2C$:] for the NHC. When the reaction between **11** and $Na[BAr^F{}_4]$ was conducted in mesitylene, the corresponding mesitylene adduct $[(ITr)Ag(\eta^3\text{-MesH})][BAr^F{}_4]$ (**13**) was formed (Scheme 4.6, Figure 4.12) which exhibits similarly long Ag–C_{arene} interactions in the range of 2.322(4)–2.719(5) Å.

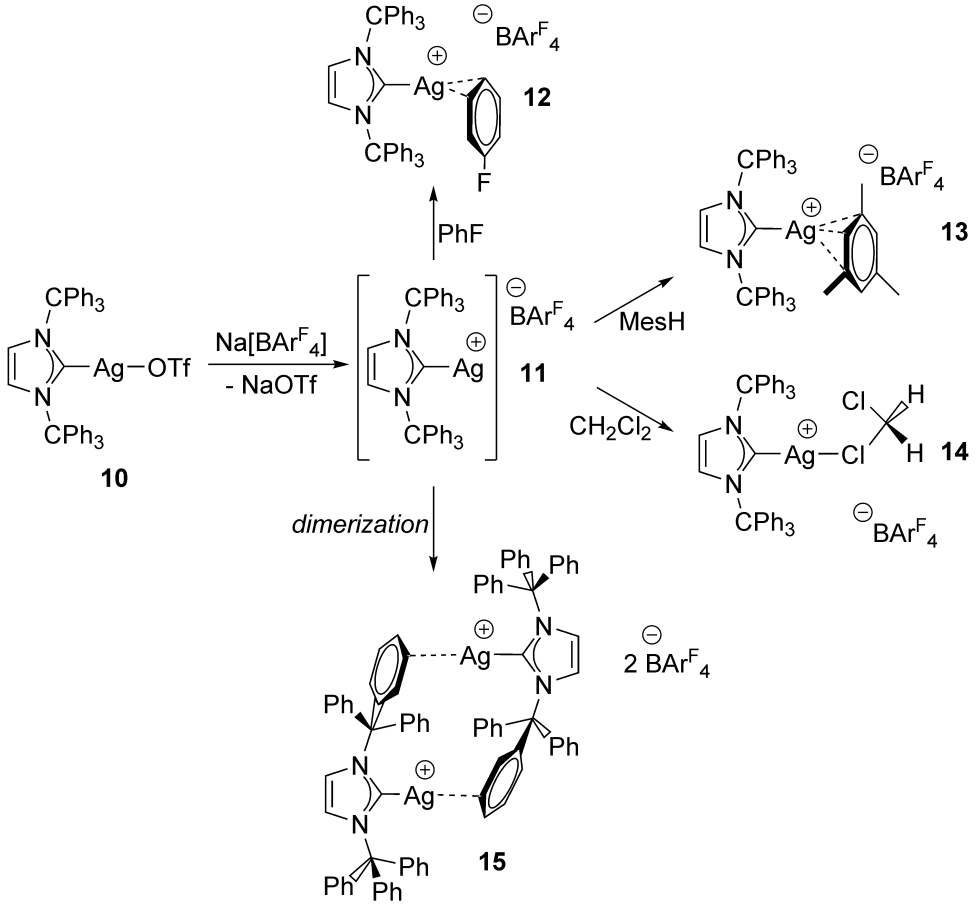

Scheme 4.6. Formation of the solvent adducts **12**–**14** of the parent $[(ITr)Ag]^+$ (**11**) ands its dimerization to form **15**.

The attempted synthesis of $[(ITr)Ag]^+$ by combining [(ITr)Ag(OTf)] (**10**) and $Na[BAr^F{}_4]$ in dichloromethane gave some very interesting results. ^{19}F and $^{11}B\{^1H\}$ NMR

spectroscopy of the soluble reaction product revealed that the $[BAr^{F}_{4}]^{-}$ anion remained intact, which was not the case when [(IPr**)AuCl] was combined with $Na[BAr^{F}_{4}]$ in CH_2Cl_2 (*vide supra*).[18] Repeated crystallization attempts yielded yellow block-like crystals which proved to be the CH_2Cl_2 adduct of **11**, $[(ITr)Ag(CH_2Cl_2)][BAr^{F}_{4}]$ (**14**) (Figure 4.13) (co-crystallized with 30 % of the 1:1 toluene adduct $[(ITr)Ag(toluene)][BAr^{F}_{4}]$). In the same product mixtures, yellow crystalline rods were also always present, which were identified as the weakly associated dimer of the target monocoordinate silver(I) cation $[(ITr)Ag]_2[BAr^{F}_{4}]_2$ (**15**) (Figure 4.14). When mixtures of **14** and **15** were re-dissolved in CH_2Cl_2 and the solvent removed, elemental analysis of the final product was consistent with a solvent-free species ''$[(ITr)Ag][BAr^{F}_{4}]$''. The bonding situation in **15** is reminiscent of the previously observed terphenyl-substituted copper(I) dimer, $[(2,6\text{-}Mes_2H_3C_6)Cu]_2$.[16g]

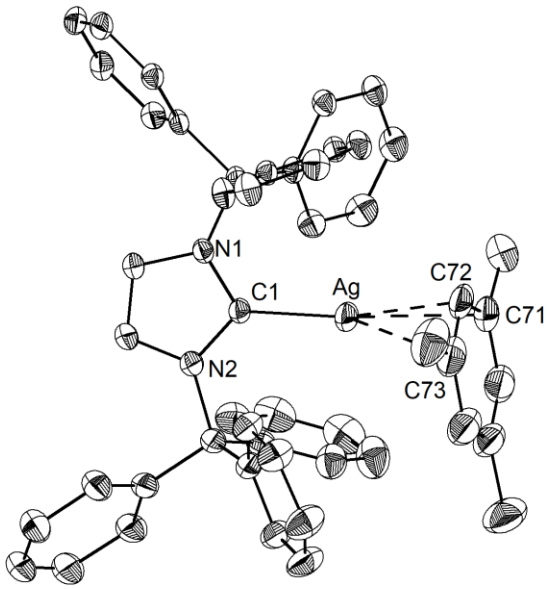

Figure 4.12. Molecular structure of $[(ITr)Ag(MesH)][BAr^{F}_{4}]$ (**13**) with thermal ellipsoids plotted at a 30 % probability level. All hydrogen atoms and the $[BAr^{F}_{4}]^{-}$ counterion and free MesH solvate have been omitted for clarity. Selected bond lengths [Å] and angles [°]: C1–Ag 2.112(3), Ag–C71 2.682(4), Ag–C72 2.323(4), Ag–C73 2.719(5); C1-Ag-C71 152.65(14), C1-Ag-C72 168.86(13), C1-Ag-C73 152.47(15).

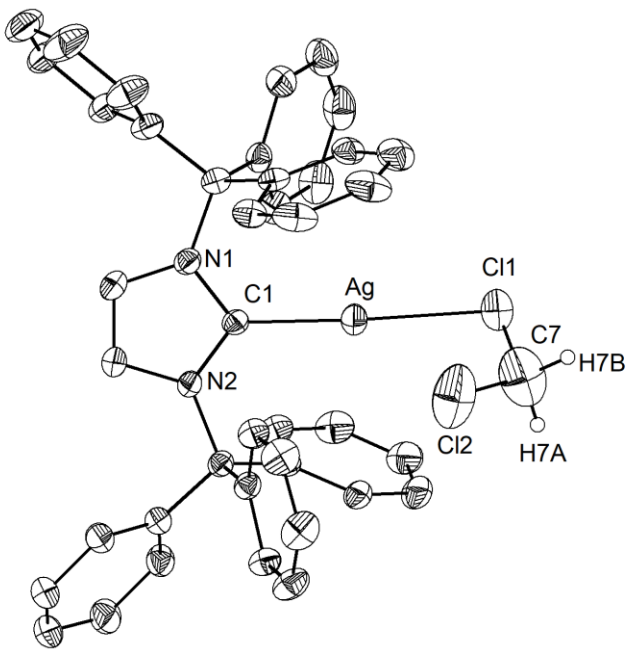

Figure 4.13. Molecular structure of $[(ITr)Ag(CH_2Cl_2)_{0.7}(\eta^3\text{-toluene})_{0.3}][BAr^F{}_4]$ (**14**) with thermal ellipsoids plotted at a 30 % probability level. All hydrogen atoms (except for CH_2Cl_2), the $[BAr^F{}_4]^-$ counterion and the 30 % η^3-coordinated toluene molecule have been omitted for clarity. Selected bond lengths [Å] and angles [°]: C1–Ag 2.098(4), Ag–Cl1 2.524(2); Cl-Ag-Cl1 170.64(12).

The dimeric dication $[(ITr)Ag]_2^{2+}$ unit in **15** arises from a set of aryl–Ag^I η^2-interactions [2.444(4) and 2.348(4) Å] involving ligand-containing $-CPh_3$ groups of a neighboring $[(ITr)Ag]^+$ cation (Figure 4.14); these Ag–arene distances are similar to those in compounds **12** and **13** [ca. 2.32–2.72 Å]. The formation of a weakly associated dimer motif in **15** leads to effective encapsulation of two electrophilic Ag^I centers within a hydrophobic core provided by the $-CPh_3$ groups.

The NMR spectra of isolated crystals of compounds **12**–**15** in C_6D_6 were each consistent with the formation of the same $[(ITr)Ag(C_6D_6)][BAr^F{}_4]$ adduct, with release of solvate (PhF, MesH and CH_2Cl_2) in the case of compounds **12**–**14**. This indicates the labile

nature of the secondary Ag^{I}–arene interactions in solution, in line with the high degree of steric protection offered by the ITr ligand (Scheme 4.6).

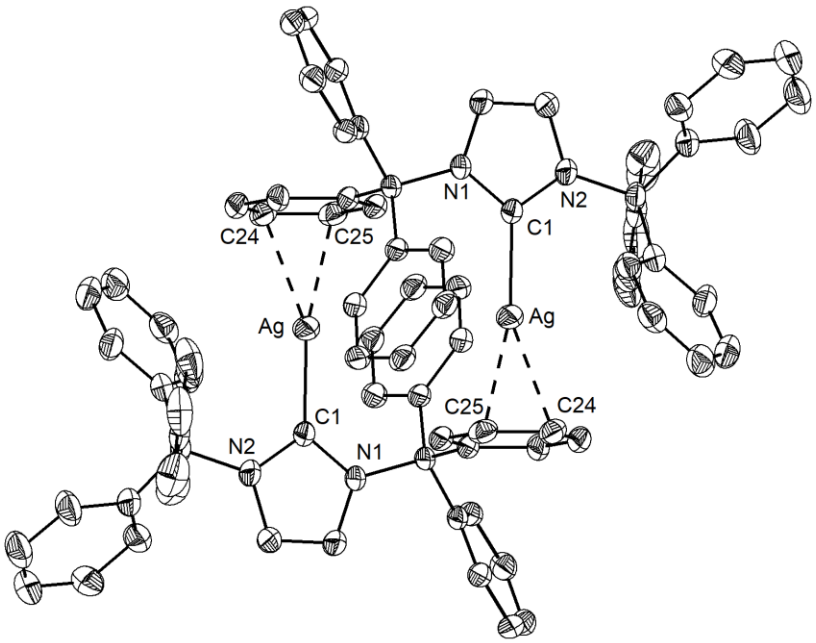

Figure 4.14. Molecular structure of $[(ITr)Ag]_2[BAr^F{}_4]_2$ (**15**) with thermal ellipsoids plotted at a 30 % probability level. All hydrogen atoms and the two $[BAr^F{}_4]^-$ counterions have been omitted for clarity. Selected bond lengths [Å] and angles [°]: C1–Ag 2.110(4), Ag–C24 2.444(4), Ag–C25 2.348(4); C1-Ag-C24 157.96(15), C1-Ag-C25 168.04(15).

Natural population analysis (NPA) of $[(ITr)Ag]^+$ (**11**) revealed a high degree of positive charge on silver (+0.71), consistent with substantial electrophilic character. We also attempted to quantify the Lewis acidity of **11** using the Childs method[25] by coordination of crotonaldehyde. The chemical shift difference between the H3 proton of free and coordinated crotonaldehyde ($\Delta\delta$ = 0.08 ppm) compares well with the relatively weak Lewis acids BPh_3 ($\Delta\delta$ = 0.05 ppm) and $B(OPh)_3$ ($\Delta\delta$ = 0.03 ppm) but shows a weaker interaction compared with $B(C_6F_5)_3$ ($\Delta\delta$ = 1.05 ppm).[25b] Given that strong coordination of crotonaldehyde to **11** may be limited by the bulky nature of ITr and the soft character of

the Ag^I center, we decided to investigate the methyl ion affinity (MIA) of this species computationally.[26] Using a truncated model for ITr, the overall reaction: $[IMe–Ag]^+ + :CH_3^- \rightarrow [IMe–Ag–CH_3]$ (IMe = $(HCNCH_3)_2C$:; $\Delta_rH = -MIA$) revealed an MIA of 780 kJ/mol. Notably, the $[(NHC)Ag]^+$ fragment has an affinity for the methyl anion on the same order of magnitude as $SiMe_3^+$ (1000 kJ/mol), $[MeZn]^+$ (1025 kJ/mol), Ph_3C^+ (836 kJ/mol) and the recently reported tin cation $[CpSn]^+$ (765 kJ/mol).[26] Interestingly, $[(NHC)Ag]^+$ has a slightly lower MIA than its copper and gold analogues (814 and 861 kJ/mol, respectively).

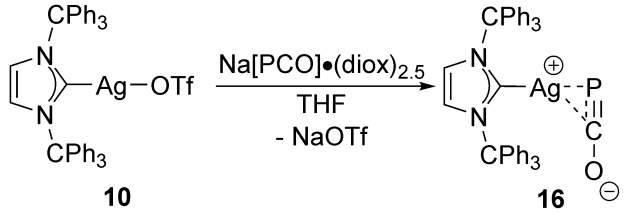

Scheme 4.7. Formation of [(ITr)Ag(η^2-PCO)] (**16**) from **10**.

Compound **10** was also combined with the recently reported, thermally stable phosphaketene salt Na[PCO]•(diox.)$_{2.5}$.[27] As expected, the –OTf group was substituted for a –PCO ligand to give [(ITr)Ag(PCO)] (**16**) (Scheme 4.7 and Figure 4.15); a similar reaction has been noted between Na[PCO]•(diox.)$_{2.5}$ and CAAC gold and copper halide complexes (CAAC = cyclic(alkyl)aminocarbene).[28] Compound **16** has a C_{NHC}–Ag–P bond angle that is slightly distorted from linearity [175.22(5)°], with Ag–P and Ag–C(6) distances of 2.4015(6) and 2.770(3) Å, respectively, indicating η^2-coordination between the PCO^- anion and Ag^I. Compound **16** yielded a broad signal in the $^{31}P\{^1H\}$ spectrum at −406 ppm at room temperature which was resolved as a sharp doublet at −80 °C due to $^{107/109}$Ag–P coupling. The Kohn–Sham molecular orbitals associated with the optimized geometry of **16** support η^2-PCO coordination (Figure 4.16) as the HOMO−1 shows electron

delocalization about the Ag–P–C unit, arising from side-on overlap of a P–C π bond with an empty s orbital on silver. The natural bonding orbitals (NBOs) further corroborate this bonding description, with the highest energy donor–acceptor interaction (second-order perturbation theory) between the $[(ITr)Ag]^+$ fragment and PCO^- being donation from a P–C π bond to an empty silver-centered s orbital (62.8 kcal/mol). A related bonding situation has been observed for [(CAAC)Cu(PCO)][28] and within phosphalkyne Ag^I complexes,[29] and supports the presence of a highly electron-deficient Ag^I center in $[(ITr)Ag]^+$.

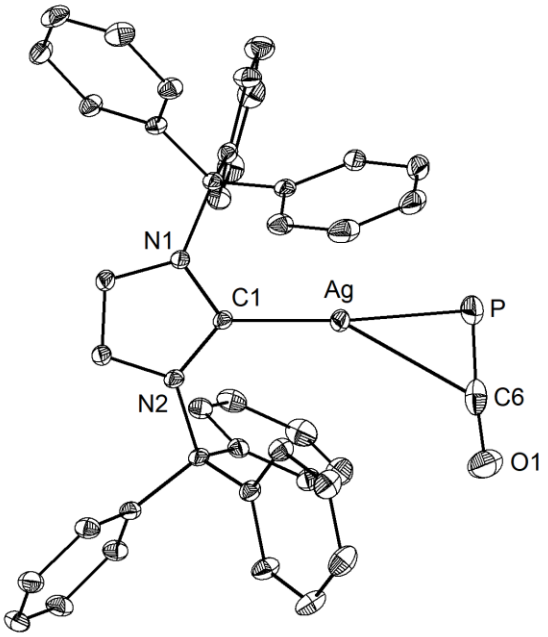

Figure 4.15. Molecular structure of [(ITr)Ag(η^2-PCO)] (**16**) with thermal ellipsoids plotted at a 30 % probability level (left). All hydrogen atoms and THF solvate have been omitted for clarity. Selected bond lengths [Å] and angles [°]: C1–Ag 2.140(2), Ag–P 2.4015(6), P–C6 1.588(3), C6–O1 1.211(4), Ag–C6 2.770(3); C1-Ag-P 175.22(5), Ag-P-C6 85.35(9), P-C6-O1 174.5(2).

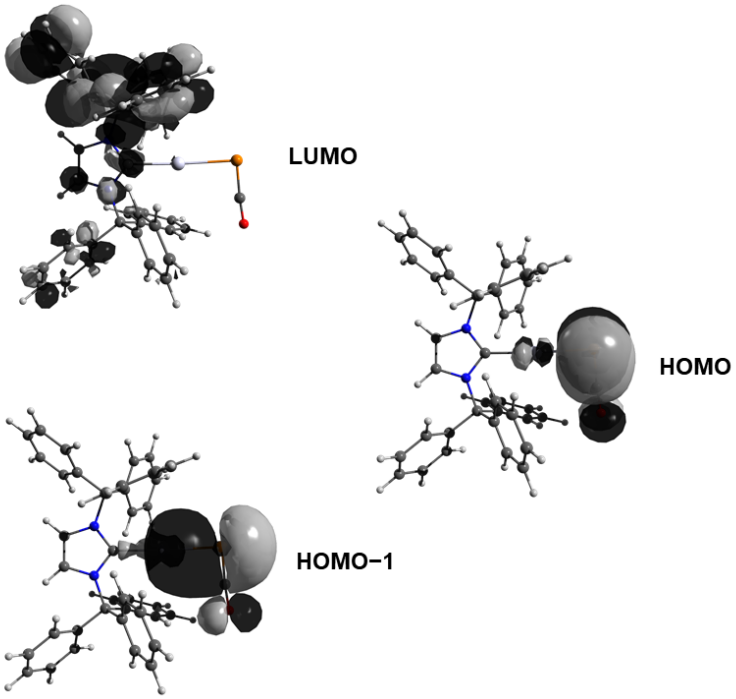

Figure 4.16. Selected molecular orbital of [(ITr)Ag(η^2-PCO)] (**16**) demonstrating the η^2-PCO bonding situation (HOMO−1).

4.3. Conclusions

A new *N*-heterocyclic carbene featuring sterically encumbered trityl (CPh_3) groups was prepared by using a synthetically efficient route and contains the highest $\%V_{bur}$ value reported to date. The ability of this ligand to act as a two-electron donor along with supplying added arene-element interactions facilitated the isolation of a quasi one-coordinate Tl^I cation, $[(ITr)Tl]^+$. This thermally stable species is a versatile transmetalation/ligation reagent and was used to generate new low-coordinate main group cations (as was exemplified by the successful synthesis of a $[GeCl]^+$ cation). Additionally, the formation of $[(ITr)Ag]^+$ complexes from the readily accessible, thermally and light, stable precursor [(ITr)Ag(OTf)] has been demonstrated. The electrophilic $[(ITr)Ag]^+$ unit engages in weak/reversible 1:1 complexation with fluorobenzene, mesitylene and dichloromethane, and yields the solvent-free, weakly associated dimer $[(ITr)Ag]_2^{2+}$. These

compounds represent rare examples of silver(I) complexes that approach monocoordination. Future work will involve modification of the umbrella-shaped CPh_3, including the formation of structurally flexible alkyl analogues,[21,30,31] and the introduction of the ITr ligand to the domain of transition metal-mediated catalysis.[32]

4.4. Experimental Details

4.4.1. General

All reactions were performed in an inert atmosphere glovebox (Innovative Technology, Inc.). Solvents were dried using a Grubbs-type solvent purification system[33] manufactured by Innovative Technologies, Inc., degassed (freeze-pump-thaw method), and stored under an atmosphere of nitrogen prior to use. Ph_3CCl, $AuCl(SMe_2)$, CuI, Cl_2Ge•diox, $K[N(SiMe_3)_2]$, MeLi (1.6 M in Et_2O), $[Rh(CO)_2Cl]_2$ and Tl(OTf) were purchased from Aldrich and used as received. Crotonaldehyde was purchased from Sigma Aldrich, degassed and dried over 4 Å molecular sieves for 2 days (to remove H_2O stabilizer) prior to use. AgOTf was purchased from Matrix Scientific and used as received. $Na[BAr^F_4]$ was dried by heating to 110 °C *in vacuo* for 24 hours prior to use. $Ph_3C(OTf)$,[34] 1-(triphenylmethyl)imidazole,[35] and $Tl[BAr^F_4]$[36] were prepared according to literature procedures. $Tl[BAr^F_4]$ was dried by heating to 110 °C *in vacuo* for 24 hours prior to use. Na[PCO]•$(dioxane)_x$ was synthesized according to the literature procedure and its dioxane content (2.5 equivalents vs. Na) was determined as described.[27] ^1H, $^{11}B\{^1H\}$, $^{13}C\{^1H\}$ and ^{19}F NMR spectra were recorded on 400, 500, 600 or 700 MHz Varian Inova instruments and were referenced externally to $SiMe_4$ (^1H, $^{13}C\{^1H\}$), $FCCl_3$ (^{19}F), 85 % H_3PO_4 ($^{31}P\{^1H\}$) or F_3B•OEt_2 ($^{11}B\{^1H\}$). Elemental analyses were performed by the Analytical and

Instrumentation Laboratory at the University of Alberta. Melting points were measured in sealed glass capillaries under nitrogen by using a MelTemp apparatus and are uncorrected.

4.4.2. X-ray Crystallography

Crystals for X-ray diffraction studies were removed from a vial (in a glovebox) and immediately coated with a thin layer of hydrocarbon oil (Paratone-N). A suitable crystal was then mounted on a glass fiber and quickly placed in a low temperature stream of nitrogen on the X-ray diffractometer.[37] All data were collected using a Bruker APEX II CCD detector/D8 or PLATFORM diffractometer using Mo K_α or Cu K_α radiation, with the crystals cooled to –80 °C or –100 °C. The data were corrected for absorption through Gaussian integration from the indexing of the crystal faces. Crystal structures were solved using intrinsic phasing (SHELXT)[38] and refined using SHELXL-2014.[39] The assignment of hydrogen atom positions were based on the sp^2 or sp^3 hybridization geometries of their attached carbon atoms and were given thermal parameters 20 % greater than those of their parent atoms.

Special refinement conditions. Compound **2**•0.5 C_4H_8O: Attempts to refine peaks of residual electron density as disordered or partial-occupancy solvent tetrahydrofuran oxygen or carbon atoms were unsuccessful. The data were corrected for disordered electron density through use of the SQUEEZE procedure as implemented in PLATON. A total solvent-accessible void volume of 618.8 $Å^3$ with a total electron count of 161 (consistent with 4 molecules of solvent tetrahydrofuran, or 0.5 molecules per formula unit of the carbene compound) was found in the unit cell. Compound **4**•C_7H_8: Distances involving the methyl carbons of the inversion-disordered solvent toluene molecules were constrained during refinement: d(C10S–C11S) = d(C20S–C21S) = 1.50(1) Å;

d(C10S···C12S) = d(C10S···C16S) = d(C20S···C22S) = d(C20S···C26S) = 2.50(1) Å. The phenyl ring carbons for each of these molecules were modelled as idealized regular hexagons, with C–C bond distances set at 1.390 Å. Compound **6**: The crystal used for data collection was found to display non-merohedral twinning. Both components of the twin were indexed with the program *CELL_NOW* (Bruker AXS Inc., Madison, WI, 2004). The second twin component can be related to the first component by 13.2º rotation about the [4 1 0] axis in real space and about the [1 0 0] axis in reciprocal space. Integrated intensities for the reflections from the two components were written into a *SHELXL-2014* HKLF 5 reflection file with the data integration program *SAINT* (version 8.37A), using all reflection data (exactly overlapped, partially overlapped and non-overlapped). The refined value of the twin fraction (*SHELXL-2014* BASF parameter) was 0.1537(16). Compound **8**: The disordered $[BAr^{F}{}_{4}]^{-}$ anion was restrained by use of the *SHELXL* SAME (interatomic distances restrained to be approximately the same as that of the ordered anion) and RIGU (the 'rigid-bond' restraint on the anisotropic displacement parameters) instructions. Compound **9**•0.75C_6H_5F: The partially-occupied/disordered solvent fluorobenzene molecules were constrained to be idealized hexagons with C–C distances of 1.39 Å and the C–F distance was restrained to be approximately 1.35(1) Å. Additionally, the C–F distances of the minor orientations of two CF_3 groups (C77 and C98) were restrained to have the approximately the value by use of the *SHELXL* SADI instruction. Compound **12**: The C–F distances within the disordered CF3 groups were restrained to be approximately equal by use of the *SHELXL* SAME instruction. Likewise, the C–F distances within the disordered coordinated fluorobenzene were also restrained to be approximately equal. Compound **13**•1.5 C_9H_{12}: (a) The $C_{aromatic}$–CH_3 bonds in the disordered solvent mesitylene

molecules were constrained during refinement: d(C11S–C17S) = d(C13S–C18S) = d(C15S–C19S) = d(C21S–C27S) = d(C23S–C28S) = d(C25S–C29S) = d(C31S–C37S) = d(C33S–C38S) = d(C35S–C39S) = 1.52(1) Å. (b) Distances between the methyl carbons and the ortho carbons in one of the disordered solvent mesitylene molecules were constrained during refinement: d(C22S···C27S) = d(C26S···C27S) = d(C22S···C28S) = d(C24S···C28S) = d(C24S···C29S) = d(C26S···C29S) = 2.50(1) Å. (c) Methyl carbon positons for one of the disordered solvent mesitylene molecules were constrained to be coplanar with the aromatic ring carbons by defining the atoms C27S, C28S, C29S, C22S, C24S, C26S as vertices of a polyhedron with a volume to not exceed 0.01 $Å^3$ (*SHELXL-2014* FLAT instruction). (d) The ring carbons of the disordered solvent mesitylene molecules were modelled as idealized regular hexagons, with C–C bond distances of 1.390 Å and bond angles of 120.0º. Compound **14**: The Cl–C distances within the coordinated dichloromethane was restrained to be approximately the same by use of the *SHELXL* SAME instruction. Likewise, the C–F distances within the CF_3 groups with carbon atoms C98 and C107 were also restrained. The coordinated toluene was constrained to be an idealized hexagon and the 1,3 interatomic distances involving the methyl group and the ortho-carbon atoms were restrained to be 2.50(1) Å. Finally, the Cl–C distances within the solvent dichloromethane molecules were restrained to be 1.80(2) Å, and the rigid-bond approximation (RIGU) was applied. Compound **15**•2 C_6H_{14}: (a) Attempts to refine peaks of residual electron density as disordered or partial-occupancy solvent hexane carbon atoms were unsuccessful. The data were corrected for disordered electron density through use of the SQUEEZE procedure as implemented in *PLATON*. A total solvent-accessible void volume of 417 $Å^3$ with a total electron count of 110 (consistent with 2 molecules of

solvent hexane) was found in the unit cell. (b) The C–F distances within the disordered CF_3 groups were restrained to be approximately the same by use of the *SHELXL* SADI instruction. Likewise, the following pairs of distances involving the disordered aryl group were also restrained: B–C81A and B–C81B distances were restrained, the C83A–C87A and C83B–C87B, and the C85A–C88A and C85B–C88B. Finally, the atoms within the disordered bis(trifluoromethyl)phenyl groups were restrained to lie in approximately the same plane by use of the *SHELXL* FLAT instruction.

4.4.3. Computational Methods

All calculations (except methyl ion affinity calculations) were carried out using the Gaussian 09, Rev. D.01 software package.[40] Input structures were optimized using the B3LYP[41] functional and 6-31G(d,p)[42] basis set in the gas phase. An effective core potential (ECP) LANL2DZ[43] was used for thallium, silver and rhodium, with added diffuse functions for the light atoms (6-31+G(d,p)). All optimized structures were then confirmed to be local energy minima on the potential energy surface by frequency analysis. In the calculation of proton affinity (PA), the thermal contribution of a proton was assumed to be 0 kcal/mol. For the calculation of methyl ion affinity (MIA), calculations were carried out using the ORCA 4.0.0.2 software package.[44] Input structures were optimized using the (RI-)BP86[45] functional and the def2-SV(P)[46] basis set in the gas phase. The optimized geometries were confirmed to be minima on the potential energy surface by frequency analysis. A truncated model was used for the ITr ligand, IMe [$(HCNCH_3)_2C$:]. The methyl ion affinity was calculated as described in the literature[26] referenced to the MIA of Me_3Si^+ calculated at the G3 level (Δ_rH = 1000 kJ/mol).[26]

Table 4.1. Computed proton affinities (kcal/mol) of selected neutral ligands.

Ligand	Proton Affinity (kcal/mol)[a]
Im*i*Pr$_2$	272.8
IPr	275.6
IPr=CH$_2$	277.0
Me$_3$P=CH$_2$	277.5
ITr	283.6

[a]proton affinity = $-\Delta_r H$ for the reaction: $L + H^+ \rightarrow LH^+$

4.4.4. Synthetic Procedures

Synthesis of [ITrH][OTf] (1). To a Schlenk flask containing trityl imidazole (3.840 g, 12.37 mmol) and Ph$_3$C(OTf) (4.866 g, 12.40 mmol) was added ca. 250 mL benzene. The reaction mixture was left to stir for 24 hours, resulting in the formation of a large amount of precipitate. From this point on, the reaction was conducted in air in a well-ventilated fumehood. The precipitate was collected on a Büchner funnel, washed with 2×20 mL portions of benzene and dissolved in 40 mL of CH_2Cl_2. The product was precipitated from the CH_2Cl_2 solution by addition of 150 mL of hexanes; the precipitate was collected on a filter funnel and dried under vacuum to yield [ITrH][OTf] (**1**) as a pale-yellow solid (6.772 g, 78 %). Crystals of **1** suitable for X-ray crystallographic analysis were obtained by storing a THF solution layered with hexanes in the freezer overnight. ^{1}H NMR ($CDCl_3$, 499.8 MHz): δ 7.92 (t, $^4J_{HH}$ = 1.9 Hz, 1H, NC*H*N), 7.54 (d, $^4J_{HH}$ = 1.9 Hz, 2H, NC*H*), 7.47–7.36 (m, 18H, *m,p*-Ar*H*), 7.19–7.11 (m, 12H, *o*-ArH). ^{13}C{^{1}H} NMR ($CDCl_3$, 176.0 MHz): δ 146.9 (N*C*H), 139.4 (Ar*C*), 137.4 (N*C*HN), 129.6 (Ar*C*), 129.5 (Ar*C*), 129.3 (Ar*C*), 125.0 (Ar*C*), 80.4 (*C*Ph$_3$). ^{19}F NMR ($CDCl_3$, 376.70 MHz): δ −78.3. M.p. 170 °C (decomp.). Anal. Calcd. for $C_{42}H_{33}F_3N_2O_3S$: C 71.78, H 4.73, N 3.99, S 4.56. Found: C 71.01, H 4.89, N 4.13, S 4.45.

Synthesis of ITr (2). To a Schlenk flask containing [ITrH][OTf] (6.575 g, 9.356 mmol) and K[N(SiMe$_3$)$_2$] (1.889 g, 9.470 mmol) was added 300 mL of toluene. The resulting slurry was stirred overnight and filtered through a ca. 2 cm plug of diatomaceous earth. The filtrate was concentrated to dryness *in vacuo*, affording an off-white solid. (4.613 g, 89 %). Crystals of ITr (**2**) suitable for X-ray crystallographic analysis were obtained by storing a THF solution layered with hexanes in the freezer overnight at −30 °C. ^{1}H NMR (C_6D_6, 499.8 MHz): δ 7.49–7.44 (m, 12H, *o*-Ar*H*), 7.08–6.99 (m, 18H, *m,p*-Ar*H*), 6.57 (s, 2H, NC*H*). ^{13}C{^{1}H} NMR (C_6D_6, 125.7 MHz): δ 225.8 (N*C*N), 145.7 (Ar*C*), 131.2 (Ar*C*), 127.5 (Ar*C*), 127.2 (Ar*C*), 120.2 (N*C*H), 77.3 (*C*Ph$_3$). M.p. 164 °C (decomp.). Anal. Calcd. for $C_{41}H_{32}N_2$: C 89.10, H 5.84, N 5.07. Found: C 88.41, H 6.08, N 4.91.

Synthesis of [(ITr)AuCl] (3). A solution of ITr (0.108 g, 0.195 mmol) in 2 mL of toluene was slowly added to a solution of [AuCl(SMe$_2$)] (0.057 g, 0.194 mmol) in 2 mL of toluene. The reaction mixture was left to stir for 4 hours and the volatiles were removed *in vacuo*, yielding [(ITr)AuCl] (**3**) as a colorless solid (0.146 g, 96 %). Crystals of **3** suitable for X-ray crystallographic analysis were obtained by slow evaporation of a benzene solution of **3** in an NMR tube. ^{1}H NMR (C_6D_6, 499.8 MHz): δ 7.25–7.20 (m, 12H, *o*-Ar*H*), 7.09-7.02 (m, 18H, *m,p*-Ar*H*), 6.49 (s, 2H, NC*H*). ^{13}C{^{1}H} NMR (C_6D_6, 125.7 MHz): δ 185.0 (N*C*N), 142.5 (Ar*C*), 130.8 (Ar*C*), 128.3 (Ar*C*), 119.6 (Ar*C*), 79.0 (*C*Ph$_3$). An Ar*C* resonance is buried under the C_6D_6 signal. M.p. 120 °C (decomp.). Anal. Calcd. for $C_{41}H_{32}AuClN_2$: C 62.72, H 4.11, N 3.57. Found: C 63.24, H 4.40, N 3.62.

Synthesis of [(ITr)CuI] (4). An 18 mL solution of ITr (0.256 g, 0.463 mmol) was added to a vial containing solid CuI (0.090 g, 0.473 mmol) in the absence of light. The mixture was stirred for two days, resulting in a colorless solution. The solvent was removed *in*

vacuo, affording [(ITr)CuI] (**4**) as an off-white solid (0.321 g, 93 %). Crystals of **4** suitable for X-ray crystallographic analysis were obtained by storing a toluene solution layered with hexanes at −30 °C for 3 days. ^{1}H NMR ($CDCl_3$, 499.8 MHz): δ 7.33–7.23 (m, 30H, Ar*H*), 7.00 (s, 2H, NC*H*). $^{13}C\{^{1}H\}$ NMR ($CDCl_3$, 125.7 MHz): δ 142.3 (Ar*C*), 129.9 (Ar*C*), 128.3 (Ar*C*), 128.1 (Ar*C*), 119.9 (N*C*H), 78.0 (*C*Ph_3). An N*C*N resonance was not observed. M.p. 170 °C (decomp.). Anal. Calcd. for $C_{41}H_{32}CuIN_2$: C 66.26, H 4.34, N 3.77. Found: C 66.24, H 4.70, N 3.45.

Synthesis of [(ITr)Rh(CO)$_2$Cl] (5). A 3 mL toluene solution of ITr (0.065 g, 0.12 mmol) was added to a vial containing a 2 mL toluene solution of $[Rh(CO)_2Cl]_2$ (0.022 g, 0.057 mmol). The mixture was stirred for 1 hour and the resulting yellow precipitate was allowed to settle. The supernatant was decanted (and discarded) and the remaining solid was dried *in vacuo* affording [(ITr)Rh(CO)$_2$Cl] (**5**) as a yellow solid (0.061 g, 72 %). Crystals of **5** suitable for X-ray crystallographic analysis were obtained by slow evaporation of a 1:1 CH_2Cl_2:Et_2O mixture over 1 week. ^{1}H NMR ($CDCl_3$, 499.8 MHz): δ 7.43–7.20 (m, 30H, Ar*H*), 6.64 (s, 2H, NC*H*). $^{13}C\{^{1}H\}$ NMR ($CDCl_3$, 125.7 MHz): δ 185.6 (d, $^{1}J_{C–Rh}$ = 57.3 Hz, N*C*N), 182.2 (d, $^{1}J_{C–Rh}$ = 79.2 Hz, *C*O), 178.9 (d, $^{1}J_{C–Rh}$ = 42.3 Hz, *C*O), 142.1 (Ar*C*), 131.2 (Ar*C*), 127.9 (Ar*C*), 127.7 (Ar*C*), 126.0 (N*C*H), 80.2 (*C*Ph_3). IR (Nujol, cm^{-1}): 2055 (νCO), 1980 (νCO). M.p. 178 °C (decomp.). Anal. Calcd. for $C_{43}H_{32}ClN_2O_2Rh$: C 69.13, H 4.32, N 3.75. Found: C 68.38, H 4.82, N 3.14.

Synthesis of [(ITr)Tl][OTf] (6). To a vial containing ITr (0.133 g, 0.241 mmol) and Tl[OTf] (0.083 g, 0.24 mmol) was added 3 mL of THF, leading to the formation of a yellow solution. The solution was stirred for 30 minutes, layered with 3 mL of hexanes and placed in a −30 °C freezer overnight. The supernatant was decanted away from the resulting

yellow precipitate and the solid dried *in vacuo* to give [(ITr)Tl][OTf] (**6**) as a pale yellow solid (0.167 g, 78 %). Crystals of **6** suitable for X-ray crystallographic analysis were obtained by storing a fluorobenzene solution layered with hexanes at −30 °C for 2 days. ^{1}H NMR (C_6D_6, 400.0 MHz): δ 7.31–7.26 (m, 12H, *o/m*-Ar*H*), 7.18–7.10 (m, 12H, *o/m*-Ar*H*), 7.00–6.90 (m, 6H, *p*-Ar*H*), 6.40 (s, 2H, NC*H*). ^{13}C{^{1}H} NMR ($CDCl_3$, 125.7 MHz): δ 142.7 (Ar*C*), 139.3 (Ar*C*), 130.5 (Ar*C*), 129.4 (Ar*C*), 129.3 (Ar*C*), 129.1 (Ar*C*), 128.9 (Ar*C*), 128.4 (Ar*C*), 123.7 (N*C*H), 80.2 (*C*Ph$_3$). An N*C*N resonance was not observed. ^{19}F (C_6D_6, 376.3 MHz): δ −77.9. M.p. 130 °C (decomp.). Anal. Calcd. for $C_{42}H_{32}F_3N_2O_3STl$: C 55.67, H 3.56, N 3.09, S 3.54. Found: C 55.67, H 3.63, N 3.03, S 3.51.

Synthesis of [(ITr)Tl][BAr$^{F}_4$] (7). A 2 mL fluorobenzene solution of ITr (0.067 g, 0.12 mmol) was added to a 1 mL fluorobenzene solution of Tl[BAr$^{F}_4$] (0.127 g, 0.119 mmol). The resulting red solution was stirred for 45 minutes. The solution was then concentrated to ca. 1.5 mL *in vacuo*, layered with ca. 2 mL of hexanes and placed in a −30 °C freezer overnight. Colorless blocks of [(ITr)Tl][BAr$^{F}_4$] (**7**) were recovered by decanting the mother liquor and washing the solid with 2×2 mL portions of hexanes. The volatiles were removed *in vacuo* yielding **7** as a colorless solid (0.132 g, 68 %). Crystals of **7** suitable for X-ray crystallographic analysis were obtained by storing a fluorobenzene solution layered with hexanes at −30 °C for 2 days. ^{1}H NMR (C_6D_6, 400.0 MHz): δ 8.40 (broad s, 8H, *o*-$C_6H_3(CF_3)_2$), 7.64 (broad s, 4H, *p*-$C_6H_3(CF_3)_2$), 7.03–6.89 (m, 20H, Ar*H*), 6.80–6.76 (m, 8H, Ar*H*), 6.66–6.60 (m, 2H, Ar*H*), 6.38 (s, 2H, NC*H*). ^{13}C{^{1}H} (C_6D_6, 125.7 MHz): δ 162.7 (q, $^{1}J_{C–B}$ = 49.0 Hz, *ipso*-$C_6H_3(CF_3)_2$), 142.3 (Ar*C*), 138.7 (Ar*C*), 135.4 (Ar*C*), 129.8 (broad, Ar*C*), 129.2 (Ar*C*), 129.0 (Ar*C*), 127.4 (q, $^{1}J_{C–F}$ = 276.5 Hz, *C*F$_3$), 118.0 (broad, N*C*H), 77.3 (*C*Ph$_3$). An N*C*N resonance was not observed. ^{11}B{^{1}H} NMR (C_6D_6, 128.3

MHz): δ -5.9 (s, BAr^F_4). ^{19}F NMR (C_6D_6, 376.3 MHz): δ -62.1 (s). M.p. 62 °C (decomp.) Anal. Calcd. for $C_{73}H_{44}BF_{24}N_2Tl$: C 54.11, H 2.74, N 1.73. Found: C 55.10, H 3.39, N 1.72.

Synthesis of [(ITr)GeCl][BAr^F_4] (8). A ca. 5 mL fluorobenzene solution of ITr (0.076 g, 0.14 mmol) was added to a vial containing a ca. 3 mL solution of Tl[BAr^F_4] (0.147 g, 0.138 mmol), leading to the formation of a red/brown solution. The mixture was stirred for 30 minutes then added to a ca. 1 mL fluorobenzene slurry of Cl_2Ge•dioxane (0.032 g, 0.14 mmol); a colorless precipitate formed immediately upon addition. The reaction mixture was left to stir for 1 hour and filtered, yielding a colorless filtrate. The filtrate was concentrated to a volume of 4 mL, layered with an equal volume of hexanes and placed in a −30 °C freezer overnight. The mother liquor was decanted, the resulting precipitate washed with 3×2 mL portions of hexanes, and the volatiles were removed *in vacuo* yielding a colorless oil. The oily residue was subsequently dissolved in ca. 4 mL of C_6H_6 and frozen by storing in a −30 °C freezer for 1 hour. The volatiles were removed from the frozen C_6H_6 *in vacuo* to afford [(ITr)GeCl][BAr^F_4] (**8**) as a colorless powder (0.178 g, 85 %). Crystals of **8** suitable for X-ray crystallographic analysis were obtained by layering a CH_2Cl_2 solution of [(ITr)GeCl][BAr^F_4] with hexanes and storing at room temperature for 1 week. ^1H NMR (C_6D_6, 399.8 MHz): δ 8.41 (broad s, 8H, *o*-$C_6H_3(CF_3)_2$), 7.62 (broad s, 4H, *p*-$C_6H_3(CF_3)_2$), 6.96–6.83 (m, 30H, Ar*H*), 6.39 (s, 2H, NC*H*). $^{13}C\{^1H\}$ (C_6D_6, 125.7 MHz): δ 173.7 (N*C*N), 162.7 (q, $^1J_{C–B}$ = 49.8 Hz, *ipso*-$C_6H_3(CF_3)_2$), 139.5 (Ar*C*), 135.4 (Ar*C*), 130.4 (Ar*C*), 129.7 (Ar*C*), 124.5 (Ar*C*), 125.2 (q, $^1J_{C–F}$ = 284.2 Hz, CF_3), 118.0 (N*C*H), 79.2 (*C*Ph_3). $^{11}B\{^1H\}$ NMR (C_6D_6, 128.3 MHz): δ −5.9 (s, BAr^F_4). ^{19}F NMR (C_6D_6, 468.7

MHz): δ −62.1 (s). M.p. 134 °C (decomp.) Anal. Calcd. for $C_{73}H_{44}BClF_{24}GeN_2$: C 57.53, H 2.91, N 1.84. Found: C 57.37, H 3.12, 1.84.

Synthesis of [(ITr)Li(OEt$_2$)][BAr$^F{}_4$] (9). A 1.6 M solution of MeLi (16.4 μL, 0.0262 mmol) in Et_2O was added to a vial containing a ca. 3 mL Et_2O solution of [(ITr)GeCl][BAr$^F{}_4$] (0.040 g, 0.026 mmol) forming a small amount of colorless precipitate. The mixture was stirred for 30 minutes and filtered yielding a colorless filtrate. The precipitate was discarded and the volatiles of the filtrate were removed *in vacuo* yielding an off-white solid (0.038 g, 97 %). Crystals of [(ITr)Li(OEt$_2$)][BAr$^F{}_4$] (**9**) suitable for X-ray crystallographic analysis were obtained by layering a PhF solution of **9** with hexanes and storing at −30 °C overnight. ^{1}H NMR ($CDCl_3$, 400.0 MHz): δ 7.70 (broad s, 8H, *o*-$C_6H_3(CF_3)_2$), 7.51 (broad s, 4H, *p*-$C_6H_3(CF_3)_2$), 7.41–7.31 (m, 18H, *m,p*-Ar*H*), 7.16–7.10 (m, 12H, *o*-Ar*H*), 7.02 (s, 1H, NC*H*), 3.16 (q, 4H, $^3J_{HH}$ = 6.7 Hz, Et_2O), 0.79 (t, 6H, $^3J_{HH}$ = 6.7 Hz, Et_2O). ^{13}C{^{1}H} ($CDCl_3$, 125.7 MHz): δ 161.7 (q, $^1J_{C–B}$ = 49.8 Hz, *ipso*-$C_6H_3(CF_3)_2$), 139.5 (Ar*C*), 135.4 (Ar*C*), 130.4 (Ar*C*), 129.7 (Ar*C*), 124.5 (Ar*C*), 124.6 (q, $^1J_{C–F}$ = 276.5 Hz, *C*F$_3$), 117.5 (N*C*H), 66.0 (*C*H$_2$CH$_3$-Et_2O), 14.2 (CH$_2$*C*H$_3$-Et_2O). N*C*N and *C*Ph$_3$ resonances were not observed. ^{11}B{^{1}H} NMR ($CDCl_3$, 128.3 MHz): δ −6.6 (s, BAr$^F{}_4$). ^{19}F NMR ($CDCl_3$, 376.3 MHz): δ −62.4 (s). ^{7}Li{^{1}H} NMR ($CDCl_3$, 155.4 MHz): δ −2.3. M.p. 120 °C (decomp.). Anal Calcd. for $C_{77}H_{54}BF_{24}LiN_2O$: C 61.78, H 3.64, N 1.87. Found: C 61.50, H 4.28, N 1.90.

Reaction of [(ITr)Li(OEt$_2$)][BAr$^F{}_4$] with Cl$_2$Ge•dioxane. A ca. 2 mL fluorobenzene solution of [(ITr)Li(OEt$_2$)][BAr$^F{}_4$] (0.023 g, 0.016 mmol) was added to a vial containing a ca. 1 mL fluorobenzene slurry of Cl_2Ge•dioxane (0.004 g, 0.017 mmol) forming a colorless slurry. The reaction mixture was stirred for 1 hour and a 1 mL aliquot was removed from

the reaction mixture and filtered yielding a colorless solution. The volatiles were removed *in vacuo* and NMR analysis revealed quantitative formation of [(ITr)GeCl][BAr^F_4] (**8**).

Synthesis of [(ITr)Ag(OTf)] (10). A ca. 10 mL solution of ITr (0.197 g, 0.356 mmol) in toluene was added to a vial containing AgOTf (0.090 g, 0.35 mmol). The resulting white slurry was stirred for 2 hours and the volatiles removed *in vacuo* affording [(ITr)Ag(OTf)] as an off-white solid (0.263 g, 93 %). Crystals suitable for X-ray crystallographic analysis were obtained by layering a fluorobenzene solution of **10** with hexanes and storing the mixture at −30 °C in a freezer overnight. ^{1}H NMR (C_6D_6, 499.8 MHz): δ 7.11–7.03 (m, 30H, Ar*H*), 6.52 (s, 2H, NC*H*). ^{13}C{^{1}H} NMR (C_6D_6, 128.0 MHz): δ 142.3 (Ar*C*), 130.0 (Ar*C*), 128.6 (Ar*C*), 128.5 (Ar*C*), 120.3 (N*C*H), 78.6 (*C*Ph$_3$). ^{19}F NMR (C_6D_6, 376.7 MHz): δ −77.1 (s). M.p. 187 °C (decomp.). Anal. Calcd. for $C_{42}H_{32}AgF_3N_2O_3S$: C 62.31, H 3.98, N 3.46, S 3.96. Found: C 62.32, H 4.04, N 3.47, S 3.74.

Synthesis of [(ITr)Ag(PhF)][BAr^F_4] (12). A ca. 12 mL fluorobenzene slurry of ITr (0.264 g, 0.478 mmol) was added to a vial containing AgOTf (0.119 g, 0.463 mmol). The resulting slurry was stirred for 1 hour and subsequently added to a vial containing Na[BAr^F_4] (0.410 g, 0.463 mmol). The reaction mixture was stirred for 1 hour and filtered. The filtrate was layered with an equal volume of hexanes and placed in a −30 °C freezer overnight, yielding pale yellow crystals of [(ITr)Ag(PhF)][BAr^F_4], which were isolated and dried (0.519 g, 69 %). Crystals suitable for X-ray crystallographic analysis were obtained by layering a fluorobenzene solution of **12** with hexanes and storing the mixture at −30 °C in a freezer overnight.

Synthesis of [(ITr)Ag(MesH)][BAr^F_4] (13). 3 mL of mesitylene (MesH) was added to a vial containing [(ITr)Ag(OTf)] (0.065 g, 0.080 mmol) and Na[BAr^F_4] (0.072 g, 0.081

mmol). The resulting white slurry was stirred overnight and filtered. The filtrate was then layered with an equal volume of hexanes and placed in a −30 °C freezer overnight to give a few colorless crystals of **13** (0.007 g, <1 % yield).

Synthesis of [(ITr)Ag(CH_2Cl_2)][BAr^F_4] (14) and [(ITr)Ag]$_2$[BAr^F_4]$_2$ (15). A ca. 5 mL solution of [(ITr)Ag(OTf)] (0.127 g, 0.157 mmol) in CH_2Cl_2 was added to a vial containing Na[BAr^F_4] (0.139 g, 0.157 mmol). After 3 minutes, the resulting slurry began to take on a bright yellow color. The slurry was stirred for 1 hour and filtered. The filtrate was a bright yellow solution and the white precipitate was discarded. The filtrate was layered with an equal volume of hexanes and placed in a −30 °C freezer overnight, yielding yellow rod-shaped crystals and yellow block-shaped crystals. A few crystals were removed for X-ray crystallographic analysis and the rod-shaped crystals were determined to be **15** and the blocks were found to be **14**. The mother liquor was decanted, the crystals washed with 2×2 mL hexanes and the volatiles were removed *in vacuo* yielding a yellow crystalline solid (0.012 g, crop 1). The mother liquor was subsequently concentrated to half its original volume, layered with an equal volume of hexanes and placed in a −30 °C freezer for 1 week affording more yellow crystals. The mother liquor was decanted again, the crystals washed with 2×2 mL hexanes yielding a mixture of **14** and **15** as a yellow crystalline solid (0.145 g, crop 2). The two crops of crystals were then combined (0.157 g). Based on the crystal morphologies, the final product contains a mixture of **14** and **15**, and thus a percentage yield is not listed. NMR analysis of the mixture in C_6D_6 gave data that was consistent with the formation of [(ITr)Ag(C_6D_6)][BAr^F_4].

NMR data for [(ITr)Ag(C_6D_6)][BAr^F_4] and analytical data for "[(ITr)Ag][BAr^F_4]". ^{1}H, ^{13}C{^{1}H}, ^{11}B{^{1}H} and ^{19}F NMR spectroscopy for compounds **12**–**15** in C_6D_6 revealed

identical NMR spectra, along with the corresponding free fluorobenzene (**12**), mesitylene (**13**) or dichloromethane (**14**) in the ^{1}H and $^{13}C\{^{1}H\}$ spectra indicating that compounds **12**–**15** are the same in C_6D_6 solution. To confirm the formation of $[(ITr)Ag(C_6D_6)][BAr^F{}_4]$ the reaction of [(ITr)Ag(OTf)] and $Na[BAr^F{}_4]$ was conducted in C_6D_6 solvent and an aliquot was filtered revealing the same traces in the NMR spectra as for when compounds **12**–**15** are dissolved in C_6D_6.

Data for $[(ITr)Ag(C_6D_6)][BAr^F{}_4]$: ^{1}H NMR (C_6D_6, 499.8 MHz): δ 8.40 (broad s, 8H, *o*-$C_6H_3(CF_3)_2$), 7.65 (broad s, 4H, *p*-$C_6H_3(CF_3)_2$), 7.00–6.95 (m, 6H, Ar*H*), 6.94–6.89 (m, 12H, Ar*H*), 6.70–6.64 (m, 12H, Ar*H*), 6.25 (broad d, 2H, $^{4}J_{H-Ag}$ = 1.9 Hz, NC*H*). $^{13}C\{^{1}H\}$ NMR (C_6D_6, 125.7 MHz): δ 163.0 (q, $^{1}J_{C-B}$ = 47.8 Hz, *ipso*-$C_6H_3(CF_3)_2$), 141.9 (Ar*C*), 135.4 (Ar*C*), 129.6 (Ar*C*), 128.7 (Ar*C*), 128.4 (Ar*C*), 125.2 (q, $^{1}J_{C-F}$ = 272.7 Hz, CF_3), 118.0 (broad, N*C*H), 78.1 (CPh_3). An N*C*N resonance was not observed. ^{19}F NMR (C_6D_6, 468.7 MHz): δ −62.1 (s, $BAr^F{}_4$). $^{11}B\{^{1}H\}$ (C_6D_6, 159.8 MHz): δ −5.9 (s, $BAr^F{}_4$).

Crystals of **14** and **15** were re-dissolved in CH_2Cl_2 and dried *in vacuo* for several hours yielding a yellow powder. NMR spectroscopy (in C_6D_6) revealed that all CH_2Cl_2 had been removed from the solid, and elemental analysis was found to be consistent with a product of the general formula $[(ITr)Ag][BAr^F{}_4]$ (most likely the solvent-free dimer **15**). M.p. 154 °C (decomp.). Anal. Calcd. for $C_{73}H_{44}AgBF_{24}N_2$: C 57.53, H 2.91, N 1.84. Found C 57.14, H 3.21, N 1.78.

Synthesis of [(ITr)Ag(PCO)] (16). A ca. 2 mL solution of Na[PCO]•$diox_{2.5}$ (0.143 g, 0.177 mmol) in THF was added to a vial containing a ca. 2 mL THF solution of [(ITr)Ag(OTf)] (0.055 g, 0.182 mmol). The resulting slurry was stirred for 20 minutes and

had turned a dark brown (originally colorless). The slurry was filtered yielding a dark brown solution. The filtrate was layered with an equal volume of hexanes and placed in a −30 °C freezer overnight. The supernatant was decanted from the resulting brown precipitate and the precipitate washed 2×2 mL hexanes. The volatiles were removed *in vacuo* affording [(ITr)Ag(PCO)] (**16**) as a brown powder (0.053 g, 42 %). Crystals of **16** suitable for X-ray crystallographic analysis were obtained by layering a THF solution with hexanes and storing in a −30 °C freezer overnight. ^{1}H NMR (C_6D_6, 400.0 MHz): δ 7.22–7.17 (m, 12H, Ar*H*), 7.13–7.02 (m, 18H, Ar*H*), 6.55 (broad s, 2H, NC*H*). ^{13}C{^{1}H} NMR (C_6D_6, 125.7 MHz): δ 172.8 (d, $^{1}J_{C–P}$ = 91.8 Hz, -P*C*O), 142.7 (Ar*C*), 130.3 (Ar*C*), 128.5 (Ar*C*), 128.3 (Ar*C*), 120.0 (broad s, N*C*H), 78.4 (*C*Ph$_3$). An N*C*N resonance was not observed. ^{31}P{^{1}H} NMR (C_6D_6, 161.9 MHz): δ −406.0 (broad s). ^{31}P{^{1}H} NMR ([D$_8$]toluene, 161.8 MHz, −80 °C): δ −404.8 (d, $^{1}J_{P–Ag}$ = 152.5 Hz). M.p. 135 °C (decomp.). Anal. Calcd. for $C_{42}H_{32}AgN_2OP$: C 70.11, H 4.48, N 3.89. Found: C 69.49, H 4.51, N 3.82.

Addition of Crotonaldehyde to "[(ITr)Ag][BAr$^{F}_4$]" (Childs Method for determining Lewis acidity). To a vial containing a 1.5 mL CD_2Cl_2 solution of "[(ITr)Ag][BAr$^{F}_4$]" (synthesized from **10** and Na[BAr$^{F}_4$] in CH_2Cl_2; 0.049 g, 0.032 mmol) was added trans-crotonaldehyde (2.7 μL, 0.033 mmol) in CD_2Cl_2. After stirring for 70 minutes an aliquot was removed for NMR analysis. ^{1}H NMR spectroscopy revealed a set of crotonaldehyde peaks shifted from free crotonaldehyde. ^{1}H NMR (CD_2Cl_2, 399.8 MHz): δ 9.12 (d, 1H, *H1*), 6.95 (m, 1H, *H3*), 5.78 (ddq, 1H, *H2*), 2.00 (dd, 3H, *H4*). Free cotonaldehyde: ^{1}H NMR (CD_2Cl_2, 399.8 MHz): δ 9.47 (d, 1H, *H1*), 6.87 (m, 1H, *H3*), 6.10 (ddq, 1H, *H2*), 2.10 (dd, 3H, *H4*). The chemical shift difference of the *H3* proton between free and coordinated crotonaldehyde was found to be: Δδ *H3* = 0.08 ppm.

4.5. Crystallographic Data

Table 4.2. Crystallographic data for compounds **1**–**3**.

Compound	**1**	**2**•0.5 C_4H_8O	**3**•0.5 C_6H_6
formula	$C_{42}H_{33}F_3N_2O_3S$	$C_{43}H_{36}N_2O_{0.5}$	$C_{44}H_{35}AuClN_2$
formula weight	702.76	588.74	824.15
crystal system	monoclinic	monoclinic	monoclinic
space group	$P2_1/c$	$C2/c$	$P2_1/c$
a [Å]	13.1231(2)	24.0402(4)	16.5574(3)
b [Å]	13.6272(3)	9.1716(2)	8.47110(10)
c [Å]	20.0432(3)	30.1712(5)	25.2746(4)
α [°]	90	90	90
β [°]	103.7187(8)	106.5359	102.5463(8)
γ [°]	90	90	90
V [Å^3]	3482.09(9)	6377.2(2)	3460.35(9)
Z	4	8	4
ρ_{calcd} [g/cm^3]	1.341	1.226	1.582
μ [mm^{-1}]	1.323	0.550	8.955
T [°C]	−100	−100	−100
$2\theta_{max}$ [°]	144.85	145.75	145.27
total data collected	23923	21783	22932
unique data (R_{int})	6884 (0.0252)	6125 (0.0597)	6876 (0.0491)
obs data [$I \geq 2\sigma(I)$]	5921	4925	6430
params	460	388	433
R_1 [$I \geq 2\sigma(I)$][a]	0.0563	0.0443	0.0322
wR_2 [all data][a]	0.1564	0.1226	0.0820
max/min $\Delta\rho$ [e/Å^3]	0.691/−0.875	0.334/−0.295	1.717/−3.145

[a] $R_1 = \sum||F_o| - |F_c||/\sum|F_o|$; $wR_2 = [\sum w(F_o^2 - F_c^2)^2/\sum w(F_o^4)]^{1/2}$

Table 4.3. Crystallographic data for compounds **4**–**6**.

Compound	**4**•C_7H_8	**5**•CH_2Cl_2	**6**
formula	$C_{48}H_{40}CuIN_2$	$C_{44}H_{34}Cl_3N_2O_2Rh$	$C_{42}H_{32}F_3N_2O_3STl$
formula weight	835.26	831.99	906.12
crystal system	triclinic	orthorhombic	orthorhombic
space group	$P\bar{1}$	$P2_12_12_1$	*Pnma*
a [Å]	10.1904(5)	8.629(5)	17.7378(13)
b [Å]	13.2838(6)	20.388(11)	22.0727(16)
c [Å]	15.8378(8)	21.937(12)	8.8464(6)
α [°]	75.8828(7)	90	90
β [°]	76.6587(7)	90	90
γ [°]	67.6146(6)	90	90
V [Å^3]	1899.63(16)	3859(4)	3463.6(4)
Z	2	4	4
ρ_{calcd} [g/cm^3]	1.460	1.432	1.738
μ [mm^{-1}]	1.424	0.690	4.784
T [°C]	−80	−100	−100
$2\theta_{max}$ [°]	55.22	51.52	52.83
total data collected	17106	28553	100710
unique data (R_{int})	8786 (0.0338)	7366 (0.1419)	4160 (0.0682)
obs data [$I \geq 2\sigma(I)$]	6721	4967	3484
params	428	469	263
R_1 [$I \geq 2\sigma(I)$][a]	0.0413	0.0599	0.0406
wR_2 [all data][a]	0.1149	0.1441	0.1119
max/min $\Delta\rho$ [e/Å^3]	1.055/−0.748	0.823/−0.798	1.306/−0.880

[a] $R_1 = \sum||F_o| - |F_c||/\sum|F_o|$; $wR_2 = [\sum w(F_o^2 - F_c^2)^2/\sum w(F_o^4)]^{1/2}$

Table 4.4. Crystallographic data for compounds **7**–**9**.

Compound	**7**•C_6H_5F	**8**	**9**•0.75C_6H_5F
formula	$C_{79}H_{49}BF_{25}N_2Tl$	$C_{73}H_{44}BClF_{24}GeN_2$	$C_{81.5}H_{57.75}BF_{24.75}LiN_2O$
formula weight	1716.38	1523.95	1569.04
crystal system	triclinic	triclinic	monoclinic
space group	$P\bar{1}$	$P\bar{1}$	$P2_1/n$
a [Å]	12.4208(3)	18.3523(8)	15.1406(3)
b [Å]	14.4589(3)	18.9809(8)	25.8236(5)
c [Å]	20.7631(4)	20.7897(9)	19.1059(4)
α [°]	101.9164(10)	70.7662(6)	90
β [°]	101.5262(9)	80.3526(7)	102.1351(11)
γ [°]	93.4973(13)	80.6592(7)	90
V [Å^3]	3554.54	6696.3(5)	7303.2(3)
Z	2	4	4
ρ_{calcd} [g/cm^3]	1.604	1.512	1.427
μ [mm^{-1}]	5.366	0.610	1.117
T [°C]	−100	−100	−100
$2\theta_{max}$ [°]	147.89	52.75	148.34
total data collected	25468	54172	51698
unique data (R_{int})	13833 (0.0302)	27309 (0.0447)	14820 (0.0538)
obs data [$I \geq 2\sigma(I)$]	13293	16310	12037
params	1090	2333	1091
R_1 [$I \geq 2\sigma(I)$][a]	0.0474	0.0758	0.0725
wR_2 [all data][a]	0.1395	0.2478	0.2059
max/min $\Delta\rho$ [e/Å^3]	1.284/−2.062	0.965/−0.982	0.976/−0.421

[a] $R_1 = \sum||F_o| - |F_c||/\sum|F_o|$; $wR_2 = [\sum w(F_o^2 - F_c^2)^2/\sum w(F_o^4)]^{1/2}$

Table 4.5. Crystallographic data for compounds **10**–**13**.

Compound	**10**	**12**	**13**•1.5 C_9H_{12}
formula	$C_{42}H_{32}AgF_3N_2O_3S$	$C_{79}H_{49}AgBF_{25}N_2$	$C_{95.5}H_{74}AgBF_{24}N_2$
formula weight	809.62	1619.88	1824.24
crystal system	monoclinic	monoclinic	triclinic
space group	$P2_1/m$	$P2_1/n$	$P\overline{1}$
a [Å]	9.4002(2)	15.1650(7)	13.0012(3)
b [Å]	20.3414(5)	26.0219(12)	16.8587(4)
c [Å]	9.8392(2)	18.5838(9)	20.2367(5)
α [°]	90	90	93.9117(15)
β [°]	104.7623(9)	101.2305(6)	100.4578(16)
γ [°]	90	90	99.6917(14)
V [Å^3]	1819.28(7)	7193.2(6)	4277.23(18)
Z	2	4	2
ρ_{calcd} [g/cm^3]	1.478	1.496	1.416
μ [mm^{-1}]	5.466	0.391	2.767
T [°C]	−100	−100	−100
$2\theta_{max}$ [°]	148.35	56.63	148.07
total data collected	13008	64785	30571
unique data (R_{int})	3746 (0.0345)	17602 (0.0374)	16677 (0.0344)
obs data [$I \geq 2\sigma(I)$]	3578	12524	13630
params	274	1006	1151
R_1 [$I \geq 2\sigma(I)$][a]	0.0317	0.0572	0.0581
wR_2 [all data][a]	0.0856	0.1714	0.1820
max/min $\Delta\rho$ [e/Å^3]	1.541/−0.841	0.889/−0.531	0.825/−0.909

[a] $R_1 = \sum||F_o| - |F_c||/\sum|F_o|$; $wR_2 = [\sum w(F_o^2 - F_c^2)^2/\sum w(F_o^4)]^{1/2}$

Table 4.6. Crystallographic data for compound **14**.

Compound	$[(ITr)Ag(CH_2Cl_2)_{0.7}(C_7H_8)_{0.3}][BAr^F{}_4]\bullet CH_2Cl_2$ (**14**)
formula	$C_{76.80}H_{49.80}AgBCl_{3.40}F_{24}N_2$
formula weight	1695.79
crystal system	monoclinic
space group	$P2_1/n$
a [Å]	15.3180(3)
b [Å]	25.8009(5)
c [Å]	18.7754(4)
α [°]	90
β [°]	101.5004(12)
γ [°]	90
V [Å^3]	7271.4(3)
Z	4
ρ_{calcd} [g/cm^3]	1.549
μ [mm^{-1}]	4.329
T [°C]	−100
$2\theta_{max}$ [°]	145.11
total data collected	50317
unique data (R_{int})	14382 (0.0464)
obs data [$I \geq 2\sigma(I)$]	11638
params	1062
R_1 [$I \geq 2\sigma(I)$][a]	0.0682
wR_2 [all data][a]	0.2056
max/min $\Delta\rho$ [e/Å^3]	0.916/−1.406

[a] $R_1 = \sum||F_o| - |F_c||/\sum|F_o|$; $wR_2 = [\sum w(F_o^2 - F_c^2)^2/\sum w(F_o^4)]^{1/2}$

Table 4.7. Crystallographic data for compounds **15** and **16**.

Compound	**15**•2 C_6H_{14}	**16**•2 C_4H_8O
formula	$C_{158}H_{116}Ag_2B_2F_{48}N_4$	$C_{50}H_{48}AgN_2O_3P$
formula weight	3219.0	863.4
crystal system	triclinic	triclinic
space group	$P\bar{1}$	$P\bar{1}$
a [Å]	15.6902(3)	11.15213(16)
b [Å]	16.2845(4)	11.75148(17)
c [Å]	16.4921(4)	16.7352(3)
α [°]	117.7485(13)	83.7416(11)
β [°]	92.4871(15)	85.9962(8)
γ [°]	105.9078(15)	71.1237(9)
V [Å^3]	3513.30(15)	2061.50(5)
Z	1	2
ρ_{calcd} [g/cm^3]	1.522	1.391
μ [mm^{-1}]	3.284	4.644
T [°C]	−100	−100
$2\theta_{max}$ [°]	145.24	147.87
total data collected	21964	14722
unique data (R_{int})	13276 (0.0514)	8024 (0.0287)
obs data [$I \geq 2\sigma(I)$]	9284	7411
params	1072	514
R_1 [$I \geq 2\sigma(I)$][a]	0.0605	0.0308
wR_2 [all data][a]	0.1720	0.0844
max/min $\Delta\rho$ [e/Å^3]	0.592/−1.316	0.774/−0.720

[a] $R_1 = \sum||F_o| - |F_c||/\sum|F_o|$; $wR_2 = [\sum w(F_o^2 - F_c^2)^2/\sum w(F_o^4)]^{1/2}$

4.6. References

1. (a) For selected reviews and articles, see: (a) Nguyen, T.; Sutton, A. D.; Brynda, M.; Fettinger, J. C.; Long, G. L.; Power, P. P. *Science* **2005**, *310*, 844; (b) Fischer, R. C.; Power, P. P. *Chem. Rev.* **2010**, *110*, 3877; (c) Mizuhata, Y.; Sasamori, T.; Tokitoh, N. *Chem. Rev.* **2009**, *109*, 3479; (d) Asay, M.; Jones, C.; Driess, M. *Chem. Rev.* **2011**, *111*, 354; (e) Sen, S.; Khan, S.; Samuel, P. P.; Roesky, H. W. *Chem. Sci.* **2012**, *3*, 659; (f) Khan, S.; Gopakumar, G.; Thiel, W.; Alcarazo, M. *Angew. Chem. Int. Ed.* **2013**, *52*, 5644; (g) Hadlington, T. J.; Hermann, M.; Frenking, G.; Jones, C. *J. Am. Chem. Soc.* **2014**, *136*, 3028; (h) Rit, A.; Campos, J.; Niu, H.; Aldridge, S. *Nat. Chem.* **2016**, *8*, 1022; (i) Martin, D.; Melaimi, M.; Soleilhavoup, M.; Bertrand, G. *Organometallics* **2011**, *30*, 5304; (j) Ochiai, T.; Franz, D.; Inoue, S. *Chem. Soc. Rev.* **2016**, *45*, 6327; (k) Milnes, K. K.; Pavelka, L. C.; Baines, K. M. *Chem. Soc. Rev.* **2016**, *45*, 1019; (l) Gray, P. A.; Burford, N. *Coord. Chem. Rev.* **2016**, *324*, 1.
2. (a) Power, P. P. *Nature* **2010**, *463*, 171; (b) Spikes, G. H.; Fettinger, J. C.; Power, P. P. *J. Am. Chem. Soc*. **2005**, *127*, 12232; (c) Hadlington, T. J.; Kefalidis, C. E.; Maron, L.; Jones, C. *ACS Catal.* **2017**, *7*, 1853. For related work concerning the use of Frustrated Lewis Pairs (FLPs) for small molecule activation, see: (d) Stephan, D. W. *Acc. Chem. Res.* **2015**, *48*, 306.
3. (a) Jones, C. *Chem. Commun.* **2001**, 2293; (b) Robinson, G. H. *Dalton Trans.* **2012**, *41*, 2601; (c) Braunschweig, H.; Dewhurst, R. D.; Hammond, K.; Mies, J.; Radacki, K.; Vargas, A. *Science* **2012**, *336*, 1420; (d) Wilson, D. J. D.; Dutton, J. L. *Chem. Eur. J.* **2013**, *19*, 13626; (e) Rivard, E. *Chem. Soc. Rev.* **2016**, *45*, 989; (f) Präsang, C.; Scheschkewitz, D. *Chem. Soc. Rev.* **2016**, *45*, 900.

4. Percent buried volumes were calculated with the SambVca 2.0 web tool (https://www.molnac.unisa.it/OMtools/sambvca2.0/) using default parameters with H atoms omitted from the calculation, see: Falivene, L.; Credendino, R.; Poater, A.; Petta, A.; Serra, L.; Oliva, R.; Scarano, V.; Cavallo, L. *Organometallics* **2016**, *35*, 2286.
5. $\%V_{bur}$ for IPr and IPr*: Gómez-Suárez, A.; Nelson, D. J.; Nolan, S. P. *Chem. Commun.* **2017**, *53*, 2650.
6. Dröge, T.; Glorius, F. *Angew. Chem. Int. Ed.* **2010**, *49*, 6940.
7. Purkait, T. K.; Swarnakar, A. K.; De Los Reyes, G. B.; Hegmann, F. A.; Rivard, E.; Veinot, J. G. C. *Nanoscale* **2015**, *7*, 2241.
8. (a) Arnold, P. L.; Scarisbrick, A. C. *Organometallics* **2004**, *23*, 2519; (b) Cole, M. L.; Davis, A. J.; Jones, C. *J. Chem. Soc., Dalton Trans.* **2001**, 2451.
9. Nakai, H.; Tang, Y.; Gantzel, P.; Mayer, K. *Chem. Commun.* **2003**, 24.
10. Cordero, B.; Gómez, V.; Platero-Prats, A. E.; Revés, M.; Echeverría, J.; Cremades, E.; Barragán, F.; Alvarez, S. *Dalton Trans.* **2008**, 2832.
11. For examples of $[RTl]_x$ (x =1 or 2) compounds, see: (a) Niemeyer, M.; Power, P. P. *Angew. Chem. Int. Ed.* **1998**, *37*, 1277; (b) Hill, M. S.; Pongtavornpinyo, R.; Hitchcock, P. B. *Chem. Commun.* **2006**, 3720; (c) Wright, R. J.; Brynda, M.; Power, P. P. *Inorg. Chem.* **2005**, *44*, 3368; (d) Wright, R. J.; Phillips, A. D.; Hino, S.; Power, P. P. *J. Am. Chem. Soc.* **2005**, *127*, 4794; (e) Dange, D.; Li, J.; Schenk, C.; Schnöckel, H.; Jones, C. *Inorg. Chem.* **2012**, *51*, 13050.
12. Mansaray, H. B.; Tang, C. Y.; Vidovic, D.; Thompson, A. L.; Aldridge, S. *Inorg. Chem.* **2012**, *51*, 13017.

13. Thimer, K. C.; Al-Rafia, S. M. I.; Ferguson, M. J.; McDonald, R.; Rivard, E. *Chem. Commun.* **2009**, 7119.

14. (a) Rit, A.; Tirfoin, R.; Aldridge, S. *Angew. Chem. Int. Ed.* **2016**, *55*, 378; For an example of a quasi one-coordinate Ge^{II} cation, see: (b) Li, J.; Schenk, C.; Winter, F.; Schere, H.; Trapp, N.; Higelin, A.; Keller, S.; Pöttgen, R.; Krossing, I.; Jones, C. *Angew. Chem. Int. Ed.* **2012**, *51*, 9557.

15. The Rivard group is currently exploring *direct* routes to $[(ITr)Li]^+$ salts that do not involve toxic thallium-based precursors.

16. (a) Lang, H.; Jakob, A.; Milde, B. *Organometallics* **2012**, *31*, 7661; (b) Dorel, R.; Echavarren, A. M. *Chem. Rev.* **2015**, *115*, 9028; (c) Halbes-Letinois, U.; Weibel, J.-M.; Pale, P. *Chem. Soc. Rev.* **2007**, *36*, 759; (d) Díez-González, S.; Marion, N.; Nolan, S. P. *Chem. Rev.* **2009**, *109*, 3612; (e) Fang, G.; Bi, X. *Chem. Soc. Rev.* **2015**, *44*, 8124; (f) Nechaev, M. S.; Rayón, V. M.; Frenking, G. *J. Phys. Chem. A* **2004**, *108*, 3134; (g) Niemeyer, M. *Organometallics* **1998**, *17*, 4649.

17. Weber, S. G.; Rominger, F.; Straub, B. F. *Eur. J. Inorg. Chem.* **2012**, 2863.

18. Weber, S. G; Zahner, D.; Rominger, F.; Straub, B. F. *Chem. Commun.* **2012**, *48*, 11325.

19. Phillips, N.; Dodson, T.; Tirfoin, R.; Bates, J. I. Aldridge, S. *Chem. Eur. J.* **2014**, *20*, 16721.

20. Collins, L. R.; Rajabi, N. A.; Macgregor, S. A.; Mahon, M. F.; Whittlesey, M. K. *Angew. Chem. Int. Ed.* **2016**, *55*, 15539.

21. Romero, E. A.; Olsen, P. M.; Jazzar, R.; Soleilhavoup, M.; Gembicky, M.; Bertrand, G. *Angew. Chem. Int. Ed.* **2017**, *56*, 4024.

22. For articles and reviews, see: (a) Reisinger, A.; Trapp, N.; Knapp, C.; Himmel, D.; Breher, F.; Rüegger, H.; Krossing, I. *Chem. Eur. J.* **2009**, *15*, 9505; (b) Reisinger, A.; Trapp, N.; Krossing, I.; Altmannshofer, S.; Herz, V.; Presnitz, M.; Scherer, W. *Angew. Chem. Int. Ed.* **2007**, *46*, 8295; (c) Dias, H. V. R.; Fianchini, M. *Angew. Chem. Int. Ed.* **2007**, *46*, 2188; (d) Dias, H. V. R.; Lovely, C. J. *Chem. Rev.* **2008**, *108*, 3223; (e) Jayaratna, N. B.; Gerus, I. I.; Mironets, R. V.; Mykhailiuk, P. K.; Yousufuddin, M.; Dias, H. V. R. *Inorg. Chem.* **2013**, *52*, 1691; (f) Dias, H. V. R.; Flores, J. A.; Wu, J.; Kroll, P. *J. Am. Chem. Soc.* **2009**, *131*, 11249.

23. (a) Gibard, C.; Fauché, K.; Guillot, R; Jouffret, L.; Traïkia, M.; Gautier, A.; Cisnetti, F. *J. Organomet. Chem.* **2017**, *840*, 70; (b) Wong, V. H. L.; White, A. J. P.; Hor, T. S. A.; Hii, K. K. *Chem. Commun.* **2015**, *51*, 17752; (c) Su, H.-L.; Pérez, L. M.; Lee, S.-J.; Reibenspies, J. H.; Bazzi, H. S.; Bergbreiter, D. E. *Organometallics* **2012**, *31*, 4063; (d) de Frémont, P.; Scott, N. M.; Stevens, E. D.; Ramnial, T.; Lightbody, O. C.; Macdonald, C. L. B.; Clyburne, J. A. C.; Abernethy, C. D.; Nolan, S. P. *Organometallics* **2005**, *24*, 6301.

24. For example: Smith, H. G.; Rundle, R. E. *J. Am. Chem. Soc.* **1958**, *80*, 5075.

25. (a) Childs, R. F.; Mulholland, D. L.; Nixon, A. *Can. J. Chem.* **1982**, *60*, 801; (b) Britovsek, G. J. P.; Ugolotti, J.; White, A. J. P. *Organometallics* **2005**, *24*, 1685.

26. (a) Böhrer, H.; Trapp, N.; Himmel, D.; Schleep, M.; Krossing, I. *Dalton Trans.* **2015**, *44*, 7489; (b) Schleep, M.; Hettich, C.; Velázquez Rojaz, J.; Kratzert, D.; Ludwig, T.; Lieberth, K.; Krossing, I. *Angew. Chem. Int. Ed.* **2017**, *56*, 2880.

27. (a) Puschmann, F. F.; Stein, D.; Heift, D.; Hendriksen, C.; Gal, Z. A.; Grützmacher, H. F.; Grützmacher, H. *Angew. Chem. Int. Ed.* **2011**, *50*, 8420; (b) Heift, D.; Benkő, Z.; Grützmacher, H. *Dalton Trans.* **2014**, *43*, 831.
28. Liu, L.; Ruiz, D. A.; Dahcheh, F.; Bertrand, G.; Suter, R.; Tondreau, A. M.; Grützmacher, H. *Chem. Sci.* **2016**, *7*, 2335.
29. Rummel, E.-M.; Mastrorilli, P.; Todisco, S.; Latronico, M.; Balázs, G.; Virovets, A. V.; Scheer, M. *Angew. Chem. Int. Ed.* **2016**, *55*, 13301.
30. Liew, S. K.; Al-Rafia, S. M. I.; Goettel, J. T.; Lummis, P. A.; McDonald, S. M.; Miedema, L. J.; Ferguson, M. J.; McDonald, R.; Rivard, E. *Inorg. Chem.* **2012**, *51*, 5471.
31. Weber, S. G.; Loos, C.; Rominger, F.; Straub, B. F. *ARKIVOC* **2012**, *iii*, 226.
32. For a recent example of bulky NHCs in catalysis, see: Lan, X.-B.; Li, Y.; Li, Y.-F.; Shen, D.-S.; Ke, Z.; Liu, F.-S. *J. Org. Chem.* **2017**, *82*, 2914.
33. Pangborn, A. B.; Giardello, M. A.; Grubbs, R. H.; Rosen, R. K.; Timmers, F. J. *Organometallics* **1996**, *15*, 1518.
34. Straus, D. A.; Zhang, C.; Tilley, T. D. *J. Organomet. Chem.* **1989**, *369*, C13.
35. Davis, D. P.; Kirk, K. A.; Cohen, L. A. *J. Heterocyclic Chem.* **1982**, *19*, 253.
36. Cullinane, J.; Jolleys, A.; Mair, F. S. *Dalton Trans.* **2013**, *42*, 11971.
37. Hope, H. *Prog. Inorg. Chem.* **1994**, *41*, 1.
38. Sheldrick, G. M. *Acta. Crystallogr. Sect. A.* **2015**, *71*, 3.
39. Sheldrick, G. M. *Acta. Crystallogr. Sect. C.* **2015**, *71*, 3.
40. Gaussian 9, Revision D.01, Frisch, M. J.; Trucks, G. W.; Schlegel, H. B.; Scuseria, G. E.; Robb, M. A.; Cheeseman, J. R.; Scalmani, G.; Barone, V.; Mennucci, B.;

Petersson, G. A.; Nakatsuji, H.; Caricato, M.; Li, X.; Hratchian, H. P.; Izmaylov, A. F.; Bloino, J.; Zheng, G.; Sonnenberg, J. L.; Hada, M.; Ehara, M.; Toyota, K.; Fukuda, R.; Hasegawa, J.; Ishida, M.; Nakajima, T.; Honda, Y.; Kitao, O.; Nakai, H.; Vreven, T.; Montgomery, J. A.; Peralta, J. E.; Ogliaro, F.; Bearpark, M.; Heyd, J. J.; Brothers, E.; Kudin, K. N.; Staroverov, V. N.; Kobayashi, R.; Normand, J.; Raghavachari, K.; Rendell, A.; Burant, J. C.; Iyengar, S. S.; Tomasi, J.; Cossi, M.; Rega, N.; Millam, J. M.; Klene, M.; Knox, J. E.; Cross, J. B.; Bakken, V.; Adamo, C.; Jaramillo, J.; Gomperts, R.; Stratmann, R. E.; Yazyev, O.; Austin, A. J.; Cammi, R.; Pomelli, C.; Ochterski, J. W.; Martin, R. L.; Morokuma, K.; Zakrzewski, V. G.; Voth, G. A.; Salvodor, P.; Dannenberg, J. J.; Dapprich, S.; Daniels, A. D.; Farkas, Ö.; Foresman, J. B.; Ortiz, J. V.; Cioslowski, J.; Fox, D. J. Gaussian, Inc., Wallingford CT, **2009**.

41. (a) Lee, C.; Yang, W.; Parr, R. G. *Phys. Rev. B* **1988**, *37*, 785; (b) Becke, A. D. *Phys. Rev. A* **1988**, *38*, 3098; (c) Stephens, P. J.; Devlin, F. J.; Chabalowski, C. F.; Frisch, M. J. *J. Phys. Chem.* **1994**, *98*, 11623.
42. (a) Hariharan, P. C.; Pople, J. A. *Theor. Chim. Acta* **1973**, *28*, 213; (b) Francl, M. M.; Pietro, W. J.; Hehre, W. J.; Binkley, J. S.; Gordon, M. S.; DeFrees, D. J.; Pople, J. A. *J. Chem. Phys.* **1982**, *77*, 3654.
43. (a) Hay, P. J.; Wadt, W. R. *J. Chem. Phys.* **1985**, *82*, 270; (b) Wadt, W. R; Hay, P. J. *J. Chem. Phys.* **1985**, *82*, 284; (c) Hay, P. J.; Wadt, W. R. *J. Chem. Phys.* **1985**, *82*, 299.
44. Neese, F. *Wiley Interdiscip. Rev.: Comput. Mol. Sci.* **2012**, *2*, 73.
45. Perdew, J. P.; *Phys. Rev. B* **1986**, *33*, 8822.

46. (a) Weigand, F.; Ahlrichs, R. *Phys. Chem. Chem. Phys.* **2005**, *7*, 3297; (b) Weigand, F. *Phys. Chem. Chem. Phys.* **2006**, *8*, 1057.

Chapter 5: Neutral, Cationic and Hydride-substituted Siloxygermylenes

5.1. Introduction

The search for new inorganic bonding motifs[1] has led to the emergence of s/p-block element-mediated catalysis,[2] and improved routes to bulk and nanodimensional materials.[3] To gain access to new reactive species for the abovementioned applications, our group[4] and others[5] have explored donor–acceptor stabilization, wherein normally unstable main group species are complexed between capping Lewis acidic (LA) and Lewis basic (LB) groups. For example, the Rivard group has prepared low-oxidation state Group 14 element hydride complexes LB•EH_2•LA and LB•H_2E–EH_2•LA (E = Si, Ge, and/or Sn)[6] as well as complexes of the inorganic acetylene analogue HBNH.[7] Of added relevance to the current study, the Lewis acid-free stabilization of reactive two-coordinate Ge^{II} cations such as $[LB•GeCl]^+$ is possible when the Lewis basic donor (LB) is very large.[8] Somewhat surprisingly, catalysis involving such cations had not been reported prior to this study, despite the presence of an accessible site for coordination at germanium.

In this chapter, the siloxy-substituted germylene IPr•$GeCl(OSiMe_3)$ (IPr = $[(HCNDipp)_2C:]$; Dipp = 2,6-*i*$Pr_2C_6H_3$) is prepared, containing labile halide and siloxy functionalities. Halide abstraction led to the formation of a rare acyclic two-coordinate Ge^{II} cation $[IPr•Ge(OSiMe_3)]^+$ which was found to participate in oxidative addition chemistry, and to catalyze the hydroborylation of ketones under mild conditions; these processes are facilitated by the presence of an open coordination site at Ge. In

addition, new experimental and computational insight into factors that govern the stability of Ge^{II} hydrides within donor–acceptor systems are described.

5.2. Results and Discussion

The Rivard group recently prepared a donor–acceptor complex of chloro-oxoborane IPr•ClB=O•$B(C_6F_5)_3$[9] by $B(C_6F_5)_3$-induced $ClSiMe_3$ loss from the dihalosiloxyborane adduct IPr•$BCl_2(OSiMe_3)$ (Scheme 5.1). Accordingly, the hitherto unknown precursor IPr•$GeCl(OSiMe_3)$ is expected to be a suitable precursor to carbene-stabilized GeO in the presence of a strong Lewis acid (Scheme 5.1).[5d, 10]

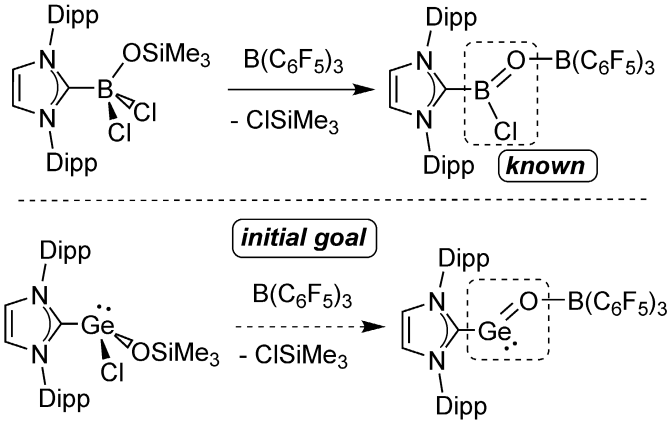

Scheme 5.1. Previous synthesis of a chlorooxoborane complex and postulated route to a GeO donor–acceptor complex; formal charges are omitted for clarity.

Fortunately, the synthesis of the requisite precursor IPr•$GeCl(OSiMe_3)$ (**1**) proceeded in a straightforward fashion (98 % isolated yield) by combining the known Ge^{II} chloride adduct IPr•$GeCl_2$[6a] with commercially available $NaOSiMe_3$ in Et_2O (Scheme 5.2). Colorless X-ray quality crystals of **1** (Mp = 146–147 °C) were obtained from a cold (−30 °C) toluene/hexanes mixture and the crystallographically determined structure is presented as Figure 5.1. The metrical parameters of **1** were similar to those of other known NHC•GeR_2 complexes[5c,6a] with a C_{NHC}–Ge distance of 2.113(2) Å, while the Ge–Cl

distance in **1** is 2.3459(7) Å [*cf.* 2.277(1) Å avg. in IPr•$GeCl_2$].[6a] As expected, a pyramidal geometry is present about the Ge atom in **1** [$\sum\alpha = 281.2(1)°$] due to the existence of a lone pair.

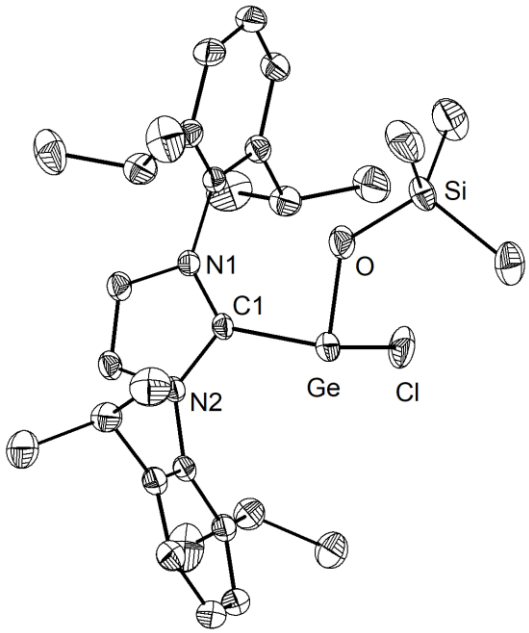

Figure 5.1. Molecular structure of IPr•GeCl($OSiMe_3$) (**1**) with thermal ellipsoids presented at the 30 % probability level. All hydrogen atoms and toluene solvate have been omitted for clarity. Selected bond lengths [Å] and angles [°]: Ge–C(1) 2.113(2), Ge–Cl 2.3459(7), Ge–O 1.8128(18); C(1)-Ge-Cl 88.86(5), C(1)-Ge-O 94.58(8), O-Ge-Cl 97.79(7).

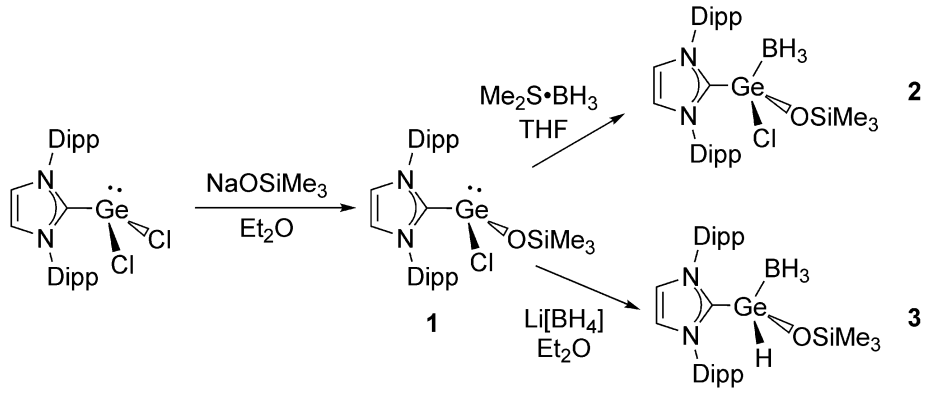

Scheme 5.2. Preparation of the siloxy-substituted germylene (**1**), its borane adduct (**2**), and the donor–acceptor germanium(II) siloxy-hydride adduct (**3**).

A stoichiometric quantity of $B(C_6F_5)_3$ was then added to IPr•GeCl($OSiMe_3$) (**1**) in toluene with the hope of instigating $ClSiMe_3$ elimination to yield the donor–acceptor complex IPr•GeO•$B(C_6F_5)_3$ (Scheme 5.1). However, analysis of the resulting product mixture showed the formation of the known adduct IPr•$GeCl_2$ (according to ^1H and $^{13}C\{^1H\}$ NMR spectroscopy)[6a] and multiple unidentified IPr and -$OSiMe_3$ containing products. One possible explanation for the formation of IPr•$GeCl_2$ is that $B(C_6F_5)_3$ promoted Cl/$OSiMe_3$ group scrambling via abstraction of one of these groups from Ge. In order to identify the possible disproportionation product IPr•Ge($OSiMe_3$)$_2$, IPr•$GeCl_2$ was mixed with two equivalents of $NaOSiMe_3$ in Et_2O. However, this reaction afforded a mixture of free IPr and several unknown -$OSiMe_3$ containing products as determined by ^1H NMR spectroscopy. Thus, it appears that the concomitant increase in steric bulk and reduction of Lewis acidity at the Ge center in the target species IPr•Ge($OSiMe_3$)$_2$, prevented its formation. In addition, this reaction yielded a few crystals of a product identified by X-ray crystallography as the germanide salt [IPrH][Na{$Ge_2(OSiMe_3)_6$}] (Figure 5.2). This divergent reactivity from the boron analogue IPr•$Cl_2B(OSiMe_3)$[9] is likely due to the relatively weak Ge–O linkage in **1** compared to the proximal Si–O bond in -$OSiMe_3$. It was reasoned, however that the -$OSiMe_3$ group in **1** should be useful both as a stabilizing π-donor ligand (allowing access to low-valent Ge^{II} compounds), and as an effective leaving group. For example, the first isolable Pb^{II} hydride was recently synthesized using the mild hydride source HBpin and an alkoxide-substituted Pb precursor (via H^-/OR^- exchange).[1k]

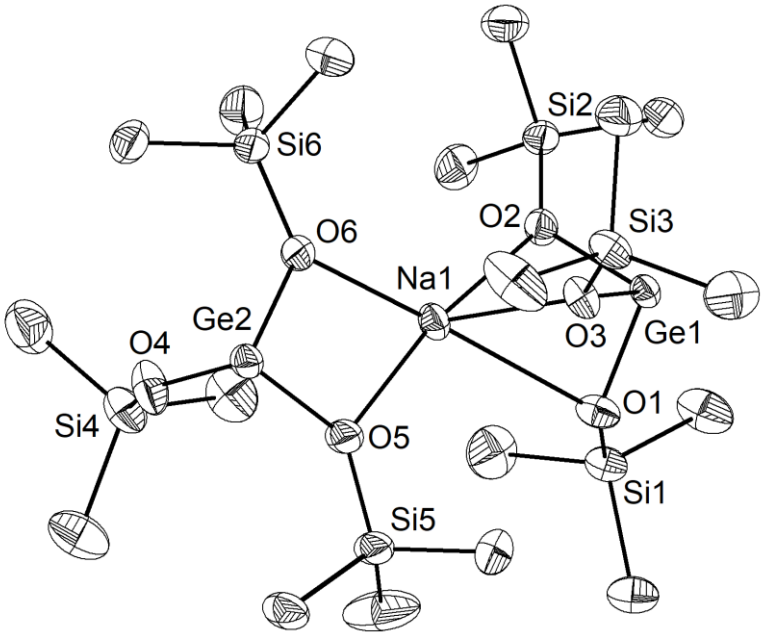

Figure 5.2. Molecular structure of [IPrH][Na{$Ge_2(OSiMe_3)_6$}] with thermal ellipsoids plotted at a 30 % probability level. The $[IPrH]^+$ counterion and all hydrogen atoms were omitted for clarity. Selected bond lengths [Å] and angles [°]: Ge1–O1 1.8639(12), Ge1–O2 1.8674(12), Ge1–O3 1.8616(11), Ge2–O4 1.8149(14), Ge2–O5 1.8709(13), Ge2–O6 1.8774(12), Na1–O1 2.8162(15), Na1–O2 2.4245(13), Na1–O3 2.3153(13), Na1–O5 2.2994(13), Na1–O6 2.3353(14); O1-Ge1-O2 92.60(6), O1-Ge1-O3 91.26(5), O4-Ge2-O5 99.05(7), O4-Ge2-O6 98.16(7).

The Ge^{II} center in IPr•$GeCl(OSiMe_3)$ (**1**) also has inherent dual nucleophilic and electrophilic character, thus these different reactivity profiles were explored in more depth. As a starting point, the germylene adduct **1** was combined with Me_2S•BH_3 in THF. If one runs the reaction at room temperature for one minute, followed by rapid work-up and crystallization of the resulting product from toluene/hexanes at −30 °C, the 1:1 complex IPr•$GeCl(OSiMe_3)$•BH_3 (**2**) can be obtained (Figure 5.3; Scheme 5.2). Leaving solutions of **2** at room temperature in toluene, Et_2O or THF for longer than 30 min., resulted in significant decomposition of **2** to give IPr•BH_3[11] as the main carbene-containing product.

In this case, BH_3 promotes decomplexation of the carbene (IPr) from the Ge to form IPr•BH_3 and presumably the unstable germylene ClGe($OSiMe_3$).

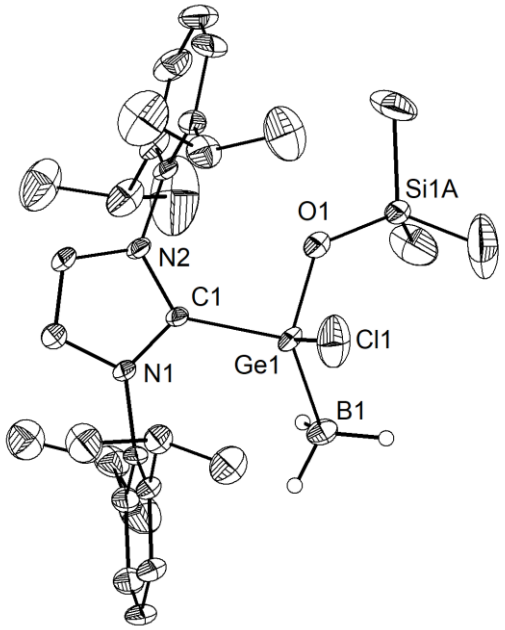

Figure 5.3. Molecular structure of IPr•GeCl($OSiMe_3$)•BH_3 (**2**) with thermal ellipsoids plotted at a 30 % probability level. All carbon-bound hydrogen atoms and toluene solvate have been omitted for clarity. Selected bond lengths [Å] and angles [°]: C1–Ge1 2.030(4), Ge1–Cl1 2.2039(15), Ge1–B1 2.030(6), Ge1–O1 1.767(3); C1-Ge1-B1 122.3(2), Cl1-Ge1-O1 102.32(13), Cl1-Ge1-B1 115.2(2).

The observed instability of the Ge^{II}-borane complex IPr•GeCl($OSiMe_3$)•BH_3 (**2**) led to a study of the thermodynamics associated with the formation of IPr•GeX($OSiMe_3$)•BH_3 (X = Cl or H) from IPr•GeX($OSiMe_3$) and BH_3 in the gas phase. As summarized in Scheme 5.3, the formation of IPr•GeCl($OSiMe_3$)•BH_3 is less favorable (Δ_rH = −98.7 kJ/mol; Δ_rG = −55.2 kJ/mol) than its Ge^{II} hydride analogue IPr•GeH($OSiMe_3$)•BH_3 (Δ_rH = −123.4 kJ/mol; Δ_rG = −77.4 kJ/mol), suggesting the more electronegative chloride ligand reduces the Lewis basicity of the germylene which affords a less thermodynamically

stable adduct with BH_3. This result is interesting as base-free Ge^{II} hydrides are often much less stable than their chloride counterparts,[2b] however the opposite stability trend is found within donor–acceptor complexes and partially explains the stability of the Ge^{II} dihydride complex IPr•GeH_2•BH_3.[6a]

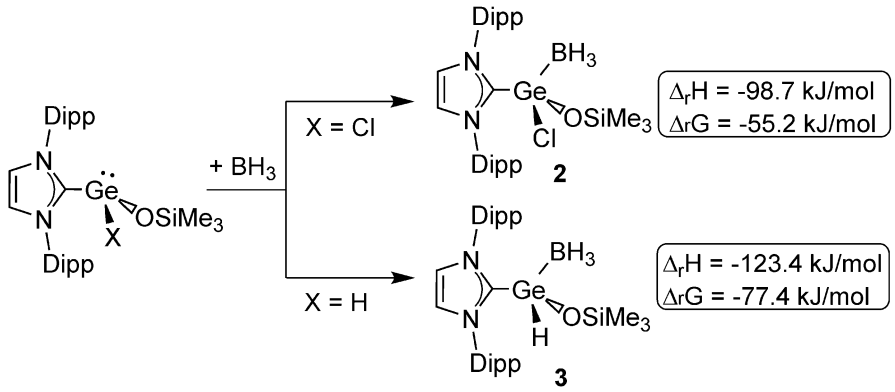

Scheme 5.3. Computed energetics [B3LYP/6-31G(d,p)] associated with the formation of IPr•GeX($OSiMe_3$)•BH_3 complexes (X = Cl or H).

These encouraging computational studies (*vide supra*) led to the attempted synthesis of the first siloxy(hydrido)germylene complex IPr•GeH($OSiMe_3$)•BH_3 (**3**). Added inspiration comes from prior work in the Rivard group concerning the conversion of Ge^{II} hydride complexes (*cf.* Ph_3PCMe_2•GeH_2•BH_3)[12] into luminescent Ge nanoparticles upon mild heating.[3b] As anticipated from computations (Scheme 5.3) IPr•GeH($OSiMe_3$)•BH_3 (**3**) could be formed in a nearly quantitative yield as a moisture-sensitive, colorless solid by combining IPr•GeCl($OSiMe_3$) (**1**) with Li[BH_4] in Et_2O (Scheme 5.2). Interestingly, **3** showed a significantly downfield shifted Ge–H signal in the ^{1}H NMR spectrum (δ 6.31 ppm in C_6D_6) compared to the corresponding Ge–H resonances in the previously reported germanium dihydrides, IPr•GeH_2•BH_3 (δ 3.92 ppm in C_6D_6)[6a] and IPr•GeH_2•$W(CO)_5$ (δ 4.23 ppm in C_6D_6).[6b] IPr•GeH($OSiMe_3$)•BH_3 (**3**) is stable for prolonged periods of time at room temperature in solution but decomposes in the solid state

upon heating to 119 °C under an atmosphere of N_2. Heating a solution of **3** in C_6D_6 at 50 °C for two days led to the formation of IPr•BH_3,[11] the dihydroaminal [$(HCNDipp)_2CH_2$] ($IPrH_2$),[6b] trace amounts of IPr•GeH_2•BH_3,[6a] and an insoluble product, tentatively assigned as germanium metal, indicating that **3** should be an effective molecular precursor to germanium nanomaterials. The molecular structure of **3** (Figure 5.4) compares well with the distorted tetrahedral geometry observed for the amido-substituted germylene, IPr•GeH(NHDipp)•BH_3.[6e] Specifically, the C_{NHC}–Ge and Ge–H distances in **3** [2.033(4) and 1.54(6) Å, respectively] are the same within experimental error as those found in IPr•GeH(NHDipp)•BH_3 [2.020(2) and 1.53(4) Å].

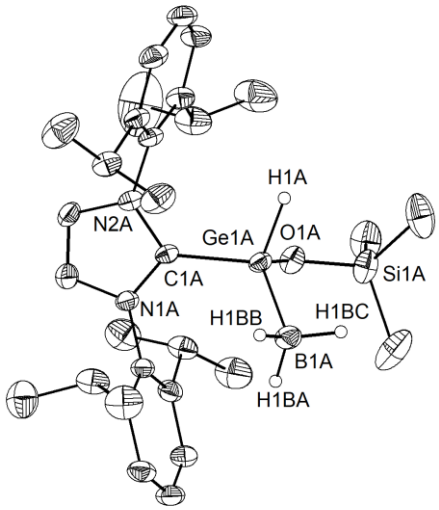

Figure 5.4. Molecular structure of IPr•GeH($OSiMe_3$)•BH_3 (**3**) with thermal ellipsoids plotted at a 30 % probability level. Two independent molecules of **3** were located in the asymmetric unit, and all carbon-bound hydrogen atoms have been omitted for clarity. Selected bond lengths [Å] and angles [°] for **3** with values corresponding to a second molecule in the asymmetric unit presented in square brackets: Ge1A–C1A 2.033(4) [2.011(5)], Ge1A–O1A 1.802(3) [1.795(9)], Ge1A–B1A 2.033(6) [2.004(16)], Ge1A–H1A 1.54(6); O1A-Ge1A-C1A 97.35(16) [91.9(4)], O1A-Ge1A-B1A 115.7(2) [116.5(15)], C1A-Ge1A-B1A 118.7(2) [117.9(14)].

Main group element alkoxides and triflates have been shown to be effective precatalysts for carbonyl reductions.[2e,13] Accordingly, the siloxy-germylene IPr•GeCl(OSiMe$_3$) (**1**) may also act as a precatalyst in a similar fashion. As such, 10 mol % **1** was added to a vial containing a 1:1 mixture of benzophenone and pinacolborane (HBpin) in C_6D_6, however stirring the mixture overnight at room temperature did not afford any of the expected hydroborylation product $Ph_2C(H)O(Bpin)$. Likewise, no hydroborylation was observed when using **2** as a precatalyst, however using the Ge^{II} hydride **3** (10 mol %) as a precatalyst led to stoichiometric (10 %) substrate conversion to $Ph_2C(H)O(Bpin)$ after stirring overnight. In order to investigate the possible formation of IPr•Ge(H)Cl[14] (via $OSiMe_3^-/H^-$ exchange with HBpin), IPr•GeCl(OSiMe$_3$) (**1**) was treated with a stoichiometric quantity of HBpin (Scheme 5.4); as stated previously, pinacolborane-mediated alkoxy/hydride exchange is a known route to main group hydrides.[1k,13a] The resulting product mixture arising from the combination of **1** and HBpin contained the expected siloxyborane $Me_3SiO–Bpin$[15] as the sole Bpin-containing product, along with IPr•$GeCl_2$ and $IPrH_2$[6b] (Scheme 5.4) as major species. This reactivity implies that any initially formed IPr•Ge(H)Cl disproportionates into IPr•$GeCl_2$ and IPr•GeH_2, of which the latter readily decomposes into $IPrH_2$ in the absence of a stabilizing Lewis acid (Scheme 4).[6b] The same procedure was repeated using DBpin in place of HBpin. Accordingly, the expected deuterated dihydroaminal ($IPrD_2$) was observed by ^1H and $^2H\{^1H\}$ NMR spectroscopy.

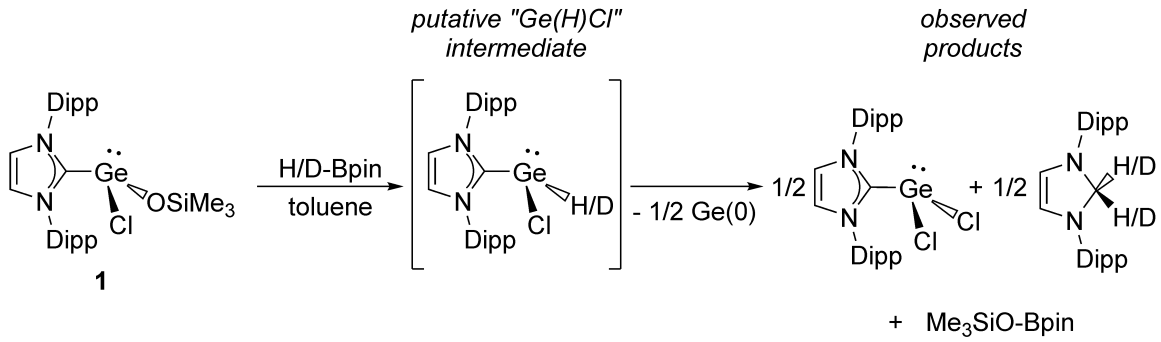

Scheme 5.4. Attempted formation of IPr•Ge(H)Cl and the observed products.

In an effort to stabilize IPr•Ge(H)Cl in the form of its BH_3 adduct IPr•GeH(Cl)•BH_3, IPr•$GeCl_2$ was combined with one equivalent of Li[BH_4] in Et_2O. NMR spectroscopic analysis of the product mixture after 1 hour (Figure 5.5) revealed a mixture of unreacted IPr•$GeCl_2$ (26 %), IPr•BH_3 (34 %), and a set of signals consistent with the formation of the desired Ge^{II} hydride complex IPr•GeH(Cl)•BH_3 (40 %). Specifically, a downfield shifted Ge–H signal (δ 6.08 ppm in C_6D_6) was found with discernable coupling to a -BH_3 unit in the $^1H\{^{11}B\}$ spectrum (quartet, $^3J_{HH}$ = ca. 4 Hz; Figure 5.5). Stirring the reaction mixture overnight revealed that IPr•GeH(Cl)•BH_3 is unstable in solution and is converted to IPr•BH_3 and an insoluble precipitate, similar to what was observed for the siloxy-functionalized adduct IPr•GeCl($OSiMe_3$)•BH_3 (**2**). IPr•$GeCl_2$ was then combined with one equivalent of Li[BD_4], and IPr•GeD(Cl)•BD_3 formation was confirmed by NMR. Due to the instability of IPr•GeH(Cl)•BH_3 in solution and its similar solubility to that of IPr•$GeCl_2$, separation of the [:Ge(H)Cl] complex from the mixture prior to its complete decomposition was not achieved, despite several attempts. In order to enhance the stability of potential Ge^{II} hydrides formed during hydroborylation catalysis, a cationic siloxy-germylene [IPr•Ge($OSiMe_3$)]$^+$ was targeted via halide abstraction from compound **1**.

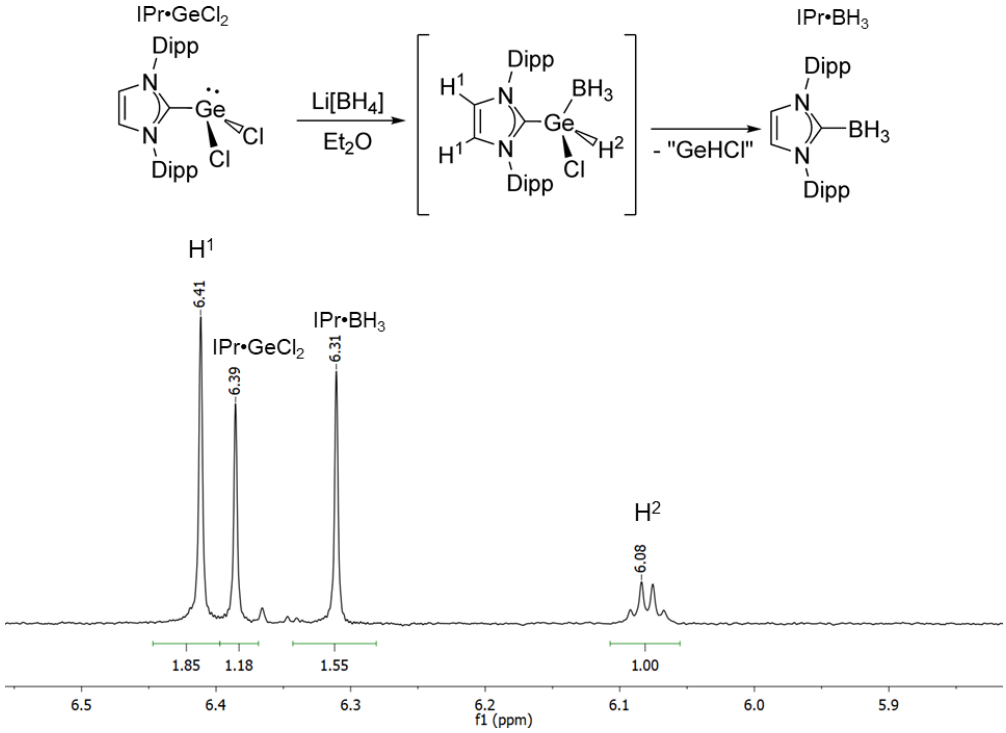

Figure 5.5. $^{1}H\{^{11}B\}$ NMR (C_6D_6, 400 MHz) spectroscopic observation of IPr•GeH(Cl)•BH_3 generated from the reaction of IPr•$GeCl_2$ with one equivalent of Li[BH_4].

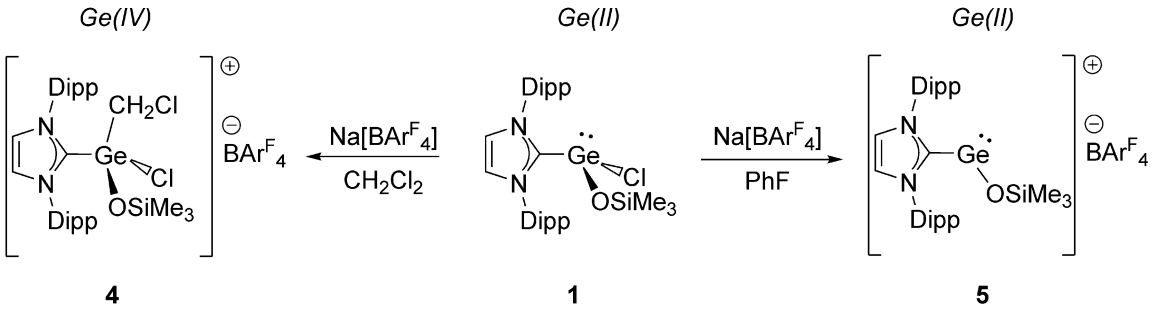

Scheme 5.5. Formation of the siloxy-germylium cation **4** via oxidative addition of CH_2Cl_2 and the initially targeted siloxy-germyliumylidene **5**.

In a first attempt to synthesize [IPr•Ge($OSiMe_3$)]$^+$, the siloxy(chloro)germylene IPr•GeCl($OSiMe_3$) (**1**) was combined with one equivalent of Na[BAr^F_4]

(Ar^F = 3,5-$(F_3C)_2C_6H_3$) in dichloromethane (Scheme 5.5). ^{1}H NMR spectroscopy of the filtrate showed a new product with a downfield shifted resonance corresponding to the NHC backbone protons (δ 7.58 ppm in $CDCl_3$), consistent with a cationic NHC adduct. Along with the expected IPr and $[BAr^F_4]^-$ resonances, a pair of leaning doublets (δ 2.69 and 2.49 ppm) were found with a coupling constant consistent with geminal H–H coupling ($^2J_{HH}$ = 12.0 Hz). X-ray crystallography identified the product as the Ge^{IV} germylium cation [IPr•GeCl($OSiMe_3$)CH_2Cl][BAr^F_4] (**4**), formed via the oxidative addition of the CH_2Cl_2 solvent to the target siloxygermanium(II) cation [IPr•Ge($OSiMe_3$)]$^+$ (Scheme 5.5). Main group element-mediated oxidative addition of CH_2Cl_2 is still a rare transformation, and suggests a high level of reactivity inherent to [IPr•Ge($OSiMe_3$)]$^+$.[16,17] For example, two-coordinate Si^{II} heterocycles (silylenes) are known to react with dichloromethane to form disilanes[16b] or undergo double insertions to yield methylene-bridged silanes.[16a] Moreover, the slow reaction (one week, room temp.) of CH_2Cl_2 with a cyclic bis-amidosilylene,[16c] and the oxidative addition of dichloromethane to [IPr•Ge{$CH(SiMe_3)_2$}]$^+$ have been reported.[17c] The molecular structure of **4** shows that Ge is in a distorted tetrahedral geometry with shortened C_{NHC}–Ge and Ge–$OSiMe_3$ bond lengths [1.968(2) and 1.7159(19) Å, respectively] compared to those of the neutral precursor IPr•GeCl($OSiMe_3$) (**1**) [2.030(4) and 1.8128(18) Å], indicating enhanced Lewis acidity of the Ge^{IV} center in **4** (Figure 5.6).

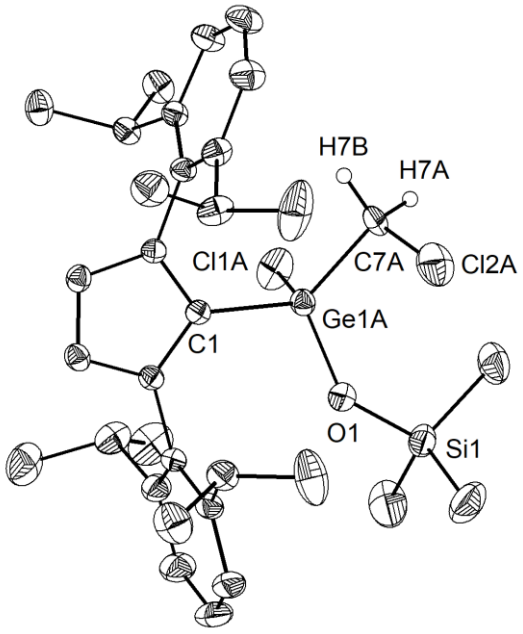

Figure 5.6. Molecular structure of [IPr•GeCl(OSiMe$_3$)CH$_2$Cl][BAr$^F{}_4$] (**4**) with thermal ellipsoids plotted at a 30 % probability level. All hydrogen atoms (except H7A, H7B), fluorobenzene solvate and the [BAr$^F{}_4$]$^-$ anion were omitted for clarity. Selected bond lengths [Å] and angles [°]: C1–Ge1A 1.968(2), Ge1A–Cl1A 2.1518(10), Ge1A–O1 1.7159(19), Ge1A–C7A 1.958(3); Cl1A-Ge1A-O1 107.58(8), Cl1A-Ge1A-C1 104.69(7), Cl1A-Ge1A-C7A 107.49(12), O1-Ge1A-C1 105.61(9).

When the reaction between Na[BAr$^F{}_4$] and **1** was repeated in fluorobenzene rather than in dichloromethane, the formation of [IPr•Ge(OSiMe$_3$)][BAr$^F{}_4$] (**5**) was observed (Scheme 5.5). X-ray crystallography revealed a bent two-coordinate geometry at Ge with a C1-Ge1-O1 angle of 96.45(10)° (Figure 5.7). As expected, the Ge–O distance in this cation [1.716(2) Å] was around 0.1 Å shorter than in the neutral adduct IPr•GeCl(OSiMe$_3$) (**1**) [1.8128(18) Å].

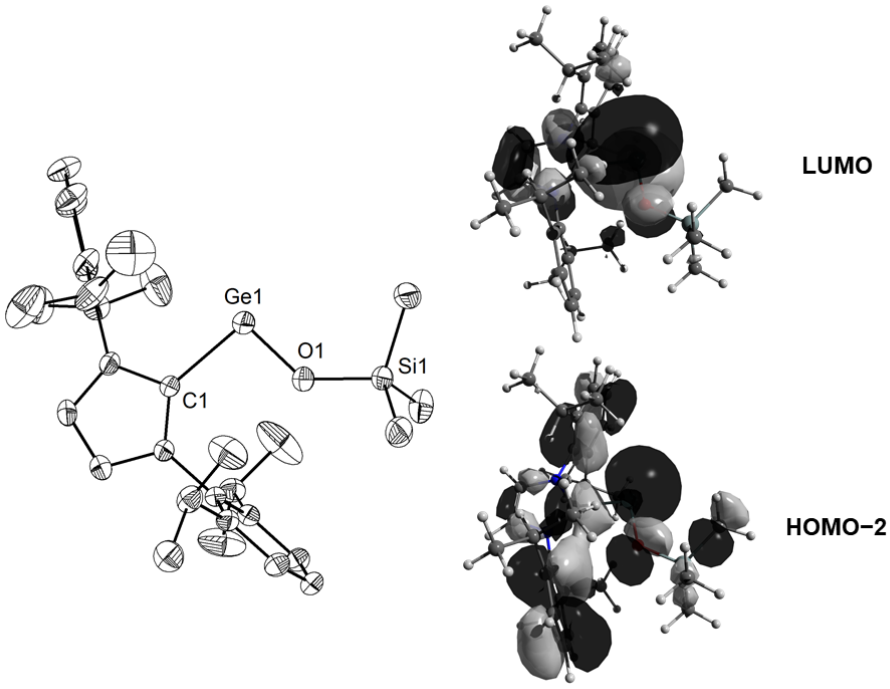

Figure 5.7. Molecular structure of [IPr•Ge(OSiMe$_3$)][BAr$^F{}_4$] (**5**) with thermal ellipsoids plotted at a 30 % probability level (left) and selected computed molecular orbitals of **5** (right). All hydrogen atoms, fluorobenzene solvate, and the [BAr$^F{}_4$]$^-$ anion were omitted for clarity. Selected bond lengths [Å] and angles [°]: C1–Ge1 2.071(3), Ge1–O1 1.716(2), Si1–O1 1.670(2); C1-Ge1-O1 96.45(10), Ge1-O1-Si1 135.71(14).

Compound **5** represents a rare example of an acyclic germylene cation[8,17,18] and only the second example of such a species which undergoes clean oxidative addition chemistry.[17c] Specifically, the dark orange, alkyl-substituted germylene cation, [IPr•Ge{CH(SiMe$_3$)$_2$}]$^+$ also participated in oxidation addition of a C–Cl bond in CH_2Cl_2.[17c] The added π-donation from the -OSiMe$_3$ group in **5** leads to an expected widening of the HOMO/LUMO gap in relation to that found in [IPr•Ge{CH(SiMe$_3$)$_2$}]$^+$,[17c] as evidenced by the pale yellow color of **5**. Accordingly, the molecular orbitals of **5** were computed at the B3LYP/6-31G(d,p) level (Figure 5.7, right). The LUMO in **5** consists of a C_{NHC}–Ge π-interaction along with π* contribution between Ge and the -OSiMe$_3$ ligand. Both the HOMO and HOMO−1 orbitals in **5** reside on the Dipp groups of IPr, whereas the

germylene lone pair was located as part of the HOMO−2. The HOMO/LUMO gap in **5** was computed to be 342 kJ/mol and the energy difference between the germanium lone pair (HOMO−2) and a vacant orbital located on germanium (LUMO) is 364 kJ/mol, almost twice that of the HOMO/LUMO gap found for the reactive Ge^{II} cation $[IPr•Ge\{CH(SiMe_3)_2\}]^+$ (187 kJ/mol).[17c]

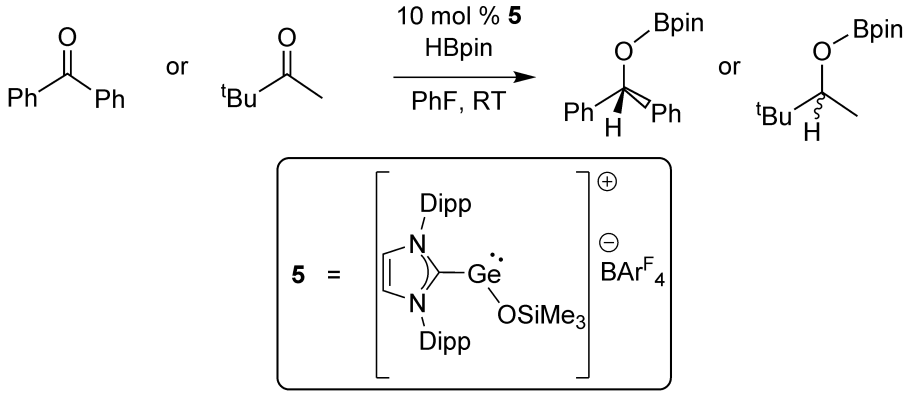

Scheme 5.6. Examples of the catalytic hydroborylation of hindered ketones using $[IPr•Ge(OSiMe_3)][BAr^F_4]$ (**5**) as a precatalyst.

Finally, $[IPr•Ge(OSiMe_3)][BAr^F_4]$ (**5**) was utilized as a precatalyst to promote the hydroborylation of hindered aryl and alkyl-substituted ketones (Scheme 5.6). To begin, 10 mol % of **5** was combined with a 1:1 mixture of benzophenone and HBpin in fluorobenzene at room temperature. After 25 min, 22 % Ph_2CO had been converted to $Ph_2C(H)O(Bpin)$[19] (as determined by ^1H NMR spectroscopy; TON = 2.2, TOF = 5.2 h^{-1}), with 61 % conversion being achieved after stirring the mixture overnight. In the same manner, the quantitative hydroborylation of the electron-rich ketone, pinacolone (*t*BuC(O)Me), was achieved with 10 mol % **5** after 25 minutes (TON = 10.2, TOF = 24.4 h^{-1}). This represents the first example of catalysis using a cationic germylene and future work will involve changing the nature of the stabilizing ligand in order to

facilitate the formation of the putative hydride catalyst [IPr•GeH]$^+$ (presumably formed via $OSiMe_3^-/H^-$ exchange with HBpin).[20]

5.3. Conclusions

A new siloxy-substituted germylene was prepared IPr•GeCl($OSiMe_3$) which proved to be an effective building block in the synthesis of the donor–acceptor stabilized siloxy(hydrido)germylene IPr•GeH($OSiMe_3$)•BH_3 and the siloxygermylene cation [IPr•Ge($OSiMe_3$)]$^+$. The [IPr•Ge($OSiMe_3$)]$^+$ cation participates in spontaneous oxidative addition chemistry with CH_2Cl_2 and catalyzes the room temperature hydroborylation of carbonyls; both processes are likely promoted by the presence of an empty coordination site at germanium. Future work will seek to generate more reactive E^{II} cations (E = Si–Pb) with a focus on preparing two-coordinate [LB•EH]$^+$ species for main group element-based catalysis.

5.4. Experimental Details

5.4.1. General

All reactions were performed in an inert atmosphere glovebox (Innovative Technology, Inc.). Fluorobenzene was dried by refluxing over calcium hydride, followed by vacuum distillation, and storage over 4 Å molecular sieves prior to use. All remaining solvents were dried using a solvent purification system provided by Innovative Technology, Inc., degassed (freeze-pump-thaw method), and stored under nitrogen prior to use. $GeCl_2$•dioxane, $NaOSiMe_3$, Me_2S•BH_3 (2.0 M solution in THF), Li[BH_4], Li[BD_4] (98 atom % D), benzophenone and HBpin were obtained from Aldrich and used as received. Na[BAr^F_4] (Ar^F = 3,5-$(F_3C)_2C_6H_3$) was purchased from Ark Pharmaceuticals and dried by

heating to 110 °C under vacuum for two days prior to use. IPr,[21] $B(C_6F_3)_3$,[22] IPr•$GeCl_2$[6a] were prepared according to literature procedures. A 1.5 M solution of DBpin in THF was synthesized according to a literature procedure[23] using 90 atom % D labelled $Na[BD_4]$; the concentration of the THF solution of DBpin was determined by the relative integrations of the DBpin methyl proton resonance and the THF resonances in the ^1H NMR spectrum.

5.4.2. X-ray Crystallography

Crystals for X-ray diffraction studies were removed from a vial (in a glovebox) and immediately coated with a thin layer of hydrocarbon oil (Paratone-N). A suitable crystal was then mounted on a glass fiber and quickly placed in a low temperature stream of nitrogen on the X-ray diffractometer.[24] All data were collected using a Bruker APEX II CCD detector/D8 or PLATFORM diffractometer using Mo K_α or Cu K_α radiation, with the crystals cooled to −80 °C or −100 °C. The data were corrected for absorption through Gaussian integration from the indexing of the crystal faces. Crystal structures were solved using intrinsic phasing (SHELXT)[25] and refined using SHELXL-2014.[26] The assignment of hydrogen atom positions was based on the sp^2 or sp^3 hybridization geometries of their attached carbon atoms and were given thermal parameters 20 % greater than those of their parent atoms.

Special refinement conditions. Compound **1**•1.5 C_7H_8: The disordered solvent toluene molecules had both bond distance restraints (DFIX) and displacement parameter restraints (RIGU) applied. Compound **2**: The crystal used for data collection was found to display non-merohedral twinning. Both components of the twin were indexed with the program *CELL_NOW* (Bruker AXS Inc., Madison, WI, 2004). The second twin component can be related to the first component by 180º rotation about the [$^{-1}/_2$ 1 0] axis in real space and

about the [0 1 $^1/_2$] axis in reciprocal space. Integrated intensities for the reflections from the two components were written into a *SHELXL-2014* HKLF 5 reflection file with the data integration program *SAINT* (version 8.38A), using all reflection data (exactly overlapped, partially overlapped and non-overlapped). The refined value of the twin fraction (*SHELXL-2014* BASF parameter) was 0.152(2). Compound **3**: The disordered Ge(H)(BH_3)($OSiMe_3$) core of molecule B was restrained to have similar bond lengths and angles as that of the order core in molecule A by use of the *SHELXL* SAME instruction. Additionally, the anisotropic displacement parameters for that group were restrained by use of the RIGU instruction. The Ge1B–H1B and Ge1C–H1C distances were restrained to be 1.50(2) Å. Compound **4**•0.5 C_6H_5F: The Ge1B–C7B and C7B–Cl2B distances were restrained to be the same as the Ge1A–C7A and C7A–Cl2A distances. Compound **5**•C_6H_5F: (a) Attempts to refine peaks of residual electron density as disordered or partial-occupancy solvent fluorobenzene fluorine or carbon atoms were unsuccessful. The data were corrected for disordered electron density through use of the SQUEEZE procedure as implemented in *PLATON*. A total solvent-accessible void volume of 928 $Å^3$ with a total electron count of 191 (consistent with 4 molecules of solvent fluorobenzene, or 1 molecule per formula unit of the germanium compound) was found in the unit cell. (b) The C–F distances within the minor orientation of all of the disorder CF_3 groups were restrained to be approximately the same by use of the SHELXL SADI instruction.

5.4.3. Computational Methods

All calculations were carried out using the Gaussian 16, Rev. A.03 software package.[27] Input structures were optimized using the B3LYP[28] functional and 6-31G(d,p)[29] basis set

in the gas phase. The optimized geometries were confirmed to be minima on the potential energy surface using frequency analysis.

5.4.4. Synthetic Procedures

Synthesis of IPr•GeCl(OSiMe$_3$) (1). An 8 mL Et_2O solution of IPr•$GeCl_2$ (0.102 g, 0.192 mmol) was added to a vial containing a solution of $NaOSiMe_3$ (0.023 g, 0.21 mmol) in 3 mL of Et_2O. The formation of a colorless precipitate was observed immediately and the resulting slurry was stirred for 1 hour. The slurry was filtered, and the volatiles were removed *in vacuo* affording IPr•GeCl($OSiMe_3$) (0.114 g, 98 %) as a colorless solid. Crystals suitable for X-ray diffraction analysis were obtained by layering a toluene solution of **1** with hexanes and storing the mixture at −30 °C overnight. ^{1}H NMR (400 MHz, C_6D_6): δ 7.22 (t, 2H, $^3J_{HH}$ = 7.8 Hz, *p*-Ar*H*), 7.09 (d, 4H, $^3J_{HH}$ = 8.0 Hz, *m*-Ar*H*), 6.37 (s, 2H, NCH), 2.90 (sept, 2H, $^3J_{HH}$ = 6.8 Hz, C*H*(CH_3)$_2$), 2.78 (sept, 2H, $^3J_{HH}$ = 6.8 Hz, C*H*(CH_3)$_2$), 1.44 (d, 12H, $^3J_{HH}$ = 6.8 Hz, CH(C*H*$_3$)$_2$), 1.01 (d, 12H, $^3J_{HH}$ = 6.8 Hz, CH(C*H*$_3$)$_2$), 0.07 (s, 9H, Si(CH_3)$_3$). ^{13}C{^{1}H} NMR (125 MHz, C_6D_6): δ 178.4 (N*C*N), 145.8 (Ar*C*), 145.6 (Ar*C*), 133.9 (Ar*C*), 130.7 (N*C*H), 124.2 (Ar*C*), 124.1 (Ar*C*), 124.0 (Ar*C*), 29.2 (*C*H(CH_3)$_2$), 29.1 (*C*H(CH_3)$_2$), 25.6 (CH(*C*H$_3$)$_2$), 25.5 (CH(*C*H$_3$)$_2$), 23.3 (CH(*C*H$_3$)$_2$), 23.2 (CH(CH_3)$_2$), 3.3 (Si(*C*H$_3$)$_3$). Anal. Calcd. for $C_{30}H_{45}ClGeN_2OSi$: C 61.50, H 7.74, N 4.78. Found: C 62.41, H 7.76, N 4.64. M.p. 146–147 °C.

Synthesis of IPr•Ge(Cl)OSiMe$_3$•BH$_3$ (2). To a vial containing a 1 mL solution of IPr•GeCl($OSiMe_3$) (0.050 g, 0.085 mmol) in THF was added Me_2S•BH_3 (2.0 M solution in THF, 43 μL, 0.086 mmol) and the mixture was stirred for 1 minute. The volatiles were then removed rapidly *in vacuo* affording IPr•Ge(Cl)$OSiMe_3$•BH_3 (0.051 g, 99 %) as a colorless solid. Colorless crystals suitable for X-ray diffraction analysis were grown by

layering a toluene solution of **2** with hexanes and storing the mixture at −30 °C overnight. Due to the instability of **2** in solution, IPr•BH_3[11] was present in the NMR spectra (ca. 15 %). $^1H\{^{11}B\}$ NMR (500 MHz, C_6D_6): δ 7.23 (t, 2H, $^3J_{HH}$ = 8.0 Hz, *p*-Ar*H*), 7.10 (d, 2H, $^3J_{HH}$ = 8.0 Hz, *m*-Ar*H*), 7.06 (d, 2H, $^3J_{HH}$ = 8.0 Hz, *m*-Ar*H*), 6.39 (s, 2H, NC*H*), 2.77 (sept, 2H, $^3J_{HH}$ = 7.0 Hz, C*H*$(CH_3)_2$), 2.67 (sept, 2H, $^3J_{HH}$ = 7.0 Hz, C*H*$(CH_3)_2$), 1.48 (d, 6H, $^3J_{HH}$ = 7.0 Hz, CH(C*H*$_3)_2$), 1.41 (d, 6H, $^3J_{HH}$ = 7.0 Hz, CH(C*H*$_3)_2$), 0.96 (d, 12H, $^3J_{HH}$ = 7.0 Hz, CH(C*H*$_3)_2$), 0.92 (broad s, 3H, BH_3), 0.09 (s, 9H, Si(C*H*$_3)_3$). $^{13}C\{^1H\}$ NMR (125 MHz, C_6D_6): δ 164.7 (N*C*N), 145.6 (Ar*C*), 145.5 (Ar*C*), 133.5 (Ar*C*), 131.5 (N*C*H), 125.5 (Ar*C*), 124.7 (Ar*C*), 124.4 (Ar*C*), 29.3 (*C*H$(CH_3)_2$), 29.2 (*C*H$(CH_3)_2$), 26.0 (CH(*C*H$_3)_2$), 25.8 (CH(*C*H$_3)_2$), 23.2 (CH(*C*H$_3)_2$), 23.1 (CH(*C*H$_3)_2$), 3.0 (Si(*C*H$_3)_3$). $^{11}B\{^1H\}$ NMR (160 MHz, C_6D_6): δ −32.6 (s) (BH_3). IR (film, cm^{-1}): 2379, 2341 (m, νB–H). Anal. Calcd. for $C_{30}H_{48}BClGeN_2OSi$: C 60.08, H 8.07, N 4.67. Found: C 60.14, H 8.10, N 4.56. M.p. 83 °C (decomp.).

Synthesis of IPr•Ge(H)OSiMe$_3$•BH_3 (3). A 2 mL solution of Li[BH_4] in Et_2O (4.0 mg, 0.18 mmol) was added to a vial containing a 3 mL solution of IPr•GeCl(OSiMe$_3$) (0.105 g, 0.179 mmol) in Et_2O. The formation of a colorless precipitate was observed and the resulting slurry was stirred for 1 hour. The slurry was filtered, and the solvent removed from the resulting filtrate *in vacuo* affording IPr•Ge(H)OSiMe$_3$•BH_3 (0.100 g, 99 %) as a colorless solid. Crystals suitable for X-ray diffraction analysis were grown by layering a toluene solution of **3** with hexanes and storing the mixture at −30 °C overnight. $^1H\{^{11}B\}$ NMR (500 MHz, C_6D_6): δ 7.22 (t, 2H, $^3J_{HH}$ = 7.8 Hz, *p*-Ar*H*), 7.08 (d, 4H, $^3J_{HH}$ = 8.0 Hz, *m*-Ar*H*), 6.48 (s, 2H, NC*H*), 6.31 (broad q, 1H, $^3J_{HH}$ = 5.0 Hz, Ge*H*), 2.78 (sept, 2H, $^3J_{HH}$ = 7.0 Hz, C*H*$(CH_3)_2$), 2.63 (sept, 2H, $^3J_{HH}$ = 7.0 Hz, C*H*$(CH_3)_2$), 1.42 (d, 6H, $^3J_{HH}$ = 7.0

Hz, CH(CH_3)$_2$), 1.41 (d, 6H, $^3J_{HH}$ = 7.0 Hz, CH(CH_3)$_2$), 0.99 (d, 6H, $^3J_{HH}$ = 7.0 Hz, CH(CH_3)$_2$), 0.98 (d, $^3J_{HH}$ = 7.0 Hz, 6H, CH(CH_3)$_2$), 0.89 (broad s, 3H, BH_3), 0.06 (s, 9H, Si(CH_3)$_3$). $^{13}C\{^1H\}$ NMR (125 MHz, C_6D_6): δ 169.2 (N*C*N), 145.8 (Ar*C*), 145.3 (Ar*C*), 133.5 (Ar*C*), 131.2 (N*C*H), 124.8 (Ar*C*), 124.4 (Ar*C*), 124.3 (Ar*C*), 29.2 (*C*H(CH$_3$)$_2$), 29.1 (*C*H(CH$_3$)$_2$), 25.5 (CH(*C*H$_3$)$_2$), 25.4 (CH(*C*H$_3$)$_2$), 23.2 (CH(*C*H$_3$)$_2$), 23.0 (CH(*C*H$_3$)$_2$), 2.8 (Si(*C*H$_3$)$_3$). $^{11}B\{^1H\}$ NMR (160 MHz, C_6D_6): δ −37.1 (s) (BH_3). IR (film, cm^{-1}): 1970 (m, ν Ge–H). Anal. Calcd. for C30H49BGeN2OSi: C 63.75, H 8.74, N 4.96. Found: C 63.40, H 8.70, N 4.70. M.p. 119 °C (decomp.).

Synthesis of [IPr•GeCl(OSiMe$_3$)CH$_2$Cl][BAr$^F_4$] (4). A slurry of Na[BAr$^F_4$] (0.246 g, 0.278 mmol) in 7 mL of CH_2Cl_2 was added to a vial containing a 1 mL solution of IPr•GeCl(OSiMe$_3$), (0.163 g, 0.278 mmol) in CH_2Cl_2. The resulting slurry was stirred overnight. The slurry was filtered and the solvent removed from the filtrate *in vacuo* affording [IPr•GeCl(OSiMe$_3$)CH$_2$Cl][BAr$^F_4$] (0.358 g, 86 %) as a colorless solid. Crystals suitable for X-ray diffraction analysis were obtained by layering a fluorobenzene solution of **5** with hexanes and storing the mixture at −30 °C overnight. ^1H NMR (400 MHz, $CDCl_3$): δ 7.70 (broad s, 8H, *o*-C$_6H_3$(CF$_3$)$_2$), 7.58 (s, 2H, NC*H*), 7.50 (broad s, 4H, *p*-C$_6H_3$(CF$_3$)$_2$), 7.43 (m, 4H, *m*-Ar*H*), 2.69 (leaning d, 1H, $^2J_{HH}$ = 12.0 Hz, Ge-CH_2Cl), 2.45 (leaning d, 1H, $^2J_{HH}$ = 12 Hz, Ge-CH_2Cl), 2.32 (broad s, 4H, C*H*(CH$_3$)$_2$), 1.37 (d, 6H, $^3J_{HH}$ = 8.0 Hz, CH(CH_3)$_2$), 1.33 (d, 6H, $^3J_{HH}$ = 8.0 Hz, CH(CH_3)$_2$), 1.15 (d, 6H, $^3J_{HH}$ = 8.0 Hz, CH(CH_3)$_2$), 1.13 (d, 6H, $^3J_{HH}$ = 8.0 Hz, CH(CH_3)$_2$), −0.13 (s, 9H, Si(CH_3)$_3$). The expected triplet resonance for the *p*-Ar*H* protons of the -Dipp groups appears to be buried by the *o*-C$_6$H$_3$(CF$_3$)$_2$ resonance (δ 7.70 ppm) and was therefore not assigned. $^{13}C\{^1H\}$ NMR (178 MHz, $CDCl_3$): δ 161.8 (1:1:1:1 q, $^1J_{CB}$ = 49.3 Hz, *ipso*-*C*$_6$H$_3$(CF$_3$)$_2$), 145.6 (N*C*H), 145.2

(Ar*C*), 144.8 (Ar*C*), 134.9 (Ar*C*), 133.6 (Ar*C*), 128.9 (q, $^{2}J_{CF}$ = 31.3 Hz, *C*CF_3), 128.8 (Ar*C*), 125.8 (Ar*C*), 125.5 (Ar*C*), 125.4 (Ar*C*), 124.6 (Ar*C*), 124.6 (q, $^{1}J_{CF}$ = 272.8 Hz, *C*F_3), 117.5 (Ar*C*), 32.1 (*C*H_2Cl), 29.5 (*C*H$(CH_3)_2$), 29.4 (CH(*C*H_3)$_2$), 26.0 (CH(*C*H_3)$_2$), 24.5 (CH(*C*H_3)$_2$), 23.6 (CH(*C*H_3)$_2$), 22.4 (CH(*C*H_3)$_2$), 1.8 (Si(*C*H_3)$_3$). An N*C*N resonance was not observed. ^{19}F NMR ($CDCl_3$, 376 MHz): δ −62.4 (s, BAr$^{F}_4$). ^{11}B{^{1}H} NMR ($CDCl_3$, 128 MHz): δ −6.6 (s, *B*Ar$^{F}_4$). Anal. Calcd. for $C_{63}H_{59}BCl_2F_{24}GeN_2OSi$: C 50.49, H 3.97, N 1.87; Found: C 51.03, H 4.18, N 1.97. M.p. 120–122 °C.

Synthesis of [IPr•Ge(OSiMe$_3$)][BAr$^{F}_4$] (5). To a vial containing IPr•GeCl(OSiMe$_3$) (0.251 g, 0.428 mmol) and Na[BAr$^{F}_4$] (0.378 g, 0.427 mmol) was added 12 mL of fluorobenzene resulting in a pale-yellow slurry. The mixture was stirred for 30 minutes and filtered. The precipitate was discarded, and the volatiles were removed from the filtrate *in vacuo* to give a pale-yellow oil. This oil was triturated with 3 mL of hexanes, affording [IPr•Ge(OSiMe$_3$)][BAr$^{F}_4$] (**5**) as a pale-yellow solid (0.357 g, 57 %). ^{1}H NMR (498 MHz, [D$_6$]DMSO): δ 8.54 (s, 2H, NC*H*), 7.70 (broad s, 4H, *p*-C$_6$*H*$_3$(CF$_3$)$_2$), 7.67 (t, $^{3}J_{HH}$ = 8.0 Hz, 2H, *p*-Ar*H*), 7.61 (broad s, 8H, *o*-C$_6$*H*$_3$(CF$_3$)$_2$), 7.51 (d, 4H, $^{3}J_{HH}$ = 8.0 Hz, *m*-Ar*H*), 2.34 (sept, 4H, $^{3}J_{HH}$ = 7.0 Hz, C*H*(CH$_3$)$_2$), 1.25 (d, 12H, $^{3}J_{HH}$ = 7.0 Hz, CH(C*H*$_3$)$_2$), 1.15 (d, 12H, $^{3}J_{HH}$ = 7.0 Hz, CH(C*H*$_3$)$_2$), 0.09 (broad s, 4H, Si(CH$_3$)$_3$), 0.01 (broad s, 5H, Si(C*H*$_3$)$_3$). ^{13}C{^{1}H} NMR (126 MHz, [D$_6$]DMSO): δ 160.9 (1:1:1:1 q, $^{1}J_{CB}$ = 50.3 Hz, *ipso*-*C*$_6$H$_3$(CF$_3$)$_2$), 144.8 (N*C*H), 134.0 (Ar*C*), 131.8 (Ar*C*), 130.0 (Ar*C*), 128.4 (q, $^{2}J_{CF}$ = 31.4 Hz, *C*CF_3), 127.2 (Ar*C*), 126.1 (Ar*C*), 124.6 (Ar*C*), 124.0 (q, $^{1}J_{CF}$ = 272.7 Hz, CF_3), 117.7 (Ar*C*), 28.6 (*C*H$(CH_3)_2$), 24.0 (CH(*C*H_3)$_2$), 23.0 (CH(*C*H_3)$_2$), 3.5 (Si(*C*H_3)$_3$). An N*C*N resonance was not observed. ^{19}F NMR (469 MHz, [D$_6$]DMSO): δ −61.6 (s, BAr$^{F}_4$). ^{11}B{^{1}H} NMR (160 MHz, [D$_6$]DMSO): δ −6.9 (s, *B*Ar$^{F}_4$). Anal Calcd. for

$C_{62}H_{57}BF_{24}GeN_2OSi$: C 52.68, H 4.06, N 1.98; Found: 52.63, H 4.16, N 1.96. M.p. 155–156 °C.

Representative ketone hydroborylation procedure. To a vial charged with Ph_2CO (0.025 g, 0.14 mmol) and 10 mol % **5** (0.019 g, 0.013 mmol) was added 1.00 mL of fluorobenzene, forming a colorless solution. HBpin was added to the solution (19.5 mL, 0.134 mmol) and the mixture was stirred at room temperature. Aliquots were removed from the mixture to monitor reaction progress. After 25 minutes, ^{1}H NMR analysis revealed 22 % conversion of Ph_2CO to $Ph_2C(H)OBpin$[18] (TON = 2.2, TOF = 5.2 h^{-1}). After stirring the remaining mixture overnight (18 hours) another 200 µL aliquot was removed, revealing a 61 % conversion (TON = 6.0, TOF = 0.3 h^{-1}). The above procedure was followed using pinacolone in place of in place of benzophenone; quantitative conversion to its hydroborylation product, *t*BuMeC(H)OBpin was observed.

NMR data for *t*BuMeC(H)OBpin (C_6D_6, 400 MHz): δ 4.10 (q, 1H, $^3J_{HH}$ = 6.0 Hz, C*H*O), 1.15 (d, 3H, $^3J_{HH}$ = 6 Hz, CC*H*$_3$), 1.01 (s, 12H, -Bpin), 0.91 (s, 9H, -tBu). ^{11}B{^{1}H} NMR (C_6D_6, 128 MHz): δ 22.6 (*B*pin).

Formation of IPr•GeH(Cl)•BH_3 from IPr•$GeCl_2$ and Li[BH_4]. To a vial charged with a 4 mL slurry of IPr•$GeCl_2$ (0.149 g, 0.280 mmol) in Et_2O was added a 2 mL Et_2O solution of Li[BH_4] (6.0 mg, 0.28 mmol). The resulting slurry was stirred for 1 hour, filtered and the volatiles were removed from the filtrate *in vacuo* yielding a colorless solid (0.139 g). NMR analysis (C_6D_6) revealed a mixture of IPr•$GeCl_2$ (28 %), IPr•BH_3[11] (32 %) and IPr•GeH(Cl)•BH_3 (40 %). IPr•BH_3 was separated from the reaction mixture by extraction with 3×1 mL toluene, however attempts to separate IPr•$GeCl_2$ and IPr•GeH(Cl)•BH_3 using toluene, benzene and fluorobenzene were unsuccessful due to their similar solubilities.

Additionally, IPr•GeH(Cl)•BH_3 is unstable in solution, forming IPr•BH_3 and an insoluble precipitate overnight. The above procedure was repeated with Li[BD_4] in place of Li[BH_4] where the formation of IPr•GeD(Cl)•BD_3 was observed along with unreacted IPr•$GeCl_2$ and IPr•BD_3.

Reaction of IPr•GeCl(OSiMe$_3$) with HBpin/DBpin. A J-Young NMR tube was loaded with a 600 μL solution of IPr•GeCl($OSiMe_3$) in C_6D_6. Subsequently, HBpin (33.4 mL, 0.230 mmol) was added to the NMR tube forming a colorless solution. After standing overnight, the reaction mixture yielded a pale-orange solution over a colorless precipitate. NMR analysis revealed the formation of IPr•$GeCl_2$ (45 %), IPrH_2 (27 %) and an unknown species (27 %). The above procedure was repeated using DBpin (1.5 M solution in THF) in place of HBpin where the formation of IPrH_2 (9 %), IPr(H)D (28 %) and IPrD_2 (9 %) were observed in addition to IPr•$GeCl_2$ and an unknown species.

5.5. Crystallographic Data

Table 5.1. Crystallographic data for compounds **1** and **[IPrH][Na{Ge$_2$(OSiMe$_3$)$_6$}]**.

Compound	**1**•1.5 C_7H_8	**[IPrH][Na{Ge$_2$(OSiMe$_3$)$_6$}]**
formula	$C_{40.5}H_{57}ClGeN_2OSi$	$C_{45}H_{91}Ge_2N_2NaO_6Si_6$
formula weight	724.01	1092.90
crystal system	monoclinic	monoclinic
space group	$P2_1/n$	$P2_1/n$
a [Å]	15.6781(4)	11.3136(2)
b [Å]	14.7142(4)	24.2049(6)
c [Å]	18.3811(5)	23.5799(5)
α [°]	90	90
β [°]	102.9394(14)	98.9136(9)
γ [°]	90	90
V [Å^3]	4132.67(19)	6379.2(2)
Z	4	4
ρ_{calcd} [g/cm^3]	1.164	1.138
μ [mm^{-1}]	2.130	2.609
T [°C]	−100	−100
$2\theta_{max}$ [°]	147.93	147.94
total data collected	26607	44878
unique data (R_{int})	8312 (0.0487)	12665 (0.0216)
obs data [$I \geq 2\sigma(I)$]	7130	11837
params	492	585
R_1 [$I \geq 2\sigma(I)$][a]	0.0485	0.0298
wR_2 [all data][a]	0.1459	0.0829
max/min $\Delta\rho$ [e/Å^3]	1.063/−0.548	0.770/−0.656

[a] $R_1 = \sum||F_o| - |F_c||/\sum|F_o|$; $wR_2 = [\sum w(F_o^2 - F_c^2)^2/\sum w(F_o^4)]^{1/2}$

Table 5.2. Crystallographic data for compounds **2** and **3**.

Compound	**2**	**3**
formula	$C_{30}H_{48}BClGeN_2OSi$	$C_{30}H_{49}BGeN_2OSi$
formula weight	599.64	565.20
crystal system	triclinic	triclinic
space group	$P\bar{1}$	$P\bar{1}$
a [Å]	9.5949(2)	10.9431(5)
b [Å]	10.1375(2)	16.7176(7)
c [Å]	20.3471(5)	18.8983(9)
α [°]	77.4969(16)	103.651(3)
β [°]	85.5238(13)	103.651(3)
γ [°]	63.1192(12)	94.561(3)
V [Å^3]	1722.97(7)	92.660(3)
Z	2	2
ρ_{calcd} [g/cm^3]	1.156	3341.4(3)
μ [mm^{-1}]	2.417	1.124
T [°C]	−100	−100
$2\theta_{max}$ [°]	147.95	140.77
total data collected	122126	22431
unique data (R_{int})	6766 (0.1591)	12303 (0.0527)
obs data [$I \geq 2\sigma(I)$]	5844	10236
params	359	742
R_1 [$I \geq 2\sigma(I)$][a]	0.0788	0.0821
wR_2 [all data][a]	0.2241	0.2087
max/min $\Delta\rho$ [e/Å^3]	1.203/−1.061	1.085/−0.636

[a] $R_1 = \sum||F_o| - |F_c||/\sum|F_o|$; $wR_2 = [\sum w(F_o^2 - F_c^2)^2/\sum w(F_o^4)]^{1/2}$

Table 5.2. Crystallographic data for compounds **4** and **5**.

Compound	**4**• $0.5C_6H_5F$	**5**•C_6H_5F
formula	$C_{66}H_{61.5}BCl_2F_{24.5}GeN_2OSi$	$C_{68}H_{62}BF_{25}GeN_2OSi$
formula weight	1546.56	1509.68
crystal system	triclinic	monoclinic
space group	$P\bar{1}$	$P2_1/c$
a [Å]	13.8897	18.2924(4)
b [Å]	14.1962(4)	18.3117(4)
c [Å]	19.4089(6)	23.1068(4)
α [°]	109.1587(14)	90
β [°]	100.5402(14)	113.1072(10)
γ [°]	90.4117(12)	90
V [Å^3]	3544.77(18)	7119.0(3)
Z	2	4
ρ_{calcd} [g/cm^3]	1.449	1.409
μ [mm^{-1}]	2.398	1.711
T [°C]	−100	−100
$2\theta_{max}$ [°]	144.48	140.81
total data collected	22517	43458
unique data (R_{int})	13315 (0.0343)	13546 (0.0415)
obs data [$I \geq 2\sigma(I)$]	11445	11261
params	962	907
R_1 [$I \geq 2\sigma(I)$][a]	0.0524	0.0647
wR_2 [all data][a]	0.1532	0.1920
max/min $\Delta\rho$ [e/Å^3]	0.737/−0.648	0.620/−1.398

[a] $R_1 = \sum||F_o| - |F_c||/\sum|F_o|$; $wR_2 = [\sum w(F_o^2 - F_c^2)^2/\sum w(F_o^4)]^{1/2}$

5.6. References

1. (a) Fischer, R. C.; Power, P. P. *Chem. Rev.* **2010**, *110*, 3877; (b) Wang, Y.; Robinson, G. H. *Inorg. Chem.* **2011**, *50*, 12326; (c) Ghadwal, R. S.; Azhakar, R.; Roesky, H. W. *Acc. Chem. Res.* **2013**, *46*, 444; (d) Brand, J.; Braunschweig, H.; Sen, S. S. *Acc. Chem. Res.* **2014**, *47*, 180; (e) Präsang, C.; Scheschkewitz, D. *Chem. Soc. Rev.* **2016**, *45*, 900; (f) Ochiai, T.; Franz, D.; Inoue, S. *Chem. Soc. Rev.* **2016**, *45*, 6327; (g) Priegert, A. M.; Rawe, B. W.; Serin, S. C.; Gates, D. P. *Chem. Soc. Rev.* **2016**, *45*, 922; (h) Melaimi, M.; Jazzar, R.; Soleilhavoup, M.; Bertrand, G. *Angew. Chem. Int. Ed.* **2017**, *56*, 10046; (i) Alvarado-Beltran, I.; Rosas-Sánchez, A.; Baceiredo, A.; Saffon-Merceron, N.; Branchadell, V.; Kato, T. *Angew. Chem. Int. Ed.* **2017**, *56*, 10481; (j) Mizuhata, Y.; Fujimori, S.; Sasamori, T.; Tokitoh, N. *Angew. Chem. Int. Ed.* **2017**, *56*, 4588; (k) Schneider, J.; Sindlinger, C. P.; Eichele, K.; Schubert, H.; Wesemann, L. *J. Am. Chem. Soc.* **2017**, *139*, 6542; (l) Wendel, D.; Reiter, D.; Porzelt, A.; Altmann, P. J.; Inoue, S.; Rieger, B. *J. Am. Chem. Soc.* **2017**, *139*, 17193; (m) Légaré, M.-A.; Bélanger-Chabot, G.; Dewhurst, R. D.; Welz, E.; Krummenacher, I.; Engels, B.; Braunschweig, H. *Science* **2018**, *359*, 896.
2. (a) Power, P. P. *Nature* **2010**, *463*, 171; (b) Hadlington, T. J.; Hermann, M.; Frenking, G. Jones, C. *Chem. Sci.* **2015**, *6*, 7249; (c) Yadav, S.; Saha, S.; Sen, S. S. *ChemCatChem* **2016**, *8*, 486; (d) Hill, M. S.; Liptrot, D. J.; Weetman, C.; *Chem. Soc. Rev.* **2016**, *45*, 972; (e) Hadlington, T. J.; Kefalidis, C. E.; Maron, L; Jones, C. *ACS Catal.* **2017**, *7*, 1853; (f) Schuhknecht, D.; Lhotzky, C.; Spaniol, T. P.; Maron, L.; Okuda, J. *Angew. Chem. Int. Ed.* **2017**, *56*, 12367; (g) Wilson, A. S. S.; Hill, M. S.;

Mahon, M. F.; Dinoi, C.; Maron, L. *Science* **2017**, *358*, 1168; (h) Nikonov, G. I. *ACS Catal.* **2017**, *7*, 7257.

3. (a) Schnepf, A. *New J. Chem.* **2010**, *34*, 2079; (b) Purkait, T. K.; Swarnakar, A. K.; De Los Reyes, G. B.; Hegmann, F. A.; Rivard, E.; Veinot, J. G. C. *Nanoscale* **2015**, *7*, 2241; (c) Yin, J.; Li, J.; Hang, Y.; Yu, J.; Tai, G.; Li, X.; Zhang, Z.; Guo, W. *Small* **2016**, *12*, 2942; (d) Rivard, E. *Chem. Soc. Rev.* **2016**, *45*, 989; (e) Haas, M.; Christopoulos, V.; Radebner, J.; Holthausen, M.; Lainer, T.; Schuh, L.; Fitzek, H.; Kothleitner, G.; Torvisco, A.; Fischer, R.; Wunnicke, O.; Stüger, H. *Angew. Chem. Int. Ed.* **2017**, *56*, 14071.
4. (a) Rivard, E. *Dalton Trans.* **2014**, *43*, 8577; (b) Roy, M. M. D.; Rivard, E. *Acc. Chem. Res.* **2017**, *50*, 2017.
5. (a) Marks, T. J. *J. Am. Chem. Soc.* **1971**, *93*, 7090; (b) Vogel, U.; Timoshkin, A. Y.; Scheer, M. *Angew. Chem. Int. Ed.* **2001**, *40*, 4409; (c) Rupar, P. A.; Jennings, M. C.; Ragogna, P. J.; Baines, K. M. *Organometallics* **2007**, *26*, 4109; (d) Zabula, A. V.; Pape, T.; Hepp, A.; Schappacher, F. M.; Rodewald, U. C.; Pöttgen, R.; Hahn, F. E. *J. Am. Chem. Soc.* **2008**, *130*, 5648; (e) Filippou, A. C.; Baars, B.; Chernov, O.; Lebedev, Y. N.; Schnakenburg, G. *Angew. Chem. Int. Ed.* **2014**, *53*, 565; (f) Stephan, D. W. *Acc. Chem. Res.* **2015**, *48*, 306; (g) Zhou, Y.-P.; Karni, M.; Yoa, S.; Apeloig, Y.; Driess, M. *Angew. Chem. Int. Ed.* **2016**, *55*, 15096; (h) Mo, Z.; Rit, A.; Campos, J.; Kolychev, E. L.; Aldridge, S. *J. Am. Chem. Soc.* **2016**, *138*, 3306; (i) Hickox, H. P.; Wang, Y.; Xie, Y.; Wei, P.; Schaeffer III, H. F.; Robinson, G. H. *J. Am. Chem. Soc.* **2016**, *138*, 9799; (j) Rodriguez, R.; Gau, D.; Saouli, J.; Baceiredo, A.; Saffon-Merceron, N.; Branchadell, V.; Kato, T. *Angew. Chem. Int. Ed.* **2017**, *56*, 3935.

6. For selected references, see: (a) Thimer, K. C.; Al-Rafia, S. M. I.; Ferguson, M. J.; McDonald, R.; Rivard, E. *Chem. Commun.* **2009**, 7119; (b) Al-Rafia, S. M. I.; Malcolm, A. C.; Liew, S. K.; Ferguson, M. J.; Rivard, E. *J. Am. Chem. Soc.* **2011**, *133*, 777; (c) Al-Rafia, S. M. I.; Malcolm, A. C.; McDonald, R.; Ferguson, M. J.; Rivard, E. *Angew. Chem. Int. Ed.* **2011**, *50*, 8354; (d) Al-Rafia, S. M. I.; Malcolm, A. C.; McDonald, R.; Ferguson, M. J.; Rivard, E. *Chem. Commun.* **2012**, *48*, 1308; (e) Al-Rafia, S. M. I.; McDonald, R.; Ferguson, M. J.; Rivard, E. *Chem. Eur. J.* **2012**, *18*, 13810; (f) Al-Rafia, S. M. I.; Momeni, M. R.; Ferguson, M. J.; McDonald, R.; Brown, A.; Rivard, E. *Organometallics* **2013**, *32*, 6658.
7. (a) Swarnakar, A. K.; Hering-Junghans, C.; Nagata, K.; Ferguson, M. J.; McDonald, R.; Tokitoh, N.; Rivard, E. *Angew. Chem. Int. Ed.* **2015**, *54*, 10666; (b) Swarnakar, A. K.; Hering-Junghans, C.; Ferguson, M. J.; McDonald, R.; Rivard, E. *Chem. Sci.* **2017**, *8*, 2337.
8. (a) Khan, S.; Gopakumar, G.; Thiel, W.; Alcazaro, M. *Angew. Chem. Int. Ed.* **2013**, *52*, 5644; (b) Roy, M. M. D.; Lummis, P. A.; Ferguson, M. J.; McDonald, R.; Rivard, E. *Chem. Eur. J.* **2017**, *23*, 11249.
9. Swarnakar, A. K.; Hering-Junghans, C.; Ferguson, M. J.; McDonald, R.; Rivard, E. *Chem. Eur. J.* **2017**, *23*, 8628.
10. Gao, Y.; Yang, Y.; Zheng, W.; Su, Y.; Zhang, X.; Roesky, H. W. *Inorg. Chem.* **2017**, *56*, 10220.
11. Wang, Y.; Quillian, B.; Wei, P.; Wannere, C. S.; Xie, Y.; King, R. B.; Schaefer III, H. F.; Schleyer, P. v. R.; Robinson, G. H. *J. Am. Chem. Soc.* **2007**, *129*, 12412.

12. Swarnakar, A. K.; McDonald, S. M.; Deutsch, K. C.; Choi, P.; Ferguson, M. J.; McDonald, R.; Rivard, E. *Inorg. Chem.* **2014**, *53*, 8662.

13. (a) Hadlington, T. J.; Hermann, M.; Frenking, G.; Jones, C. *J. Am. Chem. Soc.* **2014**, *136*, 3028; (b) Chong, C. C.; Hirao, H.; Kinjo, R. *Angew. Chem. Int. Ed.* **2015**, *54*, 190; (c) Bagherzadeh, S.; Mankad, N. P. *Chem. Commun.* **2016**, *52*, 3844; (d) Roy, M. M. D.; Ferguson, M. J.; McDonald, R.; Rivard, E. *Chem. Eur. J.* **2016**, *22*, 18236.

14. For the preparation of [:Ge(H)Cl] as a transient species, see: (a) Harper, W. W.; Clouthier, D. J. *J. Chem. Phys.* **1998**, *108*, 416; (b) Lin, W.; Kang, L.; Novick, S. E. *J. Molec. Spec.* **2005**, *230*, 93.

15. Yoshimura, A.; Yoshinaga, M.; Yamashita, H.; Igarashi, M.; Shimada, S.; Sato, K. *Chem. Commun.* **2017**, *53*, 5822.

16. (a) Ishida, S.; Iwamoto, T.; Kabuto, C.; Kira, M. *Chem. Lett.* **2001**, *30*, 1102; (b) Moser, D. F.; Bosse, T.; Moser, J. L.; Guzei, I. A.; West, R. *J. Am. Chem. Soc.* **2002**, *124*, 4186; (c) Xiong, Y.; Yao, S.; Driess, M. *Organometallics* **2009**, *28*, 1927; (d) Chu, T.; Nikonov, G. I.; *Chem. Rev.* **2018**, *118*, 3608.

17. (a) Li, J.; Schenk, C.; Winter, F.; Scherer, H.; Trapp, N.; Higelin, A.; Keller, S.; Pöttgen, R.; Krossing, I.; Jones, C. *Angew. Chem. Int. Ed.* **2012**, *51*, 9557; (b) Inomata, K.; Watanabe, T.; Tobita, H. *J. Am. Chem. Soc.* **2014**, *136*, 14341; (c) Rit, A.; Tirfoin, R.; Aldridge, S. *Angew. Chem. Int. Ed.* **2016**, *55*, 378.

18. Germyliumylidenes are most commonly stabilized within a cyclic framework, for example: (a) Cheng, F.; Dyke, J. M.; Ferrante, F.; Hector, A. L.; Levason, W.; Reid, G.; Webster, M.; Zhang, W. *Dalton Trans.* **2010**, *39*, 847; (b) Xiong, Y.; Yao, S.; Inoue, S.; Berkefeld, A.; Driess, M. *Chem. Commun.* **2012**, *48*, 12198; (c) Bouška, M.;

Dostál, L.; Růžička, A.; Jambor, R. *Organometallics* **2013**, *32*, 1995; (d) Weicker, S. A.; Dube, J. W.; Ragogna, P. J. *Organometallics* **2013**, *32*, 6681; (e) Xiong, Y.; Yao, S.; Tan, S.; Inoue, S.; Driess, M. *J. Am. Chem. Soc.* **2013**, *135*, 5004; (f) Su, B.; Ganguly, R; Li, Y.; Kinjo, R. *Angew. Chem. Int. Ed.* **2014**, *53*, 13106; (g) Ochiai, T.; Szilvási, T.; Franz, D.; Irran, E.; Inoue, S. *Angew. Chem. Int. Ed.* **2016**, *55*, 11619; (h) Su, Y.; Li, Y.; Ganguly, R.; Kinjo, R. *Eur. J. Inorg. Chem.* **2018**, 2228.

19. Arrowsmith, M.; Hadlington, T. J.; Hill, M. S.; Kociok-Köhn, G. *Chem. Commun.* **2012**, *48*, 4567.
20. The direct reaction of **5** with stoichiometric HBpin did not yield any spectroscopic evidence of $[IPr•GeH]^+$. Similar results were obtained when this reaction was repeated in the presence of the carbene $(MeCN\textit{i}Pr)_2C$: and $Ph_2PCH_2CH_2PPh_2$.
21. Jafarpour, L.; Stevens, E. D.; Nolan, S. P. *J. Organomet. Chem.* **2000**, *606*, 49.
22. Massey, A. G.; Park, A. J. *J. Organomet. Chem.* **1964**, *2*, 245.
23. Labre, F.; Gimbert, Y.; Bannwarth, P.; Olivero, S.; Duñach, E.; Chavant, P. Y. *Org. Lett.* **2014**, *16*, 2366.
24. Hope, H. *Prog. Inorg. Chem.* **1994**, *41*, 1.
25. Sheldrick, G. M. *Acta. Crystallogr. Sect. A* **2015**, *71*, 3.
26. Sheldrick, G. M. *Acta. Crystallogr. Sect. C.* **2015**, *71*, 3.
27. Gaussian 16, Revision B.01, Frisch, M. J.; Trucks, G. W.; Schlegel, H. B.; Scuseria, G. E.; Robb, M. A.; Cheeseman, J. R.; Scalmani, G.; Barone, V.; Petersson, G. A.; Nakatsuji, H.; Li, X.; Caricato, M.; Marenich, A. V.; Bloino, J.; Janesko, B. G.; Gomperts, R.; Mennucci, B.; Hratchian, H. P.; Ortiz, J. V.; Izmaylov, A. F.; Sonnenberg, J. L.; Williams-Young, D.; Ding, F.; Lipparini, F.; Egidi, F.; Goings, J.;

Peng, B.; Petrone, A.; Henderson, T.; Ranasinghe, D.; Zakrzewski, V. G.; Gao, J.; Rega, N.; Zheng, G.; Liang, W.; Hada, M.; Ehara, M.; Toyota, K.; Fukuda, R.; Hasegawa, J.; Ishida, M.; Nakajima, T.; Honda, Y.; Kitao, O.; Nakai, H.; Vreven, T.; Throssell, K.; Montgomery, J. A., Jr.; Peralta, J. E.; Ogliaro, F.; Bearpark, M. J.; Heyd, J. J.; Brothers, E. N.; Kudin, K. N.; Staroverov, V. N.; Keith, T. A.; Kobayashi, R.; Normand, J.; Raghavachari, K.; Rendell, A. P.; Burant, J. C.; Iyengar, S. S.; Tomasi, J.; Cossi, M.; Millam, J. M.; Klene, M.; Adamo, C.; Cammi, R.; Ochterski, J. W.; Martin, R. L.; Morokuma, K.; Farkas, O.; Foresman, J. B.; Fox, D. J. Gaussian, Inc., Wallingford CT, **2016**.

28. (a) Lee, C.; Yang, W.; Parr, R. G. *Phys. Rev. B* **1988**, *37*, 785; (b) Becke, A. D. *Phys. Rev. A* **1998**, *38*, 3098; (c) Stephens, P. J.; Devlin, F. J.; Chabalowski, C. F.; Frisch, M. J. *J. Phys. Chem.* **1994**, *98*, 11623.

29. (a) Hariharan, P. C.; Pople, J. A. *Theor. Chim. Acta.* **1973**, *28*, 213; (b) Francl, M. M.; Pietro, W. J.; Hehre, W. J.; Binkley, J. S.; Gordon, M. S.; DeFrees, D. J.; Pople, J. A. *J. Chem. Phys.* **1982**, *77*, 3654.

Chapter 6: A Vinyl Silylsilylene and its Activation of Strong Homo- and Heteroatomic Bonds

6.1. Introduction

The activation and functionalization of small molecules such as H_2, CO, CO_2, P_4[1] and even N_2[2] by Earth-abundant main group elements usually relies on the isolation of highly reactive element centers. In order to be synthetically viable, a delicate balance of stability and reactivity must be achieved. Amongst p-block compounds, those of Group 14 in the +II oxidation state (tetrelenes) have shown significant promise with regard to bond activation and catalysis.[3] Silylenes (R_2Si:) still remain rare relative to the other Group 14 tetrelenes, owing in part to the general instability of Si^{II} compounds.[4] While coordinatively saturated examples of silylenes (*e.g.* Cp^*_2Si; $Cp^* = \eta^5$-C_5Me_5) had been reported previously,[5] West and coworkers prepared the first example of an unsaturated two-coordinate *N*-heterocyclic silylene.[6] It was only in 2012 that the first examples of isolable two-coordinate *acyclic* silylenes were simultaneously published (**I** and **II**, Scheme 6.1);[7] in stark contrast, their heavier R_2E: congeners (E = Ge, Sn, Pb; R = anionic ligands) were first reported decades prior.[8] While a few examples of room temperature stable acyclic silylenes are known,[7,9] all have been stabilized by two heteroatom-based ligands. Herein, a bulky vinylic ligand $[^{Me}IPr{=}CH]^-$, (^{Me}IPr = [(MeCNDipp)$_2$C]; Dipp = 2,6-*i*$Pr_2C_6H_3$) is used to generate the first two-coordinate acyclic silylene stabilized by a carbon-based donor.[10] Despite the remarkable thermal stability of the title complex ($^{Me}IPrCH$)Si{$Si(SiMe_3)_3$}, this vinyl silylsilylene was able to undergo the formal oxidative addition of several strong

organic and inorganic bonds, including the regioselective activation/functionalization of white phosphorus (P_4) and the activation of a primary C-H bond at room temperature.

6.2. Results and Discussion

This study relied upon the steric bulk and potential 4-electron (2σ, 2π) donating ability of the carbon-based anionic vinylic ligand [^{Me}IPr=CH]$^-$,[11] to gain access to a two-coordinate silylene. This ligand represents the deprotonated form of its neutral *N*-heterocyclic olefin (NHO)[12] parent ^{Me}IPr=CH_2 and has been previously used by the Rivard group to isolate the first base-free divinylgermylene (^{Me}IPrCH)$_2$Ge:.[11]

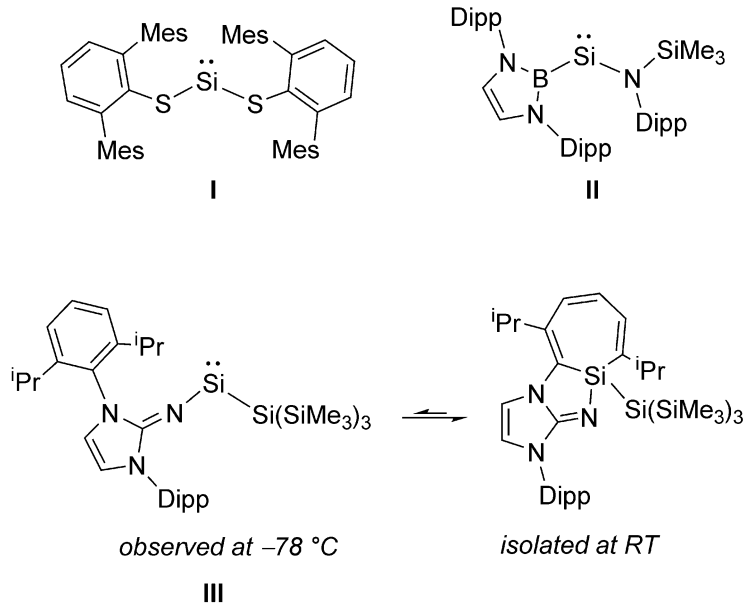

Scheme 6.1. The first isolable two-coordinate acyclic silylenes (**I** and **II**) and the spectroscopically observed iminosilylene **III**.

The first step towards accessing a new organosilylene was to install the [^{Me}IPr=CH]$^-$ ligand at silicon. This was achieved by mixing two equivalents of the olefin proligand ^{Me}IPr=CH_2 with $SiBr_4$ to give the silane (^{Me}IPrCH)$SiBr_3$ (**1**). After filtration from the flocculant [^{Me}IPrCH$_3$]Br precipitate, the target Si^{IV} precursor **1** was isolated as an off-white, crystalline solid in a 53 % yield (Scheme 6.2). Attempts to prepare the divinyl silane

(^{Me}IPrCH)$_2$SiBr$_2$ by combining **1** with an additional two equivalents of ^{Me}IPr=CH$_2$ or one equivalent of ^{Me}IPrCH(SiMe$_3$)[11] were unsuccessful. Synthetic studies were then focused on preparing a silylene directly from **1**.

Following recent reports of bulky silyl-substituted silylenes,[9a,c] (^{Me}IPrCH)SiBr$_3$ (**1**) was combined with two equivalents of hypersilyl potassium [K(THF)$_2$][Si(SiMe$_3$)$_3$] in toluene (Scheme 6.2). This resulted in the immediate formation of a deep green slurry. ^{1}H NMR spectroscopic analysis of the filtrate revealed quantitative conversion to a 1:1 mixture of a new [^{Me}IPr=CH]$^-$ containing product and BrSi(SiMe$_3$)$_3$. The vinylic proton signal in the new product exhibits two-bond coupling satellites to Si ($^2J_{H\text{-}Si}$ = 13.5 Hz), and its remarkably downfield-positioned chemical shift (δ 7.40 in C_6D_6) indicates significant transfer of electron density from the [^{Me}IPr=CH]$^-$ ligand to silicon. Additionally, the ^{29}Si{^{1}H} NMR spectrum displayed a signal at 432.9 ppm, which lies in the spectral range of known two-coordinate acyclic silylenes.[9]

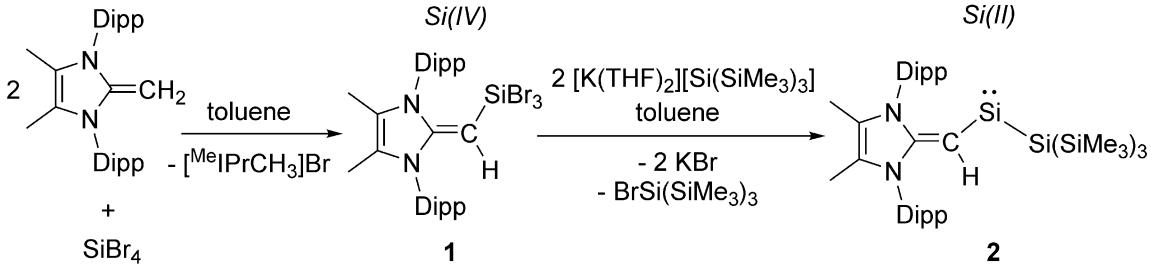

Scheme 6.2. Formation of the tribromo-vinylsilane **1** and its subsequent reduction to the vinyl silylsilylene **2**.

To confirm the formation of the two-coordinate silylene (^{Me}IPrCH)Si{Si(SiMe$_3$)$_3$} (**2**), deep-green crystals suitable for X-ray crystallographic analysis were grown from Me$_3$SiOSiMe$_3$. The molecular structure of **2** (Figure 6.1) is in good agreement with the abovementioned NMR results. Specifically, the vinylic C3–C4 bond in **2** [1.406(3) Å] is elongated relative to free NHO ^{Me}IPr=CH$_2$ [1.3489(18) Å],[13] providing added evidence for

the transfer of π-electron density to silicon. The C4-Si1-Si2 angle was found to be 101.59(7)°, in line with the presence of a high degree of *s*-character at the silicon-based lone pair. This angle implies that **2** should have a good balance of stability and reactivity. For example, the colorless dithiolato-supported silylene $Si(SAr^{Mes})_2$ (**I** in Scheme 6.1) has an R-Si-R angle of 90.519(19)° indicating a relatively low-energy Si-based lone pair of nearly pure *s*-character.[7a] While $Si(SAr^{Mes})_2$ has not been reported to cleave strong organic bonds,[14] acyclic silylenes with obtuse R-Si-R angles (and smaller HOMO-LUMO gaps) have been shown to activate small molecules such as H_2, CO_2, and NH_3.[7b,9]

(^{Me}IPrCH)Si{$Si(SiMe_3)_3$} (**2**) is remarkably stable, with no NMR spectroscopic sign of decomposition noted after storage of a benzene solution at room temperature for two months (under N_2 atmosphere). This observation contrasts the situation in Inoue and Rieger's imino silylsilylene (**III**, Scheme 6.1), which exists predominately in a 7-membered Si^{IV} ring (silepin) form (via reversible ligand activation) at ambient temperature.[9c] The Rivard group's previous attempts to generate the bis-iminosilylene $(IPrN)_2Si$: consistently afforded irreversible ligand activation products.[15] Additionally, silylenes generated using hypersilyl potassium are often contaminated with the highly soluble $BrSi(SiMe_3)_3$ byproduct,[9a,c] however in the case of **2**, the pure silylene can be obtained in moderate yield (67 %) by washing the crude residue with a minimal amount of cold (−30 °C) $Me_3SiOSiMe_3$.

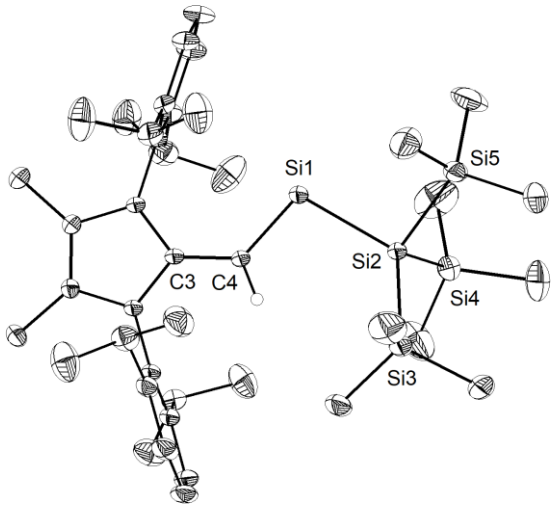

Figure 6.1. Molecular structure of (^{Me}IPrCH)Si{Si(SiMe$_3$)$_3$} (**2**) with thermal ellipsoids plotted at a 30 % probability level. All hydrogen atoms (except the vinylic hydrogen) were omitted for clarity. Selected bond lengths [Å] and angles [°]: C3-C4 1.406(3), C4-Si1 1.798(2), Si1-Si2 2.4041; Si1-C4-C3 128.74(15), Si2-Si1-C4 101.59(7).

To gain further insight into the influence of the [^{Me}IPrCH]$^-$ ligand in **2**, a series of computational (DFT) studies were conducted at the M06-2X/def2-TZVP level.[16] The computed HOMO of **2** is predominately a silicon-based lone pair whereas the HOMO−1 consists of a C–Si π bond between the vinylic ligand and the silylene center (Figure 6.2). The C–Si Wiberg Bond Index (WBI) was found to be 1.06 and the LUMO shows significant C–Si π* orbital character. Together, these analyses demonstrate the stabilizing π-donation ability of the [^{Me}IPr=CH]$^-$ ligand. Additionally, the computed natural charges show a highly polarized *Si*^{II}–*Si*R$_3$ bond (*Si*^{II}: +0.54; *Si*R$_3$: −0.51) which may enable interesting reactivity to transpire. As a result, the interaction of **2** with small molecules was investigated in detail.

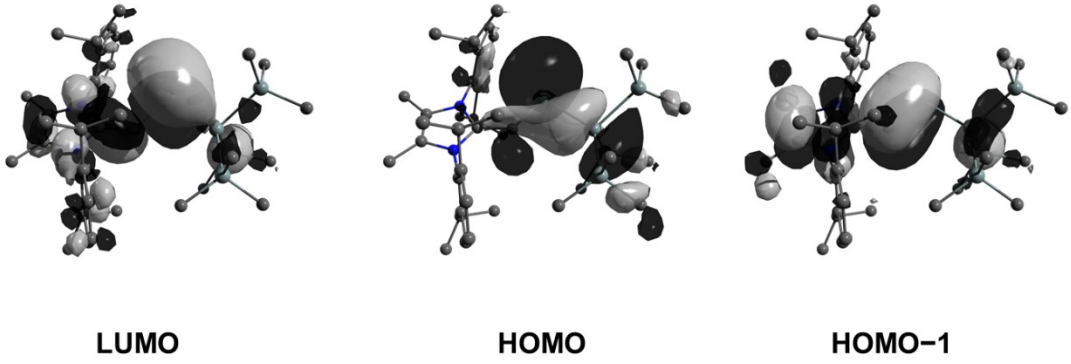

Figure 6.2. Selected molecular orbitals of the optimized structure of **2** computed at the M06-2X/def2-TZVP level of theory.

The reactivity study of **2** began by combining this silylene with the carbon-based electrophile MeOTf (OTf = $CF_3SO_3^-$). As anticipated, the deep green color of **2** dissipated upon addition of MeOTf and NMR analysis revealed the formation of a single new product. X-ray crystallography identified this species as the new triflato-silane (^{Me}IPrCH)Si(Me)OTf{Si(SiMe$_3$)$_3$} (**3**) (Scheme 6.3, Figure 6.3). Compound **3** crystallizes in a distorted tetrahedral geometry, with a covalently bound -OTf unit in the solid state [Si1-O1 = 1.8258(10) Å] and in solution (^{19}F{^{1}H} NMR: δ −75.8 ppm).

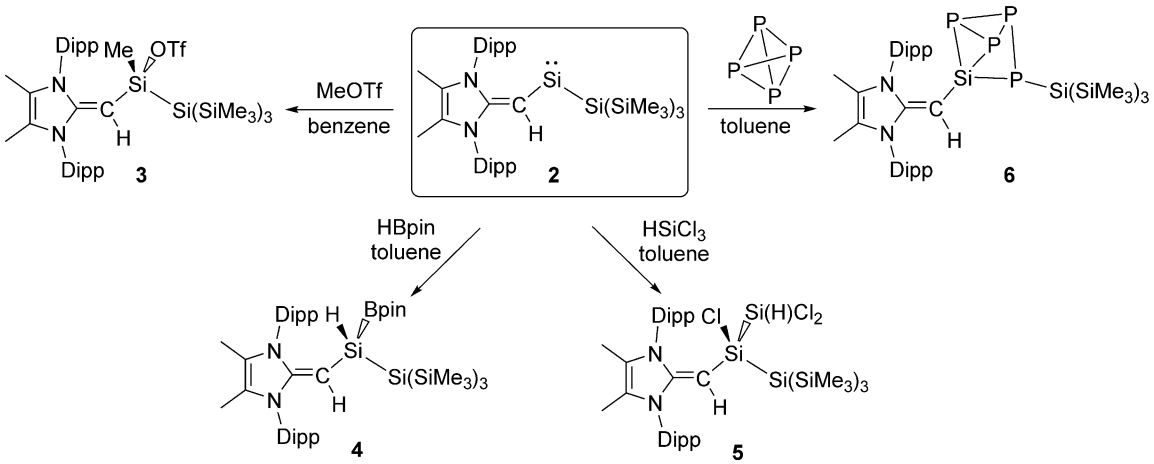

Scheme 6.3. Oxidative addition of the substrates MeOTf (**3**), HBpin (**4**), $HSiCl_3$ (**5**) and P_4 (**6**) to the reactive silylene **2**.

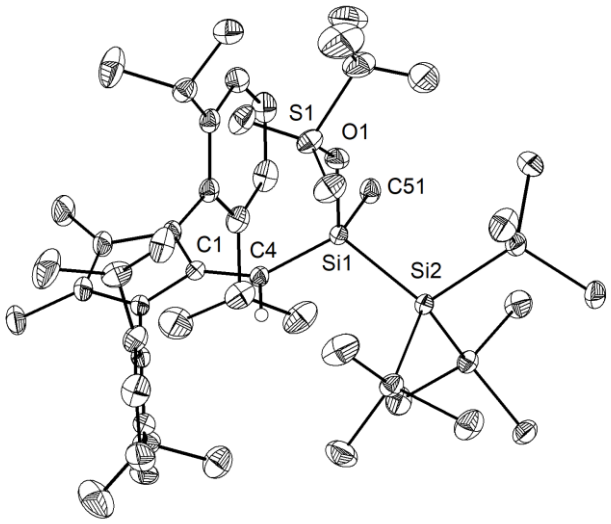

Figure 6.3. Molecular structure of (^{Me}IPrCH)Si(Me)OTf{Si(SiMe$_3$)$_3$} (**4**) with thermal ellipsoids plotted at a 30 % probability level. All hydrogen atoms (except the vinylic hydrogen) were omitted for clarity. Selected bond lengths [Å] and angles [°]: C1-C4 1.3964(17), C4-Si1 1.7929(13), Si1-O1 1.8258(10); C4-Si1-O1 111.37(5), C4-Si1-C51 121.69(6), C4-Si1-Si2 111.04(4).

Silylene **2** was then combined with the widely used hydroborylation reagent pinacolborane (HBPin), which led to oxidative addition of an H–B bond at silicon to yield (^{Me}IPrCH)Si(H)BPin{Si(SiMe$_3$)$_3$} (**4**) (Scheme 6.3). When **2** was reacted with trichlorosilane (HSiCl$_3$), a new compound was soon observed with a singlet Si–H resonance in the ^{1}H NMR spectrum (δ 3.61 ppm, $^1J_{H\text{-}Si}$ = 180.0 Hz). The lack of $^3J_{HH}$ coupling to the neighboring vinylic hydrogen implied that oxidative addition of an Si–Cl bond had transpired in place of Si–H bond activation.[16] Crystallographic analysis confirmed the formation of (^{Me}IPrCH)SiCl(HSiCl$_2$){Si(SiMe$_3$)$_3$} (**5**) (Figure 6.4). Of note, the addition of HSiCl$_3$ across a silylene (such as Cl$_2$Si:) is a key step proposed in the chemical vapour deposition (CVD) of epitaxial silicon from trichlorosilane.[17] The sterically congested nature of **5** is evident by its ^{1}H and ^{13}C{^{1}H} NMR spectra which are very broad at room temperature but are resolved at +75 °C. The molecular structure of **5** (Figure 6.4)

shows an expected distorted tetrahedral geometry at Si1 [Si2-Si1-Si3: 109.81(9)°]. Interestingly, the located silane hydrogen atom was found to exhibit an SiH-π interaction in the solid state (H---$Dipp_{centroid}$ distance: 2.33 Å). Attempts to induce dehydrochlorination of **5** (to form a dichlorodisilene, RR′Si=$SiCl_2$) using the strong Brønsted bases DABCO (DABCO = 1,4-diazabicyclo[2.2.2]octane) or the *N*-heterocyclic carbene $(MeCNMe)_2C$: were unsuccessful.[18] In both cases, no reaction was observed, perhaps owing to steric protection of the Si–H bond.

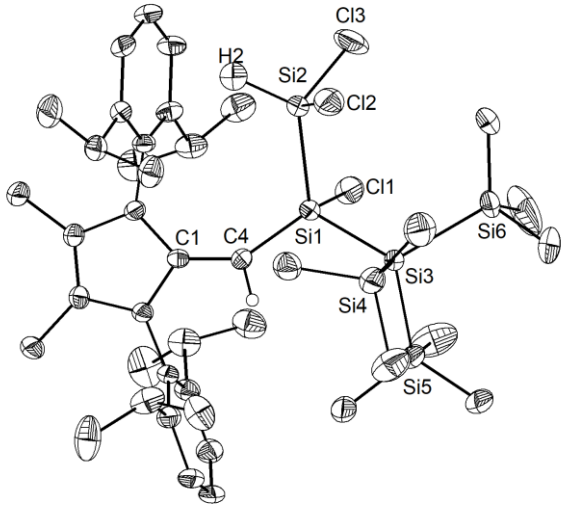

Figure 6.4. Molecular structure of (^{Me}IPrCH)SiCl($SiHCl_2$){$Si(SiMe_3)_3$} (**5**) with thermal ellipsoids plotted at a 30 % probability level. All hydrogen atoms (except the vinylic hydrogen and silane hydrogen) were omitted for clarity. Selected bond lengths [Å] and angles [°]: C1-C4 1.394(7), C4-Si1 1.789(5), Si1-Si2 2.364(2), Si1-Cl1 2.170(2), Si2-H2 1.50(7), Si2-Cl2 2.076(3), 2.074(3), Si1-Si3 2.358(2); Si2-Si1-Si3 109.81(9), Si2-Si1-Cl1 100.27(9), Si2-Si1-C4 118.15(19).

Encouraged by the activation of polarized heteroatomic bonds using **2**, the reactivity of silylene **2** with the non-polar bonds of white phosphorus (P_4) was explored. While acyclic silylenes have not yet been shown to react with P_4, several examples of cyclic silylenes reacting with P_4 are known. These reactions are limited to the oxidative addition

of a single P–P bond across a silicon center,[19] and the controlled activation/functionalization of P_4 by main group elements remains a difficult transformation.[20] Upon mixing **2** and P_4 for 20 minutes at room temperature, a pale orange solution was formed. $^{31}P\{^1H\}$ NMR analysis suggested that simple oxidative addition of a P–P bond had not occurred, as three distinct signals were observed (δ 120.0, −181.0, −316.7 ppm).[16] X-ray crystallographic analysis revealed that 1,2-migration of the hypersilyl group of **2** transpired in addition to P_4 reduction (Scheme 6.3, Figure 6.5) to yield (^{Me}IPrCH)Si(P_4){Si($SiMe_3$)$_3$} (**6**). This transformation is likely facilitated by the steric bulk of **2** and the polarized nature of the *Si*^{II}–*Si*($SiMe_3$)$_3$ bond (*vide supra*). This activation/functionalization of P_4 represents the cleavage of two P–P bonds and the regioselective formation of four new Si–P bonds. Remarkably, a search of the Cambridge Structural Database (CSD) revealed that compound **6** represents an entirely new bonding motif for the P_4^{2-} ligand.[21] Notably, silylated phosphines and phosphides are valuable precursors to element phosphide nanomaterials[22] and organophosphines[23] and thus their preparation from elemental phosphorus continues to be of great importance.

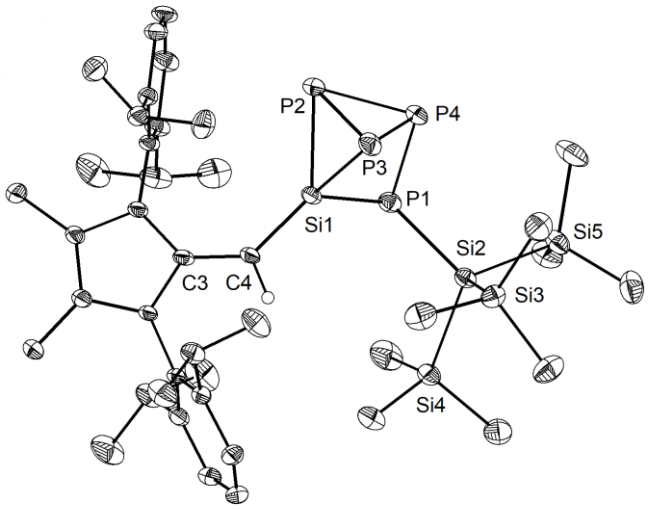

Figure 6.5. Molecular structure of (^{Me}IPrCH)Si(P$_4$){Si(SiMe$_3$)$_3$} (**6**) with thermal ellipsoids plotted at a 30 % probability level. All hydrogen atoms (except the vinylic hydrogen) were omitted for clarity. Selected bond lengths [Å] and angles [°]: C3-C4 1.380(4), C4-Si1 1.792(3), Si1-P1 2.2407(11), Si1-P2 2.2364(10), Si1-P3 2.2639(10), P2-P3 2.2555(12), P2-P4 2.2262(12), P3-P4 2.2057(13), P4-P1 2.2615(10), P1-Si2 2.2775(11); C4-Si1-P1 123.42(11), P4-P1-Si1 75.18(4), P4-P1-Si2 104.06(4), P3-P2-P4 58.96(4).

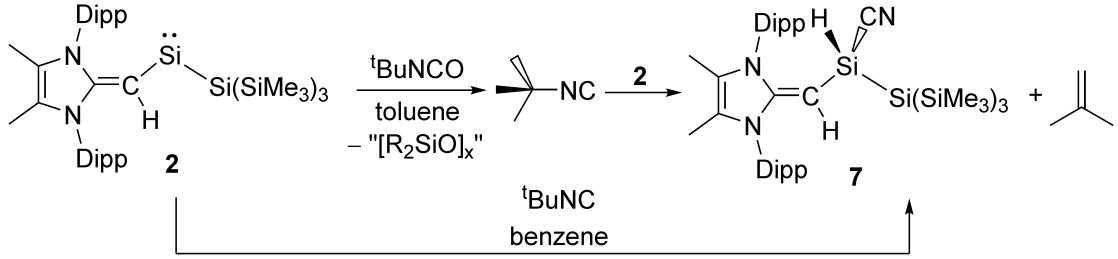

Scheme 6.4. Formation of the silyl-cyanide **7** via reaction of **2** with ^{t}BuCN.

Following the remarkable report by Rieger, Inoue and coworkers of an isolable three-coordinate silanone (formed by oxidation of **III** in Scheme 6.1 with N_2O)[24] the analogous reaction with **2** was investigated. Surprisingly, exposure of a solution of **2** to an N_2O atmosphere at −78 °C or room temperature afforded no reaction. Subsequently, **2** was combined with one equivalent of the potential oxygen-atom source *tert*-butyl isocyanate (^{t}BuNCO) which yielded a mixture of products by ^{1}H NMR spectroscopy, including

several [^{Me}IPrCH]$^{-}$ containing species, unreacted ^{t}BuNCO and isobutylene. Extraction of the mixture with hexanes and crystallization afforded crystals of the silyl-cyanide (^{Me}IPrCH)SiH(CN){Si(SiMe$_3$)$_3$} (**7**) in low (31 %) yield (Figure 6.6). Compound **7** is likely forms from the isocyanide (^{t}BuNC) by-product generated after the initial oxidation of **2** with ^{t}BuNCO (Scheme 6.4). Thus far, I have been unable to isolate and identify the other products in the mixture, including the possible silanone by-product (^{Me}IPrCH)Si(O){Si(SiMe$_3$)$_3$}. In order to give credence to the proposed mechanism, **2** was combined with one equivalent of ^{t}BuNC, which led to the quantitative formation of a 1:1 mixture of **7** and isobutylene (as determined by ^{1}H NMR spectroscopy). This transformation represents a quantitative room temperature activation of a primary C-H bond by a silylene (R$_2$Si:). Related transformations have been demonstrated previously with an acyclic germylene[25] and a disilene,[26] albeit at elevated temperatures.

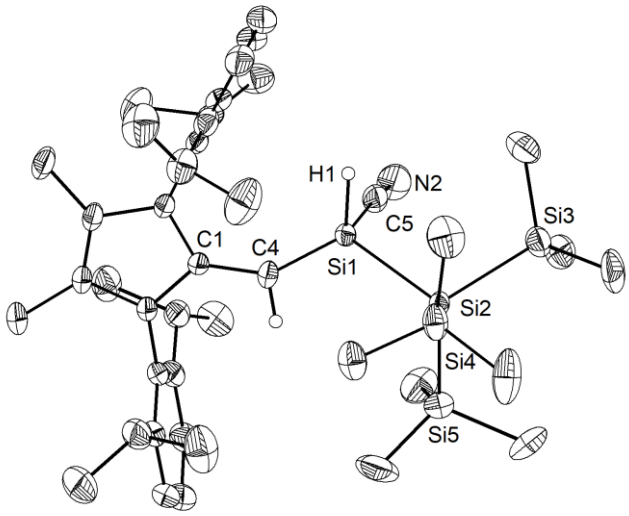

Figure 6.6. Molecular structure of (^{Me}IPrCH)SiH(CN){Si(SiMe$_3$)$_3$} (**7**) with thermal ellipsoids plotted at a 30 % probability level. All hydrogen atoms (except the vinylic and silicon-bound hydrogens) were omitted for clarity. Selected bond lengths [Å] and angles [°]: C4-Si1 1.709(3), Si1-H1 1.46(5), Si1-Si2 2.3396(15), Si1-C5 1.918(5), C5-N2 1.110(7); C4-S1-Si2 116.64(10), C4-Si1-C5 111.9(2), Si1-C5-N2 175.0(6).

6.3. Conclusions

In this work, the synthesis of a thermally stable, two-coordinate acyclic silylene (^{Me}IPrCH)Si{Si(SiMe$_3$)$_3$} was achieved, and is the first example of such a species supported by a carbon-based ligand. The stabilizing influence of [^{Me}IPrCH]$^-$ was evaluated experimentally and computationally. The high reactivity of this new silylene was demonstrated by its room temperature activations of strong homo- and heteroatomic bonds. Future work will target the synthesis of more nucleophilic sources of [^{Me}IPrCH]$^-$ which may allow for the formation of a stable divinylsilylene and related reactive species for main group element-based catalysis.

6.4. Experimental Details

6.4.1. General

All reactions were performed in an inert atmosphere glovebox (Innovative Technology, Inc.). Solvents (except Me$_3$SiOSiMe$_3$) were dried using a Grubbs-type solvent purification system[27] manufactured by Innovative Technologies, Inc., degassed (freeze-pump-thaw method), and stored under an atmosphere of nitrogen prior to use. Me$_3$SiOSiMe$_3$ was degassed (freeze-pump-thaw method) and dried over 4 Å molecular sieves prior to use. MeOTf was purchased from Aldrich and used as received. HSiCl$_3$, ^{t}BuNCO, and ^{t}BuNC were purchased from Aldrich and stored over 4 Å molecular sieves prior to use. SiBr$_4$ was purchased from Alfa Aesar and used as received. HBpin was purchased from Matrix Scientific and used as received. P$_4$ was sublimed prior to use. ^{Me}IPr=CH$_2$ was prepared according to the literature procedure.[13] [K(THF)$_2$][Si(SiMe$_3$)$_3$] was prepared according to the literature procedure and recrystallized from hexanes prior to use.[28] ^{1}H, ^{11}B{^{1}H}, ^{13}C{^{1}H}, ^{29}Si{^{1}H}, ^{31}P{^{1}H} and ^{19}F{^{1}H} NMR spectra were recorded on 400, 500, 600 or

700 MHz Varian Inova instruments and were referenced externally to $SiMe_4$ (^1H, $^{13}C\{^1H\}$, $^{29}Si\{^1H\}$), $CFCl_3$ ($^{19}F\{^1H\}$), 85 % H_3PO_4 ($^{31}P\{^1H\}$) or $BF_3{\cdot}Et_2O$ ($^{11}B\{^1H\}$). Elemental analyses were performed by the Analytical and Instrumentation Laboratory at the University of Alberta. Melting points were measured in sealed glass capillaries under nitrogen with a MelTemp apparatus and are uncorrected. UV-visible spectroscopic measurements were carried out with a Varian Carry 300 Scan spectrophotometer.

6.4.2. X-ray Crystallography

Crystals for X-ray diffraction studies were removed from a vial (in a glovebox) and immediately coated with a thin layer of hydrocarbon oil (Paratone-N). A suitable crystal was then mounted on a glass fiber and quickly placed in a low temperature stream of nitrogen on an X-ray diffractometer.[29] All data were collected using a Bruker APEX II CCD detector/D8 or PLATFORM diffractometer using Mo Kα or Cu Kα radiation, with the crystals cooled to –80 °C or –100 °C. The data were corrected for absorption through Gaussian integration from the indexing of the crystal faces. Crystal structures were solved using intrinsic phasing (*SHELXT*)[30] and refined using *SHELXL-2014*.[31] The assignment of hydrogen atom positions were based on the sp^2 or sp^3 hybridization geometries of their attached carbon atoms and were given thermal parameters 20 % greater than those of their parent atoms.

Special refinement conditions. Compound **5**: The crystal used for data collection was found to display non-merohedral twinning. Both components of the twin were indexed with the program *CELL_NOW*. The second twin component can be related to the first component by 180º rotation about the [1 0 0] axis in real space and about the [1 0 -0.227] axis in reciprocal space. Integrated intensities for the reflections from the two components were

written into a *SHELXL-2014* HKLF 5 reflection file with the data integration program *SAINT* (version 8.38A), using all reflection data (exactly overlapped, partially overlapped and non-overlapped). The refined value of the twin fraction (*SHELXL-2014* BASF parameter) was 0.4636(17). The Si6–C distances of the disordered trimethylsilyl group were restrained to be approximately the same by use of the *SHELXL* **SADI** instruction (15 restraints). Additionally, the anisotropic displacement parameters for that group were restrained by use of the *SHELXL* **RIGU** instruction (36 restraints).

6.4.3. Computational Methods

All calculations were carried out using the Gaussian 16 software package.[32] The input structure of (^{Me}IPrCH)Si{Si(SiMe$_3$)$_3$} was taken from the molecular structure obtained from X-ray crystallography and first optimized using the B3LYP[33] functional and 6-31G(d,p)[34] basis set in the gas phase. This optimized geometry was subsequently re-optimized using the M06-2X[35] functional and def2-TZVP[36] basis set and confirmed to be a minimum on the potential energy surface using frequency analysis.

6.4.4. Synthetic Procedures

Synthesis of (^{Me}IPrCH)SiBr$_3$ (1). A Schlenk flask charged with a 200 mL diethyl ether solution of ^{Me}IPr=CH$_2$ (3.046 g, 7.073 mmol). SiBr$_4$ (440.7 μL, 3.536 mmol) was added to the stirring solution, immediately affording a flocculent white precipitate. The resulting slurry was stirred overnight and filtered through a glass frit packed with a *ca.* 1 cm plug of Celite. The volatiles of the filtrate were removed *in vacuo*, affording (^{Me}IPrCH)SiBr$_3$ (1.300 g, 53 %) as a microcrystalline, off-white solid. Crystals suitable for X-ray crystallographic analysis were obtained by storing an Et$_2$O solution of **1** in a −30 °C freezer for one week. ^{1}H NMR (C$_6$D$_6$, 699.8 MHz): δ 7.19 (t, 2H, $^3J_{HH}$ = 7.5 Hz, *p*-Ar*H*), 7.10 (d,

4H, $^{3}J_{HH}$ = 7.5 Hz, *m*-Ar*H*), 3.04 (s, 1H, C*H*SiBr$_3$), 2.94 (broad s, 4H, C*H*(CH$_3$)$_2$), 1.49 (broad s, 12H, CH(C*H*$_3$)$_2$), 1.35 (s, 6H, NCC*H*$_3$), 1.09 (d, 12H, $^{3}J_{HH}$ = 7.0 Hz, CH(C*H*$_3$)$_2$). ^{13}C{^{1}H} NMR (C$_6$D$_6$, 125.7 MHz): δ 152.6 (N*C*N), 148.0 (Ar*C*), 130.8 (Ar*C*), 125.2 (Ar*C*), 119.3 (N*C*-CH$_3$), 54.1 (C=*C*H), 29.0 (*C*H(CH$_3$)$_2$), 24.6 (CH(*C*H$_3$)$_2$), 23.7 (CH(*C*H$_3$)$_2$), 9.4 (NC-*C*H$_3$). *One ArC signal is missing and likely obscured by the C$_6$D$_6$ signal.* ^{29}Si{^{1}H} NMR (C$_6$D$_6$, 79.5 MHz, DEPT): δ −59.9. Anal. Calcd. for C$_{30}$H$_{41}$Br$_3$N$_2$Si: C 51.66, H 5.93, N 4.02. Found: C 51.46, 5.97, N 3.95. M.p. 202 °C (decomp.)

Synthesis of (^{Me}IPrCH)Si{Si(SiMe$_3$)$_3$} (2). To a vial containing a 1 mL slurry of (^{Me}IPrCH)SiBr$_3$ (0.168 g, 0.241 mmol) was added a 4 mL solution of [K(THF)$_2$][Si(SiMe$_3$)$_3$] (0.211 g, 0.490 mmol), leading to the immediate formation of a deep green slurry. The resulting mixture was stirred for 20 minutes, filtered and the volatiles were removed from the filtrate *in vacuo*. The resulting deep green solid was washed with 2×1.5 mL cold (−30 °C) Me$_3$SiOSiMe$_3$ (to remove the BrSi(SiMe$_3$)$_3$ side-product). The remaining solid was dried *in vacuo*, affording (^{Me}IPrCH)Si{Si(SiMe$_3$)$_3$} as a deep green solid (0.113 g, 67 %). Crystals suitable for X-ray crystallographic analysis were obtained by storing an Me$_3$SiOSiMe$_3$ solution of **2** in a −30 °C freezer for two weeks. ^{1}H NMR (C$_6$D$_6$, 498.1 MHz): δ 7.40 (s, 1H, satellites: $^{2}J_{H\text{-}Si}$ = 13.5 Hz, C*H*Si), 7.24 (t, 2H, $^{3}J_{HH}$ = 8.0 Hz, *p*-Ar*H*), 7.10 (d, 4H, $^{3}J_{HH}$ = 8.0 Hz, *m*-Ar*H*), 2.88 (sept, 4H, $^{3}J_{HH}$ = 7.0 Hz, C*H*(CH$_3$)$_2$), 1.47 (s, 6H, NC-C*H*$_3$), 1.37 (d, 12H, $^{3}J_{HH}$ = 7.0 Hz), 1.10 (d, 12H, $^{3}J_{HH}$ = 7.0 Hz), 0.31 (s, 27H, Si(SiMe$_3$)$_3$). ^{13}C{^{1}H} NMR (C$_6$D$_6$, 125.3 MHz): δ 154.4 (N*C*N), 147.0 (Ar*C*), 132.3 (Ar*C*), 130.63 (Ar*C*), 128.3 (C=*C*H), 125.3 (Ar*C*), 121.0 (N*C*-CH$_3$), 29.2 (*C*H(CH$_3$)$_2$), 24.6 (CH(*C*H$_3$)$_2$), 23.8 (CH(*C*H$_3$)$_2$), 9.1 (NC-*C*H$_3$), 3.85 (Si(SiMe$_3$)$_3$). ^{29}Si{^{1}H} NMR (C$_6$D$_6$, 79.5 MHz, DEPT): δ 432.9 (*Si*-Si(SiMe$_3$)$_3$), −9.5 (Si-Si(*Si*Me$_3$)$_3$),

−113.4 (Si-*Si*(SiMe$_3$)$_3$). Anal. Calcd. for $C_{39}H_{68}N_2Si_5$: C 66.41, H 9.72, N 3.97. Found: C 65.58, H 9.69, N 3.89. M.p. 110–112 °C. UV-Vis: λ_{max} = 266 nm (ε = 8630 $M^{-1}cm^{-1}$), 309 nm (ε = 9500 $M^{-1}cm^{-1}$), 416 nm (ε = 3130 $M^{-1}cm^{-1}$), 583 nm (ε = 42 $M^{-1}cm^{-1}$).

Synthesis of (^{Me}IPrCH)Si(Me)OTf{Si(SiMe$_3$)$_3$} (3). To a vial containing a 1.5 mL benzene solution of **2** (0.042 g, 0.060 mmol) was added MeOTf (6.60 μL, 0.060 mmol). The resulting colorless solution was stirred for 30 seconds and the volatiles were removed *in vacuo* affording (^{Me}IPrCH)Si(Me)OTf{Si(SiMe$_3$)$_3$} as a colorless solid (0.048 g, 93 %). Crystals suitable for X-ray crystallographic analysis were grown by the slow evaporation of a 1:1 benzene:hexanes solution of **3** at room temperature. ^{1}H NMR (C_6D_6, 399.8 MHz): δ 7.30-7.20 (m, 4H, *m*-ArH), 7.13-7.03 (m, 2H, *p*-ArH), 3.53 (sept, 2H, $^3J_{HH}$ = 6.4 Hz, C*H*(CH$_3$)$_2$), 3.00 (sept, 1H, $^3J_{HH}$ = 6.4 Hz, C*H*(CH$_3$)$_2$), 2.75 (sept, 1H, $^3J_{HH}$ = 6.4 Hz, C*H*(CH$_3$)$_2$), 2.72 (s, 1H, C*H*Si), 1.66 (d, 3H, $^3J_{HH}$ = 6.4 Hz, CH(C*H*$_3$)$_2$), 1.55 (d, 3H, $^3J_{HH}$ = 6.4 Hz, CH(C*H*$_3$)$_2$), 1.37 (s, 3H, NC-C*H*$_3$), 1.33 (s, 3H, NC-C*H*$_3$), 1.31 (d, 6H, $^3J_{HH}$ = 6.4 Hz, CH(C*H*$_3$)$_2$), 1.15 (d, 3H, $^3J_{HH}$ = 6.4 Hz, CH(C*H*$_3$)$_2$), 1.12 (d, 3H, $^3J_{HH}$ = 6.4 Hz, CH(C*H*$_3$)$_2$), 1.10 (d, 3H, $^3J_{HH}$ = 6.4 Hz, CH(C*H*$_3$)$_2$), 1.09 (d, 3H, $^3J_{HH}$ = 6.4 Hz, CH(C*H*$_3$)$_2$), 0.99 (d, 3H, $^3J_{HH}$ = 6.4 Hz, CH(C*H*$_3$)$_2$), 0.24 (s, 27H, Si(SiMe$_3$)$_3$), −0.28 (s, 3H, Si-C*H*$_3$). ^{13}C{^{1}H} NMR (C_6D_6, 176.0 MHz): δ 154.1 (N*C*N), 149.5 (Ar*C*), 148.7 (Ar*C*), 147.7 (Ar*C*), 147.4 (Ar*C*), 134.7 (Ar*C*), 132.6 (Ar*C*), 130.3 (Ar*C*), 129.9 (Ar*C*), 128.5 (Ar*C*), 128.3 (Ar*C*), 125.6 (Ar*C*), 125.4 (Ar*C*), 124.8 (Ar*C*), 120.1 (N*C*-CH$_3$), 119.6 (N*C*-CH$_3$), 48.7 (C=*C*H), 28.6 (*C*H(CH$_3$)$_2$), 28.5 (*C*H(CH$_3$)$_2$), 28.2 (*C*H(CH$_3$)$_2$), 26.2 (CH(*C*H$_3$)$_2$), 25.1 (CH(*C*H$_3$)$_2$), 24.1 (CH(*C*H$_3$)$_2$), 23.6 (CH(*C*H$_3$)$_2$), 23.4 (CH(*C*H$_3$)$_2$), 23.3 (CH(*C*H$_3$)$_2$), 10.3 (CH(*C*H$_3$)$_2$), 10.2 (CH(*C*H$_3$)$_2$), 4.9 (Si-*C*H$_3$), 3.3 (Si(SiMe$_3$)$_3$). ^{29}Si{^{1}H} NMR (C_6D_6, 79.5 MHz, DEPT): δ 26.8 (*Si*-Si(SiMe$_3$)$_3$), −10.5 (Si-Si(*Si*Me$_3$)$_3$), −125.0 (Si-*Si*(SiMe$_3$)$_3$).

$^{19}F\{^{1}H\}$ NMR (C_6D_6, 376.3 MHz): δ −75.8. Anal. Calcd. for $C_{41}H_{71}F_3N_2O_3SSi_5$: C 56.64, H 8.23, N 3.22 S 3.69. Found: C 55.52, H 8.11, N 3.06, S 3.10. M.p. 240 °C (decomp.; turns red).

Synthesis of (^{Me}IPrCH)Si(H)Bpin{Si(SiMe$_3$)$_3$} (4). To a vial containing a 1 mL solution of **2** (0.024 g, 0.034 mmol) in toluene was added HBpin (4.9 μL, 0.034 mmol). The deep green color of **2** began to lighten upon the addition of HBpin, eventually turning to a pale-yellow color after 5 minutes of stirring. The resulting solution was stirred for an additional 30 minutes and the volatiles were subsequently removed *in vacuo* yielding a pale-yellow oil. The oil was triturated with 0.5 mL hexanes and dried *in vacuo*, affording (^{Me}IPrCH)Si(H)Bpin{Si(SiMe$_3$)$_3$} as a pale-yellow solid (0.017 g, 60 %). ^{1}H NMR (C_6D_6, 498.1 MHz): δ 7.30-7.18 (m, 6H, *m*-Ar*H*/*p*-Ar*H*), 3.61 (d, 1H, $^{3}J_{HH}$ = 9.3 Hz, satellites: $^{1}J_{H\text{-}Si}$ = 180.0 Hz, Si-*H*), 3.50 (sept, 1H, $^{3}J_{HH}$ = 6.5 Hz, C*H*(CH$_3$)$_2$), 3.37 (sept, 1H, $^{3}J_{HH}$ = 6.5 Hz, C*H*(CH$_3$)$_2$), 3.12-3.04 (m, 2H, C*H*(CH$_3$)$_2$), 1.72 (d, 1H, $^{3}J_{HH}$ = 9.3 Hz, C=C*H*), 1.57-1.49 (m, 12H, CH(C*H*$_3$)$_2$ and NCC*H*$_3$), 1.39 (d, 3H, $^{3}J_{HH}$ = 7.0 Hz, CH(C*H*$_3$)$_2$), 1.25 (d, 3H, $^{3}J_{HH}$ = 6.5 Hz, CH(C*H*$_3$)$_2$), 1.20-1.15 (m, 12H, CH(C*H*$_3$)$_2$), 1.10 (s, 6H, *C*H$_3$ in Bpin), 1.08 (s, 6H, *C*H$_3$ in Bpin), 0.30 (s, 27H, Si(SiMe$_3$)$_3$). $^{13}C\{^{1}H\}$ NMR (C_6D_6, 176.0 MHz): δ 153.7 (N*C*N), 149.3 (Ar*C*), 148.2 (Ar*C*), 134.6 (Ar*C*), 133.7 (Ar*C*), 129.5 (Ar*C*), 129.2 (Ar*C*), 124.7 (Ar*C*), 124.6 (Ar*C*), 124.5 (Ar*C*), 123.9 (Ar*C*), 117.7 (N*C*CH$_3$), 117.6 (N*C*CH$_3$), 82.7 (BO*C*, Bpin), 34.7 (C=*C*H), 29.0 (*C*(CH$_3$)$_2$), 28.8 (*C*(CH$_3$)$_2$, 28.7 (*C*(CH$_3$)$_2$), 28.4 (*C*(CH$_3$)$_2$, 26.9 (CH(*C*H$_3$)$_2$), 26.3 (CH(*C*H$_3$)$_2$), 25.2 (CH(*C*H$_3$)$_2$), 24.8 (CH(*C*H$_3$)$_2$), 24.8 (CH(*C*H$_3$)$_2$), 24.2 (CH(*C*H$_3$)$_2$), 23.8 (CH(*C*H$_3$)$_2$), 23.6 (CH(*C*H$_3$)$_2$), 23.2 (CH(*C*H$_3$)$_2$), 10.3 (*C*H$_3$, Bpin), 10.0 (*C*H$_3$, Bpin), 3.5 (Si(SiMe$_3$)$_3$). $^{11}B\{^{1}H\}$ 33.8 (broad s, *B*pin). $^{29}Si\{^{1}H\}$ NMR (C_6D_6, 79.5 MHz, DEPT): δ −0.5 (*Si*-Si(SiMe$_3$)$_3$), −9.6 (Si-

Si(*Si*Me$_3$)$_3$), −119.0 (Si-*Si*(SiMe$_3$)$_3$). Anal. Calcd. for $C_{45}H_{81}BN_2O_2Si_5$: C 64.85, H 9.80, N 3.36. Found: C 64.49, H 9.68, N 3.35. M.p. 194 °C (decomp.)

Synthesis of (^{Me}IPrCH)ClSi(HSiCl$_2$){Si(SiMe$_3$)$_3$} (5). To a vial containing a 1 mL toluene solution of **2** (0.021 g, 0.030 mmol) was added $HSiCl_3$ (3.0 μL, 0.030 mmol). The resultant pale-yellow solution was stirred for 20 minutes and the volatiles were removed *in vacuo* affording a pale-yellow solid. The solid was re-dissolved in C_6D_6 for NMR analysis, revealing the quantitative formation of **5**. The NMR solution was then transferred to a vial and dried *in vacuo* affording (^{Me}IPrCH)ClSi(HSiCl$_2$){Si(SiMe$_3$)$_3$} as a pale-yellow solid (0.019 g, 76 %). Crystals suitable for X-ray crystallographic analysis were obtained by slow evaporation of a hexanes solution of **5** over one week at room temperature. ^{1}H NMR (C_6D_6, 399.8 MHz): δ 7.24-7.08 (m, 6H, *m*-Ar*H*/*p*-Ar*H*), 4.64 (s, 1H, satellites: $^1J_{H\text{-}Si}$ = 248.4 Hz, $^2J_{H\text{-}Si}$ = 23.4 Hz, Si-*H*), 3.30 (broad s, 1H, C*H*(CH$_3$)$_2$), 3.14 (broad s, 2H, C*H*(CH$_3$)$_2$), 2.85 (broad sept, 1H, $^3J_{HH}$ = 5.6 Hz, C*H*(CH$_3$)$_2$), 2.53 (s, 1H, satellites: $^2J_{H\text{-}Si}$ = 55.6 Hz, $^3J_{H\text{-}Si}$ = 7.0 Hz, C*H*Si), 1.51 (broad s, 6H, CH(C*H*$_3$)$_2$), 1.43 (broad s, 6H, CH(C*H*$_3$)$_2$), 1.31 (broad s, 3H, NC-C*H*$_3$), 1.27 (broad s, 3H, NC-C*H*$_3$), 1.10 (broad d, 6H, $^3J_{HH}$ = 5.6 Hz, CH(C*H*$_3$)$_2$), 1.04 (broad s, 6H, CH(C*H*$_3$)$_2$), 0.32 (s, 27H, Si(SiMe$_3$)$_3$). ^{29}Si{^{1}H} NMR (C_6D_6, 79.5 MHz, DEPT): δ −0.5 (H*Si*Cl$_2$), −9.6 (Si-Si(*Si*Me$_3$)$_3$), −13.4 (*Si*-Si(SiMe$_3$)$_3$), −118.9 (Si-*Si*(SiMe$_3$)$_3$). *Due to significant broadening caused by hindered rotation of the -Dipp groups, a ^{13}C{^{1}H} spectrum was not recorded at room temperature. As such, ^{1}H and ^{13}C{^{1}H} spectra were recorded at +75 °C to resolve this broadening:* ^{1}H NMR (C_6D_6, 399.8 MHz, +75 °C): δ 7.24-7.17 (m, 6H, *m*-Ar*H*/*p*-Ar*H*), 4.81 (s, 1H, satellites: $^1J_{H\text{-}Si}$ = 248.4 Hz, $^2J_{H\text{-}Si}$ = 23.4 Hz, Si-*H*), 3.20 (sept, 2H, $^3J_{HH}$ = 6.8 Hz, C*H*(CH$_3$)$_2$), 3.04 (sept, 2H, $^3J_{HH}$ = 6.8 Hz, C*H*(CH$_3$)$_2$), 2.48 (s, 1H, satellites: $^2J_{H\text{-}Si}$ = 55.6

Hz, $^{3}J_{H\text{-}Si}$ = 7.0 Hz, C*H*Si), 1.46 (d, 12H, $^{3}J_{HH}$ = 6.8 Hz, CH(C*H*$_3$)$_2$), 1.36 (s, 6H, NC-C*H*$_3$), 1.12 (d, 6H, $^{3}J_{HH}$ = 6.8 Hz, CH(C*H*$_3$)$_2$), 1.06 (d, 6H, $^{3}J_{HH}$ = 6.8 Hz, CH(C*H*$_3$)$_2$), 0.29 (s, 27H, Si(SiMe$_3$)$_3$). ^{13}C{^{1}H} NMR (C$_6$D$_6$, 100.6 MHz, +75 °C): δ 155.5 (N*C*N), 148.2 (Ar*C*), 130.3 (Ar*C*), 125.6 (Ar*C*), 125.5 (Ar*C*), 120.5 (N*C*CH$_3$), 43.2 (C=*C*H), 29.0 (*C*H(CH$_3$)$_2$), 28.8 (*C*H(CH$_3$)$_2$), 25.8 (CH(*C*H$_3$)$_2$), 24.9 (CH(*C*H$_3$)$_2$), 23.8 (CH(*C*H$_3$)$_2$), 23.7 (CH(*C*H$_3$)$_2$), 10.3 (NC-*C*H$_3$), 4.1 (Si(SiMe$_3$)$_3$). Anal. Calcd. for C$_{39}$H$_{69}$Cl$_3$N$_2$Si$_6$: C 55.71, H 8.27, N 3.33. Found: C 55.72, H 8.26, N 3.29. M.p. 218 °C (decomp.; turns red).

Synthesis of (^{Me}IPrCH)Si(P$_4$){Si(SiMe$_3$)$_3$} (6). To a vial containing a 1 mL slurry of (^{Me}IPrCH)SiBr$_3$ (0.088 g, 0.13 mmol) in toluene was added a 3 mL toluene solution of [K(THF)$_2$][Si(SiMe$_3$)$_3$] (0.108 g, 0.251 mmol), immediately forming a deep green slurry (containing silylene **2** and BrSi(SiMe$_3$)$_3$). After stirring the mixture for 5 min. a 2 mL solution of P$_4$ (0.016 g, 0.129 mmol) in toluene was added. After two minutes of stirring, the mixture had changed from deep green to a red color. The mixture was stirred for an additional 20 min. after which the color had lightened to orange. The slurry was filtered and the volatiles were removed from the filtrate *in vacuo*. The solid residue was washed with 2 mL of Me$_3$SiOSiMe$_3$ and dried *in vacuo*, affording (^{Me}IPrCH)Si(P$_4$){Si(SiMe$_3$)$_3$} as a pale yellow/orange solid (0.046 g, 44 %). Crystals suitable for X-ray crystallographic analysis were grown by storing a hexanes solution of **6** in a −30 °C freezer overnight. ^{1}H NMR (C$_6$D$_6$, 400.0 MHz): δ 7.49-7.34 (m, 4H, *m*-Ar*H*), 7.15-7.07 (m, 2H, *o*-Ar*H*), 3.47 (broad sept, 2H, $^{3}J_{HH}$ = 5.6 Hz, C*H*(CH$_3$)$_2$), 3.31 (s, 1H, C*H*Si), 3.05 (broad sept, 2H, $^{3}J_{HH}$ = 5.6 Hz, C*H*(CH$_3$)$_2$), 1.78 (broad d, 6H, $^{3}J_{HH}$ = 5.6 Hz, CH(C*H*$_3$)$_2$), 1.39 (s, 6H, NC-C*H*$_3$), 1.36 (broad d, 6H, $^{3}J_{HH}$ = 5.6 Hz, CH(C*H*$_3$)$_2$), 1.21 (broad d, 6H, $^{3}J_{HH}$ = 5.6 Hz, CH(C*H*$_3$)$_2$), 1.10 (broad d, 6H, $^{3}J_{HH}$ = 5.6 Hz, CH(C*H*$_3$)$_2$), 0.42 (s, 27H, Si(SiMe$_3$)$_3$). ^{29}Si{^{1}H} NMR

(C_6D_6, 79.4 MHz, DEPT): δ −9.4 (s, Si-Si(*Si*Me_3)$_3$), −10.0 (m, *Si*-Si($SiMe_3$)$_3$), −109.6 (broad s, Si-*Si*($SiMe_3$)$_3$). $^{31}P\{^1H\}$ NMR (C_6D_6, 161.9 MHz): δ 120.0 (dd, $^1J_{P1\text{-}P2}$ = 158.2 Hz, $^2J_{P1\text{-}P3}$ = 150.6 Hz, P1), −181.0 (dt, $^1J_{P3\text{-}P2}$ = 165.1 Hz, $^2J_{P3\text{-}P1}$ = 150.6 Hz, P3), −316.7 (dt, $^1J_{P2\text{-}P3}$ = 165.1, $^1J_{P2\text{-}P1}$ = 158.2 Hz, P2). *Due to significant broadening, we were unable to collect suitable $^{13}C\{^1H\}$ NMR data at room temperature, +75 °C (C_6D_6) or +100 °C ([D_8]toluene).* Anal. Calcd. for $C_{39}H_{68}N_2P_4Si_5$: C 56.48, H 8.27, N 3.38. Found: C 55.97, H 8.18, N 3.26. M.p. 184–186 °C (melts to red). *Alternatively,* ***6*** *can be generated from the direct reaction of* ***2*** *and* P_4.

Synthesis of (^{Me}IPrCH)SiH(CN){Si($SiMe_3$)$_3$} (7) from ^{t}BuNCO. To a vial containing a 1 mL toluene solution of **2** (0.050 g, 0.071 mmol) was added ^{t}BuNCO (4.20 μL, 0.037 mmol) with no discernable color change upon addition. The mixture was stirred overnight, resulting in a pale-yellow solution. The volatiles were removed *in vacuo*, the residue extracted with 1 mL of hexanes and the solution placed in a −30 °C freezer overnight affording pale-yellow crystals, from which a few crystals were removed for X-ray crystallographic analysis. The mother liquor was decanted from the bulk sample and the volatiles were removed *in vacuo*, yielding (^{Me}IPrCH)SiH(CN){Si($SiMe_3$)$_3$} as a pale-yellow crystalline solid (0.008 g, 31 %). ^1H NMR (C_6D_6, 699.7 MHz): δ 7.36-7.32 (m, 2H, Ar*H*), 7.27-7.24 (m, 1H, Ar*H*), 7.20-7.13 (m, 3H, Ar*H*), 3.92 (d, 1H, $^3J_{HH}$ = 7.7 Hz, satellites: $^1J_{H\text{-}Si}$ = 210.7 Hz, Si-*H*), 3.22 (sept, 1H, $^3J_{HH}$ = 7.0 Hz, C*H*(CH_3)$_2$), 3.10 (sept, 2H, $^3J_{HH}$ = 7.0 Hz, C*H*(CH_3)$_2$), 2.91 (sept, 1H, $^3J_{HH}$ = 7.0 Hz, C*H*(CH_3)$_2$), 1.78 (d, 3H, $^3J_{HH}$ = 7.0 Hz, C*H*(CH_3)$_2$), 1.75 (d, 1H, $^3J_{HH}$ = 7.7 Hz, C*H*(CH_3)$_2$), 1.54 (d, 3H, $^3J_{HH}$ = 7.0 Hz, CH(C*H*$_3$)$_2$), 1.47 (s, 3H, NC-C*H*$_3$), 1.46 (s, 3H, NC-C*H*$_3$), 1.43 (d, 3H, $^3J_{HH}$ = 7.0 Hz, CH(C*H*$_3$)$_2$), 1.32 (d, 3H, $^3J_{HH}$ = 7.0 Hz, CH(C*H*$_3$)$_2$), 1.18 (d, 3H, $^3J_{HH}$ = 7.0 Hz, CH(C*H*$_3$)$_2$),

1.13 (d, 3H, $^{3}J_{HH}$ = 7.0 Hz, CH(CH_3)$_2$), 1.11 (d, 3H, $^{3}J_{HH}$ = 7.0 Hz, CH(CH_3)$_2$), 1.10 (d, 3H, $^{3}J_{HH}$ = 7.0 Hz, CH(CH_3)$_2$), 0.25 (s, 27H, Si(SiMe$_3$)$_3$). ^{13}C{^{1}H} NMR (C_6D_6, 176.0 MHz): δ 154.7 (N*C*N), 148.9 (Ar*C*), 148.7 (Ar*C*), 148.3 (Ar*C*), 147.8 (Ar*C*), 133.0 (Ar*C*), 132.5 (Ar*C*), 130.7 (Ar*C*), 129.8 (Ar*C*), 128.3 (Si-*C*N), 126.2 (Ar*C*), 124.9 (Ar*C*), 124.6 (Ar*C*), 124.1 (Ar*C*), 118.6 (N*C*-CH$_3$), 118.2 (N*C*-CH$_3$), 32.4 (C=*C*H), 29.4 (*C*H(CH$_3$)$_2$), 28.8 (*C*H(CH$_3$)$_2$), 28.7 (*C*H(CH$_3$)$_2$), 25.6 (CH(*C*H$_3$)$_2$), 25.1 (CH(*C*H$_3$)$_2$), 24.3 (CH(*C*H$_3$)$_2$), 24.2 (CH(*C*H$_3$)$_2$), 24.1 (CH(*C*H$_3$)$_2$), 23.9 (CH(*C*H$_3$)$_2$), 23.8 (CH(*C*H$_3$)$_2$), 23.2 (CH(*C*H$_3$)$_2$), 2.7 (Si(SiMe$_3$)$_3$). ^{29}Si{^{1}H} NMR (C_6D_6, 79.4 MHz, DEPT): δ −9.7 (s, Si-Si(*Si*Me$_3$)$_3$), −74.5 (*Si*-Si(SiMe$_3$)$_3$), −133.0 (Si-*Si*(SiMe$_3$)$_3$). Anal. Calcd. for $C_{40}H_{69}N_3Si_5$: C 65.59, H 9.50, N 5.74. Found C 64.99, H 9.16, N 6.16. M.p. 158 °C (decomp.)

Synthesis of (^{Me}IPrCH)SiH(CN){Si(SiMe$_3$)$_3$} (7) from ^{t}BuNC. A J. Young PTFE valve-capped NMR tube was loaded with a 0.5 mL solution of **2** (0.014 g, 0.020 mmol) to which ^{t}BuNC was added (2.24 μL, 0.0198 mmol). Upon addition of ^{t}BuNC, the deep green color of **2** immediately dissipated, forming a pale-yellow solution. After NMR analysis (which revealed a mixture of **7** and isobutylene), the solution was transferred to a vial and the volatiles were removed *in vacuo*, affording (^{Me}IPrCH)SiH(CN){Si(SiMe$_3$)$_3$} (**7**) as a pale-yellow solid (0.013 g, 89 %).

6.5. Crystallographic Data

Table 6.1. Crystallographic data for compounds **2** and **3**.

Compound	**2**	**3**
formula	$C_{39}H_{68}N_2Si_5$	$C_{41}H_{71}F_3N_2O_3SSi_5$
formula weight	705.40	869.50
crystal system	triclinic	monoclinic
space group	$P\overline{1}$	$P2_1/c$
a [Å]	10.3993(7)	20.6562(5)
b [Å]	12.5264(7)	13.3097(3)
c [Å]	18.4455(11)	19.8440(5)
α [°]	88.449(3)	90
β [°]	85.965(4)	109.6576(9)
γ [°]	75.290(3)	90
V [Å^3]	2318.2(2)	5137.7(2)
Z	2	4
ρ_{calcd} [g/cm^3]	1.011	1.124
μ [mm^{-1}]	1.617	2.048
T [°C]	−100	−100
$2\theta_{max}$ [°]	148.31	148.39
total data collected	94354	240012
unique data (R_{int})	9029 (0.0804)	10457 (0.0371)
obs data [$I \geq 2\sigma(I)$]	7429	9712
params	434	546
R_1 [$I \geq 2\sigma(I)$][a]	0.0526	0.0319
wR_2 [all data][a]	0.1667	0.0932
max/min $\Delta\rho$ [e/Å^3]	0.504/−0.609	0.300/−0.435

[a] $R_1 = \sum||F_o| - |F_c||/\sum|F_o|$; $wR_2 = [\sum w(F_o^2 - F_c^2)^2/\sum w(F_o^4)]^{1/2}$

Table 6.2. Crystallographic data for compounds **5** and **6**.

Compound	**5**	**6**
formula	$C_{39}H_{69}Cl_3N_2Si_6$	$C_{39}H_{64}N_2P_4Si_5$
formula weight	840.86	825.25
crystal system	monoclinic	triclinic
space group	$P2_1/n$	$P\bar{1}$
a [Å]	10.4358(6)	10.1314(4)
b [Å]	19.1606(5)	13.5879(6)
c [Å]	24.4753(8)	18.6001(7)
α [°]	90	78.391(3)
β [°]	95.466(3)	85.188(2)
γ [°]	90	77.406(3)
V [Å^3]	4871.7(3)	2445.70(17)
Z	4	2
ρ_{calcd} [g/cm^3]	1.146	1.121
μ [mm^{-1}]	3.320	2.802
T [°C]	−100	−100
$2\theta_{max}$ [°]	140.52	148.54
total data collected	10180	17281
unique data (R_{int})	10180 (0.0934)	9501 (0.0390)
obs data [$I \geq 2\sigma(I)$]	7477	7735
params	491	470
R_1 [$I \geq 2\sigma(I)$][a]	0.0768	0.0603
wR_2 [all data][a]	0.2177	0.1837
max/min $\Delta\rho$ [e/Å^3]	0.891/−0.589	0.819/−0.779

[a] $R_1 = \sum||F_o| - |F_c||/\sum|F_o|$; $wR_2 = [\sum w(F_o^2 - F_c^2)^2/\sum w(F_o^4)]^{1/2}$

Table 6.3. Crystallographic data for **7**.

Compound	**7**
formula	$C_{40}H_{69}N_3Si_5$
formula weight	732.43
crystal system	monoclinic
space group	$P2_1/m$
a [Å]	11.3610(2)
b [Å]	18.2937(4)
c [Å]	11.6759(2)
α [°]	90
β [°]	105.7582(8)
γ [°]	90
V [Å^3]	2335.46(8)
Z	2
ρ_{calcd} [g/cm^3]	1.042
μ [mm^{-1}]	1.628
T [°C]	−100
$2\theta_{max}$ [°]	148.57
total data collected	16666
unique data (R_{int})	4908 (0.0163)
obs data [$I \geq 2\sigma(I)$]	4547
params	325
R_1 [$I \geq 2\sigma(I)$][a]	0.0786
wR_2 [all data][a]	0.2282
max/min $\Delta\rho$ [e/Å^3]	1.562/−0.469

[a] $R_1 = \sum||F_o| - |F_c||/\sum|F_o|$; $wR_2 = [\sum w(F_o^2 - F_c^2)^2/\sum w(F_o^4)]^{1/2}$

6.6. References

1. For recent reviews and articles, see: (a) Chu, T.; Nikonov, G. I. *Chem. Rev.* **2018**, *118*, 3608; (b) Power, P. P. *Nature* **2010**, *463*, 171; (c) Weetman, C.; Inoue, S. *ChemCatChem.* **2018**, *10*, 4213; (d) Melen, R. L. *Science* **2019**, *363*, 479; (e) Wilson, A. S. S.; Hill, M. S.; Mahon, M. F.; Dinoi, C.; Maron, L. *Science* **2017**, *358*, 1168; (f) Fontaine, F.-G.; Rochette, E. *Acc. Chem. Res.* **2018**, *51*, 454; (g) Hicks, J.; Vasko, P.; Goicoechea, J. M.; Aldridge, S. *Nature* **2018**, *557*, 92.
2. Légaré, M.-A.; Bélanger-Chabot, G.; Dewhurst, R. D.; Welz, E.; Krummenacher, I.; Engels, B.; Braunschweig, H. *Science* **2018**, *359*, 896.
3. (a) Miller, K. A.; Watson, T. W.; Bender, J. E.; Banaszak Holl, M. M.; Kampf, J. W. *J. Am. Chem. Soc.* **2001**, *123*, 982; (b) Peng, Y.; Ellis, B. D.; Wang, X.; Power, P. P. *J. Am. Chem. Soc.* **2008**, *130*, 12268; (c) Peng, Y.; Guo, J.-D.; Ellis, B. D.; Zhu, Z.; Fettinger, J. C.; Nagase, S.; Power, P. P. *J. Am. Chem. Soc.* **2009**, *131*, 16272; (d) Mandal, S. K.; Roesky, H. W. *Acc. Chem. Res.* **2011**, *45*, 298; (e) Inomata, K.; Watanabe, T.; Miyazaki, Y.; Tobita, H. *J. Am. Chem. Soc.* **2015**, *137*, 11935; (f) Protchenko, A. V.; Bates, J. I.; Saleh, L. M. A.; Blake, M. P.; Schwarz, A. D.; Kolychev, E. L.; Thompson, A. L.; Jones, C.; Mountford, P.; Aldridge, S. *J. Am. Chem. Soc.* **2016**, *138*, 4555; (g) Roy, M. M. D.; Fujimori, S.; Ferguson, M. J.; McDonald, R.; Tokitoh, N.; Rivard, E. *Chem. Eur. J.* **2018**, *24*, 14392; (h) Hadlington, T. J.; Driess, M.; Jones, C. *Chem. Soc. Rev.* **2018**, *47*, 4176.
4. (a) Mizuhata, Y.; Sasamori, T.; Tokitoh, N. *Chem. Rev.*, **2009**, *109*, 3479; (b) Asay, M.; Jones, C.; Driess, M. *Chem. Rev.* **2011**, *111*, 354; (c) Rivard, E. *Chem. Soc. Rev.* **2016**, *45*, 989.

5. (a) Jutzi, P.; Holtmann, U.; Kanne, D.; Krüger, C.; Blom, R.; Gleiter, R.; Hyla-Kryspin, I. *Chem. Ber.* **1989**, *122*, 1629; (b) Karsch, H. H.; Keller, U.; Gamper, S.; Müller, G. *Angew. Chem. Int. Ed. Engl.* **1990**, *29*, 295.
6. Denk, M.; Lennon, R.; Hayashi, R.; West, R.; Belyakov, A. V.; Verne, H. P.; Haaland, A.; Wagner, M.; Metzler, N. *J. Am. Chem. Soc.*, **1994**, *116*, 2691.
7. (a) Rekken, B. D.; Brown, T. M.; Fettinger, J. C.; Tuononen, H. M.; Power, P. P. *J. Am. Chem. Soc.* **2012**, *134*, 6504; (b) Protchenko, A. V.; Birjkumar, K. H.; Dange, D.; Schwarz, A. D.; Vidovic, D.; Jones, C.; Kaltsoyannis, N.; Mountford, P.; Aldridge, S. *J. Am. Chem. Soc.* **2012**, *134*, 6500.
8. Gynane, M. J. S.; Harris, D. H.; Lappert, M. F.; Power, P. P.; Rivière, P.; Rivière-Baudet, M. *J. Chem. Soc., Dalton Trans.* **1977**, 2004.
9. (a) Protchenko, A. V.; Schwarz, A. D.; Blake, M. P.; Jones, C.; Kaltsoyannis, N.; Mountford, P.; Aldridge, S. *Angew. Chem. Int. Ed.* **2013**, *52*, 568; (b) Hadlington, T. J.; Abdalla, J. A. B.; Tirfoin, R.; Aldridge, S.; Jones, C. *Chem. Commun.* **2016**, *52*, 1717; (c) Wendel, D.; Porzelt, A.; Herz, F. A. D.; Sakar, D.; Jandl, C.; Inoue, S.; Rieger, B. *J. Am. Chem. Soc.* **2017**, *139*, 8134; (d) Loh, Y. K.; Ying, L. Fuentes, M. Á.; Do, D. C. H.; Aldridge, S. *Angew. Chem. Int. Ed.* **2019**, *58*, 4847.
10. A cyclic dialkylsilylene has been previously reported: Kira, M.; Ishida, S.; Iwamoto, T.; Kabuto, C. *J. Am. Chem. Soc.* **1999**, *121*, 9722
11. (a) Hering-Junghans, C.; Andreiuk, P.; Ferguson, M. J.; McDonald, R.; Rivard, E. *Angew. Chem. Int. Ed.* **2017**, *56*, 6272; (b) For an example of a base-stabilized divinylgermylene, see: Walewska, M.; Baumgartner, J.; Marschner, C. *Chem. Commun.* **2015**, *51*, 276.

12. For reviews on NHO ligands, see: (a) Ghadwal, R. S. *Dalton Trans.* **2016**, *45*, 16081; (b) Crocker, R. D.; Nguyen, T. V. *Chem. Eur. J.* **2016**, *22*, 2208; (*c*) Roy, M. M. D.; Rivard, E. *Acc. Chem. Res.* **2017**, *50*, 2017.
13. Powers, K.; Hering-Junghans, C.; McDonald, R.; Ferguson, M. J.; Rivard, E. *Polyhedron* **2016**, *108*, 8.
14. Dithiolatosilylenes have been reported to reversibly bind ethylene: Lips, F.; Fettinger, J. C.; Mansikkamäki, A.; Tuononen, H. M.; Power, P. P. *J. Am. Chem. Soc.* **2014**, *136*, 634.
15. Lui, M. W.; Merten, C.; Ferguson, M. J.; McDonald, R.; Xu, Y.; Rivard, E. *Inorg. Chem.* **2015**, *54*, 2040.
16. A similar reaction has been previously reported for a cyclic silylene, however a mixture of two products was observed: Xiong, Y.; Yao, S.; Driess, M. *Organometallics* **2009**, *28*, 1927.
17. Swihart, M. T.; Carr, R. W. *J. Phys. Chem. A* **1998**, *102*, 1542.
18. Hydrodechlorination of chlorosilanes using strong neutral bases is known. For example: Ghadwal, R. S.; Roesky, H. W.; Merkel, S.; Henn, H.; Stalke, D. *Angew. Chem. Int. Ed.* **2009**, *48*, 5683.
19. (a) Driess, M.; Fanta, A. D.; Powell, D. R.; West, R. *Angew. Chem. Int. Ed. Engl.* **1989**, *28*, 1038; (b) Xiong, Y.; Yao, S.; Brym, M.; Driess, M. *Angew. Chem. Int. Ed.* **2007**, *46*, 4511; (c) Sen, S. S.; Khan, S.; Roesky, H. W.; Kratzert, D.; Meindl, K.; Henn, J.; Stalke, D.; Demers, J.-P.; Lange, A. *Angew. Chem. Int. Ed.* **2011**, *50*, 2322.
20. For selected reviews of P_4 activation by main group elements, see: (a) Scheer, M.; Balázs, g.; Seitz, A. *Chem. Rev.* **2010**, *110*, 4236; (b) Khan, S.; Sen, S. S.; Roesky, H.

W. *Chem. Commun.* **2012**, *48*, 2169; (c) Borger, J. E.; Ehlers, A. W.; Slootweg, J. C.; Lammertsma, K. *Chem. Eur. J.* **2017**, *23*, 11738.

21. The activation of P_4 by H_2Si: has been studied computationally. Interestingly, none of the located minima on the potential energy surface correspond to compound **6**: Damrauer, R.; Pusede, S. E. *Organometallics* **2009**, *28*, 1289.
22. For example: Gary, D. C.; Cossairt, B. M. *Chem. Mater.* **2013**, *25*, 2463.
23. Geeson, M. B.; Cummins, C. C. *Science* **2018**, *359*, 1383.
24. Wendel, D.; Reiter, D.; Porzelt, A.; Altmann, P. J.; Inoue, S.; Rieger, B. *J. Am. Chem. Soc.* **2017**, *139*, 17193.
25. Brown, Z. D.; Vasko, P.; Fettinger, J. C.; Tuononen, H. M.; Power, P. P. *J. Am. Chem. Soc.* **2012**, *134*, 4045.
26. Takeda, N.; Kajiwara, T.; Suzuki, H.; Okazaki, R.; Tokitoh, N. *Chem. Eur. J.* **2003**, *9*, 3530.
27. Pangborn, A. B.; Giardello, M. A.; Grubbs, R. H.; Rosen, R. K.; Timmers, F. J. *Organometallics* **1996**, *15*, 1518.
28. Marschner, C. *Eur. J. Inorg. Chem.* **1998**, 221.
29. Hope, H. *Prog. Inorg. Chem.* **1994**, *41*, 1.
30. Sheldrick, G. M. *Acta. Crystallogr. Sect. A* **2015**, *71*, 3.
31. Sheldrick, G. M. *Acta. Crystallogr. Sect. C* **2015**, *71*, 3.
32. Gaussian 16, Revision B.01, Frisch, M. J.; Trucks, G. W.; Schlegel, H. B.; Scuseria, G. E.; Robb, M. A.; Cheeseman, J. R.; Scalmani, G.; Barone, V.; Petersson, G. A.; Nakatsuji, H.; Li, X.; Caricato, M.; Marenich, A. V.; Bloino, J.; Janesko, B. G.; Gomperts, R.; Mennucci, B.; Hratchian, H. P.; Ortiz, J. V.; Izmaylov, A. F.;

Sonnenberg, J. L.; Williams-Young, D.; Ding, F.; Lipparini, F.; Egidi, F.; Goings, J.; Peng, B.; Petrone, A.; Henderson, T.; Ranasinghe, D.; Zakrzewski, V. G.; Gao, J.; Rega, N.; Zheng, G.; Liang, W.; Hada, M.; Ehara, M.; Toyota, K.; Fukuda, R.; Hasegawa, J.; Ishida, M.; Nakajima, T.; Honda, Y.; Kitao, O.; Nakai, H.; Vreven, T.; Throssell, K.; Montgomery, J. A., Jr.; Peralta, J. E.; Ogliaro, F.; Bearpark, M. J.; Heyd, J. J.; Brothers, E. N.; Kudin, K. N.; Staroverov, V. N.; Keith, T. A.; Kobayashi, R.; Normand, J.; Raghavachari, K.; Rendell, A. P.; Burant, J. C.; Iyengar, S. S.; Tomasi, J.; Cossi, M.; Millam, J. M.; Klene, M.; Adamo, C.; Cammi, R.; Ochterski, J. W.; Martin, R. L.; Morokuma, K.; Farkas, O.; Foresman, J. B.; Fox, D. J. Gaussian, Inc., Wallingford CT, **2016**.

33. (a) Lee, C.; Yang, W.; Parr, R. G. *Phys. Rev. B* **1988**, *37*, 785; (b) Becke, A. D. *Phys. Rev. A* **1988**, *38*, 3098; (c) Stephens, P. J.; Devlin, F. J.; Chabalowski, C. F.; Frisch, M. J. *J. Phys. Chem.* **1994**, *98*, 11623.
34. (a) Hariharan, P. C.; Pople, J. A. *Theor. Chim. Acta* **1973**, *28*, 213; (b) Francl, M. M.; Pietro, W. J.; Hehre, W. J.; Binkley, J. S.; Gordon, M. S.; DeFrees, D. J.; Pople, J. A. *J. Chem. Phys.* **1982**, *77*, 3654.
35. Zhao, Y.; Truhlar, D. J. *Theor. Chem. Acc.* **2008**, *120*, 215.
36. Weigend, F.; Ahlrichs, R. *Phys. Chem. Chem. Phys.* **2005**, *7*, 3297.

Chapter 7: The Group 14 Series of Homoleptic Divinyltetrelenes R_2E: (E = Si–Pb)

1.1. Introduction

Since the seminal isolation of the dialkyl tetrelenes (**I**, Figure 7.1) by Lappert and coworkers in the 1970s,[1] the field of low-coordinate main group chemistry has flourished.[2] While Lappert's dialkyl tetrelenes are monomeric in solution, they form weak E–E bonded dimers in the solid state (E = Ge–Pb). The use of bulky carbon-based ligands as substituents kinetically inhibits oligomerization of the resulting two-coordinate tetrelenes in solution. Since these early reports, this strategy has been extended to silicon(II). For example, using the pentamethylcyclopentadienyl ligand ($C_5Me_5^-$), Jutzi and coworkers isolated the coordinatively saturated silylene **II**,[3] which was followed by the cyclic dialkyl silylene **III**[4] by Kira and coworkers (Figure 7.1). Additionally, bulky diarylgermylenes (**IV**), stannylenes (**V**) and plumbylenes (**VI**) have been reported.[5] Since these early reports, several of these (and related) species have been shown to exhibit transition-metal like reactivity, such as the oxidative addition of strong bonds.[6] Despite these advances, a homologous tetrelene series has not been reported for carbon-based donors, thus limiting the direct comparison of the E^{II} series (E = Si–Pb).[7] This is likely due to the relative instability of the silicon(II) oxidation state, with known stable silylenes being limited to cyclic systems[4,8] (such as **III**), coordinatively saturated examples[3,9] (such as **II**) and those stabilized by heteroatom donors.[10] In this chapter, the first completed divinyltetrelene series is reported consisting of the bulky carbon-based vinylic donor, $[^{Me}IPr{=}CH]^-$; (^{Me}IPr = [(MeCNDipp)$_2$C]; Dipp = 2,6-*i*Pr$_2$C$_6$H$_3$).

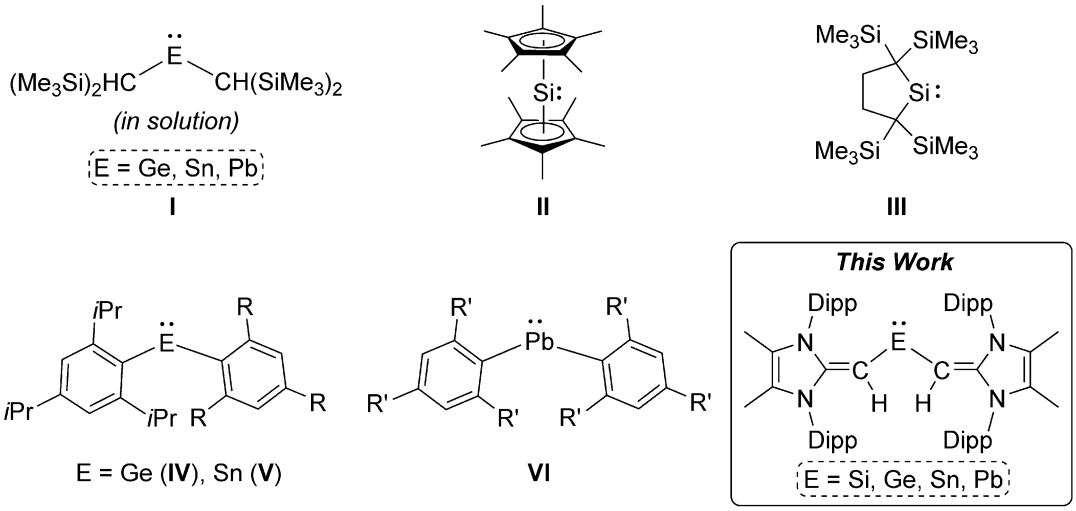

Figure 7.1. Selected early examples of alkyl- and aryl-substituted tetrelenes; R = $CH(SiMe_3)_2$, R′ = CF_3.

7.2. Results and Discussion

In order to form a sufficiently stable two-coordinate acyclic silylene using only carbon-based donors, the *N*-heterocyclic vinyl ligand $[^{Me}IPr{=}CH]^-$ was selected. Previously, this ligand was accessed via *in situ* deprotonation of its *N*-heterocyclic olefin (NHO)[11] parent $^{Me}IPr{=}CH_2$ in the presence of an element halide (Scheme 7.1; top left). While this strategy has shown to be viable in certain cases[12] it is not universally successful. For example, the Rivard group has utilized this strategy to isolate the divinylgermylene $(^{Me}IPrCH)_2Ge:$,[13] however attempts to install the ligand on tin or lead starting from $:ECl_2$ (E = Sn, Pb), $^{Me}IPr{=}CH_2$ and base were unsuccessful. Additionally, in Chapter 6 it was demonstrated that attempts to install a second equivalent of the $[^{Me}IPr{=}CH]^-$ ligand onto a Si^{IV} center [to form $(^{Me}IPrCH)_2SiBr_2$] was unsuccessful, with the reaction halting at the mono-substituted product $(^{Me}IPrCH)SiBr_3$. Therefore, it was desirable to first find an improved method to install the $[^{Me}IPr{=}CH]^-$ ligand and thus a lithiated *N*-heterocyclic olefin ligand $(^{Me}IPrCH)Li$ was targeted.

The direct deprotonation of the *N*-heterocyclic olefin, IPr=CH_2 [IPr = $(HCNDipp)_2C$:] has been previously investigated using alkyllithium reagents, however it was shown that the *N*-heterocycle backbone was deprotonated in preference to an exocyclic C–H bond due to the polarized nature of the terminal $^{\delta+}C{=}CH_2{}^{\delta-}$ olefin.[14] Unsurprisingly, attempts to deprotonate the backbone protected ^{Me}IPr=CH_2 using either *n*BuLi, *t*BuLi or *n*BuLi/TMEDA (TMEDA = tetramethylethylenediamine) resulted in no reaction and so the iodinated NHO ^{Me}IPr=CH(I) (**1**) was first prepared.

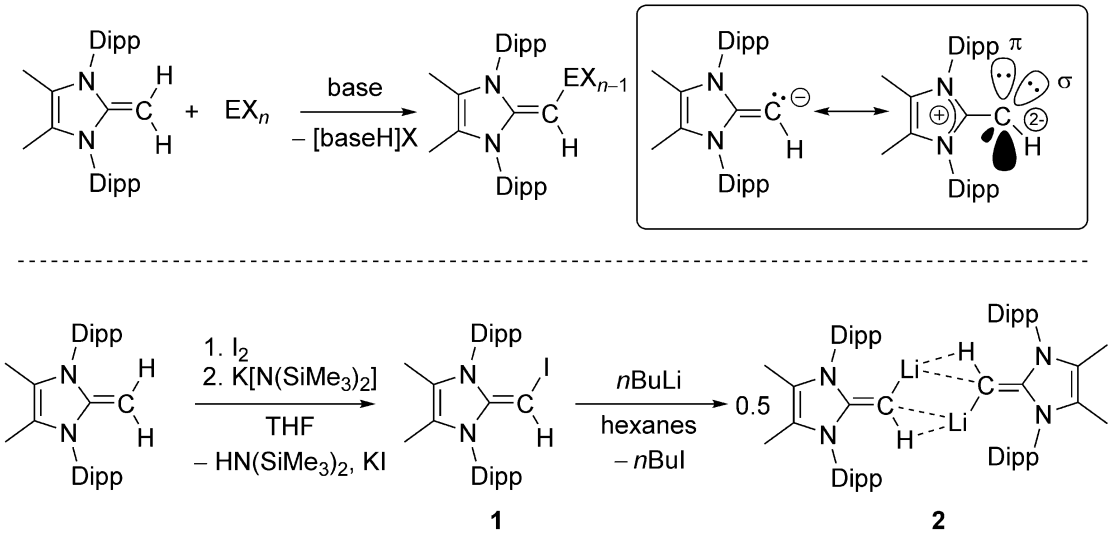

Scheme 7.1. General route to vinyl-substituted p-block elements (top left); illustration of the 2σ, 2π donor capability of *N*-heterocyclic vinyl ligands (top right); *N*-heterocyclic olefin iodination (forming **1**) and subsequent lithiation forming **2** (bottom).

When ^{Me}IPr=CH_2 was combined with elemental iodine in THF, a bright yellow precipitate formed, tentatively assigned as the imidazolium salt [^{Me}IPrCH_2(I)]I.[15] Upon addition of the strong amide base K[N($SiMe_3$)$_2$], the precipitate was consumed and afforded the thermally sensitive target compound ^{Me}IPr=CH(I) (**1**) after extraction into hexanes and filtration (Scheme 7.1, Figure 7.2). X-ray crystallography confirmed the formation of the desired iodinated NHO, ^{Me}IPr=CH(I) (**1**) which crystallizes as a monomer in the solid state with an sp^2-character exocyclic carbon atom [C2-C1-I1: 128.1(3)°].

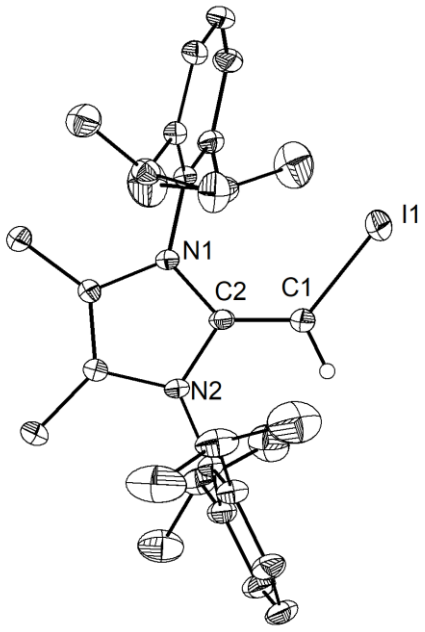

Figure 7.2. Molecular structure of ^{Me}IPr=CH(I) (**1**) with thermal ellipsoids plotted at a 30 % probability level. All hydrogen atoms (except the vinylic hydrogen) were omitted for clarity. Selected bond lengths [Å] and angles [°]: C1-I1 2.068(3), C2-C1 1.360(5); C2-C1-I1 128.1(3).

With compound **1** in hand, its lithiation with *n*BuLi was investigated. Indeed, upon addition of *n*BuLi to a hexanes solution of **1**, a bright orange precipitate began to form. Crystallization from a saturated hexanes solution at −30 °C afforded crystals of the target (^{Me}IPrCH)Li (**2**, Scheme 7.1). Compound **2** crystallizes as a centrosymmetric dimer [(^{Me}IPrCH)Li]$_2$ (Figure 7.3). Interestingly, rather than dimerizing via the polarized vinylic C=C bond, compound **2** forms a rhomboid dimer that is supported through agostic (CH)···Li interactions as evidenced by close C–Li contacts [2.117(5) Å] with the retention of double bond character of the exocyclic olefin [C1–C4: 1.341(6) Å].[16] To test whether **2** would act as an effective source of the [^{Me}IPr=CH]$^-$ ligand, **2** was combined with Cl_2Ge•dioxane in Et_2O. The formation of the previously reported deep-red germylene

(^{Me}IPrCH)$_2$Ge: (**3**) was observed[13] and was purified by its extraction into hexanes and subsequent crystallization in a 49 % yield (Scheme 7.2). Given that previous attempts to form the tin and lead analogues were unsuccessful, it was reasoned that **2** should provide access to such species. In an analogous fashion to the synthesis of **3**, the vinyl lithium precursor [(^{Me}IPrCH)Li]$_2$ (**2**) was combined with $SnCl_2$ in Et_2O. Upon addition, the immediate formation of a deep violet solution was observed. Subsequent workup and crystallization from hexanes afforded reddish-pink crystals of the target divinyl stannylene (^{Me}IPrCH)$_2$Sn: (**4**) in a 32 % yield (Scheme 7.2).

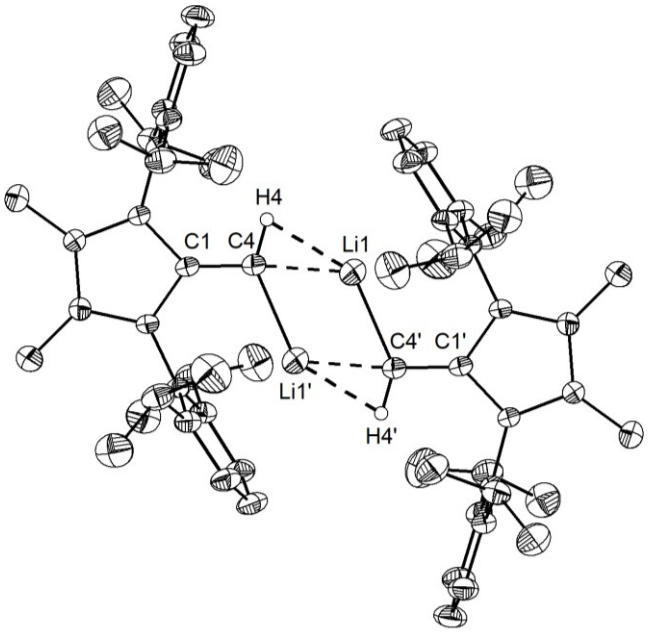

Figure 7.3. Molecular structure of [(^{Me}IPrCH)Li]$_2$ (**2**) with thermal ellipsoids plotted at a 30 % probability level. All hydrogen atoms (except the vinylic hydrogens) were omitted for clarity. Selected bond lengths [Å] and angles [°]: C1-C4 1.341(3), C4-H4 0.94(3), C4-Li1′ 2.117(5), C4-Li1 2.027(5); C1-C4-Li1′ 111.94(19).

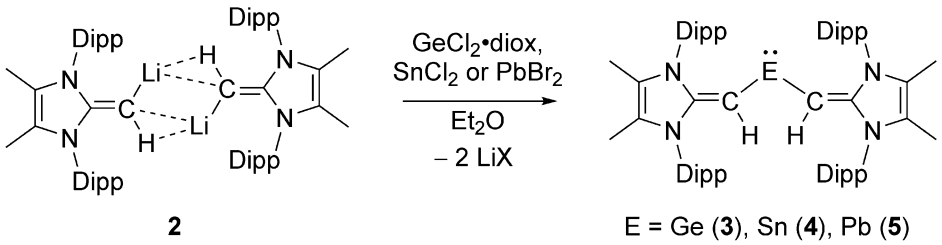

2 E = Ge (**3**), Sn (**4**), Pb (**5**)

Scheme 7.2. Formation of the divinylgermylene **3**, divinylstannylene **4** and divinylplumbylene **5** from vinyl lithium **2**.

Interestingly, unlike the divinyl germylene (^{Me}IPrCH)$_2$Ge: (**3**) which exhibits a lengthening of the vinylic C=C bond [1.364(3) Å] relative to free ^{Me}IPr=CH$_2$ [1.3489(18) Å][17] (indicating π-donation from the vinyl ligands), the related C=C bond in stannylene **4** [1.352(5) Å] is the same as ^{Me}IPr=CH$_2$ within error. Additionally, the C-Sn-C bond angle in **4** of 90.83(14)° suggests the tin-based lone pair is of essentially pure *s*-character. During initial attempts to crystallize **4**, a few yellow crystals were isolated and X-ray crystallography identified the crystals to be an alternate constitutional isomer of **4** (**6**, Scheme 7.3). This alternate form may be viewed as resulting from the formal C–H activation of an -*i*Pr group residing on one of the ligand -Dipp groups of stannylene **4** (Figure 7.5, Scheme 7.3). Specifically, the molecular structure of **6** also shows transfer of the hydrogen atom to one of the vinyl ligands, now forming an ylidic C–Sn linkage. The long H$_2$C–Sn [C54-Sn1: 2.428(5) Å] and C–CH$_2$ [C51-C54: 1.418(7) Å] bonds are indicative of a neutral donor interaction similar to known NHO•LA (LA = Lewis acid) adducts.[11] This compound may arise from the intramolecular activation of a C–H bond of **4**, either through σ-bond metathesis or an oxidative addition/reductive elimination mechanism. While only a few crystals of **6** were isolated, attempts to intentionally synthesize **6** are currently underway. Thus far, attempts to form **6** by the mild heating of **4**

have been unsuccessful, yielding only ^{Me}IPr=CH_2 and tin metal, indicating that **6** may arise from an alternate mechanism of (^{Me}IPrCH)Li and $SnCl_2$.

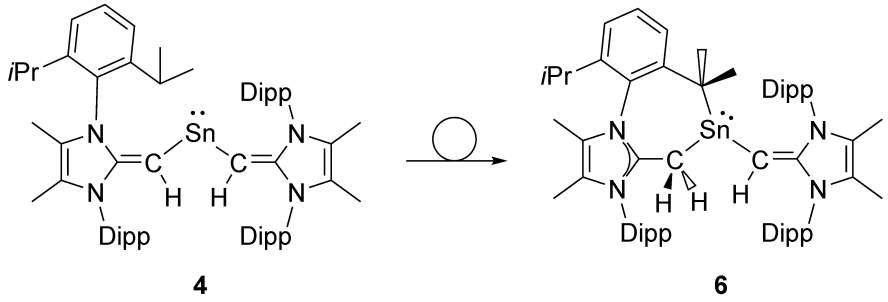

Scheme 7.3. The observed three-coordinate stannylene **6** may be formed from the intramolecular C–H activation of divinylstannylene **4**.

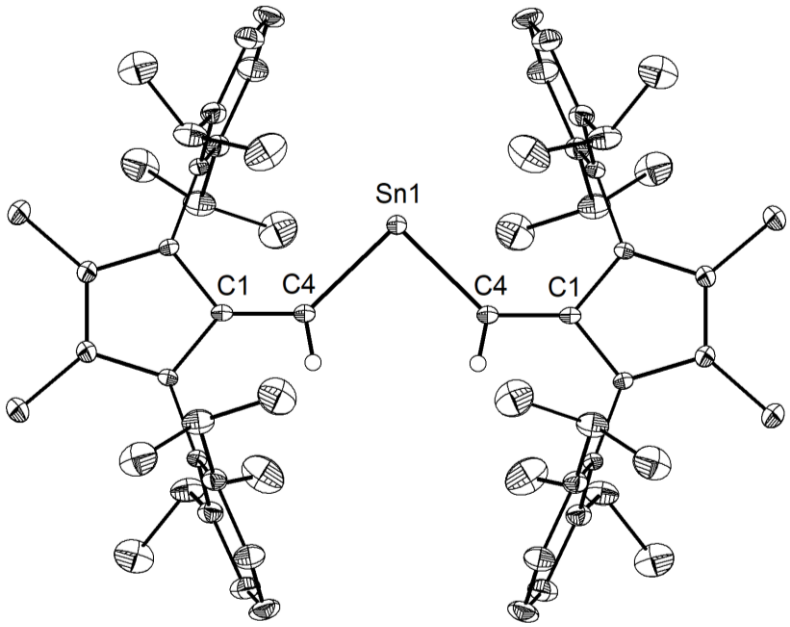

Figure 7.4. Molecular structure of (^{Me}IPrCH)$_2$Sn: (**4**) with thermal ellipsoids plotted at a 30 % probability level. All hydrogen atoms (except the vinylic hydrogens) were omitted for clarity. Selected bond lengths [Å] and angles [°]: C1-C4 1.352(5), C4-Sn1 2.109(3); C4-Sn1-C4 90.83(14).

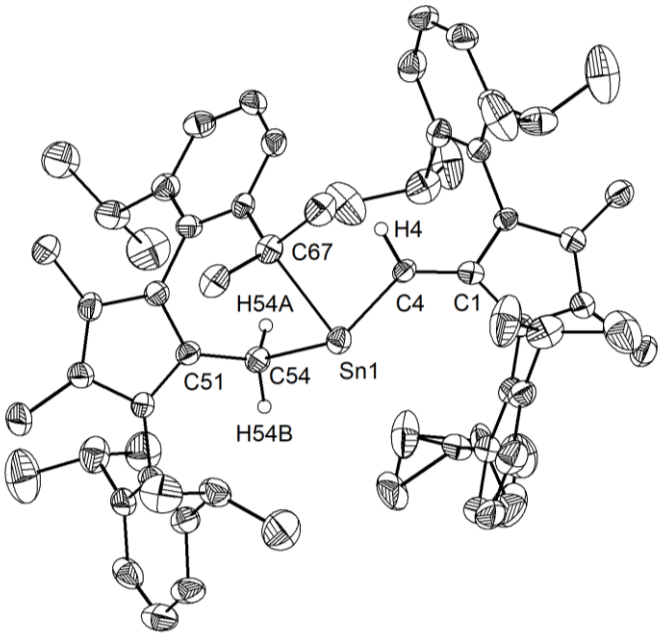

Figure 7.5. Molecular structure of the Lewis base stabilized stannylene **6** with thermal ellipsoids plotted at a 30 % probability level. All hydrogen atoms (except the vinylic/olefinic hydrogens) were omitted for clarity. Selected bond lengths [Å] and angles [°]: Sn1-C4 2.168(6), Sn1-C54 2.428(5), Sn1-C67 2.358(6), C1-C4 1.355(7), C51-C54 1.418(7); C4-Sn1-C54 94.5(2), C4-Sn1-C67 92.47(19), C54-Sn1-C67 89.82(19), Sn1-C54-C51 110.2(4), Sn1-C4-C1 135.0(4).

Additionally, the monomeric lead analogue (^{Me}IPrCH)$_2$Pb: (**5**) was synthesized by combining [(^{Me}IPrCH)Li]$_2$ (**2**) with $PbBr_2$ in Et_2O, followed by extraction into hexanes and crystallization (Scheme 7.2, 49 % yield). The resulting deep blue crystals of **5** were analyzed by X-ray crystallography. Similar to stannylene **4**, the C-Pb-C atoms form nearly a right angle [88.6(2)°] indicating the Pb lone pair is of pure *s*-character. This angle is more contracted than known diarylplumbylenes, such **VI** in Figure 7.1 which has a C-Pb-C angle of 94.5°.[5c] Additionally, the C4-Pb1 distance in **5** [2.210(4) Å] is shorter than in **VI** [2.361(4) Å] suggesting a stronger interaction of the [^{Me}IPrCH]$^-$ ligand with Pb^{II}.

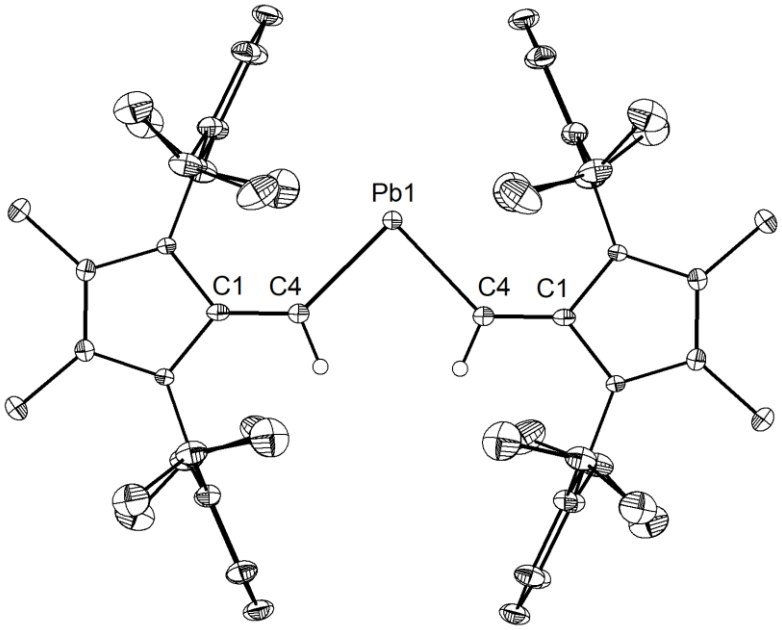

Figure 7.6. Molecular structure of (^{Me}IPrCH)$_2$Pb: (**5**) with thermal ellipsoids plotted at a 30 % probability level. All hydrogen atoms (except the vinylic/olefinic hydrogens) were omitted for clarity. Selected bond lengths [Å] and angles [°]: C4-Pb1 2.210(4), C1-C4 1.342(7); C1-C4-Pb1 134.30(10), C4-Pb1-C4 88.6(2).

While the divinyl germylene (**3**), stannylene (**4**) and plumbylene (**5**) were readily synthesized from [(^{Me}IPrCH)Li]$_2$ (**2**) and commercially available dihalotetrelenes (Cl_2Ge•dioxane, $SnCl_2$ or $PbBr_2$), Si^{II} is far more reactive and such silicon(II) precursors are not readily available. Accordingly, Roesky's *N*-heterocyclic carbene (NHC)-stabilized dichlorosilylene IPr•$SiCl_2$[18] was prepared and combined with **2**, however no evidence of the target silylene (^{Me}IPrCH)$_2$Si: was observed. After stirring the reaction mixture in toluene overnight, ^{1}H NMR analysis of an aliquot of the reaction mixture revealed primarily unreacted starting materials, along with ^{Me}IPr=CH_2 (which is also observed upon thermal decomposition of **2**). This lack of reactivity may be due to the presence of strong Si–Cl bonds and so Filippou's more labile precursor IPr•$SiBr_2$ was synthesized.[19] When

IPr•$SiBr_2$ was reacted with **2** for 1 hour, the expected release of the free carbene (IPr) was observed by ^{1}H NMR spectroscopy, along with ^{Me}IPr=CH_2 and a small set of signals (< 5 %) whose pattern matched those of compounds **3**–**5**. The presence of significant quantities of ^{Me}IPr=CH_2 is likely due to the competitive deprotonation of the IPr backbone protons of IPr•$SiBr_2$. In order to circumvent this competitive pathway, the methyl backbone-protected analogue ^{Me}IPr•$SiBr_2$ (**7**) was prepared. While this compound has been previously reported from the disproportionation of Si_2Br_6,[20] its separation from the concomitantly formed Si^{IV} product ^{Me}IPr•$SiBr_4$ was not demonstrated, so an improved synthesis of this compound was first explored.

Recently, it has been shown that acyclic silyl-silylenes such as (^{Me}IPrCH)Si{$Si(SiMe_3)_3$} (Chapter 6) can be generated from Si^{IV} precursors appended with appropriately bulky (and stabilizing) substituents.[21] When $RSiBr_3$ precursors (R = bulky group) are combined with two equivalents of the hypersilyl anion source $[K(THF)_2][Si(SiMe_3)_3]$, the corresponding hypersilyl-substituted silylene RSi{$Si(SiMe_3)_3$} can be generated (Scheme 7.4). In this reaction, one equivalent of the $[Si(SiMe_3)_3]^-$ anion is a source of silyl ligand and the other equivalent serves to reduce Si^{IV} to Si^{II}. When using one equivalent of $[K(THF)_2][Si(SiMe_3)_3]$ in the presence of the *N*-heterocyclic carbene ^{Me}IPr and $SiBr_4$, it was found to act solely as a reducing agent, cleanly forming the corresponding Si^{II} dibromide adduct ^{Me}IPr•$SiBr_2$ (**7**). The expected hypersilyl bromide byproduct $BrSi(SiMe_3)_3$ was also identified by ^{1}H NMR and could be easily removed by washing with cold (−30 °C) hexanes, affording **7** in 64 % isolated yield.

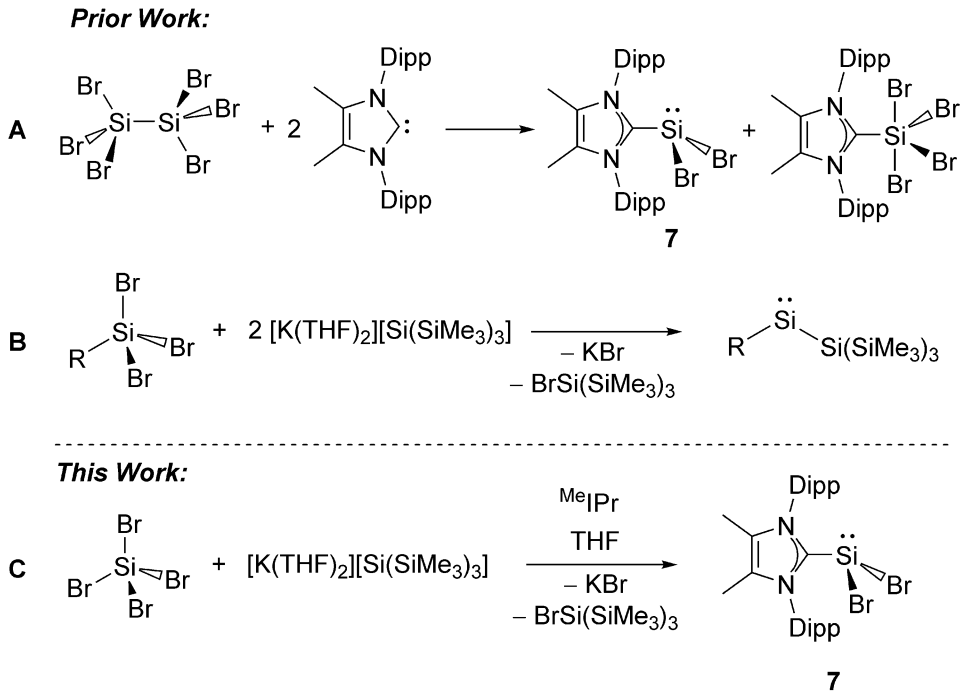

Scheme 7.4. A) Synthesis of ^{Me}IPr•SiBr$_2$ by the disproportionation of Si_2Br_6, B) Formation of silyl-silylenes from RSiBr$_3$ (R = bulky substituent), C) The synthesis of ^{Me}IPr•SiBr$_2$ (**7**) using a related strategy.

With an efficient synthesis of **7** now available, the preparation of the target divinylsilylene (^{Me}IPrCH)$_2$Si: was again attempted. When **7** was combined with [(^{Me}IPrCH)Li]$_2$ (**2**) in toluene, the immediate formation of a deep-yellow/brown mixture was observed. After stirring for 1 hour, the volatiles of the reaction mixture were removed *in vacuo*, the crude residue extracted into hexanes, filtered and the filtrate placed in a −30 °C freezer, affording deep-yellow crystals of (^{Me}IPrCH)$_2$Si: (**8**) in a 75 % yield (Scheme 7.5, Figure 7.7). As shown in Figure 7.7, the elongated C=C bond length in **8** [C1-C4: 1.375(2) Å] relative to ^{Me}IPr=CH$_2$ [1.3489(18) Å][17] indicates π-donation from the vinylic C=CH bond to the empty silicon-based *p*-orbital. Additionally, the C-Si-C angle of 100.58(8)° suggests some degree of *s*/*p* orbital mixing in the Si-based lone pair, as expected for the lighter tetrel element silicon.

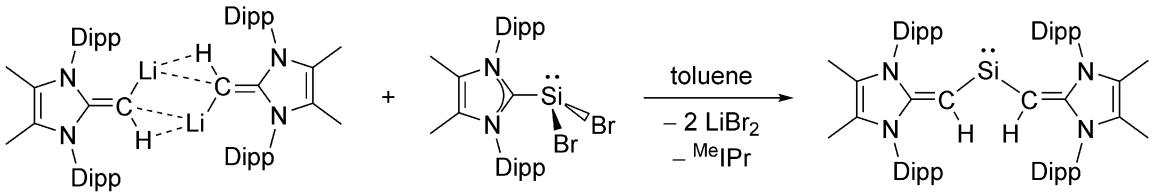

Scheme 7.5. Formation of the divinylsilylene **8** from **2** and the Si^{II} precursor **7**.

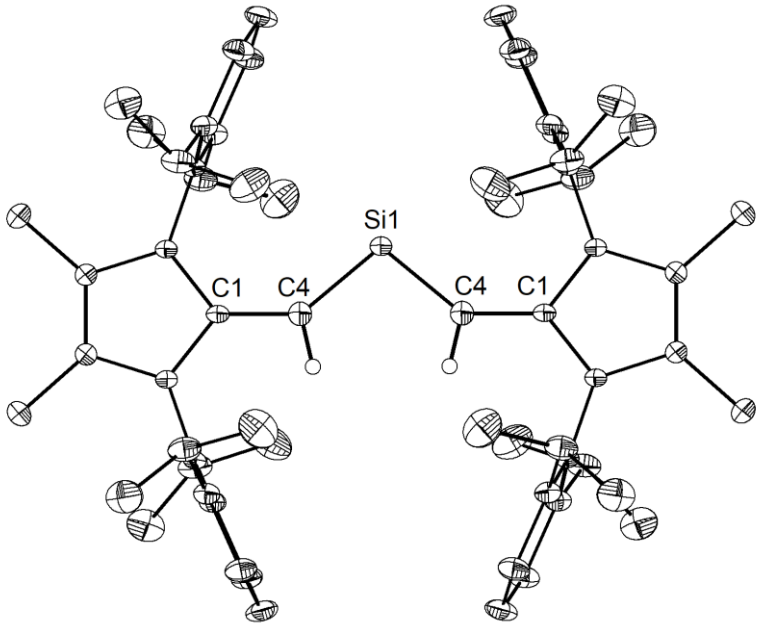

Figure 7.7. Molecular structure of (^{Me}IPrCH)$_2$Si: (**8**) with thermal ellipsoids plotted at a 30 % probability level. All hydrogen atoms (except the vinylic/olefinic hydrogens) were omitted for clarity. Selected bond lengths [Å] and angles [°]: C1-C4 1.375(2), C4-Si1 1.7620(14); C1-C4-Si1 140.29(4), C4-Si1-C4 100.58(8).

With the completed homoleptic divinyltetrelene (^{Me}IPrCH)$_2$E: (E = Si−Pb) series prepared, structural comparison between these heavy carbene homologues can be conducted, and general trends may be extrapolated. Upon descending the Group 14 elements (from Si–Pb), one can observe a distinct shortening of the vinylic C–C bond length as π-donation from the vinyl group (to the tetrelene empty *p*-orbital) decreases

descending the group due to worse C–E orbital overlap (Table 7.1). The inert pair effect manifests itself in the C-E-C bond angles, which approach 90° upon descending the group. Additionally, π-donation from the vinyl substituent to the element worsens down the group, causing a decrease in the HOMO(π)/LUMO(π*) gap energies, $\Delta E_{H/L}$ (Table 7.1).

Table 7.1. Comparison of the structural features and energies of the divinyltetrelene series.

	C–C [Å]	C–E–C [°]	$\Delta E_{H/L}$ [kJ/mol][b]
(^{Me}IPrCH)$_2$Si:	1.375(2)	100.58(8)	306.7
(^{Me}IPrCH)$_2$Ge:	1.364(3)[a]	96.56(10)[a]	290.5
(^{Me}IPrCH)$_2$Sn:	1.352(5)	90.83(14)	264.3
(^{Me}IPrCH)$_2$Pb:	1.342(7)	88.6(2)	248.8

[a]Data from ref. 13
[b]Computed at the B3LYP/cc-pVDZ level of theory

7.3. Conclusions

In this chapter, a nucleophilic source of the [^{Me}IPr=CH]$^-$ ligand was prepared by a one-pot iodination protocol of the parent *N*-heterocyclic olefin ^{Me}IPr=CH$_2$ and subsequent lithiation. Using the dimeric [(^{Me}IPrCH)Li]$_2$ precursor, the series of divinyltetrelenes (^{Me}IPrCH)$_2$E: (E = Si–Pb) was synthesized from various EX$_2$ precursors (X = halogen). In the case of silicon, a new, efficient synthesis of the Si^{II} source ^{Me}IPr•SiBr$_2$ was reported and this species used in the formation of the divinylsilylene (^{Me}IPrCH)$_2$Si:. This new protocol represents a general synthesis of base-stabilized :SiBr$_2$ adducts which may extend to a wide array of Lewis bases. Future work will include oxidation of the divinyltetrelenes using oxygen atom transfer reagents (such as N$_2$O) to their corresponding "heavy ketones" (^{Me}IPrCH)$_2$E=O.[22,23]

7.4. Experimental Details

7.4.1. General

All reactions were performed in an inert atmosphere glovebox (Innovative Technology, Inc.). Solvents were dried using a Grubbs-type solvent purification system[24] manufactured by Innovative Technologies, Inc., degassed (freeze-pump-thaw method), and stored under an atmosphere of nitrogen prior to use. Cl_2Ge•dioxane, $SnCl_2$ and $PbBr_2$ were purchased from Aldrich and used as received. $SiBr_4$ was purchased from Alfa Aesar and used as received. ^{Me}IPr,[25] ^{Me}IPr=CH_2,[26] and $[K(THF)_2][Si(SiMe_3)_3]$[27] were prepared according to literature procedures. ^{1}H, $^{13}C\{^1H\}$, ^{29}Si and ^{119}Sn NMR spectra were recorded on 400, 500, 600 or 700 MHz Varian Inova instruments and were referenced externally to $SiMe_4$ (^{1}H, $^{13}C\{^1H\}$, ^{29}Si) or $SnMe_4$ (^{119}Sn). Elemental analyses were performed by the Analytical and Instrumentation Laboratory at the University of Alberta. Melting points were measured in sealed glass capillaries under nitrogen by using a MelTemp apparatus and are uncorrected.

7.4.2. X-ray Crystallography

Crystals for X-ray diffraction studies were removed from a vial (in a glovebox) and immediately coated with a thin layer of hydrocarbon oil (Paratone-N). A suitable crystal was then mounted on a glass fiber and quickly placed in a low temperature stream of nitrogen on an X-ray diffractometer.[28] All data were collected using a Bruker APEX II CCD detector/D8 or PLATFORM diffractometer using Mo Kα or Cu Kα radiation, with the crystals cooled to –80 °C or –100 °C. The data were corrected for absorption through Gaussian integration from the indexing of the crystal faces. Crystal structures were solved using intrinsic phasing (*SHELXT*)[29] and refined using *SHELXL-2014*.[30] The assignment of hydrogen atom positions were based on the sp^2 or sp^3 hybridization geometries of their

attached carbon atoms and were given thermal parameters 20 % greater than those of their parent atoms.

7.4.3. Computational Methods

All calculations were carried out using the Gaussian 16 software package.[31] The input structures were taken from the molecular structure obtained from X-ray crystallography and optimized using the B3LYP[32] functional and cc-pVDZ[33] basis set in the gas phase. Optimized geometries were confirmed to be a minima on the potential energy surface using frequency analysis.

7.4.4. Synthetic Procedures

Synthesis of ^{Me}IPr=CH(I) (1). A solution of I_2 in 20 mL THF (1.153 g, 4.543 mmol) was added via syringe to a solution of ^{Me}IPrCH$_2$ (1.997 g, 4.637 mmol) in 150 mL of THF in a Schlenk flask. Upon addition of I_2, a flocculant, bright-yellow precipitate began to form. Once the addition was complete, the resulting mixture was stirred for an additional 140 minutes. *From this point on, all manipulations were conducted in the absence of ambient light*. A solution of K[N(SiMe$_3$)$_2$] (0.920 g, 4.612 mmol) in THF was transferred via cannula to the yellow mixture. Upon addition of amide, the yellow precipitate was slowly consumed to form a brown slurry. This mixture was stirred for 70 minutes and the volatiles were subsequently removed *in vacuo*. The solid residue was extracted with 100 mL of hexanes and filtered through a frit packed with a *ca.* 1 cm plug of diatomaceous earth. The resulting dark yellow filtrate was concentrated to 20 mL and placed in a −30 °C freezer overnight, which afforded bright yellow crystals of ^{Me}IPr=CH(I) (1.127 g). The mother liquor was then concentrated to half its original volume and placed in a −30 °C freezer overnight, yielding a second crop of crystals (0.326 g; combined yield: 1.453 g, 57 %).

Crystals suitable for X-ray diffraction analysis were obtained by dissolving **1** in a minimal amount of hexanes and storing the solution at −30 °C for one week. ^{1}H NMR (400 MHz, C_6D_6): δ 7.28 (t, 1H, $^{3}J_{HH}$ = 7.6 Hz, *p*-ArH), 7.18-7.11 (m, 3H, ArH), 7.06 (d, 2H, $^{3}J_{HH}$ = 7.6 Hz, *m*-ArH), 3.19 (sept, 2H, $^{3}J_{HH}$ = 6.8 Hz, C*H*$(CH_3)_2$), 3.09 (sept, 2H, $^{3}J_{HH}$ = 6.8 Hz, C*H*$(CH_3)_2$), 2.21 (s, 1H, C*H*I), 1.53 (d, 6H, $^{3}J_{HH}$ = 6.8 Hz, CH(C*H*$_3)_2$), 1.48 (s, 3H, NCC*H*$_3$), 1.42 (s, 3H, NCC*H*$_3$), 1.28 (d, 6H, $^{3}J_{HH}$ = 6.8 Hz, CH(C*H*$_3)_2$), 1.14 (d, 6H, $^{3}J_{HH}$ = 6.8 Hz, CH(C*H*$_3)_2$), 1.11 (d, 6H, $^{3}J_{HH}$ = 6.8 Hz, CH(C*H*$_3)_2$). ^{13}C{^{1}H} NMR (100 MHz, C_6D_6): δ 148.9 (Ar*C*), 148.8 (Ar*C*), 145.2 (N*C*N), 132.6 (Ar*C*), 132.2 (Ar*C*), 129.5 (Ar*C*), 129.3 (Ar*C*), 124.4 (Ar*C*), 123.4 (Ar*C*), 116.6 (N*C*-CH_3), 116.2 (N*C*-CH_3), 28.7 (*C*H$(CH_3)_2$), 28.5 (*C*H$(CH_3)_2$), 24.4 (CH(*C*$H_3)_2$), 23.9 (CH(*C*$H_3)_2$), 23.5 (CH(*C*$H_3)_2$), 9.1 (NC-*C*H_3), 9.0 (NC-*C*H_3), −7.5 (*C*HI). Anal. Calcd. for $C_{30}H_{41}IN_2$: C 64.74, H 7.43, N 5.03; Found: C 64.89, H 7.45, N 4.86. M.p. 150 °C (decomp.)

Synthesis of (^{Me}IPrCH)Li (2). A 2.5 M solution of *n*BuLi in hexanes (208 μL, 0.519 mmol) was added to a yellow solution of ^{Me}IPr=CH(I) (0.289 g, 0.519 mmol) in 4 mL of hexanes. After 2 minutes of stirring, the solution began to turn a bright orange/red color. After 20 minutes of stirring, an orange/red solid began to precipitate from solution. The mixture was placed in a −30 °C freezer overnight, the mother liquor was decanted (and discarded) and the volatiles were removed *in vacuo* yielding (^{Me}IPrCH)Li (**2**) as a bright orange/red solid (0.185 g, 82 %). Crystals suitable for X-ray crystallographic analysis were obtained by storing a hexanes solution of **2** in a −30 °C freezer for 10 days. *Compound 2 slowly decomposes at room temperature, even when stored in an inert atmosphere in the solid state. As such, batches of **2** were always stored as solids at −30 °C in a glovebox.* ^{1}H NMR (C_6D_6, 700 MHz): δ 7.41 (t, 2H, $^{3}J_{HH}$ = 8.0 Hz, *p*-Ar*H*), 7.32 (d, 4H, $^{3}J_{HH}$ = 8.0 Hz,

m-Ar*H*), 7.04 (d, 4H, $^{3}J_{HH}$ = 8.0 Hz, *m*-Ar*H*), 6.88 (t, 2H, $^{3}J_{HH}$ = 8.0 Hz, *p*-Ar*H*), 3.40-3.13 (m, C*H*(CH_3)$_2$), 1.67 (s, 6H, NC-CH_3), 1.65 (s, 6H, NC-CH_3), 1.40 (d, 12H, $^{3}J_{HH}$ = 7.0 Hz, CH(CH_3)$_2$), 1.31 (d, 12H, $^{3}J_{HH}$ = 7.0 Hz, CH(CH_3)$_2$), 1.30 (d, 12H, $^{3}J_{HH}$ = 7.0 Hz, CH(CH_3)$_2$), 1.11 (d, 12H, $^{3}J_{HH}$ = 7.0 Hz, CH(CH_3)$_2$), 0.87 (broad s, 2H, C*H*Li). $^{13}C\{^{1}H\}$ NMR (C_6D_6, 176 MHz): δ 159.0 (N*C*N), 150.5 (Ar*C*), 150.4 (Ar*C*), 136.6 (Ar*C*), 136.0 (Ar*C*), 129.4 (Ar*C*), 128.3 (Ar*C*), 126.0 (Ar*C*), 123.7 (Ar*C*), 115.6 (N*C*CH_3), 113.6 (N*C*CH_3), 69.7 (broad, C=*C*H), 28.7 (*C*H(CH_3)$_2$), 28.5 (*C*H(CH_3)$_2$), 25.4 (CH(*C*H_3)$_2$), 24.5 (CH(*C*H_3)$_2$), 24.3 (CH(*C*H_3)$_2$), 23.9 (CH(*C*H_3)$_2$), 10.3 (NC*C*H_3), 10.1 (NC*C*H_3). M.p. 188–190 °C.

Synthesis of (^{Me}IPrCH)$_2$Ge: (3). A solution of (^{Me}IPrCH)Li (0.067 g, 0.15 mmol) in 4 mL of Et_2O was added to a slurry of Cl_2Ge•diox (0.018 g, 0.077 mmol) in 1 mL Et_2O. After stirring for 1 minute, the resulting mixture had turned deep red. After stirring for an additional 2 hours, the volatiles were removed *in vacuo*, the residue extracted with 5 mL of hexanes and filtered. The filtrate was concentrated to a volume of 2 mL and placed in a −30 °C freezer for one week. The mother liquor was decanted away from the resulting deep orange/red crystals of **3** and dried (0.035 g, 49 %). ^{1}H and $^{13}C\{^{1}H\}$ data for **3** are consistent with the literature.[13]

Synthesis of (^{Me}IPrCH)$_2$Sn: (4). A solution of (^{Me}IPrCH)Li (0.043 g, 0.095 mmol) in 4 mL of Et_2O was added to a slurry of $SnCl_2$ (0.010 g, 0.053 mmol) in 1 mL of Et_2O. After stirring for 1 minute, the resulting mixture had turned a deep violet. After stirring for an additional 30 minutes, the volatiles were removed *in vacuo*, the residue extracted with 4 mL of hexanes and filtered. The filtrate was concentrated to a volume of 2 mL and placed in a −30 °C freezer for one week. A few crystals were removed for X-ray crystallographic

analysis. The mother liquor was decanted from the bulk crystals and the crystals dried *in vacuo* affording (^{Me}IPrCH)$_2$Sn: (**4**) as a deep reddish pink crystalline solid (0.015 g, 32 %). ^{1}H NMR (C_6D_6, 700 MHz): δ 7.33 (t, 2H, $^3J_{HH}$ = 8.0 Hz, *p*-Ar*H*), 7.22 (t, 2H, $^3J_{HH}$ = 8.0 Hz, *p*-Ar*H*), 7.15 (d, 4H, $^3J_{HH}$ = 8.0 Hz, *m*-Ar*H*), 7.14 (d, 4H, $^3J_{HH}$ = 8.0 Hz, *m*-Ar*H*), 5.20 (s, 2H, C*H*Sn), 3.20 (sept, 4H, $^3J_{HH}$ = 7.0 Hz, C*H*(CH$_3$)$_2$), 3.04 (sept, 4H, $^3J_{HH}$ = 7.0 Hz, C*H*(CH$_3$)$_2$), 1.59 (s, 6H, NC-C*H*$_3$), 1.58 (s, 6H, NC-C*H*$_3$), 1.34 (d, 12H, $^3J_{HH}$ = 7.0 Hz, CH(C*H*$_3$)$_2$), 1.21 (d, 12H, $^3J_{HH}$ = 7.0 Hz, CH(C*H*$_3$)$_2$), 1.17 (d, 12H, $^3J_{HH}$ = 7.0 Hz, CH(C*H*$_3$)$_2$), 1.14 (d, 12H, $^3J_{HH}$ = 7.0 Hz, CH(C*H*$_3$)$_2$). ^{13}C{^{1}H} NMR (C_6D_6, 176 MHz): δ 157.7 (N*C*N), 149.0 (Ar*C*), 148.0 (Ar*C*), 135.0 (Ar*C*), 133.4 (Ar*C*), 129.4 (Ar*C*), 128.8 (Ar*C*), 126.6 (Ar*C*), 125.5 (Ar*C*), 124.1 (Ar*C*), 117.6 (N*C*CH$_3$), 116.7 (N*C*CH$_3$), 49.1 (C=*C*H), 28.8 (*C*H(CH$_3$)$_2$), 28.7 (*C*H(CH$_3$)$_2$), 25.0 (CH(*C*H$_3$)$_2$), 24.9 (CH(*C*H$_3$)$_2$), 24.2 (CH(*C*H$_3$)$_2$), 24.0 (CH(*C*H$_3$)$_2$), 9.8 (NC*C*H$_3$), 9.6 (NC*C*H$_3$). ^{119}Sn{^{1}H} NMR ([D$_8$]toluene, 149 MHz, −20 °C): δ 1163.4 (broad s). *Tin satellites were not observed in the ^{1}H NMR spectrum nor was any coupling observed in proton coupled ^{119}Sn NMR experiments. A ^{1}H/^{119}Sn HSQC experiment was attempted which did not show the expected cross peak.* Anal. Calcd. for $C_{60}H_{82}N_4Sn$: C 73.68, H 8.45, N 5.73. Found: C 72.62, H 8.25, N 5.22. M.p. 185 °C (decomp.)

Synthesis of (^{Me}IPrCH)$_2$Pb: (5). A solution of (^{Me}IPrCH)Li (0.067 g, 0.18 mmol) in 4 mL of Et$_2$O was added to a slurry of PbBr$_2$ (0.033 g, 0.090 mmol) in 1 mL of Et$_2$O. After stirring for 1 minute, the resulting mixture had turned a deep blue. After stirring for an additional 20 minutes, the volatiles were removed *in vacuo*, the residue extracted with 4 mL of hexanes and filtered. The filtrate was concentrated to 2 mL and placed in a −30 °C freezer for one week. A few crystals were removed for X-ray crystallographic analysis.

The mother liquor was decanted from the bulk crystals and the crystals were dried *in vacuo* affording (^{Me}IPrCH)$_2$Pb: (**5**) as a deep blue crystalline solid (0.047 g, 49 %). ^{1}H NMR (C_6D_6, 700 MHz): δ 7.35 (t, 2H, $^3J_{HH}$ = 8.0 Hz, *p*-Ar*H*), 7.24 (s, C*H*Pb), 7.20 (t, 2H, $^3J_{HH}$ = 8.0 Hz, *p*-Ar*H*), 7.17 (d, 4H, $^3J_{HH}$ = 8.0 Hz, *m*-Ar*H*), 7.14 (d, 4H, $^3J_{HH}$ = 8.0 Hz), 3.24 (sept, 4H, $^3J_{HH}$ = 7.0 Hz, C*H*(CH$_3$)$_2$), 3.08 (sept, 4H, $^3J_{HH}$ = 7.0 Hz, C*H*(CH$_3$)$_2$), 1.61 (s, 12H, NC-C*H*$_3$), 1.27 (d, 12H, $^3J_{HH}$ = 7.0 Hz, CH(C*H*$_3$)$_2$), 1.22 (d, 12H, $^3J_{HH}$ = 7.0 Hz, CH(C*H*$_3$)$_2$), 1.16 (d, 12H, $^3J_{HH}$ = 7.0 Hz, CH(C*H*$_3$)$_2$), 1.15 (d, 12H, $^3J_{HH}$ = 7.0 Hz, CH(C*H*$_3$)$_2$). ^{13}C{^{1}H} NMR (C_6D_6, 176 MHz): δ 160.3 (N*C*N), 149.3 (Ar*C*), 148.4 (Ar*C*), 135.0 (Ar*C*), 133.7 (Ar*C*), 129.4 (Ar*C*), 128.8 (Ar*C*), 126.6 (Ar*C*), 125.5 (Ar*C*), 124.1 (Ar*C*), 116.9 (N*C*CH$_3$), 116.7 (N*C*CH$_3$), 49.8 (C=*C*H), 28.8 (*C*H(CH$_3$)$_2$), 28.7 (*C*H(CH$_3$)$_2$), 25.0 (CH(*C*H$_3$)$_2$), 24.9 (CH(*C*H$_3$)$_2$), 24.1 (CH(*C*H$_3$)$_2$), 24.0 (CH(*C*H$_3$)$_2$), 9.9 (NC*C*H$_3$), 9.7 (NC*C*H$_3$). *A ^{207}Pb{^{1}H} NMR signal was located between 1000–10000 ppm*. M.p. 85 °C (decomp.)

Synthesis of ^{Me}IPr•SiBr$_2$ (7). To a vial containing solution of ^{Me}IPr (0.147 g, 0.353 mmol) in 5 mL of THF was added a solution of [K(THF)$_2$][Si(SiMe$_3$)$_3$] (0.152 g, 0.353 mmol) in 3 mL of THF followed by the rapid addition of SiBr$_4$ (44.0 µL, 0.353 mmol). Upon the addition of SiBr$_4$, the formation of a colorless precipitate was observed. The reaction mixture was stirred for 1 hour and filtered through diatomaceous Earth affording an orange filtrate. The volatiles were removed *in vacuo* and the resultant residue washed with 2×2 mL cold (−30 °C) hexanes affording **7** as an orange powder (0.131 g, 61 %). While **7** has been previously reported and characterized,[20] several of the reported NMR resonances were not assigned correctly. ^{1}H NMR (C_6D_6, 499.8 MHz): δ 7.24 (t, $^3J_{HH}$ = 7.5 Hz, 2H, *p*-Ar*H*), 7.09 (d, $^3J_{HH}$ = 7.5 Hz, 4H, *m*-Ar*H*), 2.72 (sept, $^3J_{HH}$ = 7.0 Hz, 4H, C*H*(CH$_3$)$_2$),

1.50 (d, $^{3}J_{HH}$ = 7.0 Hz, 12H, CH(CH_3)$_2$), 1.40 (s, 6H, NC(CH)$_3$), 0.96 (d, $^{3}J_{HH}$ = 7.0 Hz, 12 H, CH(CH_3)$_2$). ^{13}C{^{1}H} NMR (C_6D_6, 125.7 MHz): δ 162.5 (N*C*N), 146.1 (Ar*C*), 131.7 (Ar*C*), 131.1 (Ar*C*), 128.6 (N*C*(CH$_3$)), 124.9 (Ar*C*), 29.1 (*C*H(CH$_3$)$_2$), 24.6 (CH(*C*H$_3$)$_2$), 24.3 CH(*C*H$_3$)$_2$), 9.3 (NC(*C*H$_3$)).

Synthesis of (^{Me}IPrCH)$_2$Si: (8). A solution of (^{Me}IPrCH)Li (0.119 g, 0.264 mmol) in 4 mL of toluene was added to a vial containing a slurry of ^{Me}IPr•SiBr$_2$ (0.080 g, 0.13 mmol) in 1 mL of toluene. Upon addition, the reaction mixture turned a dark yellow/brown. After stirring for 15 minutes, the volatiles of the mixture were removed *in vacuo*, the residue was extracted with 5 mL of hexanes and filtered. The dark yellow/brown filtrate was concentrated to a volume of 2 mL and placed in a −30 °C freezer overnight. A few crystals were removed for X-ray crystallographic analysis. The mother liquor was decanted from the bulk crystals and the crystals dried *in vacuo* affording (^{Me}IPrCH)$_2$Si: (**8**) as a dark yellow crystalline solid (0.088 g, 75 %). ^{1}H NMR (C_6D_6, 700 MHz): δ 7.30 (t, 2H, $^{3}J_{HH}$ = 8.0 Hz, *p*-Ar*H*), 7.25 (t, 2H, $^{3}J_{HH}$ = 8.0 Hz, *p*-Ar*H*), 7.13-7.09 (m, 8H, *m*-Ar*H*), 4.25 (s, 2H, C*H*Si), 3.11 (sept, 4H, $^{3}J_{HH}$ = 7.0 Hz, C*H*(CH$_3$)$_2$), 2.96 (sept, 4H, $^{3}J_{HH}$ = 7.0 Hz, C*H*(CH$_3$)$_2$), 1.62 (s, 6H, NC-CH_3), 1.54 (s, 6H, NC-CH_3), 1.32 (d, 12H, $^{3}J_{HH}$ = 7.0 Hz, CH(CH_3)$_2$), 1.23 (d, 12H, $^{3}J_{HH}$ = 7.0 Hz, CH(CH_3)$_2$), 1.17 (d, 12H, $^{3}J_{HH}$ = 7.0 Hz, CH(CH_3)$_2$), 1.14 (d, 12H, $^{3}J_{HH}$ = 7.0 Hz, CH(CH_3)$_2$). ^{13}C{^{1}H} NMR (C_6D_6, 176 MHz): δ 158.1 (N*C*N), 148.8 (Ar*C*), 147.7 (Ar*C*), 134.9 (Ar*C*), 132.9 (Ar*C*), 129.2 (Ar*C*), 128.9 (Ar*C*), 124.8 (Ar*C*), 123.9 (Ar*C*), 118.3 (N*C*CH$_3$), 116.9 (N*C*CH$_3$), 100.0 (C=*C*H), 28.9 (*C*H(CH$_3$)$_2$), 28.8 (*C*H(CH$_3$)$_2$), 24.5 (CH(*C*H$_3$)$_2$), 23.8 (CH(*C*H$_3$)$_2$), 9.8 (NC*C*H$_3$), 9.3 (NC*C*H$_3$). ^{29}Si{^{1}H} NMR (C_6D_6, 79.4 MHz): δ 272.0 (s). Anal. Calcd. for $C_{60}H_{82}N_4Si$: C 81.21, H 9.31, N 6.31. Found: C 80.20, H 9.77, N 5.69. M.p. 155–157 °C (decomp.)

7.5. Crystallographic Data

Table 7.2. Crystallographic data for compounds **1**, **2** and **4**.

Compound	**1**	**2**•C_6H_{14}	**4**•C_6H_{14}
formula	$C_{30}H_{41}IN_2$	$C_{66}H_{96}Li_2N_4$	$C_{66}H_{96}N_4Sn$
formula weight	556.55	959.34	1064.15
crystal system	triclinic	monoclinic	monoclinic
space group	$P\overline{1}$	$P2_1/n$	$I2/m$
a [Å]	9.0297(18)	12.287(4)	12.0876(3)
b [Å]	9.5889(19)	20.074(7)	20.5096(6)
c [Å]	18.373(4)	12.726(4)	12.7329(3)
α [°]	84.60(3)	90	90
β [°]	86.53(3)	103.325(4)	99.9583(9)
γ [°]	64.76(3)	90	90
V [Å^3]	1432.2(6)	3054.4(18)	3109.08(14)
Z	2	2	2
ρ_{calcd} [g/cm^3]	1.291	1.043	1.137
μ [mm^{-1}]	8.905	0.059	3.557
T [°C]	−100	−80	−100
$2\theta_{max}$ [°]	149.66	50.00	145.03
total data collected	5579	20795	10892
unique data (R_{int})	5579 (0.0537)	5378 (0.0511)	3166 (0.0182)
obs data [$I \geq 2\sigma(I)$]	5406	3431	3165
params	309	331	174
R_1 [$I \geq 2\sigma(I)$][a]	0.0420	0.0537	0.0477
wR_2 [all data][a]	0.1168	0.1671	0.1122
max/min $\Delta\rho$ [e/Å^3]	2.764/−0.705	0.349/−0.221	0.227/−0.828

[a] $R_1 = \sum||F_o| - |F_c||/\sum|F_o|$; $wR_2 = [\sum w(F_o^2 - F_c^2)^2/\sum w(F_o^4)]^{1/2}$

Table 7.3. Crystallographic data for compounds **5**, **6** and **8**.

Compound	**5**•C_6H_{14}	**6**	**8**•C_6H_{14}
formula	$C_{66}H_{96}N_4Pb$	$C_{60}H_{82}N_4Sn$	$C_{66}H_{96}N_4Si$
formula weight	1151.64	977.98	973.55
crystal system	monoclinic	monoclinic	monoclinic
space group	*I*2/*m*	$P2_1/n$	*I*2/*m*
a [Å]	12.0808(3)	10.683(2)	12.1119(2)
b [Å]	20.5866(5)	36.042(7)	20.0684(3)
c [Å]	12.7242(3)	14.412(3)	12.7422(2)
α [°]	90	90	90
β [°]	99.9820(10)	90.658(3)	99.7980(9)
γ [°]	90	90	90
V [Å^3]	3116.64(13)	5548.6(19)	3052.02(8)
Z	2	4	2
ρ_{calcd} [g/cm^3]	1.228	1.171	1.059
μ [mm^{-1}]	5.550	0.500	0.633
T [°C]	−100	−80	−100
$2\theta_{max}$ [°]	147.89	50.50	148.30
total data collected	68854	38142	10850
unique data (R_{int})	3216 (0.0257)	10052 (0.1240)	3086 (0.0267)
obs data [$I \geq 2\sigma(I)$]	3216	5180	2771
params	175	620	179
R_1 [$I \geq 2\sigma(I)$][a]	0.0446	0.0603	0.0413
wR_2 [all data][a]	0.1162	0.1847	0.1142
max/min $\Delta\rho$ [e/Å^3]	1.016/−2.162	0.999/−0.745	0.241/−0.275

[a] $R_1 = \sum||F_o| - |F_c||/\sum|F_o|$; $wR_2 = [\sum w(F_o^2 - F_c^2)^2/\sum w(F_o^4)]^{1/2}$

7.6. References

1. a) Davidson, P. J.; Lappert, M. F. *J. Chem. Soc., Chem. Commun.* **1973**, 317; (b) Goldberg, D. E.; Harris, D. H.; Lappert, M. F.; Thomas, K. M. *J. Chem. Soc., Chem. Commun.* **1976**, 261; (c) Hitchcock, P. B.; Lappert, M. F.; Miles, S. J.; Thorne, A. J. *J. Chem. Soc., Chem. Commun.* **1984**, 480; (d) Goldberg, D. E.; Hitchcock, P. B.; Lappert, M. F.; Thomas, K. M. *J. Chem. Soc., Chem. Commun.* **1986**, 2387.
2. For selected recent reviews and articles, see: (a) Fischer, R. C.; Power, P. P. *Chem. Rev.* **2010**, *110*, 3877; (b) Wang, Y.; Robinson, G. H. *Inorg. Chem.* **2011**, *50*, 12326; (c) Ghadwal, R. S.; Azhakar, R.; Roesky, H. W. *Acc. Chem. Res.* **2013**, *46*, 444; (d) Brand, J.; Braunschweig, H.; Sen, S. S. *Acc. Chem. Res.* **2014**, *47*, 180; (e) Präsang, C.; Scheschkewitz, D. *Chem. Soc. Rev.* **2016**, *45*, 900; (f) Ochiai, T.; Franz, D.; Inoue, S. *Chem. Soc. Rev.* **2016**, *45*, 6327; (g) Melaimi, M.; Jazzar, R.; Soleilhavoup, M.; Bertrand, G. *Angew. Chem. Int. Ed.* **2017**, *56*, 10046; (h) Schneider, J.; Sindlinger, C. P.; Eichele, K.; Schubert, H.; Wesemann, L. *J. Am. Chem. Soc.* **2017**, *139*, 6542; (i) Légaré, M.-A.; Bélanger-Chabot, G.; Dewhurst, R. D.; Welz, E.; Krummenacher, I.; Engels, B.; Braunschweig, H. *Science* **2018**, *359*, 896; (j) Nesterov, V.; Reiter, D.; Bag, P.; Frisch, P.; Holzner, R.; Porzelt, A.; Inoue, S. *Chem. Rev.* **2018**, *118*, 9678; (k) Légaré, M.-A.; Rang, M.; Bélanger-Chabot, G.; Schweizer, J. I.; Krummenacher, I.; Bertermann, R.; Arrowsmith, M.; Holthausen, M. C.; Braunschweig, H. *Science* **2019**, *363*, 1329.
3. Jutzi, P.; Holtmann, U.; Kanne, D.; Krüger, C.; Blom, R.; Gleiter, R.; Hyla-Kryspin, I. *Chem. Ber.* **1989**, *122*, 1629.
4. Kira, M.; Ishida, S.; Iwamoto, T.; Kabuto, C. *J. Am. Chem. Soc.* **1999**, *121*, 9722.

5. (a) Tokitoh, N.; Manmaru, K.; Okazaki, R. *Organometallics* **1994**, *13*, 167; (b) Tokitoh, N.; Saito, M.; Okazaki, R. *J. Am. Chem. Soc.* **1993**, *115*, 2065; (c) Brooker, S.; Buijink, J.-K.; Edelmann, F. T. *Organometallics* **1991**, *10*, 25.
6. (a) Miller, K. A.; Watson, T. W.; Bender, J. E.; Banaszak Holl, M. M.; Kampf, J. W. *J. Am. Chem. Soc.* **2001**, *123*, 982; (b) Peng, Y.; Ellis, B. D.; Wang, X.; Power, P. P. *J. Am. Chem. Soc.* **2008**, *130*, 12268; (c) Peng, Y.; Guo, J.-D.; Ellis, B. D.; Zhu, Z.; Fettinger, J. C.; Nagase, S.; Power, P. P. *J. Am. Chem. Soc.* **2009**, *131*, 16272; (d) Mandal, S. K.; Roesky, H. W. *Acc. Chem. Res.* **2011**, *45*, 298; (e) Inomata, K.; Watanabe, T.; Miyazaki, Y.; Tobita, H. *J. Am. Chem. Soc.* **2015**, *137*, 11935; (f) Protchenko, A. V.; Bates, J. I.; Saleh, L. M. A.; Blake, M. P.; Schwarz, A. D.; Kolychev, E. L.; Thompson, A. L.; Jones, C.; Mountford, P.; Aldridge, S. *J. Am. Chem. Soc.* **2016**, *138*, 4555; (g) Roy, M. M. D.; Fujimori, S.; Ferguson, M. J.; McDonald, R.; Tokitoh, N.; Rivard, E. *Chem. Eur. J.* **2018**, *24*, 14392; (h) Hadlington, T. J.; Driess, M.; Jones, C. *Chem. Soc. Rev.* **2018**, *47*, 4176.
7. A homologous tetrelene series was recently reported using bulky alkoxide ligands: Loh, Y. K.; Ying, L.; Fuentes, M.-A.; Huan Do, D. C.; Aldridge, S. *Angew. Chem. Int. Ed.* **2019**, *58*, 4847.
8. Such as: Denk, M.; Lennon, R.; Hayashi, R.; West, R.; Belyakov, A. V.; Verne, H. P.; Haaland, A.; Wagner, M.; Metzler, N. *J. Am. Chem. Soc.* **1994**, *116*, 2691.
9. Such as: Karsch, H. H.; Keller, U.; Gamper, S.; Müller, G. *Angew. Chem. Int. Ed. Engl.* **1990**, *29*, 295.
10. Two-coordinate acyclic silylenes stabilized by heteroatom donors are known: (a) Rekken, B. D.; Brown, T. M.; Fettinger, J. C.; Tuononen, H. M.; Power, P. P. *J. Am.*

Chem. Soc. **2012**, *134*, 6504; (b) Protchenko, A. V.; Birjkumar, K. H.; Dange, D.; Schwarz, A. D.; Vidovic, D.; Jones, C.; Kaltsoyannis, N.; Mountford, P.; Aldridge, S. *J. Am. Chem. Soc.* **2012**, *134*, 6500; (c) Hadlington, T. J.; Abdalla, J. A. B.; Tirfoin, R.; Aldridge, S.; Jones, C. *Chem. Commun.* **2016**, *52*, 1717.

11. For reviews on NHO ligands, see: (a) Ghadwal, R. S. *Dalton Trans.* **2016**, ***45***, 16081; (b) Crocker, R. D.; Nguyen, T. V. *Chem. Eur. J.* **2016**, *22*, 2208; (*c*) Roy, M. M. D.; Rivard, E. *Acc. Chem. Res.* **2017**, *50*, 2017.
12. For example: (a) Al-Rafia, S. M. I.; Ferguson, M. J.; Rivard, E. *Inorg. Chem.* **2011**, *50*, 10543; (b) Ghadwal, R. S.; Reichmann, S. O.; Engelhardt, F.; Andrada, D. M.; Frenking, G. *Chem. Commun.* **2013**, *49*, 9440; (c) Wünsche, M. A.; Witteler, T.; Dielmann, F. *Angew. Chem. Int. Ed.* **2018**, *57*, 7234.
13. Hering-Junghans, C.; Andreiuk, P.; Ferguson, M. J.; McDonald, R.; Rivard, E. *Angew. Chem. Int. Ed.* **2017**, *56*, 6272.
14. Gentner, T. X.; Ballmann, G.; Pahl, J.; Elsen, H.; Harder, S. *Organometallics* **2018**, *37*, 4473.
15. Kuhn, N.; Bohnen, H.; Henkel, G.; Kreutzberg, J. *Z. Naturforsch.* **1996**, *51b*, 1267.
16. Braga, D.; Grepioni, F.; Biradha, K.; Desiraju, G. R. *J. Chem. Soc., Dalton Trans.* **1996**, 3925.
17. Powers, K.; Hering-Junghans, C.; McDonald, R.; Ferguson, M. J.; Rivard, E. *Polyhedron* **2016**, *108*, 8.
18. Ghadwal, R. S.; Roesky, H. W.; Merkel, S.; Henn, J.; Stalke, D. *Angew. Chem. Int. Ed.* **2009**, *48*, 5683.

19. Filippou, A. C.; Chernov, O.; Schnackenburg, G. *Angew. Chem. Int. Ed.* **2009**, *48*, 5687.

20. Schweizer, J. I.; Sturm, A. G.; Porsch, T.; Berger, M.; Bolte, M.; Auner, N.; Holthausen, M. C. *Z. Anorg. Allg. Chem.* **2018**, *644*, 982.

21. (a) Protchenko, A. V.; Schwarz, A. D.; Blake, M. P.; Jones, C.; Kaltsoyannis, N.; Mountford, P.; Aldridge, S. *Angew. Chem. Int. Ed.*,**2013**, *52*, 568; (b) Wendel, D.; Porzelt, A.; Herz, F. A. D.; Sakar, D.; Jandl, C.; Inoue, S.; Rieger, B. *J. Am. Chem. Soc.* **2017**, *139*, 8134; (c) Roy, M. M. D.; Ferguson, M. J.; McDonald, R.; Zhou, Y.; Rivard, E. *Chem. Sci.* **2019**, *10*, 6476.

22. Wendel, D.; Reiter, D.; Porzelt, A.; Altmann, P. J.; Inoue, S.; Rieger, B. *J. Am. Chem. Soc.* **2017**, *139*, 17193.

23. A three-coordinate germanone has also been previously reported: Li, L.; Fukawa, T.; Matsuo, T.; Hashizume, D.; Fueno, H.; Tanaka, K.; Tamao, K. *Nat. Chem.* **2012**, *4*, 361.

24. Pangborn, A. B.; Giardello, M. A.; Grubbs, R. H.; Rosen, R. K.; Timmers, F. J. *Organometallics* **1996**, *15*, 1518.

25. Ryan, S. J.; Schimler, S. D.; Bland, D. C.; Sanford, M. S. *Org. Lett.* **2015**, *17*, 1866.

26. Hupf, E.; Kaiser, F.; Lummis, P. A.; Roy, M. M. D.; McDonald, R.; Ferguson, M. J.; Kühn, F. E.; Rivard, E. *unpublished results (manuscript submitted)*.

27. Marschner, C. *Eur. J. Inorg. Chem.* **1998**, 221.

28. Hope, H. *Prog. Inorg. Chem.* **1994**, *41*, 1.

29. Sheldrick, G. M. *Acta. Crystallogr. Sect. A* **2015**, *71*, 3.

30. Sheldrick, G. M. *Acta. Crystallogr. Sect. C* **2015**, *71*, 3.

31. Gaussian 16, Revision B.01, Frisch, M. J.; Trucks, G. W.; Schlegel, H. B.; Scuseria, G. E.; Robb, M. A.; Cheeseman, J. R.; Scalmani, G.; Barone, V.; Petersson, G. A.; Nakatsuji, H.; Li, X.; Caricato, M.; Marenich, A. V.; Bloino, J.; Janesko, B. G.; Gomperts, R.; Mennucci, B.; Hratchian, H. P.; Ortiz, J. V.; Izmaylov, A. F.; Sonnenberg, J. L.; Williams-Young, D.; Ding, F.; Lipparini, F.; Egidi, F.; Goings, J.; Peng, B.; Petrone, A.; Henderson, T.; Ranasinghe, D.; Zakrzewski, V. G.; Gao, J.; Rega, N.; Zheng, G.; Liang, W.; Hada, M.; Ehara, M.; Toyota, K.; Fukuda, R.; Hasegawa, J.; Ishida, M.; Nakajima, T.; Honda, Y.; Kitao, O.; Nakai, H.; Vreven, T.; Throssell, K.; Montgomery Jr., J. A.; Peralta, J. E.; Ogliaro, F.; Bearpark, M. J.; Heyd, J. J.; Brothers, E. N.; Kudin, K. N.; Staroverov, V. N.; Keith, T. A.; Kobayashi, R.; Normand, J.; Raghavachari, K.; Rendell, A. P.; Burant, J. C.; Iyengar, S. S.; Tomasi, J.; Cossi, M.; Millam, J. M.; Klene, M.; Adamo, C.; Cammi, R.; Ochterski, J. W.; Martin, R. L.; Morokuma, K.; Farkas, O.; Foresman, J. B.; Fox, D. J. Gaussian, Inc., Wallingford CT, **2016**.

32. (a) Lee, C.; Yang, W.; Parr, R. G. *Phys. Rev. B* **1988**, *37*, 785; (b) Becke, A. D. *Phys. Rev. A* **1988**, *38*, 3098; (c) Stephens, P. J.; Devlin, F. J.; Chabalowski, C. F.; Frisch, M. J. J. *Phys. Chem.* **1994**, *98*, 11623.

33. (a) Dunning Jr., T. H.; *J. Chem. Phys.* **1989**, *90*, 1007; (b) Woon, D. E.; Dunning Jr., T. H. *J. Chem. Phys.* **1993**, *98*, 1358.

Chapter 8: Summary and Future Directions

Chapter 2 described the attempted synthesis of *N*-heterocyclic carbene (NHC)-stabilized cadmium and mercury hydrides. Unlike their lighter congener zinc which forms stable NHC-zinc hydride adducts, the Cd and Hg hydride complexes were found to be unstable. However, several cadmium and mercury triflate precursors were synthesized, and the cadmium bis-triflate adduct dimer $[IPr•Cd(OTf)_2]_2$ (IPr = [(HCNDipp)$_2$C:]; Dipp = 2,6-*i*Pr$_2$C$_6$H$_3$) was found to be an active hydrosilylation/borylation precatalyst (presumably via an *in situ* generated Cd–H species) whereas the zinc triflate analogue was unreactive. The lack of catalytic activity of the zinc triflate was reasoned to be due to the presence of strong Zn–O bonds which inhibit the formation of zinc hydride linkages during catalysis (which are known to promote carbonyl reduction). Future zinc precatalysts may involve alkylated zinc adducts (such as $IPr•ZnMe_2$) which should generate reactive zinc hydrides in the presence of excess silane or borane.

The work presented in Chapter 3 outlined the unsuccessful attempts to trap the $[Cl_2P=N]$ unit through a donor/acceptor approach. The formation of the target $IPr•PCl_2N•LA$ (LA = Lewis acid) is limited by preferential halide/azide abstraction from $IPr•PCl_2N_3$ in the presence of strong Lewis acids rather than P^{III} oxidation (via N_2 loss). An alternative source of the $[Cl_2P=N]$ unit may be the previously reported anthracenylamide-substituted phosphine, $Cl_2P–N(C_{14}H_{10})$.[1] As shown in Scheme 8.1, $Cl_2P–N(C_{14}H_{10})$ may deliver a $[Cl_2P=N]$ unit to a $[Cl_2PN]_3$ ring, thus forming the 8-membered dichlorophosphazene oligomer driven by the release of anthracene. This

controlled, step-wise ring expansion may serve to model the formation of polydichlorophosphazene $[Cl_2PN]_n$ from hexachlorophosphazene.

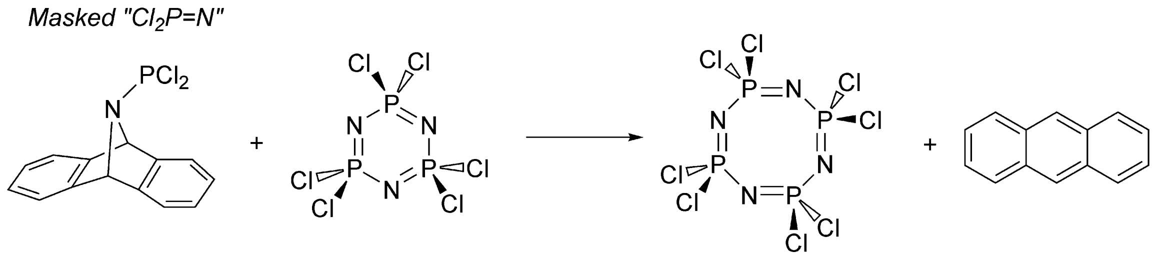

Scheme 8.1. Proposed $[Cl_2P{=}N]$ delivery using $Cl_2P–N(C_{14}H_{10})$.

The preparation of an extremely bulky *N*-heterocyclic carbene ligand ITr [ITr = $(HCNCPh_3)_2C$:] was described in Chapter 4. It was demonstrated that this ligand is most suitable for the isolation of low-coordinate inorganic cations such as $[Ag]^+$, $[:Tl]^+$ and $[:GeCl]^+$. While tetrelene monocations $[:ER]^+$ are now known,[2] tetrelene dications are far more rare. In 2008, Baines and coworkers reported the first example of a germanium(II) cation supported by a cryptand ligand.[3] Despite the high degree of positive charge, the known reactivity of this species is limited likely due to the absence of vacant coordination sites. Thus, an ITr-supported germanium dication $[ITr–Ge]^{2+}$ may be a stable species while maintaining a high degree of reactivity. This compound is expected to be a strong Lewis acid (which may lend itself to Lewis acid catalysis for example). Additionally, the presence of a lone pair of electrons may allow for ambiphilic reactivity, in contrast with typical strong Lewis acids such as $B(C_6F_5)_3$. This compound could possibly be prepared by halide abstraction from $[(ITr)GeCl]^+$ which itself was reported in Chapter 4 (Scheme 8.2).

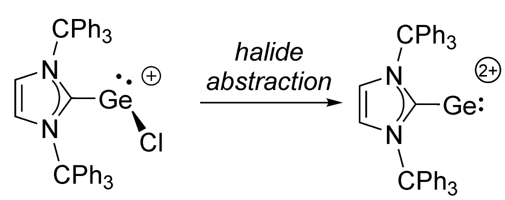

Scheme 8.2. Proposed synthesis of the monocoordinate germylene dication $[(ITr)Ge]^{2+}$.

In Chapter 5, an array of new germanium(II) compounds ligated by the trimethylsiloxy ligand –$OSiMe_3$ were reported. Most interestingly, the siloxygermylene cation $[IPr•Ge(OSiMe_3)]^+$ was found to oxidatively add a C–Cl bond of the CH_2Cl_2 solvent as well as promote the catalytic reduction of carbonyls. While the latter process may involve a germanium hydride active catalyst such as $[IPr•GeH]^+$, attempts to isolate such a species were unsuccessful. The stabilizing influence of –$OSiR_3$ ligands may also prove to be useful in low-valent main group molecules free from coordinated Lewis bases (such as NHCs) provided that –R is sufficiently bulky. For example, the commercially available chloro-tris(trimethylsilyl)silane $ClSi(SiMe_3)_3$ could possibly be converted to a siloxy ligand precursor $Li[OSi(SiMe_3)_3]$ and used to stabilize low-coordinate main group environments such as a bis(siloxy)silylene (Scheme 8.3).

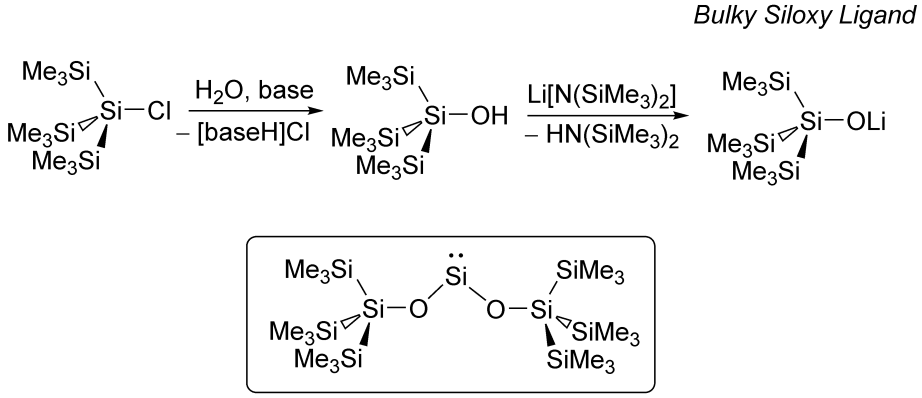

Scheme 8.3. Proposed synthesis of a bulky siloxy ligand and a bis(siloxy)silylene, $:Si\{OSi(SiMe_3)_3\}_2$.

The two-coordinate acyclic silylene $(^{Me}IPrCH)Si\{Si(SiMe_3)_3\}$ was reported in Chapter 6 and shown to undergo the oxidative addition of a variety of small molecules. While the initial goal of this project was to synthesize the divinylsilylene $(^{Me}IPrCH)_2Si:$, the installation of a second equivalent of vinyl ligand onto silicon proved to be difficult at

this point. This challenge was overcome in Chapter 7 with the synthesis of a lithiated source of the bulky vinyl ligand, (^{Me}IPrCH)Li. Using this precursor, the initially desired divinylsilylene and the complete heavy Group 14 divinyl tetrelene series (^{Me}IPrCH)$_2$E: (E = Si–Pb) were synthesized. A natural extension of this work would be to oxidize the divinyltetrelenes to their corresponding oxo-complexes. Such species represent heavy ketone analogues which have been a highly sought-after target in synthetic main group chemistry. While a diarylgermanone was reported in 2012,[4] an RR′Si=O fragment in 2017 using bulky imino and silyl groups,[5] and a cyclic dialkylsilanone reported this year,[6] the target (^{Me}IPrCH)$_2$Si=O would represent the first true silanone (acyclic, 3-coordinate, carbon ligands). Using the unique tetrelene series reported in Chapter 7, a complete series of heavy ketone analogues (^{Me}IPrCH)$_2$E=O (E = Si–Pb) may be accessible via N_2O oxidation and their relative bonding properties investigated (Scheme 8.4).

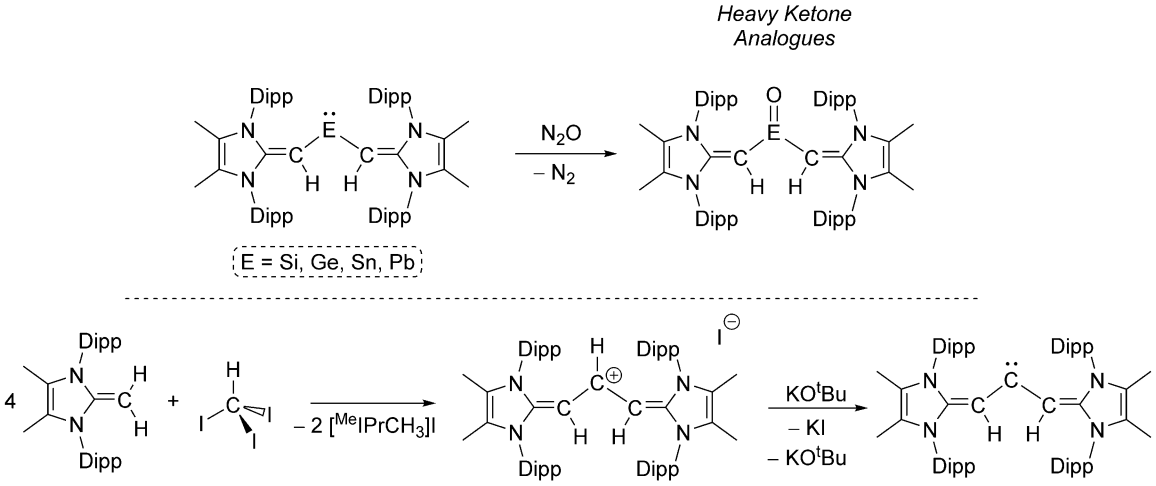

Scheme 8.4. Proposed heavy divinyl ketone synthesis (top) and proposed divinylcarbene synthesis (bottom).

Additionally, the divinyltetrelene series may be expanded to include carbon. As illustrated in Scheme 8.4, the combination of iodoform with 4 equivalents of ^{Me}IPr=CH$_2$ may give a divinyl carbenium which could be deprotonated to the divinylcarbene using a

strong base (such as KO^{t}Bu). Both the carbenium intermediate and the final target carbene are expected to be stabilized by the strong π-donation offered by the flanking [^{Me}IPr=CH]$^-$ fragments. This was shown to be a strong stabilizing influence in the case of the isolated silylenes described in Chapters 6 and 7.

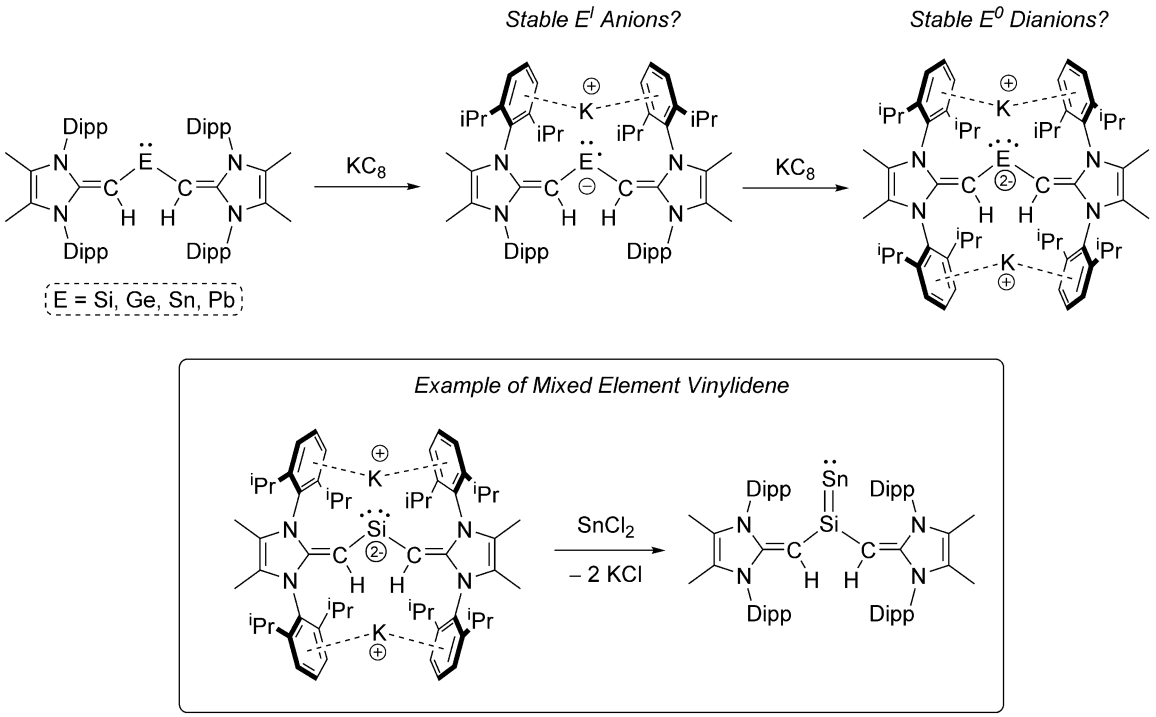

Scheme 8.5. Proposed synthesis of E^I radical anions and E^0 dianions by the reduction of divinyltetrelenes (top) and proposed synthesis of a heavy mixed-element vinylidene (bottom).

Finally, in addition to serving as precursors to heavy ketones, the divinyltetrelenes may also be reduced using a strong reducing agent (such as KC_8). A single-electron reduction would afford E^I radical anions. The molecular structures of the divinyl tetrelenes (established in Chapter 7) all exhibit flanking -Dipp groups (perpendicular to the C-E-C plane) which may effectively coordinate alkali metal atoms and enhance the stability of the target reduced species (Scheme 8.4). A two-electron reduction of the (^{Me}IPrCH)$_2$E: series

should afford E^0 dianions of the form $K_2[(^{Me}IPrCH)_2E]$. These may serve as precursors to heavy mixed-element vinylidenes, $(^{Me}IPrCH)_2E{=}E'$ (see Scheme 8.4 for an example).

The research presented in this thesis focused on the isolation of reactive, abundant elements spanning Groups 12, 13, 14 and 15 of the periodic table of elements. In order to facilitate their isolation, new stabilizing ligands (and ligand precursors) were designed. In several cases, Earth-abundant elements (such as silicon) were stabilized in low oxidation states and demonstrated to cleave strong organic bonds. Other newly reported molecules were shown to catalyze the reduction of carbonyl-containing molecules using mild hydride sources. Overall, this work illustrated that main group elements can indeed mimic the reactivity of transition metals. As the field of main group chemistry continues to progress, we draw ever closer to the use of main group elements as catalysts in chemical industry.

References

1. Velian, A.; Cummins, C. C. *J. Am. Chem. Soc.* **2012**, *134*, 13978.
2. Swamy, V. S. V. S. N.; Pal, S.; Khan, S.; Sen, S. S. *Dalton Trans.* **2015**, *44*, 12903.
3. Rupar, P. A.; Staroverov, V. N.; Baines, K. M. *Science* **2008**, *322*, 1360.
4. Li, L.; Fukawa, T.; Matsuo, T.; Hashizume, D.; Fueno, H.; Tanaka, K.; Tamao, K. *Nat. Chem.* **2012**, *4*, 361.
5. Wendel, D.; Reiter, D.; Porzelt, A.; Altmann, P. J.; Inoue, S.; Rieger, B. *J. Am. Chem. Soc.* **2017**, *139*, 17193.
6. Kobayashi, R.; Ishida, S.; Iwamoto, T. *Angew. Chem. Int. Ed.* **2019**, *58*, 9425.

Complete Bibliography

Chapter 1

1. (a) Kealy, T. J.; Pauson, P. J. *Nature* **1951**, *168*, 1039; (b) Wilkinson, G.; Rosenblum, M.; Whiting, M. C.; Woodward, R. B. *J. Am. Chem. Soc.* **1952**, *74*, 2125.
2. (a) Vaska, L.; DiLuzio, J. W. *J. Am. Chem. Soc.* **1961**, *83*, 2784; (b) Vaska, L.; DiLuzio, J. W. *J. Am. Chem. Soc.* **1962**, *84*, 679.
3. Osborne, J. A.; Jardine, F. H.; Young, J. F.; Wilkinson, G. *J. Chem. Soc. A* **1966**, 1711.
4. Cotton, F. A.; Wilkinson, G. *Advanced Inorganic Chemistry*, *Fourth Edition*; Wiley-Interscience, New York, 1980; pp 377.
5. Jutzi, P. *Angew. Chem. Int. Ed. Engl.* **1975**, *14*, 232.
6. West, R.; Fink, M. J. *Science* **1981**, *214*, 1343.
7. Yoshifuji, M.; Shima, I.; Inamoto, N. *J. Am. Chem. Soc.* **1981**, *103*, 4587.
8. Miller, R. D.; Michl, J. *Chem. Rev.* **1989**, *89*, 1359.
9. Drahnak, T. J.; Michl, J.; West, R. *J. Am. Chem. Soc.* **1979**, *101*, 5427.
10. Daly, J. J. *J. Chem. Soc.* **1964**, 6147.
11. (a) Davidson, P. J.; Lappert, M. F. *J. Chem. Soc., Chem. Commun.* **1973**, 317; (b) Goldberg, D. E.; Harris, D. H.; Lappert, M. F.; Thomas, K. M. *J. Chem. Soc., Chem. Commun.* **1976**, 261; (c) Hitchcock, P. B.; Lappert, M. F.; Miles, S. J.; Thorne, A. J. *J. Chem. Soc., Chem. Commun.* **1984**, 480; (d) Goldberg, D. E.; Hitchcock, P. B.; Lappert, M. F.; Thomas, K. M. *J. Chem. Soc., Chem. Commun.* **1986**, 2387.
12. Fink, M. J.; Michalczyk, M. J.; Haller, K. J.; West, R.; Michl, J. *J. Chem. Soc., Chem. Commun.* **1983**, 1010.

13. (a) Drago, R. S. *J. Phys. Chem.* **1958**, *62*, 353; (b) Schwerdtfeger, P.; Heath, G. A.; Dolg, M.; Bennett, M. A. *J. Am. Chem. Soc.* **1992**, *114*, 7518.

14. While the complete X-ray data for :Pb{CH(SiMe$_3$)$_2$}$_2$ has not been published, the structural features listed in Table 1.1 were published in reference 4c of the following manuscript: Stürmann, M.; Weidenbruch, M.; Klinkhammer, K. W.; Lissner, F.; Marsmann, H. *Organometallics* **1998**, *17*, 4425.

15. Sekiguchi, A.; Kinjo, R.; Ichinohe, M. *Science* **2004**, *305*, 1755.

16. Wedler, H. B.; Wendelboe, P.; Power, P. P. *Organometallics* **2018**, *37*, 2929.

17. Hardman, N. J.; Wright, R. J.; Phillips, A. D.; Power, P. P. *Angew. Chem. Int. Ed.* **2002**, *41*, 2842.

18. Wright, R. J.; Phillips, A. D.; Hardman, N. J.; Power, P. P. *J. Am. Chem. Soc.* **2002**, *124*, 8538.

19. Wright, R. J.; Phillips, A. D.; Hino, S.; Power, P. P. *J. Am. Chem. Soc.* **2005**, *127*, 4794.

20. Grigsby, W. J.; Power, P. P. *J. Am. Chem. Soc.* **1996**, *118*, 7981.

21. (a) Wright, R. J.; Phillips, A. D.; Power, P. P. *J. Am. Chem. Soc.* **2003**, *125*, 10784; (b) Agou, T.; Nagata, K.; Tokitoh, N. *Angew. Chem. Int. Ed.* **2013**, *52*, 10818.

22. Cowley, A. H.; Lasch, J. G.; Norman, N. C.; Pakulski, M. *J. Am. Chem. Soc.* **1983**, *105*, 5506.

23. Tokitoh, N.; Arai, Y.; Sasamori, T.; Okazaki, R.; Nagase, S.; Uekusa, H.; Oshashi, Y. *J. Am. Chem. Soc.* **1998**, *120*, 433.

24. Tokitoh, N.; Arai, Y.; Okazaki, R.; Nagase, S. *Science* **1997**, *277*, 78.

25. Mindiola, D. J.; Holland, P. J.; Warren, T. H. in: *Inorganic Syntheses, Volume 35*; John Wiley & Sons, Hoboken, NJ, 2010, pp 4–19.
26. Kays, D. L. *Chem. Soc. Rev.* **2016**, *45*, 1004.
27. Ochiai, T.; Franz, D.; Inoue, S. *Chem. Soc. Rev.* **2016**, *45*, 6327.
28. Niemeyer, M.; Power, P. P. *Inorg. Chem.* **1996**, *35*, 7264.
29. Segawa, Y.; Yamashita, M.; Nozaki, K. *Science* **2006**, *314*, 113.
30. For example, a bis(boryl)diphosphene has been reported: Asami, S.-S.; Okamoto, M.; Suzuki, K.; Yamashita, M. *Angew. Chem. Int. Ed.* **2016**, *55*, 12827.
31. Rekken, B. D.; Brown, T. M.; Fettinger, J. C.; Tuononen, H. M.; Power, P. P. *J. Am. Chem. Soc.* **2012**, *134*, 6504.
32. Protchenko, A. V.; Birjkumar, K. H.; Dange, D.; Schwarz, A. D.; Vidovic, D.; Jones, C.; Kaltsoyannis, N.; Mountford, P.; Aldridge, S. *J. Am. Chem. Soc.* **2012**, *134*, 6500.
33. Cui, C.; Roesky, H. W.; Schmidt, H.-G.; Noltemeyer, M.; Hao, H.; Cimpoesu, F. *Angew. Chem. Int. Ed.* **2000**, *39*, 4274.
34. Rit, A.; Campos, J.; Niu, H.; Aldridge, S. *Nat. Chem.* **2016**, *8*, 1022.
35. Wendel, D.; Reiter, D.; Porzelt, A.; Altmann, P. J.; Inoue, S.; Rieger, B. *J. Am. Chem. Soc.* **2017**, *139*, 17193.
36. Igau, A.; Grützmacher, H.; Baceiredo, A.; Bertrand, G. *J. Am. Chem. Soc.* **1988**, *110*, 6463.
37. Arduengo III, A. J.; Harlow, R. L.; Kline, M. *J. Am. Chem. Soc.* **1991**, *113*, 361.
38. (a) Nesterov, V.; Reiter, D.; Bag, P.; Frisch, P.; Holzner, R.; Porzelt, A; Inoue, S. *Chem. Rev.* **2018**, *118*, 9678. (b) Nolan, S. P. *N-Heterocyclic Carbenes: Effective Tools for Organometallic Synthesis*; Wiley-VCH, Weinheim, 2014.

39. Lavallo, V.; Canac, Y.; Präsang, C.; Donnadieu, B.; Bertrand, G. *Angew. Chem. Int. Ed.* **2005**, *44*, 5705.

40. (a) Kuhn, N.; Bohnen, H.; Kreutzberg, H.; Blässer, D.; Boese, R. *Chem. Commun.* **1993**, 1136; (b) Kuhn, N.; Bohnen, H.; Blässer, D.; Boese, R. *Chem. Ber.* **1994**, *127*, 1405.

41. Roy, M. M. D.; Rivard, E. *Acc. Chem. Res.* **2017**, *50*, 2017.

42. Wang, Y.; Quillian, B.; Wei, P.; Wannere, C. S.; Xie, Y.; King, R. B.; Schaefer III, H. F.; Schleyer, P. v. R.; Robinson, G. H. *J. Am. Chem. Soc.* **2007**, *129*, 12412.

43. Ghadwal, R. S.; Schürmann, C. J.; Engelhardt, F.; Steinmetzger, C. *Eur. J. Inorg. Chem.* **2014**, 4921.

44. Braunschweig, H.; Dewhurst, R. D.; Hammond, K.; Mies, J.; Radacki, K.; Vargas, A. *Science* **2012**, *336*, 1420.

45. Böhnke, J.; Braunschweig, H.; Ewing, W. C.; Hörl, C.; Kramer, T.; Krummenacher, I.; Mies, J.; Vargas, A. *Angew. Chem. Int. Ed.* **2014**, *53*, 9082.

46. Wang, Y.; Xie, Y.; Wei, P.; King, R. B.; Schaefer III, H. F.; Schleyer, P. v. R.; Robinson, G. H. *Science* **2008**, *321*, 1069.

47. (a) Sidiropoulos, A.; Jones, C.; Stasch, A.; Klein, S.; Frenking, G. *Angew. Chem. Int. Ed.* **2009**, *48*, 9701; (b) Jones, C.; Sidiropoulos, A.; Holzmann, N.; Frenking, G.; Stasch, A. *Chem. Commun.* **2012**, 9855.

48. Mondal, K. C.; Roy, S.; Dittrich, B.; Andrada, D. M.; Frenking, G.; Roesky, H. W. *Angew. Chem. Int. Ed.* **2016**, *55*, 3158.

49. (a) Mondal, K. C.; Roesky, H. W.; Schwarzer, M. C.; Frenking, G.; Niepötter, B.; Wolf, H.; Herbst-Irmer, R.; Stalke, D. *Angew. Chem. Int. Ed.* **2013**, *52*, 2963; (b) Li,

Y.; Mondal, K. C.; Roesky, H. W.; Zhu, H.; Stollberg, P.; Herbst-Irmer, R.; Stalke, D.; Andrada, D. M. *J. Am. Chem. Soc.* **2013**, *135*, 12422.

50. Wang, Y.; Xie, Y.; Wei, P.; King, B. R.; Schaefer III, H. F.; Schleyer, P. v. R.; Robinson, G. H. *J. Am. Chem. Soc.* **2008**, *130*, 14970.
51. Arrowsmith, M.; Braunschweig, H.; Celik, M. A.; Dellermann, T.; Dewhurst, R. D.; Ewing, W. C.; Hammond, K.; Kramer, T.; Krummenacher, I.; Mies, J.; Radacki, K.; Schuster, J. K. *Nat. Chem.* **2016**, *8*, 890.
52. Spikes, G. H.; Fettinger, J. C.; Power, P. P. *J. Am. Chem. Soc.* **2005**, *127*, 12232.
53. Chu, T.; Nikonov, G. I. *Chem. Rev.* **2018**, *118*, 3608.
54. Chu, T.; Korobkov, I.; Nikonov, G. I. *J. Am. Chem. Soc.* **2014**, *136*, 9195.
55. Arrowsmith, M.; Böhnke, J.; Braunschweig, H.; Celik, M. A.; Dellerman, T.; Hammond, K. *Chem. Eur. J.* **2016**, *22*, 17169.
56. Wendel, D.; Szilvási, T.; Jandl, C.; Inoue, S.; Rieger, B. *J. Am. Chem. Soc.* **2017**, *139*, 9156.
57. Yao, S.; Wüllen, C. v.; Sun, X.-Y.; Driess, M. *Angew. Chem. Int. Ed.* **2008**, *47*, 3250.
58. Summerscales, O. T.; Fettinger, J. C.; Power, P. P. *J. Am. Chem. Soc.* **2011**, *133*, 11960.
59. Hicks, J.; Vasko, P.; Goicoechea, J. M.; Aldridge, S. *Nature* **2018**, *557*, 92.
60. Junold, K.; Nutz, M.; Baus, J. A.; Burschka, C.; Guerra, C. F.; Bickelhapt, F. M.; Tacke, R. *Chem. Eur. J.* **2014**, *20*, 9319.
61. Crimmin, M. R.; Butler, M. J.; White, A. J. P. *Chem. Commun.* **2015**, *51*, 15994.
62. Chu, T.; Boyko, Y.; Korobkov, I.; Nikonov, G. I. *Organometallics* **2015**, *34*, 5363.
63. Bakewell, C.; White, A. J. P.; Crimmin, M. R. *Angew. Chem. Int. Ed.* **2018**, *57*, 6638.

64. Bakewell, C.; White, A. J. P.; Crimmin, M. R. *J. Am. Chem. Soc.* **2016**, *138*, 12763.

65. Jones, C. *Nat. Rev.* **2017**, *1*, 0059.

66. Légaré, M.-A.; Bélanger-Chabot, G.; Dewhurst, R. D.; Welz, E.; Krummenacher, I.; Engels, B.; Braunschweig, H. *Science* **2018**, *359*, 896.

67. Holland, P. L. *Dalton Trans.* **2010**, *39*, 5415.

68. Protchenko, A. V.; Bates, J. I.; Saleh, L. M. A.; Blake, M. P.; Schwarz, A. D.; Kolychev, E. L.; Thompson, A. L.; Jones, C.; Mountford, P.; Aldridge, S. *J. Am. Chem. Soc.* **2016**, *138*, 4555.

69. Lips, F.; Fettinger, J. C.; Mansikkamäki, A.; Tuonen, H. M.; Power, P. P. *J. Am. Chem. Soc.* **2014**, *136*, 634.

70. Hinz, A.; Schulz, A.; Villinger, A. *Angew. Chem. Int. Ed.* **2016**, *55*, 12214.

71. Welch, G. C.; San Juan, R. R.; Masuda, J. D.; Stephan, D. W. *Science* **2006**, *314*, 1124.

72. McCahill, J. S. J.; Welch, G. C.; Stephan, D. W. *Angew. Chem. Int. Ed.* **2007**, *46*, 4968.

73. Chase, P. A.; Welch, G. C.; Jurca, T.; Stephan, D. W. *Angew. Chem. Int. Ed.* **2007**, *46*, 8050.

74. Chase, P. A.; Jurca, T.; Stephan, D. W. *Chem. Commun.* **2008**, 1701.

75. Lam, J.; Szkop, K. M.; Mosaferi, E.; Stephan, D. W. *Chem. Soc. Rev.* **2019**, *48*, 3592.

76. Frank, H. G. *Industrial Aromatic Chemistry*; Springer, Berlin, 1988.

77. Parks, D. J.; Piers, W. E. *J. Am. Chem. Soc.* **1996**, *118*, 9440.

78. Parks, D. J.; Blackwell, J. M.; Piers, W. E. *J. Org. Chem.* **2000**, *65*, 3090.

79. Douvris, C.; Ozerov, O. V. *Science* **2008**, *321*, 1188.

80. (a) Gu, W.; Haneline, M. R.; Douvris, C.; Ozerov, O. V. *J. Am. Chem. Soc.* **2009**, *131*, 11203; (b) Caputo, C. B.; Hounjet, L. J.; Dobrovetsky, R.; Stephan, D. W. *Science* **2013**, *341*, 1374.

81. Mango, J.; Dunetz, J. R. *Org. Process Res. Dev.* **2012**, *16*, 1156.

82. Koren-Selfridge, L.; Londino, H. N.; Vellucci, J. K.; Simmons, B. J.; Casey, C. P.; Clark, T. B. *Organometallics* **2009**, *28*, 2085.

83. Chong, C. C.; Kinjo, R.; *ACS Catal.* **2015**, *5*, 3238.

84. Brown, H. C.; Schlesinger, H. I.; Burg, A. B. *J. Am. Chem. Soc.* **1939**, *61*, 673.

85. (a) Corey, E. J.; Bakshi, R. K.; Shibata, S. *J. Am. Chem. Soc.* **1987**, *109*, 5551; (b) Corey, E. J.; Shibata, S.; Bakshi, R. *J. Org. Chem.* **1988**, *53*, 2861.

86. Arrowsmith, M.; Hadlington, T. J.; Hill, M. S.; Kociok-Köhn, G. *Chem. Commun.* **2012**, *48*, 4567.

87. Rit, A.; Spaniol, T. P.; Maron, L.; Okuda, J. *Angew. Chem. Int. Ed.* **2013**, *52*, 4664.

88. Lummis, P. A.; Momeni, M. R.; Lui, M. W.; McDonald, R.; Ferguson, M. J.; Miskolzie, M.; Brown, A.; Rivard, E. *Angew. Chem. Int. Ed.* **2014**, *53*, 9347.

89. Rit, A.; Zanardi, A.; Spaniol, T. P.; Maron, L.; Okuda, J. *Angew. Chem. Int. Ed.* **2014**, *53*, 13273.

90. Hadlington, T. J.; Hermann, M.; Frenking, G.; Jones, C. *J. Am. Chem. Soc.* **2014**, *136*, 3028.

91. Chong, C. C.; Hirao, H.; Kinjo, R. *Angew. Chem. Int. Ed.* **2015**, *54*, 190.

92. Adams, M. R.; Tien, C.-H.; McDonald, R.; Speed, A. H. W. *Angew. Chem. Int. Ed.* **2017**, *56*, 16660.

Chapter 2

1. (a) Aldridge, S.; Downs, A. J. *Chem. Rev.* **2001**, *101*, 3305; (b) Ding, Y.; Hao, H.; Roesky, H. W.; Noltemeyer, M.; Schmidt, H.-G. *Organometallics* **2001**, *20*, 4806; (c) Mankad, N.P.; Laitar, D. S.; Sadighi, J. P. *Organometallics* **2004**, *23*, 3369; (d) Zhu, Z.; Brynda, M.; Wright, R. J.; Fischer, R. C.; Merrill, W. A.; Rivard, E.; Wolf, R.; Fettinger, J. C.; Olmstead, M. M.; Power, P. P. *J. Am. Chem. Soc.* **2007**, *129*, 10847; (e) Rivard, E. *Dalton Trans.* **2014**, *43*, 8577; (f) Marquardt, C.; Jurca, T.; Schwan, K.-C.; Stauber, A.; Virovets, A. V.; Whittell, G. R.; Manners, I.; Scheer, M. *Angew. Chem. Int. Ed.* **2015**, *54*, 13469; (g) Rivard, E. *Chem. Soc. Rev.* **2016**, *45*, 989; (h) Pagano, J. K.; Dorhout, J. M.; Czerwinski, K. R.; Morris, D. E.; Scott, B. L.; Waterman, R.; Kiplinger, J. L. *Organometallics* **2016**, *35*, 617, and references therein.
2. (a) Finholt, A. E.; Bond Jr., A. C.; Schlesinger, H. I. *J. Am. Chem. Soc.* **1947**, *69*, 1199; (b) Barbaras, G. D.; Dillard, C.; Finholt, A. E.; Wartik, T.; Wilzbach, K. E.; Schlesinger, H. I. *J. Am. Chem. Soc.* **1951**, *73*, 4585; (c) Shayesteh, A.; Yu, S.; Bernath, P. F. *Chem. Eur. J.* **2005**, *11*, 4709.
3. Rit, A.; Spaniol, T. P.; Maron, L.; Okuda, J. *Angew. Chem. Int. Ed.* **2013**, *52*, 4664.
4. Lummis, P. A.; Momeni, M. R.; Lui, M. W.; McDonald, R.; Ferguson, M. J.; Miskolzie, M.; Brown, A.; Rivard, E. *Angew. Chem. Int. Ed.* **2014**, *53*, 9347.
5. For selected examples of molecular cadmium and mercury hydrides, see: (a) Reger, D. L.; Mason, S. S.; Rheingold, A. L. *J. Am. Chem. Soc.* **1993**, *115*, 10406; (b) Dowling, C. M.; Parkin, G. *Polyhedron* **2001**, *20*, 285; (c) Nakamura, E.; Yu, Y.; Mori, S.; Yamago, S. *Angew. Chem. Int. Ed. Engl.* **1997**, *36*, 374.

6. For related studies and review articles, see: (a) Rit, A.; Zanardi, A.; Spaniol, T. P.; Maron, L.; Okuda, J. *Angew. Chem. Int. Ed.* **2014**, *53*, 13273; (b) Wiegand, A.-K.; Rit, A.; Okuda, J. *Coord. Chem. Rev.* **2016**, *314*, 71; (c) Revunova, K.; Nikonov, G. I. *Dalton Trans.* **2015**, *44*, 840; (d) Chong, C. C.; Kinjo, R. *ACS Catal.* **2015**, *5*, 3238; (e) Marinos, N. A.; Enthaler, S.; Driess, M. *ChemCatChem* **2010**, *2*, 846; (f) Mukherjee, D.; Ellern, A.; Sadow, A. D. *J. Am. Chem. Soc.* **2010**, *132*, 7582; (g) Bendt, G.; Schulz, S.; Spielmann, J.; Schmidt, S.; Bläser, D.; Wölper, C. *Eur. J. Inorg. Chem.* **2012**, 3725; (h) Jochmann, P.; Stephan, D. W. *Angew. Chem. Int. Ed.* **2013**, *52*, 9831; (i) Roberts, A. J.; Clegg, W.; Kennedy, A. R.; Probert, M. R.; Robertson, S. D.; Hevia, E. *Dalton Trans.* **2015**, *44*, 8169; (j) Sattler, W.; Ruccolo, S.; Chaijan, M. R.; Allah, T. N.; Parkin, G. *Organometallics* **2015**, *34*, 4717; (k) Bagherzadeh, S.; Mankad, N. P. *Chem. Commun.* **2016**, *52*, 3844; (l) Dawkins, M. J. C.; Middleton, E.; Kefalidis, C. E.; Dange, D.; Juckel, M. M.; Maron, L.; Jones, C. *Chem. Commun.* **2016**, *52*, 10490.

7. Al-Rafia, S. M. I.; Lummis, P. A.; Swarnakar, A. K.; Deutsch, K. C.; Ferguson, M. J.; McDonald, R.; Rivard, E. *Aust. J. Chem.* **2013**, *66*, 1235.

8. Ma, M.; Sidiropoulos, A.; Ralte, L.; Stasch, A.; Jones, C. *Chem. Commun.* **2013**, *49*, 48.

9. Pelz, S.; Mohr, F. *Organometallics* **2011**, *30*, 383.

10. Al-Rafia, S. M. I.; Malcolm, A. C.; Liew, S. K.; Ferguson, M. J.; Rivard, E. *J. Am. Chem. Soc.* **2011**, *133*, 777.

11. Halide bridging to form M_2I_2 rings is a common structural arrangement within Group 12 element chemistry: He, G.; Shynkaruk, O.; Lui, M. W.; Rivard, E. *Chem. Rev.* **2014**, *114*, 7815.
12. (a) Hegemann, C.; Tyrra, W.; Neudörfl, J.-M.; Marthur, S. *Organometallics* **2013**, *32*, 1654; (b) Gan, Q.; Ronson, T. K.; Vosburg, D. A.; Thoburn, J. D.; Nitschke, J. R. *J. Am. Chem. Soc.* **2015**, *137*, 1770.
13. Ruiz, D. A.; Melaimi, M.; Bertrand, G. *Chem. Commun.* **2014**, *50*, 7837.
14. Wang, D.; Wurst, K.; Buchmeiser, M. R. *J. Organomet. Chem.* **2004**, *689*, 2123.
15. Although THF is present within the coordination sphere of Hg in the X-ray structure of **5**•THF, coordinated THF was not observed in the ^{1}H NMR spectrum of **5** after this compound was dissolved in THF and stirred for one hour, followed by removal of the solvent under vacuum.
16. Richards, A. F.; Phillips, A. D.; Olmstead, M. M.; Power, P. P. *J. Am. Chem. Soc.* **2003**, *125*, 3204.
17. (a) Parks, D. J.; Blackwell, J. M.; Piers, W. E. *J. Org. Chem.* **2000**, *65*, 3090; (b) Oestreich, M.; Hermeke, J.; Mohr, J. *Chem. Soc. Rev.* **2015**, *44*, 2202.
18. Uhlig, W. *Chem. Ber.* **1992**, *125*, 47.
19. Hadlington, T. J.; Hermann, M.; Frenking, G.; Jones, C. *J. Am. Chem. Soc.* **2014**, *136*, 3028.
20. Chong, C. C.; Hirao, H.; Kinjo, R. *Angew. Chem. Int. Ed.* **2015**, *54*, 190.
21. (a) Cotton, F. A.; Wilkinson, G. in: *Advanced Inorganic Chemistry*, *4th ed.*, Wiley-Interscience, New York, **1980**, pp. 593–597; For selected examples of well-defined R*MM*R complexes (*M* = group 12 element), see: (b) Resa, I.; Carmona, E.; Gutierrez-

Puebla, E.; Monge, A. *Science* **2004**, *305*, 1136; (c) Zhu, Z.; Wright, R. J.; Olmstead, M. M.; Rivard, E.; Brynda, M.; Power, P. P. *Angew. Chem. Int. Ed.* **2006**, *45*, 5807; (d) Hicks, J.; Underhill, E. J.; Kefalidis, C. E.; Maron, L.; Jones, C. *Angew. Chem. Int. Ed.* **2015**, *54*, 10000.

22. (a) Jones, C. *Chem. Commun.* **2001**, 2293; (b) Kuhn, N.; Al-Sheikh, A. *Coord. Chem. Rev.* **2005**, *249*, 829; (c) Prabusankar, G.; Sathyanarayana, A.; Suresh, P.; Babu, C. N.; Srinivas, K.; Metla, B. P. R. *Coord. Chem. Rev.* **2014**, *269*, 829; (d) Wang, Y.; Robinson, G. H. *Inorg. Chem.* **2014**, *53*, 11815.
23. Baker, R. J.; Farley, R. D.; Jones, C. Kloth, M.; Murphy, D. M. *Chem. Commun.* **2002**, 1196.
24. For selected examples of mercury halide motifs with ≥ 3 Hg atoms (e.g. $[Hg_5Cl_{11}]^-$), see: (a) Brodersen, K.; Jensen, K.-P.; Thiele, G. *Z. Naturforsch.* **1980**, *35b*, 253; (b) Polyakova, N. I.; Poznyak, A. L.; Segienko, V. S. *Zh. Neorg. Khim.* **2000**, *45*, 1992; (c) Herler, S.; Mayer, P.; Nöth, H.; Schulz, A.; Suter, M.; Vogt, M. *Angew. Chem. Int. Ed.* **2001**, *40*, 3173; (d) Nockemann, P.; Pantenburg, I.; Meyer, G. *Z. Anorg. Allg. Chem.* **2007**, *633*, 814.
25. Baker, R. J.; Bettentrup, H.; Jones, C. *Eur. J. Inorg. Chem.* **2003**, 2446.
26. Pangborn, A. B.; Giardello, M. A.; Grubbs, R. H.; Rosen, R. K.; Timmers, F. J. *Organometallics* **1996**, *15*, 1518.
27. Jafarpour, L.; Stevens, E. D.; Nolan, S. P. *J. Organomet. Chem.* **2000**, *606*, 49.
28. Pelta, M. D.; Morris, G. A.; Stchedroff, M. J.; Hammond, S. J. *Magn. Reason. Chem.* **2002**, *40*, S147.
29. Botana, A.; Aguilar, J. A.; Nilsson, M.; Morris, G. A. *J. Magn. Reson.* **2011**, *208*, 270.

30. Connell, M. A.; Bowyer, P. J.; Bone, P. A.; Davis, A. L.; Swanson, A. G.; Nilsson, M.; Morris, G. A. *J. Magn. Reson.* **2009**, *198*, 121.

31. Hope, H. *Prog. Inorg. Chem.* **1994**, *41*, 1.

32. Sheldrick, G. M. *Acta. Crystallogr. Sect. A* **2015**, *71*, 3.

33. Sheldrick, G. M. *Acta. Crystallogr. Sect. C* **2015**, *71*, 3.

34. Spek, L. *Acta. Crystallogr. Sect. C* **2015**, *71*, 9.

35. Gaussian 9, Revision D.01, Frisch, M. J.; Trucks, G. W.; Schlegel, H. B.; Scuseria, G. E.; Robb, M. A.; Cheeseman, J. R.; Scalmani, G.; Barone, V.; Mennucci, B.; Petersson, G. A.; Nakatsuji, H.; Caricato, M.; Li, X.; Hratchian, H. P.; Izmaylov, A. F.; Bloino, J.; Zheng, G.; Sonnenberg, J. L.; Hada, M.; Ehara, M.; Toyota, K.; Fukuda, R.; Hasegawa, J.; Ishida, M.; Nakajima, T.; Honda, Y.; Kitao, O.; Nakai, H.; Vreven, T.; Montgomery, J. A.; Peralta, J. E.; Ogliaro, F.; Bearpark, M.; Heyd, J. J.; Brothers, E.; Kudin, K. N.; Staroverov, V. N.; Kobayashi, R.; Normand, J.; Raghavachari, K.; Rendell, A.; Burant, J. C.; Iyengar, S. S.; Tomasi, J.; Cossi, M.; Rega, N.; Millam, J. M.; Klene, M.; Knox, J. E.; Cross, J. B.; Bakken, V.; Adamo, C.; Jaramillo, J.; Gomperts, R.; Stratmann, R. E.; Yazyev, O.; Austin, A. J.; Cammi, R.; Pomelli, C.; Ochterski, J. W.; Martin, R. L.; Morokuma, K.; Zakrzewski, V. G.; Voth, G. A.; Salvodor, P.; Dannenberg, J. J.; Dapprich, S.; Daniels, A. D.; Farkas, Ö.; Foresman, J. B.; Ortiz, J. V.; Cioslowski, J.; Fox, D. J. Gaussian, Inc., Wallingford CT, **2009**.

36. (a) Lee, C.; Yang, W.; Parr, R. G. *Phys. Rev. B* **1988**, *37*, 785; (b) Becke, A. D. *Phys. Rev. A* **1988**, *38*, 3098; (c) Stephens, P. J.; Devlin, F. J.; Chabalowski, C. F.; Frisch, M. J. J. *Phys. Chem.* **1994**, *98*, 11623.

37. (a) Hariharan, P. C.; Pople, J. A. *Theor. Chim. Acta* **1973**, *28*, 213; (b) Francl, M. M.; Pietro, W. J.; Hehre, W. J.; Binkley, J. S.; Gordon, M. S.; DeFrees, D. J.; Pople, J. A. *J. Chem. Phys.* **1982**, *77*, 3654.
38. Zhao, Y.; Truhlar, D. G. *Theor. Chem. Acc.* **2008**, *120*, 215.
39. Kendall, R. A.; Dunning Jr., T. H.; Harrison, R. J. *J. Chem. Phys.* **1992**, *96*, 6796.
40. Figgen, D.; Rauhut, G.; Dolg, M.; Stoll, H. *Chem. Phys.* **2005**, *311*, 227.
41. Peterson, K. A.; Puzzarini, C. *Theor. Chem. Acc.* **2005**, *114*, 283.
42. Arrowsmith, M.; Hadlington, T. J.; Hill, M. S. Kociok-Köhn, G. *Chem. Commun.* **2012**, *48*, 4567.
43. Chakraborty, S.; Blacque, O.; Fox, T.; Berke, H. *ACS Catal.* **2013**, *3*, 2208.

Chapter 3

1. (a) Stokes, H. N. *Am. Chem. J.* **1895**, *17*, 275; (b) Stokes, H. N. *Am. Chem. J.* **1896**, *18*, 629.
2. (a) Allcock, H. R.; Kugel, R. L. *J. Am. Chem. Soc.* **1965**, *87*, 4216; (b) Allcock, H. R.; Kugel, R. L.; Valan, K. J. *Inorg. Chem.* **1966**, *5*, 1709; (c) Allcock, H. R.; Kugel, R. L. *Inorg. Chem.* **1966**, 5, 1716; For selected review articles, see: (d) Neilson, R. H.; Wisian-Neilson, P. *Chem. Rev.* **1988**, *88*, 541; (e) Allen, C. W. *Coord. Chem. Rev.* **1994**, *130*, 137; (f) Manners, I. *Angew. Chem., Int. Ed. Engl.* **1996**, *35*, 1602; (g) Priegert, A. M.; Rawe, B. W.; Serin, S. C.; Gates, D. P. *Chem. Soc. Rev.* **2016**, *45*, 922.
3. (a) Lund, L. G.; Paddock, N. L.; Proctor, J. E.; Searle, H. T. *J. Chem. Soc.* **1960**, 2542; (b) Chandrasekhar, V.; Thilagar, P.; Murugesa Pandian, B. *Coord. Chem. Rev.* **2007**,

251, 1045; (c) Zhang, Y.; Huynh, K.; Manners, I.; Reed, C. A. *Chem. Commun.* **2008**, 494.

4. Tun, Z.-M.; Heston, A. J.; Panzner, M. J.; Medvetz, D. A.; Wright, B. D.; Savant, D.; Dudipala, V. R.; Banerjee, D.; Rinaldi, P. L.; Youngs, W. J.; Tessier, C. A. *Inorg. Chem.* **2011**, *50*, 8937 and references therein.
5. (a) Boomishankar, R.; Ledger, J.; Guilbaud, J.-B.; Campbell, N. L.; Bacsa, J.; Bonar-Law, R.; Khimyak, Y. Z.; Steiner, A. *Chem. Commun.* **2007**, 5152; (b) Al-Rafia, S. M. I.; Ferguson, M. J.; Rivard, E. *Inorg. Chem.* **2011**, *50*, 10543.
6. (a) Honeyman, C. H.; Manners, I.; Morrissey, C. T.; Allcock, H. R. *J. Am. Chem. Soc.* **1995**, *117*, 7035; (b) Rivard, E.; Lough, A. J.; Manners, I. *Inorg. Chem.* **2004**, *43*, 2765; (c) Rivard, E.; Huynh, K.; Lough, A. J.; Manners, I. *J. Am. Chem. Soc.* **2004**, *126*, 2286; (d) Huynh, K.; Lough, A. J.; Forgeron, M. A. M.; Bendle, M.; Soto, A. P.; Wasylishen, R. E.; Manners, I. *J. Am. Chem. Soc.* **2009**, *131*, 7905.
7. (a) Dielmann, F.; Back, O.; Henry-Ellinger, M.; Jerabek, P.; Frenking, G.; Bertrand, G. *Science* **2012**, *337*, 1526; (b) Dielmann, F.; Bertrand, G. *Chem. Eur. J.* **2015**, *21*, 191.
8. For relevant review articles, see: (a) Rivard, E. *Dalton Trans.* **2014**, *43*, 8577; (b) Rivard, E. *Chem. Soc. Rev.* **2016**, *45*, 989; (c) Roy, M. M. D.; Rivard, E. *Acc. Chem. Res.* **2017**, *50*, 2017.
9. For the use of Lewis bases to stabilize reactive phosphorus-based species, see the following selected references: (a) Gray, P. A.; Burford, N. *Coord. Chem. Rev.* **2016**, *324*, 1; (b) Burford, N.; Cameron, T. S.; Ragogna, P. J.; Ocando-Mavarez, E.; Gee, M.; McDonald, R.; Wasylishen, R. E. *J. Am. Chem. Soc.* **2001**, *123*, 7947; (c)

Schwedtmann, K.; Hennersdorf, F.; Bauzá, A.; Frontera, A.; Fischer, R.; Weigand, J. J. *Angew. Chem., Int. Ed.* **2017**, *56*, 6218; (d) Macdonald, C. L. B.; Binder, J. F.; Swidan, A.; Nguyen, J. H.; Kosnik, S. C.; Ellis, B. D. *Inorg. Chem.* **2016**, *55*, 7152; (e) Dube, J. W.; Macdonald, C. L. B.; Ragogna, P. J. *Angew. Chem., Int. Ed.* **2012**, *51*, 13026; (f) Graham, C. M. E.; Pritchard, T. E.; Boyle, P. D.; Valjus, J.; Tuononen, H. M.; Ragogna, P. J. *Angew. Chem., Int. Ed.* **2017**, *56*, 6236; (g) Price, A. N.; Nichol, G. S.; Cowley, M. J. *Angew. Chem., Int. Ed.* **2017**, *56*, 9953; (h) Wang, Y.; Hickox, H. P.; Xie, Y.; Wei, P.; Cui, D.; Walter, M. R.; Schaefer, H. F., III; Robinson, G. H. *Chem. Commun.* **2016**, *52*, 5746; (i) Majhi, P. K.; Chow, K. C. F.; Hsieh, T. H. H.; Bowes, E. G.; Schnakenburg, G.; Kennepohl, P.; Streubel, R.; Gates, D. P. *Chem. Commun.* **2016**, *52*, 998; (j) Graham, C. M. E.; Millet, C. R. P.; Price, A. N.; Valjus, J.; Cowley, M. J.; Tuononen, H. M.; Ragogna, P. J. *Chem. Eur. J.* **2018**, *24*, 672.

10. (a) Swarnakar, A. K.; Hering-Junghans, C.; Nagata, K.; Ferguson, M. J.; McDonald, R.; Tokitoh, N.; Rivard, E. *Angew. Chem., Int. Ed.* **2015**, *54*, 10666; (b) Swarnakar, A. K.; Hering-Junghans, C.; Ferguson, M. J.; McDonald, R.; Rivard, E. *Chem. Sci.* **2017**, *8*, 2337.
11. The Rivard group has also shown that donor-acceptor complexes can effectively release their trapped molecular cargo, as evidenced by the use of GeH_2 complexes to yield luminescent germanium nanoparticles: (a) Purkait, T. K.; Swarnakar, A. K.; De Los Reyes, G. B.; Hegmann, F. A.; Rivard, E.; Veinot, J. G. C. *Nanoscale* **2015**, *7*, 2241; (b) Thimer, K. C.; Al-Rafia, S. M. I.; Ferguson, M. J.; McDonald, R.; Rivard, E. *Chem. Commun.* **2009**, 7119.

12. For related examples of NHC-stabilized P^{III}-azides and chlorides, see: (a) Henne, F. D.; Schnöckelborg, E.-M.; Feldmann, K.-O.; Grunenberg, J.; Wolf, R.; Weigand, J. J. *Organometallics* **2013**, *32*, 6674; (b) Henne, F. D.; Dickschat, A. T.; Hennersdorf, F.; Feldmann, K.-O.; Weigand, J. J. *Inorg. Chem.* **2015**, *54*, 6849.
13. (a) Dumrath, A.; Lübbe, C.; Neumann, H.; Jackstell, R.; Beller, M. *Chem. Eur. J.* **2011**, *17*, 9599; (b) Wünsche, M. A.; Mehlmann, P.; Witteler, T.; Buß, F.; Rathmann, P.; Dielmann, F. *Angew. Chem., Int. Ed.* **2015**, *54*, 11857; (c) Paisley, N. R.; Lui, M. W.; McDonald, R.; Ferguson, M. J.; Rivard, E. *Dalton Trans.* **2016**, *45*, 9860; (d) Lui, M. W.; Shynkaruk, O.; Oakley, M. S.; Sinelnikov, R.; McDonald, R.; Ferguson, M. J.; Meldrum, A.; Klobukowski, M.; Rivard, E. *Dalton Trans.* **2017**, *46*, 5946.
14. For the related use of $[N_3–BR_3]^-$ anions to yield Lewis acid coordinated uranium nitrides (after N_2 loss), see: Fox, A. R.; Arnold, P. L.; Cummins, C. C. *J. Am. Chem. Soc.* **2010**, *132*, 3250.
15. Gillespie, R. J. *Coord. Chem. Rev.* **2008**, *252*, 1315.
16. Wang, Y.; Xie, Y.; Abraham, M. Y.; Gilliard, R. J., Jr.; Wei, P.; Schaefer, H. F., III; Schleyer, P. v. R.; Robinson, G. H. *Organometallics* **2010**, *29*, 4778.
17. Burford, N.; Cameron, T. S.; Conroy, K. D.; Ellis, B.; Macdonald, C. L. B.; Ovans, R.; Phillips, A. D.; Ragogna, P. J.; Walsh, D. *Can. J. Chem.* **2002**, 80, 1404.
18. Gololobov, Y. G.; Kasukhin, L. F. *Tetrahedron* **1992**, *48*, 1353.
19. For reviews of N-heterocyclic imines in main group chemistry, see: (a) Ochiai, T.; Franz, D.; Inoue, S. *Chem. Soc. Rev.* **2016**, *45*, 6327; (b) Todd, A. D. K.; McClennan, W. L.; Masuda, J. D. *RSC Adv.* **2016**, *6*, 69270.
20. Kinjo, R.; Donnadieu, B.; Bertrand, G. *Angew. Chem., Int. Ed.* **2010**, *49*, 5930.

21. (a) Monot, J.; Brahmi, M. M.; Ueng, S.-H.; Robert, C.; Murr, M. D.-E.; Curran, D. P.; Malacria, M.; Fensterbank, L.; Lacôte, E. *Org. Lett.* **2009**, *11*, 4914; (b) Al-Rafia, S. M. I.; Lummis, P. A.; Swarnakar, A. K.; Deutsch, K. C.; Ferguson, M. J.; McDonald, R.; Rivard, E. *Aust. J. Chem.* **2013**, *66*, 1235.

22. Dillon, K. B.; Platt, A. W. G.; Waddington, T. C. J. *Chem. Soc., Dalton Trans.* **1980**, 1036.

23. Betley, T. A.; Peters, J. C. *J. Am. Chem. Soc.* **2004**, *126*, 6252.

24. Pangborn, A. B.; Giardello, M. A.; Grubbs, R. H.; Rosen, R. K.; Timmers, F. J. *Organometallics* **1996**, *15*, 1518.

25. Tamm, M.; Randoll, S.; Herdtweck, E.; Kleigrewe, N.; Kehr, G.; Erker, G.; Rieger, B. *Dalton Trans.* **2006**, 459.

26. (a) Kuprat, M.; Lehmann, M.; Schulz, A.; Villinger, A. *Organometallics* **2010**, *29*, 1421; (b) Massey, A. G.; Park, A. J. *J. Organomet. Chem.* **1964**, *2*, 245.

27. Kolychev, E. L.; Bannenberg, T.; Freytag, M.; Daniliuc, C. G.; Jones, P. G.; Tamm, M. *Chem. Eur. J.* **2012**, *18*, 16938.

28. Hope, H. *Prog. Inorg. Chem.* **1994**, *41*, 1.

29. (a) Sheldrick, G. M. *Acta Crystallogr. Sect. A* **2015**, *71*, 3; (b) Sheldrick, G. M. *Acta. Crystallogr. Sect. C* **2015**, *71*, 3.

30. Gaussian 9, Revision D.01, Frisch, M. J.; Trucks, G. W.; Schlegel, H. B.; Scuseria, G. E.; Robb, M. A.; Cheeseman, J. R.; Scalmani, G.; Barone, V.; Mennucci, B.; Petersson, G. A.; Nakatsuji, H.; Caricato, M.; Li, X.; Hratchian, H. P.; Izmaylov, A. F.; Bloino, J.; Zheng, G.; Sonnenberg, J. L.; Hada, M.; Ehara, M.; Toyota, K.; Fukuda, R.; Hasegawa, J.; Ishida, M.; Nakajima, T.; Honda, Y.; Kitao, O.; Nakai, H.; Vreven,

T.; Montgomery, J. A.; Peralta, J. E.; Ogliaro, F.; Bearpark, M.; Heyd, J. J.; Brothers, E.; Kudin, K. N.; Staroverov, V. N.; Kobayashi, R.; Normand, J.; Raghavachari, K.; Rendell, A.; Burant, J. C.; Iyengar, S. S.; Tomasi, J.; Cossi, M.; Rega, N.; Millam, J. M.; Klene, M.; Knox, J. E.; Cross, J. B.; Bakken, V.; Adamo, C.; Jaramillo, J.; Gomperts, R.; Stratmann, R. E.; Yazyev, O.; Austin, A. J.; Cammi, R.; Pomelli, C.; Ochterski, J. W.; Martin, R. L.; Morokuma, K.; Zakrzewski, V. G.; Voth, G. A.; Salvodor, P.; Dannenberg, J. J.; Dapprich, S.; Daniels, A. D.; Farkas, Ö.; Foresman, J. B.; Ortiz, J. V.; Cioslowski, J.; Fox, D. J. Gaussian, Inc., Wallingford CT, **2009**.

31. (a) Lee, C.; Yang, W. Parr, R. G. *Phys. Rev. B* **1988**, *37*, 785; (b) Becke, A. D. *Phys. Rev. A* **1988**, *38*, 3098; (c) Stephens, P. J.; Devlin, F. J.; Chabalowski, C. F.; Frisch, M. J.; *J. Phys. Chem.* **1994**, *98*, 11623.
32. (a) Hariharan, P. C.; Pople, J. A. *Theor. Chim. Acta* **1973**, *28*, 213; (b) Francl, M. M.; Pietro, W. J.; Hehre, W. J.; Binkley, J. S.; Gordon, M. S.; DeFrees, D. J.; Pople, J. A. *J. Chem. Phys.*, **1982**, *77*, 3654.

Chapter 4

1. (a) For selected reviews and articles, see: (a) Nguyen, T.; Sutton, A. D.; Brynda, M.; Fettinger, J. C.; Long, G. L.; Power, P. P. *Science* **2005**, *310*, 844; (b) Fischer, R. C.; Power, P. P. *Chem. Rev.* **2010**, *110*, 3877; (c) Mizuhata, Y.; Sasamori, T.; Tokitoh, N. *Chem. Rev.* **2009**, *109*, 3479; (d) Asay, M.; Jones, C.; Driess, M. *Chem. Rev.* **2011**, *111*, 354; (e) Sen, S.; Khan, S.; Samuel, P. P.; Roesky, H. W. *Chem. Sci.* **2012**, *3*, 659; (f) Khan, S.; Gopakumar, G.; Thiel, W.; Alcarazo, M. *Angew. Chem. Int. Ed.* **2013**, *52*, 5644; (g) Hadlington, T. J.; Hermann, M.; Frenking, G.; Jones, C. *J. Am. Chem. Soc.* **2014**, *136*, 3028; (h) Rit, A.; Campos, J.; Niu, H.; Aldridge, S. *Nat. Chem.* **2016**,

8, 1022; (i) Martin, D.; Melaimi, M.; Soleilhavoup, M.; Bertrand, G. *Organometallics* **2011**, *30*, 5304; (j) Ochiai, T.; Franz, D.; Inoue, S. *Chem. Soc. Rev.* **2016**, *45*, 6327; (k) Milnes, K. K.; Pavelka, L. C.; Baines, K. M. *Chem. Soc. Rev.* **2016**, *45*, 1019; (l) Gray, P. A.; Burford, N. *Coord. Chem. Rev.* **2016**, *324*, 1.

2. (a) Power, P. P. *Nature* **2010**, *463*, 171; (b) Spikes, G. H.; Fettinger, J. C.; Power, P. P. *J. Am. Chem. Soc*. **2005**, *127*, 12232; (c) Hadlington, T. J.; Kefalidis, C. E.; Maron, L.; Jones, C. *ACS Catal.* **2017**, *7*, 1853. For related work concerning the use of Frustrated Lewis Pairs (FLPs) for small molecule activation, see: (d) Stephan, D. W. *Acc. Chem. Res.* **2015**, *48*, 306.
3. (a) Jones, C. *Chem. Commun.* **2001**, 2293; (b) Robinson, G. H. *Dalton Trans.* **2012**, *41*, 2601; (c) Braunschweig, H.; Dewhurst, R. D.; Hammond, K.; Mies, J.; Radacki, K.; Vargas, A. *Science* **2012**, *336*, 1420; (d) Wilson, D. J. D.; Dutton, J. L. *Chem. Eur. J.* **2013**, *19*, 13626; (e) Rivard, E. *Chem. Soc. Rev.* **2016**, *45*, 989; (f) Präsang, C.; Scheschkewitz, D. *Chem. Soc. Rev.* **2016**, *45*, 900.
4. Percent buried volumes were calculated with the SambVca 2.0 web tool (https://www.molnac.unisa.it/OMtools/sambvca2.0/) using default parameters with H atoms omitted from the calculation, see: Falivene, L.; Credendino, R.; Poater, A.; Petta, A.; Serra, L.; Oliva, R.; Scarano, V.; Cavallo, L. *Organometallics* **2016**, *35*, 2286.
5. $\%V_{bur}$ for IPr and IPr*: Gómez-Suárez, A.; Nelson, D. J.; Nolan, S. P. *Chem. Commun.* **2017**, *53*, 2650.
6. Dröge, T.; Glorius, F. *Angew. Chem. Int. Ed.* **2010**, *49*, 6940.

7. Purkait, T. K.; Swarnakar, A. K.; De Los Reyes, G. B.; Hegmann, F. A.; Rivard, E.; Veinot, J. G. C. *Nanoscale* **2015**, *7*, 2241.

8. (a) Arnold, P. L.; Scarisbrick, A. C. *Organometallics* **2004**, *23*, 2519; (b) Cole, M. L.; Davis, A. J.; Jones, C. *J. Chem. Soc., Dalton Trans.* **2001**, 2451.

9. Nakai, H.; Tang, Y.; Gantzel, P.; Mayer, K. *Chem. Commun.* **2003**, 24.

10. Cordero, B.; Gómez, V.; Platero-Prats, A. E.; Revés, M.; Echeverría, J.; Cremades, E.; Barragán, F.; Alvarez, S. *Dalton Trans.* **2008**, 2832.

11. For examples of $[RTl]_x$ (x =1 or 2) compounds, see: (a) Niemeyer, M.; Power, P. P. *Angew. Chem. Int. Ed.* **1998**, *37*, 1277; (b) Hill, M. S.; Pongtavornpinyo, R.; Hitchcock, P. B. *Chem. Commun.* **2006**, 3720; (c) Wright, R. J.; Brynda, M.; Power, P. P. *Inorg. Chem.* **2005**, *44*, 3368; (d) Wright, R. J.; Phillips, A. D.; Hino, S.; Power, P. P. *J. Am. Chem. Soc.* **2005**, *127*, 4794; (e) Dange, D.; Li, J.; Schenk, C.; Schnöckel, H.; Jones, C. *Inorg. Chem.* **2012**, *51*, 13050.

12. Mansaray, H. B.; Tang, C. Y.; Vidovic, D.; Thompson, A. L.; Aldridge, S. *Inorg. Chem.* **2012**, *51*, 13017.

13. Thimer, K. C.; Al-Rafia, S. M. I.; Ferguson, M. J.; McDonald, R.; Rivard, E. *Chem. Commun.* **2009**, 7119.

14. (a) Rit, A.; Tirfoin, R.; Aldridge, S. *Angew. Chem. Int. Ed.* **2016**, *55*, 378; For an example of a quasi one-coordinate Ge^{II} cation, see: (b) Li, J.; Schenk, C.; Winter, F.; Schere, H.; Trapp, N.; Higelin, A.; Keller, S.; Pöttgen, R.; Krossing, I.; Jones, C. *Angew. Chem. Int. Ed.* **2012**, *51*, 9557.

15. The Rivard group is currently exploring *direct* routes to $[(ITr)Li]^+$ salts that do not involve toxic thallium-based precursors.

16. (a) Lang, H.; Jakob, A.; Milde, B. *Organometallics* **2012**, *31*, 7661; (b) Dorel, R.; Echavarren, A. M. *Chem. Rev.* **2015**, *115*, 9028; (c) Halbes-Letinois, U.; Weibel, J.-M.; Pale, P. *Chem. Soc. Rev.* **2007**, *36*, 759; (d) Díez-González, S.; Marion, N.; Nolan, S. P. *Chem. Rev.* **2009**, *109*, 3612; (e) Fang, G.; Bi, X. *Chem. Soc. Rev.* **2015**, *44*, 8124; (f) Nechaev, M. S.; Rayón, V. M.; Frenking, G. *J. Phys. Chem. A* **2004**, *108*, 3134; (g) Niemeyer, M. *Organometallics* **1998**, *17*, 4649.

17. Weber, S. G.; Rominger, F.; Straub, B. F. *Eur. J. Inorg. Chem.* **2012**, 2863.

18. Weber, S. G; Zahner, D.; Rominger, F.; Straub, B. F. *Chem. Commun.* **2012**, *48*, 11325.

19. Phillips, N.; Dodson, T.; Tirfoin, R.; Bates, J. I. Aldridge, S. *Chem. Eur. J.* **2014**, *20*, 16721.

20. Collins, L. R.; Rajabi, N. A.; Macgregor, S. A.; Mahon, M. F.; Whittlesey, M. K. *Angew. Chem. Int. Ed.* **2016**, *55*, 15539.

21. Romero, E. A.; Olsen, P. M.; Jazzar, R.; Soleilhavoup, M.; Gembicky, M.; Bertrand, G. *Angew. Chem. Int. Ed.* **2017**, *56*, 4024.

22. For articles and reviews, see: (a) Reisinger, A.; Trapp, N.; Knapp, C.; Himmel, D.; Breher, F.; Rüegger, H.; Krossing, I. *Chem. Eur. J.* **2009**, *15*, 9505; (b) Reisinger, A.; Trapp, N.; Krossing, I.; Altmannshofer, S.; Herz, V.; Presnitz, M.; Scherer, W. *Angew. Chem. Int. Ed.* **2007**, *46*, 8295; (c) Dias, H. V. R.; Fianchini, M. *Angew. Chem. Int. Ed.* **2007**, *46*, 2188; (d) Dias, H. V. R.; Lovely, C. J. *Chem. Rev.* **2008**, *108*, 3223; (e) Jayaratna, N. B.; Gerus, I. I.; Mironets, R. V.; Mykhailiuk, P. K.; Yousufuddin, M.; Dias, H. V. R. *Inorg. Chem.* **2013**, *52*, 1691; (f) Dias, H. V. R.; Flores, J. A.; Wu, J.; Kroll, P. *J. Am. Chem. Soc.* **2009**, *131*, 11249.

23. (a) Gibard, C.; Fauché, K.; Guillot, R; Jouffret, L.; Traïkia, M.; Gautier, A.; Cisnetti, F. *J. Organomet. Chem.* **2017**, *840*, 70; (b) Wong, V. H. L.; White, A. J. P.; Hor, T. S. A.; Hii, K. K. *Chem. Commun.* **2015**, *51*, 17752; (c) Su, H.-L.; Pérez, L. M.; Lee, S.-J.; Reibenspies, J. H.; Bazzi, H. S.; Bergbreiter, D. E. *Organometallics* **2012**, *31*, 4063; (d) de Frémont, P.; Scott, N. M.; Stevens, E. D.; Ramnial, T.; Lightbody, O. C.; Macdonald, C. L. B.; Clyburne, J. A. C.; Abernethy, C. D.; Nolan, S. P. *Organometallics* **2005**, *24*, 6301.

24. For example: Smith, H. G.; Rundle, R. E. *J. Am. Chem. Soc.* **1958**, *80*, 5075.

25. (a) Childs, R. F.; Mulholland, D. L.; Nixon, A. *Can. J. Chem.* **1982**, *60*, 801; (b) Britovsek, G. J. P.; Ugolotti, J.; White, A. J. P. *Organometallics* **2005**, *24*, 1685.

26. (a) Böhrer, H.; Trapp, N.; Himmel, D.; Schleep, M.; Krossing, I. *Dalton Trans.* **2015**, *44*, 7489; (b) Schleep, M.; Hettich, C.; Velázquez Rojaz, J.; Kratzert, D.; Ludwig, T.; Lieberth, K.; Krossing, I. *Angew. Chem. Int. Ed.* **2017**, *56*, 2880.

27. (a) Puschmann, F. F.; Stein, D.; Heift, D.; Hendriksen, C.; Gal, Z. A.; Grützmacher, H. F.; Grützmacher, H. *Angew. Chem. Int. Ed.* **2011**, *50*, 8420; (b) Heift, D.; Benkő, Z.; Grützmacher, H. *Dalton Trans.* **2014**, *43*, 831.

28. Liu, L.; Ruiz, D. A.; Dahcheh, F.; Bertrand, G.; Suter, R.; Tondreau, A. M.; Grützmacher, H. *Chem. Sci.* **2016**, *7*, 2335.

29. Rummel, E.-M.; Mastrorilli, P.; Todisco, S.; Latronico, M.; Balázs, G.; Virovets, A. V.; Scheer, M. *Angew. Chem. Int. Ed.* **2016**, *55*, 13301.

30. Liew, S. K.; Al-Rafia, S. M. I.; Goettel, J. T.; Lummis, P. A.; McDonald, S. M.; Miedema, L. J.; Ferguson, M. J.; McDonald, R.; Rivard, E. *Inorg. Chem.* **2012**, *51*, 5471.

31. Weber, S. G.; Loos, C.; Rominger, F.; Straub, B. F. *ARKIVOC* **2012**, *iii*, 226.
32. For a recent example of bulky NHCs in catalysis, see: Lan, X.-B.; Li, Y.; Li, Y.-F.; Shen, D.-S.; Ke, Z.; Liu, F.-S. *J. Org. Chem.* **2017**, *82*, 2914.
33. Pangborn, A. B.; Giardello, M. A.; Grubbs, R. H.; Rosen, R. K.; Timmers, F. J. *Organometallics* **1996**, *15*, 1518.
34. Straus, D. A.; Zhang, C.; Tilley, T. D. *J. Organomet. Chem.* **1989**, *369*, C13.
35. Davis, D. P.; Kirk, K. A.; Cohen, L. A. *J. Heterocyclic Chem.* **1982**, *19*, 253.
36. Cullinane, J.; Jolleys, A.; Mair, F. S. *Dalton Trans.* **2013**, *42*, 11971.
37. Hope, H. *Prog. Inorg. Chem.* **1994**, *41*, 1.
38. Sheldrick, G. M. *Acta. Crystallogr. Sect. A.* **2015**, *71*, 3.
39. Sheldrick, G. M. *Acta. Crystallogr. Sect. C.* **2015**, *71*, 3.
40. Gaussian 9, Revision D.01, Frisch, M. J.; Trucks, G. W.; Schlegel, H. B.; Scuseria, G. E.; Robb, M. A.; Cheeseman, J. R.; Scalmani, G.; Barone, V.; Mennucci, B.; Petersson, G. A.; Nakatsuji, H.; Caricato, M.; Li, X.; Hratchian, H. P.; Izmaylov, A. F.; Bloino, J.; Zheng, G.; Sonnenberg, J. L.; Hada, M.; Ehara, M.; Toyota, K.; Fukuda, R.; Hasegawa, J.; Ishida, M.; Nakajima, T.; Honda, Y.; Kitao, O.; Nakai, H.; Vreven, T.; Montgomery, J. A.; Peralta, J. E.; Ogliaro, F.; Bearpark, M.; Heyd, J. J.; Brothers, E.; Kudin, K. N.; Staroverov, V. N.; Kobayashi, R.; Normand, J.; Raghavachari, K.; Rendell, A.; Burant, J. C.; Iyengar, S. S.; Tomasi, J.; Cossi, M.; Rega, N.; Millam, J. M.; Klene, M.; Knox, J. E.; Cross, J. B.; Bakken, V.; Adamo, C.; Jaramillo, J.; Gomperts, R.; Stratmann, R. E.; Yazyev, O.; Austin, A. J.; Cammi, R.; Pomelli, C.; Ochterski, J. W.; Martin, R. L.; Morokuma, K.; Zakrzewski, V. G.; Voth, G. A.;

Salvodor, P.; Dannenberg, J. J.; Dapprich, S.; Daniels, A. D.; Farkas, Ö.; Foresman, J. B.; Ortiz, J. V.; Cioslowski, J.; Fox, D. J. Gaussian, Inc., Wallingford CT, **2009**.

41. (a) Lee, C.; Yang, W.; Parr, R. G. *Phys. Rev. B* **1988**, *37*, 785; (b) Becke, A. D. *Phys. Rev. A* **1988**, *38*, 3098; (c) Stephens, P. J.; Devlin, F. J.; Chabalowski, C. F.; Frisch, M. J. *J. Phys. Chem.* **1994**, *98*, 11623.
42. (a) Hariharan, P. C.; Pople, J. A. *Theor. Chim. Acta* **1973**, *28*, 213; (b) Francl, M. M.; Pietro, W. J.; Hehre, W. J.; Binkley, J. S.; Gordon, M. S.; DeFrees, D. J.; Pople, J. A. *J. Chem. Phys.* **1982**, *77*, 3654.
43. (a) Hay, P. J.; Wadt, W. R. *J. Chem. Phys.* **1985**, *82*, 270; (b) Wadt, W. R; Hay, P. J. *J. Chem. Phys.* **1985**, *82*, 284; (c) Hay, P. J.; Wadt, W. R. *J. Chem. Phys.* **1985**, *82*, 299.
44. Neese, F. *Wiley Interdiscip. Rev.: Comput. Mol. Sci.* **2012**, *2*, 73.
45. Perdew, J. P.; *Phys. Rev. B* **1986**, *33*, 8822.
46. (a) Weigand, F.; Ahlrichs, R. *Phys. Chem. Chem. Phys.* **2005**, *7*, 3297; (b) Weigand, F. *Phys. Chem. Chem. Phys.* **2006**, *8*, 1057.

Chapter 5

1. (a) Fischer, R. C.; Power, P. P. *Chem. Rev.* **2010**, *110*, 3877; (b) Wang, Y.; Robinson, G. H. *Inorg. Chem.* **2011**, *50*, 12326; (c) Ghadwal, R. S.; Azhakar, R.; Roesky, H. W. *Acc. Chem. Res.* **2013**, *46*, 444; (d) Brand, J.; Braunschweig, H.; Sen, S. S. *Acc. Chem. Res.* **2014**, *47*, 180; (e) Präsang, C.; Scheschkewitz, D. *Chem. Soc. Rev.* **2016**, *45*, 900; (f) Ochiai, T.; Franz, D.; Inoue, S. *Chem. Soc. Rev.* **2016**, *45*, 6327; (g) Priegert, A. M.; Rawe, B. W.; Serin, S. C.; Gates, D. P. *Chem. Soc. Rev.* **2016**, *45*, 922; (h) Melaimi, M.; Jazzar, R.; Soleilhavoup, M.; Bertrand, G. *Angew. Chem. Int. Ed.* **2017**,

56, 10046; (i) Alvarado-Beltran, I.; Rosas-Sánchez, A.; Baceiredo, A.; Saffon-Merceron, N.; Branchadell, V.; Kato, T. *Angew. Chem. Int. Ed.* **2017**, *56*, 10481; (j) Mizuhata, Y.; Fujimori, S.; Sasamori, T.; Tokitoh, N. *Angew. Chem. Int. Ed.* **2017**, *56*, 4588; (k) Schneider, J.; Sindlinger, C. P.; Eichele, K.; Schubert, H.; Wesemann, L. *J. Am. Chem. Soc.* **2017**, *139*, 6542; (l) Wendel, D.; Reiter, D.; Porzelt, A.; Altmann, P. J.; Inoue, S.; Rieger, B. *J. Am. Chem. Soc.* **2017**, *139*, 17193; (m) Légaré, M.-A.; Bélanger-Chabot, G.; Dewhurst, R. D.; Welz, E.; Krummenacher, I.; Engels, B.; Braunschweig, H. *Science* **2018**, *359*, 896.

2. (a) Power, P. P. *Nature* **2010**, *463*, 171; (b) Hadlington, T. J.; Hermann, M.; Frenking, G. Jones, C. *Chem. Sci.* **2015**, *6*, 7249; (c) Yadav, S.; Saha, S.; Sen, S. S. *ChemCatChem* **2016**, *8*, 486; (d) Hill, M. S.; Liptrot, D. J.; Weetman, C.; *Chem. Soc. Rev.* **2016**, *45*, 972; (e) Hadlington, T. J.; Kefalidis, C. E.; Maron, L; Jones, C. *ACS Catal.* **2017**, *7*, 1853; (f) Schuhknecht, D.; Lhotzky, C.; Spaniol, T. P.; Maron, L.; Okuda, J. *Angew. Chem. Int. Ed.* **2017**, *56*, 12367; (g) Wilson, A. S. S.; Hill, M. S.; Mahon, M. F.; Dinoi, C.; Maron, L. *Science* **2017**, *358*, 1168; (h) Nikonov, G. I. *ACS Catal.* **2017**, *7*, 7257.

3. (a) Schnepf, A. *New J. Chem.* **2010**, *34*, 2079; (b) Purkait, T. K.; Swarnakar, A. K.; De Los Reyes, G. B.; Hegmann, F. A.; Rivard, E.; Veinot, J. G. C. *Nanoscale* **2015**, *7*, 2241; (c) Yin, J.; Li, J.; Hang, Y.; Yu, J.; Tai, G.; Li, X.; Zhang, Z.; Guo, W. *Small* **2016**, *12*, 2942; (d) Rivard, E. *Chem. Soc. Rev.* **2016**, *45*, 989; (e) Haas, M.; Christopoulos, V.; Radebner, J.; Holthausen, M.; Lainer, T.; Schuh, L.; Fitzek, H.; Kothleitner, G.; Torvisco, A.; Fischer, R.; Wunnicke, O.; Stüger, H. *Angew. Chem. Int. Ed.* **2017**, *56*, 14071.

4. (a) Rivard, E. *Dalton Trans.* **2014**, *43*, 8577; (b) Roy, M. M. D.; Rivard, E. *Acc. Chem. Res.* **2017**, *50*, 2017.

5. (a) Marks, T. J. *J. Am. Chem. Soc.* **1971**, *93*, 7090; (b) Vogel, U.; Timoshkin, A. Y.; Scheer, M. *Angew. Chem. Int. Ed.* **2001**, *40*, 4409; (c) Rupar, P. A.; Jennings, M. C.; Ragogna, P. J.; Baines, K. M. *Organometallics* **2007**, *26*, 4109; (d) Zabula, A. V.; Pape, T.; Hepp, A.; Schappacher, F. M.; Rodewald, U. C.; Pöttgen, R.; Hahn, F. E. *J. Am. Chem. Soc.* **2008**, *130*, 5648; (e) Filippou, A. C.; Baars, B.; Chernov, O.; Lebedev, Y. N.; Schnakenburg, G. *Angew. Chem. Int. Ed.* **2014**, *53*, 565; (f) Stephan, D. W. *Acc. Chem. Res.* **2015**, *48*, 306; (g) Zhou, Y.-P.; Karni, M.; Yoa, S.; Apeloig, Y.; Driess, M. *Angew. Chem. Int. Ed.* **2016**, *55*, 15096; (h) Mo, Z.; Rit, A.; Campos, J.; Kolychev, E. L.; Aldridge, S. *J. Am. Chem. Soc.* **2016**, *138*, 3306; (i) Hickox, H. P.; Wang, Y.; Xie, Y.; Wei, P.; Schaeffer III, H. F.; Robinson, G. H. *J. Am. Chem. Soc.* **2016**, *138*, 9799; (j) Rodriguez, R.; Gau, D.; Saouli, J.; Baceiredo, A.; Saffon-Merceron, N.; Branchadell, V.; Kato, T. *Angew. Chem. Int. Ed.* **2017**, *56*, 3935.

6. For selected references, see: (a) Thimer, K. C.; Al-Rafia, S. M. I.; Ferguson, M. J.; McDonald, R.; Rivard, E. *Chem. Commun.* **2009**, 7119; (b) Al-Rafia, S. M. I.; Malcolm, A. C.; Liew, S. K.; Ferguson, M. J.; Rivard, E. *J. Am. Chem. Soc.* **2011**, *133*, 777; (c) Al-Rafia, S. M. I.; Malcolm, A. C.; McDonald, R.; Ferguson, M. J.; Rivard, E. *Angew. Chem. Int. Ed.* **2011**, *50*, 8354; (d) Al-Rafia, S. M. I.; Malcolm, A. C.; McDonald, R.; Ferguson, M. J.; Rivard, E. *Chem. Commun.* **2012**, *48*, 1308; (e) Al-Rafia, S. M. I.; McDonald, R.; Ferguson, M. J.; Rivard, E. *Chem. Eur. J.* **2012**, *18*, 13810; (f) Al-Rafia, S. M. I.; Momeni, M. R.; Ferguson, M. J.; McDonald, R.; Brown, A.; Rivard, E. *Organometallics* **2013**, *32*, 6658.

7. (a) Swarnakar, A. K.; Hering-Junghans, C.; Nagata, K.; Ferguson, M. J.; McDonald, R.; Tokitoh, N.; Rivard, E. *Angew. Chem. Int. Ed.* **2015**, *54*, 10666; (b) Swarnakar, A. K.; Hering-Junghans, C.; Ferguson, M. J.; McDonald, R.; Rivard, E. *Chem. Sci.* **2017**, *8*, 2337.
8. (a) Khan, S.; Gopakumar, G.; Thiel, W.; Alcazaro, M. *Angew. Chem. Int. Ed.* **2013**, *52*, 5644; (b) Roy, M. M. D.; Lummis, P. A.; Ferguson, M. J.; McDonald, R.; Rivard, E. *Chem. Eur. J.* **2017**, *23*, 11249.
9. Swarnakar, A. K.; Hering-Junghans, C.; Ferguson, M. J.; McDonald, R.; Rivard, E. *Chem. Eur. J.* **2017**, *23*, 8628.
10. Gao, Y.; Yang, Y.; Zheng, W.; Su, Y.; Zhang, X.; Roesky, H. W. *Inorg. Chem.* **2017**, *56*, 10220.
11. Wang, Y.; Quillian, B.; Wei, P.; Wannere, C. S.; Xie, Y.; King, R. B.; Schaefer III, H. F.; Schleyer, P. v. R.; Robinson, G. H. *J. Am. Chem. Soc.* **2007**, *129*, 12412.
12. Swarnakar, A. K.; McDonald, S. M.; Deutsch, K. C.; Choi, P.; Ferguson, M. J.; McDonald, R.; Rivard, E. *Inorg. Chem.* **2014**, *53*, 8662.
13. (a) Hadlington, T. J.; Hermann, M.; Frenking, G.; Jones, C. *J. Am. Chem. Soc.* **2014**, *136*, 3028; (b) Chong, C. C.; Hirao, H.; Kinjo, R. *Angew. Chem. Int. Ed.* **2015**, *54*, 190; (c) Bagherzadeh, S.; Mankad, N. P. *Chem. Commun.* **2016**, *52*, 3844; (d) Roy, M. M. D.; Ferguson, M. J.; McDonald, R.; Rivard, E. *Chem. Eur. J.* **2016**, *22*, 18236.
14. For the preparation of [:Ge(H)Cl] as a transient species, see: (a) Harper, W. W.; Clouthier, D. J. *J. Chem. Phys.* **1998**, *108*, 416; (b) Lin, W.; Kang, L.; Novick, S. E. *J. Molec. Spec.* **2005**, *230*, 93.

15. Yoshimura, A.; Yoshinaga, M.; Yamashita, H.; Igarashi, M.; Shimada, S.; Sato, K. *Chem. Commun.* **2017**, *53*, 5822.

16. (a) Ishida, S.; Iwamoto, T.; Kabuto, C.; Kira, M. *Chem. Lett.* **2001**, *30*, 1102; (b) Moser, D. F.; Bosse, T.; Moser, J. L.; Guzei, I. A.; West, R. *J. Am. Chem. Soc.* **2002**, *124*, 4186; (c) Xiong, Y.; Yao, S.; Driess, M. *Organometallics* **2009**, *28*, 1927; (d) Chu, T.; Nikonov, G. I.; *Chem. Rev.* **2018**, *118*, 3608.

17. (a) Li, J.; Schenk, C.; Winter, F.; Scherer, H.; Trapp, N.; Higelin, A.; Keller, S.; Pöttgen, R.; Krossing, I.; Jones, C. *Angew. Chem. Int. Ed.* **2012**, *51*, 9557; (b) Inomata, K.; Watanabe, T.; Tobita, H. *J. Am. Chem. Soc.* **2014**, *136*, 14341; (c) Rit, A.; Tirfoin, R.; Aldridge, S. *Angew. Chem. Int. Ed.* **2016**, *55*, 378.

18. Germyliumylidenes are most commonly stabilized within a cyclic framework, for example: (a) Cheng, F.; Dyke, J. M.; Ferrante, F.; Hector, A. L.; Levason, W.; Reid, G.; Webster, M.; Zhang, W. *Dalton Trans.* **2010**, *39*, 847; (b) Xiong, Y.; Yao, S.; Inoue, S.; Berkefeld, A.; Driess, M. *Chem. Commun.* **2012**, *48*, 12198; (c) Bouška, M.; Dostál, L.; Růžička, A.; Jambor, R. *Organometallics* **2013**, *32*, 1995; (d) Weicker, S. A.; Dube, J. W.; Ragogna, P. J. *Organometallics* **2013**, *32*, 6681; (e) Xiong, Y.; Yao, S.; Tan, S.; Inoue, S.; Driess, M. *J. Am. Chem. Soc.* **2013**, *135*, 5004; (f) Su, B.; Ganguly, R; Li, Y.; Kinjo, R. *Angew. Chem. Int. Ed.* **2014**, *53*, 13106; (g) Ochiai, T.; Szilvási, T.; Franz, D.; Irran, E.; Inoue, S. *Angew. Chem. Int. Ed.* **2016**, *55*, 11619; (h) Su, Y.; Li, Y.; Ganguly, R.; Kinjo, R. *Eur. J. Inorg. Chem.* **2018**, 2228.

19. Arrowsmith, M.; Hadlington, T. J.; Hill, M. S.; Kociok-Köhn, G. *Chem. Commun.* **2012**, *48*, 4567.

20. The direct reaction of **5** with stoichiometric HBpin did not yield any spectroscopic evidence of $[IPr•GeH]^+$. Similar results were obtained when this reaction was repeated in the presence of the carbene $(MeCN\textit{i}Pr)_2C$: and $Ph_2PCH_2CH_2PPh_2$.
21. Jafarpour, L.; Stevens, E. D.; Nolan, S. P. *J. Organomet. Chem.* **2000**, *606*, 49.
22. Massey, A. G.; Park, A. J. *J. Organomet. Chem.* **1964**, *2*, 245.
23. Labre, F.; Gimbert, Y.; Bannwarth, P.; Olivero, S.; Duñach, E.; Chavant, P. Y. *Org. Lett.* **2014**, *16*, 2366.
24. Hope, H. *Prog. Inorg. Chem.* **1994**, *41*, 1.
25. Sheldrick, G. M. *Acta. Crystallogr. Sect. A* **2015**, *71*, 3.
26. Sheldrick, G. M. *Acta. Crystallogr. Sect. C.* **2015**, *71*, 3.
27. Gaussian 16, Revision B.01, Frisch, M. J.; Trucks, G. W.; Schlegel, H. B.; Scuseria, G. E.; Robb, M. A.; Cheeseman, J. R.; Scalmani, G.; Barone, V.; Petersson, G. A.; Nakatsuji, H.; Li, X.; Caricato, M.; Marenich, A. V.; Bloino, J.; Janesko, B. G.; Gomperts, R.; Mennucci, B.; Hratchian, H. P.; Ortiz, J. V.; Izmaylov, A. F.; Sonnenberg, J. L.; Williams-Young, D.; Ding, F.; Lipparini, F.; Egidi, F.; Goings, J.; Peng, B.; Petrone, A.; Henderson, T.; Ranasinghe, D.; Zakrzewski, V. G.; Gao, J.; Rega, N.; Zheng, G.; Liang, W.; Hada, M.; Ehara, M.; Toyota, K.; Fukuda, R.; Hasegawa, J.; Ishida, M.; Nakajima, T.; Honda, Y.; Kitao, O.; Nakai, H.; Vreven, T.; Throssell, K.; Montgomery, J. A., Jr.; Peralta, J. E.; Ogliaro, F.; Bearpark, M. J.; Heyd, J. J.; Brothers, E. N.; Kudin, K. N.; Staroverov, V. N.; Keith, T. A.; Kobayashi, R.; Normand, J.; Raghavachari, K.; Rendell, A. P.; Burant, J. C.; Iyengar, S. S.; Tomasi, J.; Cossi, M.; Millam, J. M.; Klene, M.; Adamo, C.; Cammi, R.; Ochterski, J. W.;

Martin, R. L.; Morokuma, K.; Farkas, O.; Foresman, J. B.; Fox, D. J. Gaussian, Inc., Wallingford CT, **2016**.

28. (a) Lee, C.; Yang, W.; Parr, R. G. *Phys. Rev. B* **1988**, *37*, 785; (b) Becke, A. D. *Phys. Rev. A* **1998**, *38*, 3098; (c) Stephens, P. J.; Devlin, F. J.; Chabalowski, C. F.; Frisch, M. J. *J. Phys. Chem.* **1994**, *98*, 11623.
29. (a) Hariharan, P. C.; Pople, J. A. *Theor. Chim. Acta.* **1973**, *28*, 213; (b) Francl, M. M.; Pietro, W. J.; Hehre, W. J.; Binkley, J. S.; Gordon, M. S.; DeFrees, D. J.; Pople, J. A. *J. Chem. Phys.* **1982**, *77*, 3654.

Chapter 6

1. For recent reviews and articles, see: (a) Chu, T.; Nikonov, G. I. *Chem. Rev.* **2018**, *118*, 3608; (b) Power, P. P. *Nature* **2010**, *463*, 171; (c) Weetman, C.; Inoue, S. *ChemCatChem.* **2018**, *10*, 4213; (d) Melen, R. L. *Science* **2019**, *363*, 479; (e) Wilson, A. S. S.; Hill, M. S.; Mahon, M. F.; Dinoi, C.; Maron, L. *Science* **2017**, *358*, 1168; (f) Fontaine, F.-G.; Rochette, E. *Acc. Chem. Res.* **2018**, *51*, 454; (g) Hicks, J.; Vasko, P.; Goicoechea, J. M.; Aldridge, S. *Nature* **2018**, *557*, 92.
2. Légaré, M.-A.; Bélanger-Chabot, G.; Dewhurst, R. D.; Welz, E.; Krummenacher, I.; Engels, B.; Braunschweig, H. *Science* **2018**, *359*, 896.
3. (a) Miller, K. A.; Watson, T. W.; Bender, J. E.; Banaszak Holl, M. M.; Kampf, J. W. *J. Am. Chem. Soc.* **2001**, *123*, 982; (b) Peng, Y.; Ellis, B. D.; Wang, X.; Power, P. P. *J. Am. Chem. Soc.* **2008**, *130*, 12268; (c) Peng, Y.; Guo, J.-D.; Ellis, B. D.; Zhu, Z.; Fettinger, J. C.; Nagase, S.; Power, P. P. *J. Am. Chem. Soc.* **2009**, *131*, 16272; (d) Mandal, S. K.; Roesky, H. W. *Acc. Chem. Res.* **2011**, *45*, 298; (e) Inomata, K.; Watanabe, T.; Miyazaki, Y.; Tobita, H. *J. Am. Chem. Soc.* **2015**, *137*, 11935; (f)

Protchenko, A. V.; Bates, J. I.; Saleh, L. M. A.; Blake, M. P.; Schwarz, A. D.; Kolychev, E. L.; Thompson, A. L.; Jones, C.; Mountford, P.; Aldridge, S. *J. Am. Chem. Soc.* **2016**, *138*, 4555; (g) Roy, M. M. D.; Fujimori, S.; Ferguson, M. J.; McDonald, R.; Tokitoh, N.; Rivard, E. *Chem. Eur. J.*, **2018**, *24*, 14392; (h) Hadlington, T. J.; Driess, M.; Jones, C. *Chem. Soc. Rev.*, **2018**, *47*, 4176.

4. (a) Mizuhata, Y.; Sasamori, T.; Tokitoh, N. *Chem. Rev.* **2009**, *109*, 3479; (b) Asay, M.; Jones, C.; Driess, M. *Chem. Rev.* **2011**, *111*, 354; (c) Rivard, E. *Chem. Soc. Rev.*, **2016**, *45*, 989.
5. (a) Jutzi, P.; Holtmann, U.; Kanne, D.; Krüger, C.; Blom, R.; Gleiter, R.; Hyla-Kryspin, I. *Chem. Ber.* **1989**, *122*, 1629; (b) Karsch, H. H.; Keller, U.; Gamper, S.; Müller, G. *Angew. Chem. Int. Ed. Engl.*, **1990**, *29*, 295.
6. Denk, M.; Lennon, R.; Hayashi, R.; West, R.; Belyakov, A. V.; Verne, H. P.; Haaland, A.; Wagner, M.; Metzler, N. *J. Am. Chem. Soc.*, **1994**, *116*, 2691.
7. (a) Rekken, B. D.; Brown, T. M.; Fettinger, J. C.; Tuononen, H. M.; Power, P. P. *J. Am. Chem. Soc.* **2012**, *134*, 6504; (b) Protchenko, A. V.; Birjkumar, K. H.; Dange, D.; Schwarz, A. D.; Vidovic, D.; Jones, C.; Kaltsoyannis, N.; Mountford, P.; Aldridge, S. *J. Am. Chem. Soc.* **2012**, *134*, 6500.
8. Gynane, M. J. S.; Harris, D. H.; Lappert, M. F.; Power, P. P.; Rivière, P.; Rivière-Baudet, M. *J. Chem. Soc., Dalton Trans.* **1977**, 2004.
9. (a) Protchenko, A. V.; Schwarz, A. D.; Blake, M. P.; Jones, C.; Kaltsoyannis, N.; Mountford, P.; Aldridge, S. *Angew. Chem. Int. Ed.* **2013**, *52*, 568; (b) Hadlington, T. J.; Abdalla, J. A. B.; Tirfoin, R.; Aldridge, S.; Jones, C. *Chem. Commun.* **2016**, *52*, 1717; (c) Wendel, D.; Porzelt, A.; Herz, F. A. D.; Sakar, D.; Jandl, C.; Inoue, S.;

Rieger, B. *J. Am. Chem. Soc.* **2017**, *139*, 8134; (d) Loh, Y. K.; Ying, L. Fuentes, M. Á.; Do, D. C. H.; Aldridge, S. *Angew. Chem. Int. Ed.* **2019**, *58*, 4847.

10. A cyclic dialkylsilylene has been previously reported: Kira, M.; Ishida, S.; Iwamoto, T.; Kabuto, C. *J. Am. Chem. Soc.* **1999**, *121*, 9722
11. (a) Hering-Junghans, C.; Andreiuk, P.; Ferguson, M. J.; McDonald, R.; Rivard, E. *Angew. Chem. Int. Ed.* **2017**, *56*, 6272; (b) For an example of a base-stabilized divinylgermylene, see: Walewska, M.; Baumgartner, J.; Marschner, C. *Chem. Commun.* **2015**, *51*, 276.
12. For reviews on NHO ligands, see: (a) Ghadwal, R. S. *Dalton Trans.* **2016**, *45*, 16081; (b) Crocker, R. D.; Nguyen, T. V. *Chem. Eur. J.* **2016**, *22*, 2208; (*c*) Roy, M. M. D.; Rivard, E. *Acc. Chem. Res.*, **2017**, *50*, 2017.
13. Powers, K.; Hering-Junghans, C.; McDonald, R.; Ferguson, M. J.; Rivard, E. *Polyhedron* **2016**, *108*, 8.
14. Dithiolatosilylenes have been reported to reversibly bind ethylene: Lips, F.; Fettinger, J. C.; Mansikkamäki, A.; Tuononen, H. M.; Power, P. P. *J. Am. Chem. Soc.* **2014**, *136*, 634.
15. Lui, M. W.; Merten, C.; Ferguson, M. J.; McDonald, R.; Xu, Y.; Rivard, E. *Inorg. Chem.* **2015**, *54*, 2040.
16. A similar reaction has been previously reported for a cyclic silylene, however a mixture of two products was observed: Xiong, Y.; Yao, S.; Driess, M. *Organometallics* **2009**, *28*, 1927.
17. Swihart, M. T.; Carr, R. W. *J. Phys. Chem. A* **1998**, *102*, 1542.

18. Hydrodechlorination of chlorosilanes using strong neutral bases is known. For example: Ghadwal, R. S.; Roesky, H. W.; Merkel, S.; Henn, H.; Stalke, D. *Angew. Chem. Int. Ed.* **2009**, *48*, 5683.

19. (a) Driess, M.; Fanta, A. D.; Powell, D. R.; West, R. *Angew. Chem. Int. Ed. Engl.* **1989**, *28*, 1038; (b) Xiong, Y.; Yao, S.; Brym, M.; Driess, M. *Angew. Chem. Int. Ed.* **2007**, *46*, 4511; (c) Sen, S. S.; Khan, S.; Roesky, H. W.; Kratzert, D.; Meindl, K.; Henn, J.; Stalke, D.; Demers, J.-P.; Lange, A. *Angew. Chem. Int. Ed.* **2011**, *50*, 2322.

20. For selected reviews of P_4 activation by main group elements, see: (a) Scheer, M.; Balázs, G.; Seitz, A. *Chem. Rev.* **2010**, *110*, 4236; (b) Khan, S.; Sen, S. S.; Roesky, H. W. *Chem. Commun.* **2012**, *48*, 2169; (c) Borger, J. E.; Ehlers, A. W.; Slootweg, J. C.; Lammertsma, K. *Chem. Eur. J.* **2017**, *23*, 11738.

21. The activation of P_4 by H_2Si: has been studied computationally. Interestingly, none of the located minima on the potential energy surface correspond to compound **6**: Damrauer, R.; Pusede, S. E. *Organometallics* **2009**, *28*, 1289.

22. For example: Gary, D. C.; Cossairt, B. M. *Chem. Mater.* **2013**, *25*, 2463.

23. Geeson, M. B.; Cummins, C. C. *Science* **2018**, *359*, 1383.

24. Wendel, D.; Reiter, D.; Porzelt, A.; Altmann, P. J.; Inoue, S.; Rieger, B. *J. Am. Chem. Soc.* **2017**, *139*, 17193.

25. Brown, Z. D.; Vasko, P.; Fettinger, J. C.; Tuononen, H. M.; Power, P. P. *J. Am. Chem. Soc.* **2012**, *134*, 4045.

26. Takeda, N.; Kajiwara, T.; Suzuki, H.; Okazaki, R.; Tokitoh, N. *Chem. Eur. J.* **2003**, *9*, 3530.

27. Pangborn, A. B.; Giardello, M. A.; Grubbs, R. H.; Rosen, R. K.; Timmers, F. J. *Organometallics* **1996**, *15*, 1518.

28. Marschner, C. *Eur. J. Inorg. Chem.* **1998**, 221.

29. Hope, H. *Prog. Inorg. Chem.* **1994**, *41*, 1.

30. Sheldrick, G. M. *Acta. Crystallogr. Sect. A* **2015**, *71*, 3.

31. Sheldrick, G. M. *Acta. Crystallogr. Sect. C* **2015**, *71*, 3.

32. Gaussian 16, Revision B.01, Frisch, M. J.; Trucks, G. W.; Schlegel, H. B.; Scuseria, G. E.; Robb, M. A.; Cheeseman, J. R.; Scalmani, G.; Barone, V.; Petersson, G. A.; Nakatsuji, H.; Li, X.; Caricato, M.; Marenich, A. V.; Bloino, J.; Janesko, B. G.; Gomperts, R.; Mennucci, B.; Hratchian, H. P.; Ortiz, J. V.; Izmaylov, A. F.; Sonnenberg, J. L.; Williams-Young, D.; Ding, F.; Lipparini, F.; Egidi, F.; Goings, J.; Peng, B.; Petrone, A.; Henderson, T.; Ranasinghe, D.; Zakrzewski, V. G.; Gao, J.; Rega, N.; Zheng, G.; Liang, W.; Hada, M.; Ehara, M.; Toyota, K.; Fukuda, R.; Hasegawa, J.; Ishida, M.; Nakajima, T.; Honda, Y.; Kitao, O.; Nakai, H.; Vreven, T.; Throssell, K.; Montgomery, J. A., Jr.; Peralta, J. E.; Ogliaro, F.; Bearpark, M. J.; Heyd, J. J.; Brothers, E. N.; Kudin, K. N.; Staroverov, V. N.; Keith, T. A.; Kobayashi, R.; Normand, J.; Raghavachari, K.; Rendell, A. P.; Burant, J. C.; Iyengar, S. S.; Tomasi, J.; Cossi, M.; Millam, J. M.; Klene, M.; Adamo, C.; Cammi, R.; Ochterski, J. W.; Martin, R. L.; Morokuma, K.; Farkas, O.; Foresman, J. B.; Fox, D. J. Gaussian, Inc., Wallingford CT, **2016**.

33. (a) Lee, C.; Yang, W.; Parr, R. G. *Phys. Rev. B* **1988**, *37*, 785; (b) Becke, A. D. *Phys. Rev. A* **1988**, *38*, 3098; (c) Stephens, P. J.; Devlin, F. J.; Chabalowski, C. F.; Frisch, M. J. *J. Phys. Chem.* **1994**, *98*, 11623.

34. (a) Hariharan, P. C.; Pople, J. A. *Theor. Chim. Acta* **1973**, *28*, 213; (b) Francl, M. M.; Pietro, W. J.; Hehre, W. J.; Binkley, J. S.; Gordon, M. S.; DeFrees, D. J.; Pople, J. A. *J. Chem. Phys.* **1982**, *77*, 3654.
35. Zhao, Y.; Truhlar, D. J. *Theor. Chem. Acc.* **2008**, *120*, 215.
36. Weigend, F.; Ahlrichs, R. *Phys. Chem. Chem. Phys.* **2005**, *7*, 3297.

Chapter 7

1. a) Davidson, P. J.; Lappert, M. F. *J. Chem. Soc., Chem. Commun.* **1973**, 317; (b) Goldberg, D. E.; Harris, D. H.; Lappert, M. F.; Thomas, K. M. *J. Chem. Soc., Chem. Commun.* **1976**, 261; (c) Hitchcock, P. B.; Lappert, M. F.; Miles, S. J.; Thorne, A. J. *J. Chem. Soc., Chem. Commun.* **1984**, 480; (d) Goldberg, D. E.; Hitchcock, P. B.; Lappert, M. F.; Thomas, K. M. *J. Chem. Soc., Chem. Commun.* **1986**, 2387.
2. For selected recent reviews and articles, see: (a) Fischer, R. C.; Power, P. P. *Chem. Rev.* **2010**, *110*, 3877; (b) Wang, Y.; Robinson, G. H. *Inorg. Chem.* **2011**, *50*, 12326; (c) Ghadwal, R. S.; Azhakar, R.; Roesky, H. W. *Acc. Chem. Res.* **2013**, *46*, 444; (d) Brand, J.; Braunschweig, H.; Sen, S. S. *Acc. Chem. Res.* **2014**, *47*, 180; (e) Präsang, C.; Scheschkewitz, D. *Chem. Soc. Rev.* **2016**, *45*, 900; (f) Ochiai, T.; Franz, D.; Inoue, S. *Chem. Soc. Rev.* **2016**, *45*, 6327; (g) Melaimi, M.; Jazzar, R.; Soleilhavoup, M.; Bertrand, G. *Angew. Chem. Int. Ed.* **2017**, *56*, 10046; (h) Schneider, J.; Sindlinger, C. P.; Eichele, K.; Schubert, H.; Wesemann, L. *J. Am. Chem. Soc.* **2017**, *139*, 6542; (i) Légaré, M.-A.; Bélanger-Chabot, G.; Dewhurst, R. D.; Welz, E.; Krummenacher, I.; Engels, B.; Braunschweig, H. *Science* **2018**, *359*, 896; (j) Nesterov, V.; Reiter, D.; Bag, P.; Frisch, P.; Holzner, R.; Porzelt, A.; Inoue, S. *Chem. Rev.* **2018**, *118*, 9678; (k) Légaré, M.-A.; Rang, M.; Bélanger-Chabot, G.; Schweizer, J. I.; Krummenacher, I.;

Bertermann, R.; Arrowsmith, M.; Holthausen, M. C.; Braunschweig, H. *Science* **2019**, *363*, 1329.

3. Jutzi, P.; Holtmann, U.; Kanne, D.; Krüger, C.; Blom, R.; Gleiter, R.; Hyla-Kryspin, I. *Chem. Ber.* **1989**, *122*, 1629.
4. Kira, M.; Ishida, S.; Iwamoto, T.; Kabuto, C. *J. Am. Chem. Soc.* **1999**, *121*, 9722.
5. (a) Tokitoh, N.; Manmaru, K.; Okazaki, R. *Organometallics* **1994**, *13*, 167; (b) Tokitoh, N.; Saito, M.; Okazaki, R. *J. Am. Chem. Soc.* **1993**, *115*, 2065; (c) Brooker, S.; Buijink, J.-K.; Edelmann, F. T. *Organometallics* **1991**, *10*, 25.
6. (a) Miller, K. A.; Watson, T. W.; Bender, J. E.; Banaszak Holl, M. M.; Kampf, J. W. *J. Am. Chem. Soc.* **2001**, *123*, 982; (b) Peng, Y.; Ellis, B. D.; Wang, X.; Power, P. P. *J. Am. Chem. Soc.* **2008**, *130*, 12268; (c) Peng, Y.; Guo, J.-D.; Ellis, B. D.; Zhu, Z.; Fettinger, J. C.; Nagase, S.; Power, P. P. *J. Am. Chem. Soc.* **2009**, *131*, 16272; (d) Mandal, S. K.; Roesky, H. W. *Acc. Chem. Res.* **2011**, *45*, 298; (e) Inomata, K.; Watanabe, T.; Miyazaki, Y.; Tobita, H. *J. Am. Chem. Soc.* **2015**, *137*, 11935; (f) Protchenko, A. V.; Bates, J. I.; Saleh, L. M. A.; Blake, M. P.; Schwarz, A. D.; Kolychev, E. L.; Thompson, A. L.; Jones, C.; Mountford, P.; Aldridge, S. *J. Am. Chem. Soc.* **2016**, *138*, 4555; (g) Roy, M. M. D.; Fujimori, S.; Ferguson, M. J.; McDonald, R.; Tokitoh, N.; Rivard, E. *Chem. Eur. J.* **2018**, *24*, 14392; (h) Hadlington, T. J.; Driess, M.; Jones, C. *Chem. Soc. Rev.* **2018**, *47*, 4176.
7. A homologous tetrelene series was recently reported using bulky alkoxide ligands: Loh, Y. K.; Ying, L.; Fuentes, M.-A.; Huan Do, D. C.; Aldridge, S. *Angew. Chem. Int. Ed.* **2019**, *58*, 4847.

8. Such as: Denk, M.; Lennon, R.; Hayashi, R.; West, R.; Belyakov, A. V.; Verne, H. P.; Haaland, A.; Wagner, M.; Metzler, N. *J. Am. Chem. Soc.* **1994**, *116*, 2691.
9. Such as: Karsch, H. H.; Keller, U.; Gamper, S.; Müller, G. *Angew. Chem. Int. Ed. Engl.* **1990**, *29*, 295.
10. Two-coordinate acyclic silylenes stabilized by heteroatom donors are known: (a) Rekken, B. D.; Brown, T. M.; Fettinger, J. C.; Tuononen, H. M.; Power, P. P. *J. Am. Chem. Soc.* **2012**, *134*, 6504; (b) Protchenko, A. V.; Birjkumar, K. H.; Dange, D.; Schwarz, A. D.; Vidovic, D.; Jones, C.; Kaltsoyannis, N.; Mountford, P.; Aldridge, S. *J. Am. Chem. Soc.* **2012**, *134*, 6500; (c) Hadlington, T. J.; Abdalla, J. A. B.; Tirfoin, R.; Aldridge, S.; Jones, C. *Chem. Commun.* **2016**, *52*, 1717.
11. For reviews on NHO ligands, see: (a) Ghadwal, R. S. *Dalton Trans.*, **2016**, *45*, 16081; (b) Crocker, R. D.; Nguyen, T. V. *Chem. Eur. J.*, **2016**, *22*, 2208; (*c*) Roy, M. M. D.; Rivard, E. *Acc. Chem. Res.*, **2017**, *50*, 2017.
12. For example: (a) Al-Rafia, S. M. I.; Ferguson, M. J.; Rivard, E. *Inorg. Chem.* **2011**, *50*, 10543; (b) Ghadwal, R. S.; Reichmann, S. O.; Engelhardt, F.; Andrada, D. M.; Frenking, G. *Chem. Commun.* **2013**, *49*, 9440; (c) Wünsche, M. A.; Witteler, T.; Dielmann, F. *Angew. Chem. Int. Ed.* **2018**, *57*, 7234.
13. Hering-Junghans, C.; Andreiuk, P.; Ferguson, M. J.; McDonald, R.; Rivard, E. *Angew. Chem. Int. Ed.* **2017**, *56*, 6272.
14. Gentner, T. X.; Ballmann, G.; Pahl, J.; Elsen, H.; Harder, S. *Organometallics* **2018**, *37*, 4473.
15. Kuhn, N.; Bohnen, H.; Henkel, G.; Kreutzberg, J. *Z. Naturforsch.* **1996**, *51b*, 1267.

16. Braga, D.; Grepioni, F.; Biradha, K.; Desiraju, G. R. *J. Chem. Soc., Dalton Trans.* **1996**, 3925.

17. Powers, K.; Hering-Junghans, C.; McDonald, R.; Ferguson, M. J.; Rivard, E. *Polyhedron* **2016**, *108*, 8.

18. Ghadwal, R. S.; Roesky, H. W.; Merkel, S.; Henn, J.; Stalke, D. *Angew. Chem. Int. Ed.* **2009**, *48*, 5683.

19. Filippou, A. C.; Chernov, O.; Schnackenburg, G. *Angew. Chem. Int. Ed.* **2009**, *48*, 5687.

20. Schweizer, J. I.; Sturm, A. G.; Porsch, T.; Berger, M.; Bolte, M.; Auner, N.; Holthausen, M. C. *Z. Anorg. Allg. Chem.* **2018**, *644*, 982.

21. (a) Protchenko, A. V.; Schwarz, A. D.; Blake, M. P.; Jones, C.; Kaltsoyannis, N.; Mountford, P.; Aldridge, S. *Angew. Chem. Int. Ed.*,**2013**, *52*, 568; (b) Wendel, D.; Porzelt, A.; Herz, F. A. D.; Sakar, D.; Jandl, C.; Inoue, S.; Rieger, B. *J. Am. Chem. Soc.* **2017**, *139*, 8134; (c) Roy, M. M. D.; Ferguson, M. J.; McDonald, R.; Zhou, Y.; Rivard, E. *Chem. Sci.* **2019**, *10*, 6476.

22. Wendel, D.; Reiter, D.; Porzelt, A.; Altmann, P. J.; Inoue, S.; Rieger, B. *J. Am. Chem. Soc.* **2017**, *139*, 17193.

23. A three-coordinate germanone has also been previously reported: Li, L.; Fukawa, T.; Matsuo, T.; Hashizume, D.; Fueno, H.; Tanaka, K.; Tamao, K. *Nat. Chem.* **2012**, *4*, 361.

24. Pangborn, A. B.; Giardello, M. A.; Grubbs, R. H.; Rosen, R. K.; Timmers, F. J. *Organometallics* **1996**, *15*, 1518.

25. Ryan, S. J.; Schimler, S. D.; Bland, D. C.; Sanford, M. S. *Org. Lett.* **2015**, *17*, 1866.

26. Hupf, E.; Kaiser, F.; Lummis, P. A.; Roy, M. M. D.; McDonald, R.; Ferguson, M. J.; Kühn, F. E.; Rivard, E. *unpublished results (manuscript submitted).*
27. Marschner, C. *Eur. J. Inorg. Chem.* **1998**, 221.
28. Hope, H. *Prog. Inorg. Chem.* **1994**, *41*, 1.
29. Sheldrick, G. M. *Acta. Crystallogr. Sect. A.* **2015**, *71*, 3.
30. Sheldrick, G. M. *Acta. Crystallogr. Sect. C.* **2015**, *71*, 3.
31. Gaussian 16, Revision B.01, Frisch, M. J.; Trucks, G. W.; Schlegel, H. B.; Scuseria, G. E.; Robb, M. A.; Cheeseman, J. R.; Scalmani, G.; Barone, V.; Petersson, G. A.; Nakatsuji, H.; Li, X.; Caricato, M.; Marenich, A. V.; Bloino, J.; Janesko, B. G.; Gomperts, R.; Mennucci, B.; Hratchian, H. P.; Ortiz, J. V.; Izmaylov, A. F.; Sonnenberg, J. L.; Williams-Young, D.; Ding, F.; Lipparini, F.; Egidi, F.; Goings, J.; Peng, B.; Petrone, A.; Henderson, T.; Ranasinghe, D.; Zakrzewski, V. G.; Gao, J.; Rega, N.; Zheng, G.; Liang, W.; Hada, M.; Ehara, M.; Toyota, K.; Fukuda, R.; Hasegawa, J.; Ishida, M.; Nakajima, T.; Honda, Y.; Kitao, O.; Nakai, H.; Vreven, T.; Throssell, K.; Montgomery Jr., J. A.; Peralta, J. E.; Ogliaro, F.; Bearpark, M. J.; Heyd, J. J.; Brothers, E. N.; Kudin, K. N.; Staroverov, V. N.; Keith, T. A.; Kobayashi, R.; Normand, J.; Raghavachari, K.; Rendell, A. P.; Burant, J. C.; Iyengar, S. S.; Tomasi, J.; Cossi, M.; Millam, J. M.; Klene, M.; Adamo, C.; Cammi, R.; Ochterski, J. W.; Martin, R. L.; Morokuma, K.; Farkas, O.; Foresman, J. B.; Fox, D. J. Gaussian, Inc., Wallingford CT, **2016**.
32. (a) Lee, C.; Yang, W.; Parr, R. G. *Phys. Rev. B* **1988**, *37*, 785; (b) Becke, A. D. *Phys. Rev. A* **1988**, *38*, 3098; (c) Stephens, P. J.; Devlin, F. J.; Chabalowski, C. F.; Frisch, M. J. J. *Phys. Chem.* **1994**, *98*, 11623.

33. (a) Dunning Jr., T. H.; *J. Chem. Phys.* **1989**, *90*, 1007; (b) Woon, D. E.; Dunning Jr., T. H. *J. Chem. Phys.* **1993**, *98*, 1358.

Chapter 8

1. Velian, A.; Cummins, C. *J. Am. Chem. Soc.* **2012**, *134*, 13978.
2. Swamy, V. S. V. S. N.; Pal, S.; Khan, S.; Sen, S. S. *Dalton Trans.* **2015**, *44*, 12903.
3. Rupar, P. A.; Staroverov, V. N.; Baines, K. M. *Science* **2008**, *322*, 1360.
4. Li, L.; Fukawa, T.; Matsuo, T.; Hashizume, D.; Fueno, H.; Tanaka, K.; Tamao, K. *Nat. Chem.* **2012**, *4*, 361.
5. Wendel, D.; Reiter, D.; Porzelt, A.; Altmann, P. J.; Inoue, S.; Rieger, B. *J. Am. Chem. Soc.* **2017**, *139*, 17193.